

Accepted
Vermont
Master of

POST-GLACIAL FLUVIAL TERRACES
IN THE WINOOSKI DRAINAGE BASIN, VERMONT

Thesis Examination Committee:

A Thesis Presented
by
Timothy Nash Whalen
to
The Faculty of the Graduate College
of
The University of Vermont

Date: December 1, 1997

In Partial Fulfillment of the Requirements
for the Degree of Master of Science
Specializing in Geology

March, 1998

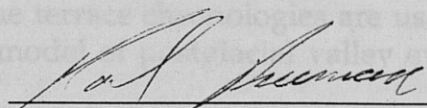
ABSTRACT

Accepted by the Faculty of the Graduate College, The University of Vermont, in partial fulfillment of the requirements for the degree of Master of Science, specializing in Geology.

The survey data are used to correlate the terraces with proglacial lake levels and with each other. Combined with previously dated baselevels, previously dated glaciolacustrine and new terrace dates, the survey data were used to produce dated terrace chronologies for each valley.

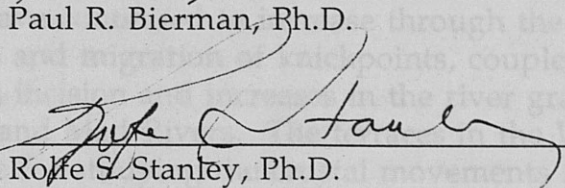
The terrace chronologies imply that following the deposition of the first

Thesis Examination Committee:

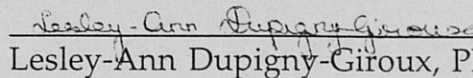


Paul R. Bierman, Ph.D.

Advisor



Rolfe S. Stanley, Ph.D.



Lesley-Ann Dupigny-Giroux, Ph.D.

Chairperson



Andrew R. Bodman, Ph.D.

Interim Dean,
Graduate College

Date: December 4, 1997

ABSTRACT

I have surveyed, trenched, and dated flights of river terraces in the Huntington, Little, and Mad River Valleys of the Winooski Drainage Basin. The survey data are used to correlate the terraces with proglacial lake levels and with each other. Combined with previously dated baselevels, previously dated alluvial fans, and new terrace dates, the survey data were used to produce dated terrace chronologies for each valley.

The terrace chronologies imply that following the deposition of the first terrace which caps the glaciolacustrine fill in each valley, incision was first controlled by proglacial lake lowerings and then possibly by widespread climate changes. The terrace chronologies are used to place the terraces within a five stage model of postglacial valley evolution.

Terrace gradients have continued to increase through the Holocene. Baselevel lowerings and migration of knickpoints, coupled with climate changes, resulted in incision and increases in the river gradients along the Huntington, Little, and Mad Rivers. The terraces in the Winooski Drainage Basin are unsuitable for studying the crustal movements associated with glacio-isostatic rebound because there is no consistent river gradient from which to make measurements.

To all of the geologists whose support **ACKNOWLEDGMENTS**

This research was supported by Sigma Xi Grants-in-Aid of Research and Geological Society of America awards to myself, and by the University of Vermont through my advisor, Dr. Paul Bierman.

I sincerely appreciated the cooperation of all the landowners in the Huntington, Little, and Mad River Valleys for access to survey their terraces. The Department of Forests, Parks and Recreation provided me access to the Little River State Park and Waterbury Reservoir. The completion of the surveying would not have been possible if not for all the help I received from the following people (in alphabetical order): Mike Abbott, Cathy Bliss, Sean Lampert, Anne Katzenberg, Megan Kelton, Mike Loso, Arif Malik, Aziza Malik, Martha McConnell, Chris Valin, John Whalen, Julie Williams, Stephen Wright, and Paul Zehfuss. Also, thanks to J. Milo Robinson from the National Geodetic Survey for Benchmark locations and elevations.

In addition to allowing me access to survey, the Moulthrop, Aldrich, and Rodger families were also kind enough to permit excavations on their properties. The 1995 Geomorphology class dug the shovel pits on the Moulthrop property and Mr. Henry Moulthrop excavated the trenches on his and the Aldrich properties. Their assistance is greatly appreciated because without it, I would have never gained such insight into the terrace stratigraphy. Paul Bierman, Cathy Bliss, Chris Valin, and Paul Zehfuss braved the trenches, helping me scrape and log the trench walls and search for the elusive charcoal pieces.

To all of the geology graduate and undergraduate students whose support and friendship have kept me going the past three years, I say thanks. A big thanks goes to (in alphabetical order): Mike Abbott, Beth Nadeau Astley, Amy Church, Lin Li, Laura Mallard, Kim Marsella, Todd Martin, Nilah Mazza, Jessica Murray, Alexis Richardson, Adam Schoonmaker, Dave Shaw, Tanya Unger, Chris Valin, and Paul Zehfuss.

There are many other important people who made this thesis possible. Dr. Stephen Wright helped me so much in the field, encouraged me to lead field trips, and enlightened me in the ways of Vermont geology. My thesis committee has been great. Thank you for your encouragement and patience, especially during the preparation of the final drafts. All my family, including my cousins, brothers, parents, grandfathers, aunts and uncles, have been unbelievably generous to me during my whole graduate career.

Finally, I must say thanks to Keely Kane. I can not imagine that I would be finishing this thesis with any sanity intact if she had not been there to make me smile during all these long days and nights of thesis writing.

Background	4
Northeast Rebound Studies	10
Summary	59
CLIMATE HISTORY OF THE NORTHEAST	61
Background	60
Climate Proxies in the Northeast	62
Summary	67
RIVER TERRACES	70
Conditions for Development of Terraces	72
Terrace Classification	73

TABLE OF CONTENTS

ACKNOWLEDGMENTS.....	ii
TABLE OF CONTENTS.....	iv
LIST OF TABLES	vii
LIST OF FIGURES	viii
CHAPTER 1: INTRODUCTION	1
STATEMENT OF PROBLEM.....	1
OVERVIEW OF THESIS.....	2
FIELD AREA	3
CHAPTER 2: PREVIOUS RESEARCH	11
DEGLACIATION OF THE CHAMPLAIN AND WINOOSKI VALLEYS.....	11
Winooski Valley.....	11
Champlain Valley.....	25
Summary	39
GLACIO-ISOSTATIC REBOUND.....	43
Background	43
Northeast Rebound Studies	49
Summary	59
CLIMATE HISTORY OF THE NORTHEAST.....	60
Background	60
Climate Proxies in the Northeast.....	62
Summary	71
RIVER TERRACES.....	72
Conditions for Development of Terraces.....	72
Terrace Classification	81

Interpretation of Terrace Remnants as Related to Tilting.....	84
CHAPTER 1 Interpretation of Terrace Remnants as Related to Environmental Changes.....	85
Local Studies of River Terraces.....	87
Summary.....	90
CHAPTER 3: METHODS AND DATA	91
SURVEYING.....	91
Methods	91
Survey Data: Huntington River.....	94
Survey Data: Little River.....	99
Survey Data: Mad River.....	104
TRENCHING.....	108
Methods	108
Trench Logs: Huntington River.....	108
Trench Logs: Mad River.....	126
DATING.....	133
Methods	133
Radiocarbon Dates: Huntington River	137
Radiocarbon Dates: Mad River	138
CHAPTER 4: RESULTS AND CALCULATIONS.....	140
DATED TERRACE CHRONOLOGY	140
Terrace Chronology: Huntington River Valley.....	140
Terrace Chronology: Little River Valley.....	143
Terrace Chronology: Mad River Valley	145
TERRACE GRADIENTS.....	147

Gradients: Huntington River Valley.....	149
Gradients: Mad River Valley.....	154
CHAPTER 5: DISCUSSION	159
TERRACE FORMATION IN THE WINOOSKI DRAINAGE	
Table 2.1: Mean terrace gradients.....	159
Table 2.2: Mean terrace gradients.....	159
Table 2.3: Mean terrace gradients.....	159
Table 2.4: Mean terrace gradients.....	159
Table 2.5: Mean terrace gradients.....	159
Table 2.6: Mean terrace gradients.....	159
GENERAL MODEL FOR VALLEY EVOLUTION	162
GRADIENT	166
IMPLICATIONS OF TERRACE GRADIENTS IN GLACIATED	
REGIONS.....	169
Table 3.1: Mean terrace gradients.....	169
Table 3.2: Mean terrace gradients.....	169
Table 3.3: Mean terrace gradients.....	169
Table 3.4: Mean terrace gradients.....	169
Table 3.5: Mean terrace gradients.....	169
RELATIONSHIP BETWEEN ALLUVIAL FANS AND RIVER	
TERRACES.....	172
Table 3.6: Mean terrace gradients.....	172
CHAPTER 6: CONCLUSIONS	176
BIBLIOGRAPHY	178
APPENDIX A: STELLA MODEL	187
APPENDIX B: HUNTINGTON RIVER DATA.....	190
HUNTINGTON RIVER SURVEY DATA.....	190
HUNTINGTON RIVER CROSS-VALLEY PROFILES	239
APPENDIX C: LITTLE RIVER DATA.....	246
LITTLE RIVER SURVEY DATA.....	246
LITTLE RIVER CROSS-VALLEY PROFILES.....	257
APPENDIX D: MAD RIVER DATA	261
MAD RIVER SURVEY DATA.....	261
MAD RIVER CROSS-VALLEY PROFILES	275

LIST OF TABLES

Table 2.1: Winooski Valley Lake Level Correlations.....	13
Table 2.2: Winooski Valley Lake Levels and Ice Positions	14
Table 2.3: Champlain Valley Water Level Correlations.....	26
Table 2.4: Champlain Valley Lake Levels and Ice Positions.....	27
Table 2.5: Baselevel Controls in the Winooski Valley	42
Table 2.6: Summary of Glacio-isostatic Rebound Studies Across the Northeast.....	50
Table 3.1: Terrace and River Elevations for Huntington River Longitudinal Profile.....	95
Table 3.2: Terrace and River Elevations for Little River Longitudinal Profile	100
Table 3.3: Terrace and River Elevations for Mad River Longitudinal Profile	105
Table 3.4: Huntington River Basal Fan Radiocarbon Ages.....	135
Table 3.5: Huntington River Terrace Radiocarbon Ages.....	136
Table 3.6: Mad River Terrace Radiocarbon Ages.....	139
Table 4.1: Huntington River Terrace Chronology	141
Table 4.3: Little River Terrace Chonology	144
Table 4.3: Mad River Terrace Chonology	146
Table 4.4: Huntington River Terrace Gradients.....	151
Table 4.5: Mad River Terrace Gradients.....	156
Champlain Valley.....	
Figure 2.15: Graph of Effect of k on Rate of Rebound	41
Figure 2.16: Graph of Different Rebound Scenarios.....	45
Figure 2.17: Graph of Change in Tilt for Four Uplift Scenarios.....	47
Figure 2.18: Location of Glacio-isostatic studies in the Northeast.....	51
Figure 2.19: Upper Atmosphere Circulation Patterns.....	61
Figure 2.20: Location of Climate Studies in the Northeast.....	63
Figure 2.21: Results From Climate Studies Across The Northeast.....	64
Figure 2.22: Schematic Diagram of Changes in Conditions in the White Mountains.....	66
Figure 2.23: Types of Equilibria in River Systems.....	74
Figure 2.24: Types of River Terraces.....	82
Figure 2.25: Effect Of Glacio-isostatic Rebound On Terrace Gradients	96
Figure 3.1: Examples of Cross-Valley Profiles.....	93
Figure 3.2: Map of Survey Locations and Longitudinal Profile in the Huntington River Basin.....	96
Figure 3.3: Longitudinal Profile of Terraces in the Huntington River Valley.....	97
Figure 3.4: Map of Survey Locations and Longitudinal Profile Location in the Little River Basin.....	101
Figure 3.5: Longitudinal Profile of Terraces in the Little River Valley.....	102

Figure 3.4. Map of Survey Locations and Longitudinal Profile in the Huntington River Valley

LIST OF FIGURES	
Figure 1.1: Map Of Winooski Drainage Basin	4
Figure 1.2: Map of Huntington River Basin	6
Figure 1.3: Map of Mad River Basin	7
Figure 1.4: Map of Little River Basin.....	9
Figure 2.1: Extent of Stage I Lakes in the Winooski Drainage Basin	16
Figure 2.2: Extent of Stage II Lakes in the Winooski Drainage Basin.....	17
Figure 2.3: Schematic Cross Sections through the Huntington Valley During Stages I-V.....	19
Figure 2.4: Extent of Stage III Lakes in the Winooski Drainage Basin.....	21
Figure 2.5: Extent of Stage IV Lakes in the Winooski Drainage Basin.....	23
Figure 2.6: Extent of Stage V Lakes in the Winooski Drainage Basin	24
Figure 2.7: Location of Major Moraines of the Hudson-Champlain Lobe.....	28
Figure 2.8: Extent of Lake Quaker Springs.....	29
Figure 2.9: Extent of Lake Coveville	31
Figure 2.10: Extent of Lake Fort Ann I.....	33
Figure 2.11: Extent of Upper Marine.....	35
Figure 2.12: Extent of Lake Champlain.....	37
Figure 2.13: Correlation Diagram of Deglacial Events in the Southern Champlain Valley.....	40
Figure 2.14: Correlation Diagram of Deglacial Events in the Northern Champlain Valley.....	41
Figure 2.15: Graph of Effect of k on Rate of Rebound	45
Figure 2.16: Graph of Different Rebound Scenarios.....	46
Figure 2.17: Graph of Change inTilt for Four Uplift Scenarios.....	47
Figure 2.18: Location of Glacio-isostatic Studies in the Northeast.....	51
Figure 2.19: Upper Atmosphere Circulation Patterns.....	61
Figure 2.20: Location of Climate Studies in the Northeast.....	63
Figure 2.21: Results From Climate Studies Across The Northeast.....	64
Figure 2.22: Schematic Diagram of Changes in Conditions in the White Mountains	68
Figure 2.23: Types of Equilibria in River Systems.....	74
Figure 2.24: Types of River Terraces	82
Figure 2.25: Effect Of Glacio-isostatic Rebound On Terrace Gradients	86
Figure 3.1: Examples of Cross-Valley Profiles.....	93
Figure 3.2: Map of Survey Locations and Longitudinal Profile in the Huntington River Basin	96
Figure 3.3: Longitudinal Profile of Terraces in the Huntington River Valley.....	97
Figure 3.4: Map of Survey Locations and Longitudinal Profile Location in the Little River Basin.....	101
Figure 3.5: Longitudinal Profile of Terraces in the Little River Valley.....	102

Figure 3.6: Map of Survey Locations and Longitudinal Profile in the Mad River Basin	106
Figure 3.7: Longitudinal Profile of Terraces in the Mad River Valley	107
Figure 3.8: Location Map of Trenches and Pits in the Huntington Valley.....	109
Figure 3.9: T8-T6 Pits-Huntington River.....	111
Figure 3.10: T6 Trench-Huntington River	114
Figure 3.11: T5 Pits 1-3-Huntington River.....	117
Figure 3.12: T5 Trench-Huntington River	119
Figure 3.13: T2 Pit and ALD-6 Trench Walls-Huntington River	121
Figure 3.14: ALD-8 Trench-Huntington River.....	123
Figure 3.15: ALD-7 Trench Walls-Huntington River.....	124
Figure 3.16: Location Map of Trenches and Pits in the Mad Valley.....	127
Figure 3.17: T8 Trench-Mad River	128
Figure 3.18: T5 Trench-Mad River	130
Figure 3.19: T4 Trench-Mad River	132
Figure 4.1: Example of Best-fit Lines for Terrace Elevations	148
Figure 4.2: Reaches of the Huntington River.....	150
Figure 4.3: Gradients for Terraces in the Huntington River.....	152
Figure 4.4: Graph of Huntington River Terrace Gradients Versus Time.....	153
Figure 4.5: Reaches of the Mad River.....	155
Figure 4.6: Gradients for Terraces in the Mad River.....	157
Figure 4.7: Graph of Mad River Terrace Gradients Versus Time.....	158
Figure 5.1: Comparison of Forcings on River Terrace Formation.....	160
Figure 5.2: Schematic Valley Evolution.....	163
Figure 5.3: Schematic Graphs of Terrace Gradients over Time	167

CHAPTER 1: INTRODUCTION

STATEMENT OF PROBLEM

Studies of post-glacial landforms in Vermont have focused primarily on interpreting the style and chronology of deglaciation and therefore have examined the features associated with ice positions and proglacial lake levels. Few studies have attempted to quantify the geomorphic changes that have occurred since the Laurentide ice sheet retreated from Vermont.

Flights of river terraces are present in nearly every river valley in Vermont, making them a significant feature of the landscape. Early geomorphologists in New England recognized river terraces and theorized on their formation. For example, Davis (1902) held the view that "the terracing rivers have slowly degraded their aggraded valleys while swinging from side to side, in combined response to a northerly uplift and a gradual decrease in load, and in spite of a probable decrease of volume." Several important observations were made by Davis, including: 1) initially river valleys had aggraded to some level; 2) differential uplift was a potential force to initiate incision; 3) the sediment load had decreased since deglaciation; and 4) the volume of water carried by the river may have decreased over time. However, none of Davis' interpretations are specific enough to warrant a model of terrace formation in New England. What is lacking from Davis' statements, and from the literature since his time, is a quantitative and systematic approach to when, how, and why river terraces developed in New England.

In recent years, archaeologists have been the primary workers to investigate river terraces in New England. Because river terraces are former flood plains and are ubiquitous in river valleys, they make excellent sites for

locating paleo-indian occupation surfaces. Archaeologists may even date some of the occupation surfaces, but because these ages usually indicate only the presence of humans on the terrace, the limiting ages may poorly bracket when the terraces formed. Furthermore, an archaeological investigation is not primarily concerned with the sedimentology of the terrace deposit (how the river behaved while the terrace formed) or with the processes that initiated river incision (why the terrace formed). Therefore, although river terraces have been investigated in Vermont, no study has completely addressed when, how, and why Vermont river terraces formed.

The purposes of this thesis are threefold: 1) to establish a dated river terrace chronology for tributaries in the Winooski Drainage Basin; 2) to use this chronology to infer the timing and cause of river incision; and 3) to develop a conceptual model of landscape evolution which considers how changing baselevels, glacio-isostatic rebound, changing climate regimes, and human land use have influenced landscape development in Vermont since deglaciation.

OVERVIEW OF THESIS

I have structured this thesis to provide sufficient background information about rivers and their responses to the different factors which may have influenced valley evolution in Vermont since deglaciation so that my data are placed in context. The remaining section of Chapter 1 describes the physical setting of the field area. In Chapter 2, I first present the previous research pertaining to deglaciation, glacio-isostatic rebound, and climate change in north-central Vermont and the Northeast before reviewing ideas about fluvial dynamics and the formation of river terraces. Next in Chapter

3, I describe my methods and present my three data sets (survey data, trench logs, and radiocarbon dates). In Chapter 4, I synthesize my data with results from previous research to establish dated terrace chronologies for the three studied valleys, and I calculate gradients for different reaches. In Chapter 5, I discuss my results in terms of a model for postglacial valley evolution that accounts for my observations and interpretations of river terrace development. I also evaluate the validity of using river terraces for interpreting crustal movements in formerly glaciated regions and provide a discussion of the link between river terraces and alluvial fans in Vermont. Chapter 6 presents the conclusions of my study.

FIELD AREA

My field area is composed of three valleys of the Winooski Drainage Basin, located in north-central Vermont (Figure 1.1). I chose to study the north-flowing Huntington and Mad Rivers and the south-flowing Little River. These three valleys have similar lithologic and structural controls as well as similar drainage area, relief, and climate, and land use. By choosing rivers with nearly identical physical properties, I expected that they display similar responses to disturbances and therefore similar terrace histories.

The orientation of the valleys is controlled by the Green Mountain Anticlinorium, a NNE-SSW trending belt of folded metamorphic rocks in which anticlines and synclines, coupled with ductile shear zones, control the topography (Stanley, personal communication, 1997). The Huntington River Valley rests in a syncline on the west limb of the Green Mountain Axial Anticline. The Mad River and Little River Valleys lie in a ductile shear zone.

The geology of all three valleys is similar; the bedrock consists of schists and phyllites (Doll et al., 1961) and the surficial deposits contain till, sand, and gravel (Doll et al., 1961; Goss, 1970). The Huntington Branch Valley is

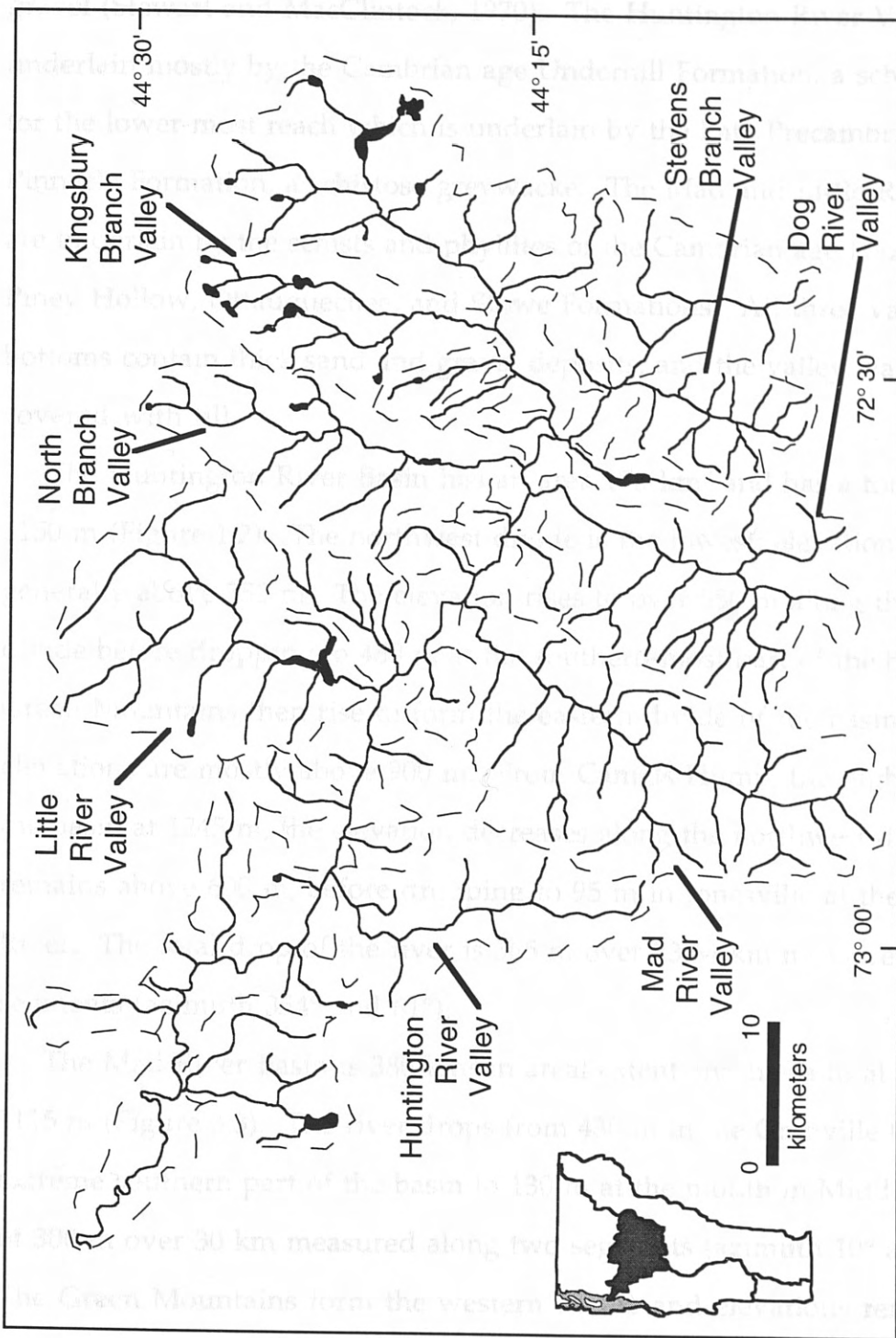


Figure 1.1: Map of Winooski Drainage Basin. Major tributary basins are labeled. Base from USGS 1:250,000 Lake Champlain Sheet.

The geology of all three valleys is similar; the bedrock consists of schists and phyllites (Doll et al., 1961) and the surficial deposits contain till, sand, and gravel (Stewart and MacClintock, 1970). The Huntington River Valley is underlain mostly by the Cambrian age Underhill Formation, a schist, except for the lower-most reach which is underlain by the Late Precambrian age Pinnacle Formation, a schistose greywacke. The Mad and Little River Valleys are underlain by the schists and phyllites of the Cambrian age Hazens Notch, Piney Hollow, Ottauquechee, and Stowe Formations. All three valley bottoms contain thick sand and gravel deposits, and the valley walls are covered with till.

The Huntington River Basin has an area 175 km² and has a total relief of 1150 m (Figure 1.2). The northwest divide is the lowest; elevations are generally above 350 m. The elevation rises to over 550 m along the southwest divide before dropping to 460 m at the southern-most part of the basin. The Green Mountains then rise to form the eastern divide of the basin, where elevations are mostly above 900 m. From Camels Hump, the highest peak in the basin at 1245 m, the elevation decreases along the northwest divide, but remains above 600 m, before dropping to 95 m in Jonesville at the Winooski River. The total drop of the river is 365 m over 23.64 km measured along two segments (azimuth 354° and 61°).

The Mad River Basin is 380 km² in areal extent and has a total relief of 1115 m (Figure 3.3). The river drops from 430 m in the Granville Gulf at the extreme southern part of the basin to 130 m at the mouth in Middlesex, a total of 300 m over 30 km measured along two segments (azimuth 10° and 40°). The Green Mountains form the western divide and elevations remain mostly above 850 m, reaching 1245 m on Mt. Ellen. The Northfield Mountains

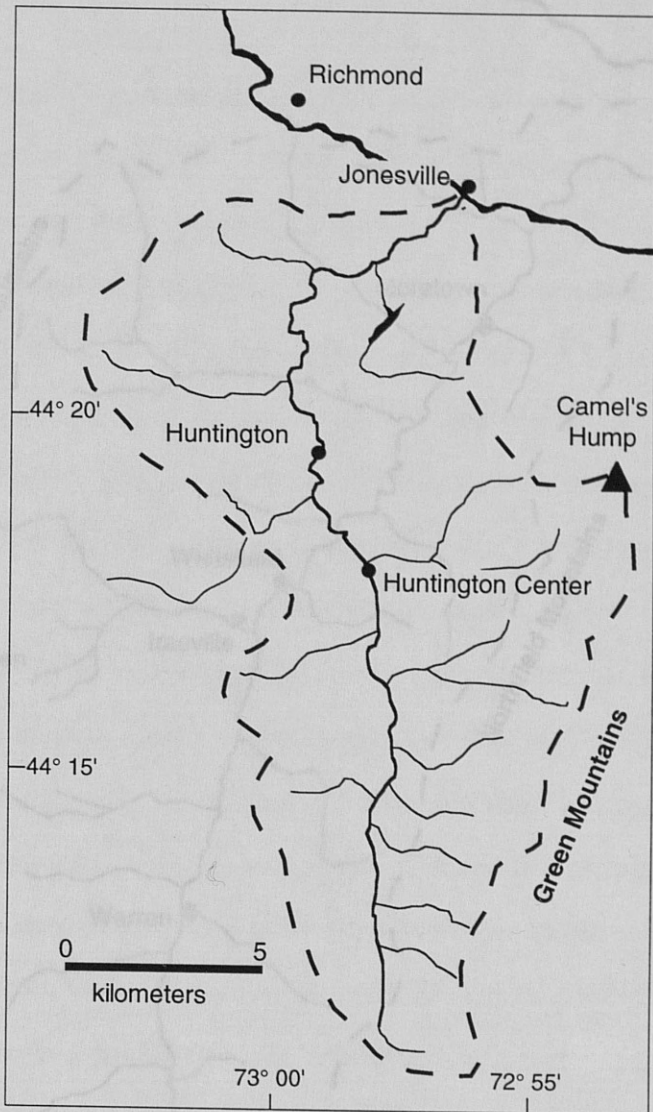


Figure 1.2: Map of Huntington River Basin. Base map from USGS 1:100,00 sheet.

Figure 1.3: Map of Head River Basin. Base map from USGS 1:100,00 sheet.

define the eastern divide and they are lower than the Green Mountains.

Elevations are mostly below 600 m, and the highest point in the basin is 987 m.

The Little River Basin covers an area of 380 km² with a mean elevation of 1,200 m (Figure 1.4). The divide between the Mad River and the Connecticut River is bounded by a 6 km long ridge. The Green Mountains form the western divide, rising to 1,600 m. The highest point in the basin is Mt. Ellen at 1,349 m, lies in the northeast corner of the basin. Along the northern divide, the elevation drops to 800 m and then rises to the east, reaching 1,000 m at Mt. Warren. To the south of the Green Mountains, generally above 750 m in elevation, the divide remains high and drops to 300 m in thebury Center. In the southeast, the Northfield Mountains, generally above 750 m in elevation, drop to 300 m in thebury Center. The climate of the region varies dramatically by location (data presented in Meeks, 1996). Summers are warm and humid, with average temperatures above 20 °C and numerous thunderstorms. Winters are cold and dry, with average temperatures near -8 °C. Precipitation is relatively constant, with slightly higher amounts falling during the summer. The valleys receive at least 100 cm of precipitation a year and the mountains receive up to 180 cm. Although westerly frontal storms bring frequent precipitation to the region and account for the majority of the yearly total, Nor'easters, in some years, can bring more precipitation than the highest precipitation event. Nor'easters can occur at any time of the year, bringing

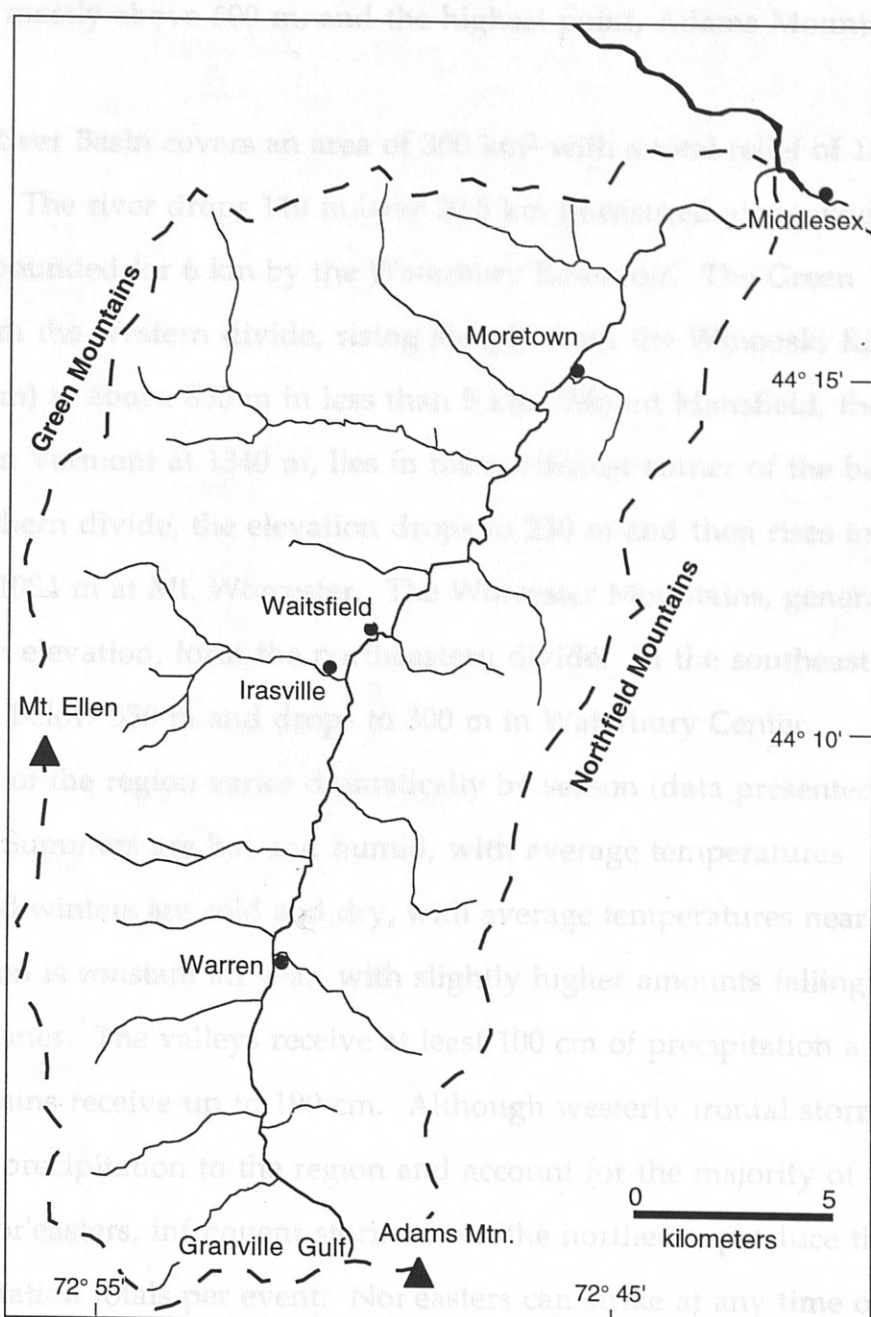


Figure 1.3: Map of Mad River Basin. Base map from USGS 1:100,000 sheet.

define the eastern divide and they are lower than the Green Mountains. Elevations are mostly above 600 m, and the highest point, Adams Mountain, is 987 m.

The Little River Basin covers an area of 300 km² with a total relief of 1220 m (Figure 1.4). The river drops 110 m over 20.5 km (measured along azimuth 30°) and is impounded for 6 km by the Waterbury Reservoir. The Green Mountains form the western divide, rising steeply from the Winooski River (elevation 120 m) to above 850 m in less than 5 km. Mount Mansfield, the highest point in Vermont at 1340 m, lies in the northwest corner of the basin. Along the northern divide, the elevation drops to 230 m and then rises to the east, reaching 1084 m at Mt. Worcester. The Worcester Mountains, generally above 750 m in elevation, form the northeastern divide. In the southeast, the divide remains below 550 m and drops to 300 m in Waterbury Center.

The climate of the region varies dramatically by season (data presented in Meeks, 1986). Summers are hot and humid, with average temperatures above 20 °C and winters are cold and dry, with average temperatures near -8 °C. Precipitation is constant all year, with slightly higher amounts falling during the summer. The valleys receive at least 100 cm of precipitation a year and the mountains receive up to 190 cm. Although westerly frontal storms bring frequent precipitation to the region and account for the majority of the yearly total, Nor'easters, infrequent storms from the northeast, produce the highest precipitation totals per event. Nor'easters can strike at any time of year, bringing significant amounts of rain or snow to the region. Convective thunderstorms, which form during the summer, may rival the precipitation totals of Nor'easters for a location, but are limited in their extent. Hurricanes

and lesser tropical storms are infrequent, but may sometimes enter the region

In the summer.

The history of land use in the basin is reflected in the names of the three basins (Meeks 1986).

In the late 1700's and early 1800's, settlers cleared the valley bottoms and upper slopes for timber and moisture land.

Although a few timber companies still exist, most of the forests were cleared from the

area, today forests are scarce (Meeks 1986). The area has a population of about 700 people.

Large ski areas and resort developments have been built in the basin, particularly along the river.

Valleys are the major drainage areas, and the basin contains several large lakes and ponds.

Elevations range from 1,000 m to over 2,000 m. Historically, timber harvesting along the rivers was the major economic activity in the basin.

Valleys were used for agriculture, and the basin contains several large lakes and ponds.

Large ski areas and resort developments have been built in the basin, particularly along the river.

Large ski areas and resort developments have been built in the basin, particularly along the river.

Large ski areas and resort developments have been built in the basin, particularly along the river.

Large ski areas and resort developments have been built in the basin, particularly along the river.

Large ski areas and resort developments have been built in the basin, particularly along the river.

Large ski areas and resort developments have been built in the basin, particularly along the river.

Large ski areas and resort developments have been built in the basin, particularly along the river.

Large ski areas and resort developments have been built in the basin, particularly along the river.

Large ski areas and resort developments have been built in the basin, particularly along the river.

Large ski areas and resort developments have been built in the basin, particularly along the river.

Large ski areas and resort developments have been built in the basin, particularly along the river.

Large ski areas and resort developments have been built in the basin, particularly along the river.

Large ski areas and resort developments have been built in the basin, particularly along the river.

Large ski areas and resort developments have been built in the basin, particularly along the river.

Large ski areas and resort developments have been built in the basin, particularly along the river.

Large ski areas and resort developments have been built in the basin, particularly along the river.

Large ski areas and resort developments have been built in the basin, particularly along the river.

Large ski areas and resort developments have been built in the basin, particularly along the river.

Large ski areas and resort developments have been built in the basin, particularly along the river.

Large ski areas and resort developments have been built in the basin, particularly along the river.

Large ski areas and resort developments have been built in the basin, particularly along the river.

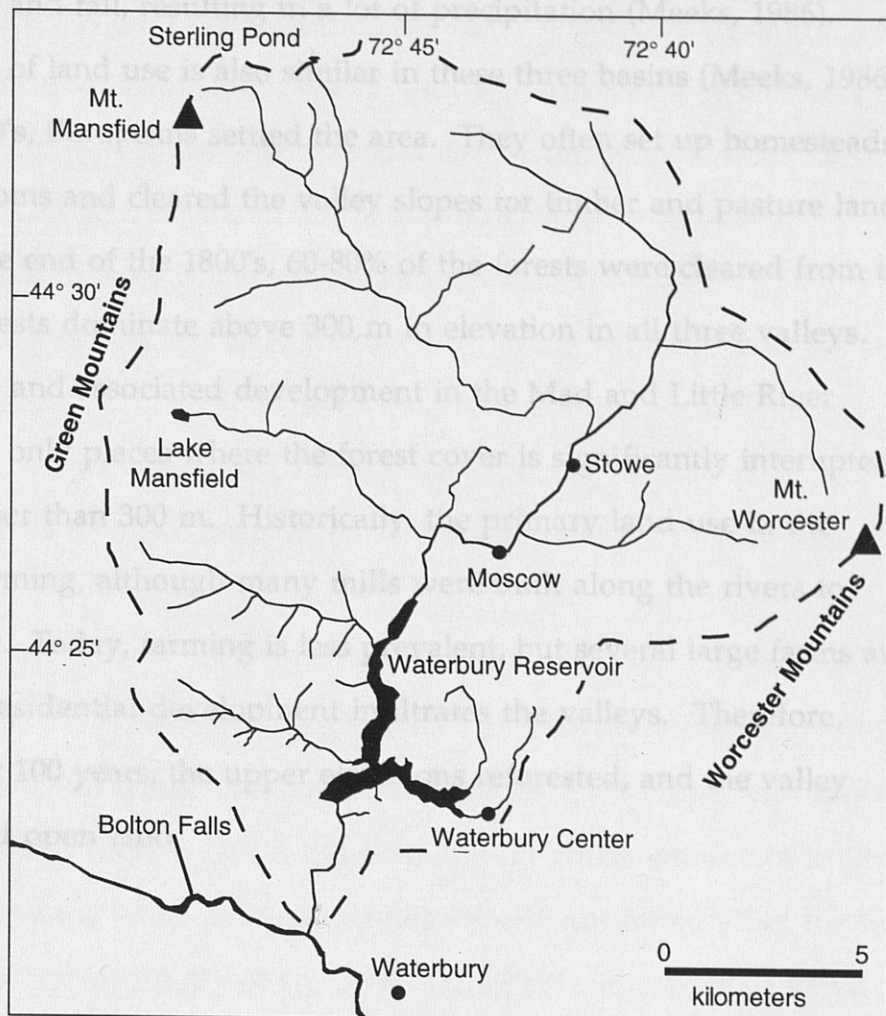


Figure 1.4: Map of Little River Basin. Base map from USGS 1:100,000 sheet.

and lesser tropical storms are infrequent, but may sometimes enter the region in the summer and fall, resulting in a lot of precipitation (Meeks, 1986).

The history of land use is also similar in these three basins (Meeks, 1986).

In the late 1700's, Europeans settled the area. They often set up homesteads in the valley bottoms and cleared the valley slopes for timber and pasture land. Although at the end of the 1800's, 60-80% of the forests were cleared from the area, today forests dominate above 300 m in elevation in all three valleys.

Large ski areas and associated development in the Mad and Little River Valleys are the only places where the forest cover is significantly interrupted at elevations higher than 300 m. Historically, the primary land use in the valleys was farming, although many mills were built along the rivers to process lumber. Today, farming is less prevalent, but several large farms are still active as residential development infiltrates the valleys. Therefore, during the past 100 years, the upper elevations reforested, and the valley floors remained open land.

Merwin (1916) has disputed the interpretation of multiple proglacial lakes in the Winooski Drainage Basin. He attributed all of the shoreline deposits to one body of water, a marine invasion which isolated New England from the rest of the continent via the Hudson and Champlain Valleys. More recent work by Larson (1972, 1987a & b), and Wagner (1972) has generally supported Merwin's (1908) chronology of lake levels.

Stewart and MacClintock (1969) present a different sequence of lake levels. Instead of attributing the delta and shoreline deposits found in the Winooski Valley to local high level lakes, Stewart and MacClintock interpreted some of these deposits to be formed by waters confluent with Lake Quaker Springs in the Champlain Valley. Deltas and terraces in the Huntington, Mad, and Winooski Valleys do occur near elevations of Lake Quaker Springs as defined

CHAPTER 2: PREVIOUS RESEARCH

DEGLACIATION OF THE CHAMPLAIN AND WINOOSKI VALLEYS

The deglacial record of the Champlain and Winooski Valleys is one of northwestward ice retreat, ice lowering, and decreasing proglacial lake levels. As the Hudson-Champlain lobe of the Laurentide ice sheet retreated, proglacial lakes developed in the valleys and left behind a scattered record of deltas and shorelines. As the lakes withdrew from the valleys, rivers began to incise the lake deposits. The purpose of this section is to review the history of the glacial lakes in the Winooski Drainage Basin and to identify when the transition occurred between lacustrine and fluvial processes in each valley.

Lake levels in the Winooski Valley follows a five stage evolution (Table

Winooski Valley

Early work in the Winooski Valley by Merwin (1908) established a chronology of lake levels that has been modified relatively little with more recent work. Only Fairchild (1916) has disputed the interpretation of multiple proglacial lakes in the Winooski Drainage Basin. He attributed all of the shoreline deposits to one body of water, a marine invasion which isolated New England from the rest of the continent via the Hudson and Champlain Valleys. More recent work by Larsen (1972, 1987a & b), and Wagner (1972) has generally supported Merwin's (1908) chronology of lake levels.

Stewart and MacClintock (1969) present a different sequence of lake levels. Instead of attributing the delta and shoreline deposits found in the Winooski Valley to local, high level lakes, Stewart and MacClintock interpreted some of these deposits to be formed by waters confluent with Lake Quaker Springs in the Champlain Valley. Deltas and terraces in the Huntington, Mad, and Winooski Valleys do occur near elevations of Lake Quaker Springs as defined

by Stewart and MacClintock, but other workers (Connally and Sirkin, 1973) placed the northern limit of Lake Quaker Springs south of the Winooski Drainage Basin. Therefore, these deposits are best explained by high level lakes. Table 2.1 shows the correlations of Winooski Valley lake levels from previous studies used to construct the history presented below.

Larsen (1972, 1987a & b) produced the most complete chronology of proglacial lakes in the eastern Winooski Valley, and his five stages of lake development are presented here as a model for the entire region. Work in the Huntington Valley (Wagner, 1972; Bryan, 1995) and in the Little River Valley (Merwin, 1908; Connally, 1972) also demonstrates that the chronology of lake levels in the Winooski Valley follows a five stage evolution (Table 2.2). Stage I lakes were limited to single north-draining valleys because they were bordered to the north by the retreating ice. These lakes drained over southern divides at different elevations into other drainage basins. During Stage II, the individual lakes coalesced, from southeast to northwest in a time-transgressive manner following the retreating ice, into a single lake whose elevation was controlled by the lowest Stage I outlet. Stage III began when the lake drained over a threshold at Gillett Pond west through the Huntington Valley into the Champlain Valley. During Stage IV, the lake continued to drain into the Champlain Valley, but the controlling threshold switched to the Hollow Brook divide. Stage IV ended when the ice retreated from where the Winooski Valley exits the Green Mountains. During Stage V, the proglacial lake waters from the Champlain Valley extended into the Winooski Basin and then withdrew to the Green Mountain Front by the close of Stage V.

Table 2.1: Winooski Valley Lake Level Correlations

	Merwin, 1908	Stewart and MacClintock, 1969	Connally, 1972	Larsen, 1972; 1987 a&b	Wagner, 1972	This Study	Elevation
Lake Winooski I	Lake Quaker Springs	-	Lake Winooski	-	Stage II	279 m at Williamstown Divide	
Lake Mansfield	Lake Quaker Springs	Lake Mansfield I	Lake Mansfield I	Lake Gillett	Stage III	229 m at Gillett Pond Threshold	
Lake Mansfield	Lake Quaker Springs	Lake Mansfield	Lake Mansfield II	Lake Huntington	Stage IV	204 m at Hollow Brook Divide	
Lake Coveville	Lake Coveville	Lake Coveville	Lake Coveville	Lake Hollow Brook & Lake Jericho	Stage V	195 m at North Williston Hill	

Ice Retreat to Green Mountain to Johns Brook to Stone Creek
 Lake Mansfield to Mansfield Brook to Stowe
 Lake Coveville to Waterbury to Floddingen to Moscow
 Lake Mansfield II to Gillett Pond to Huntington to Jericho
 Lake Gillett to Hollow Brook to Coveville to Jericho

Lake Mansfield II to Gillett Pond to Hollow Brook to Jericho
 Lake Gillett to Hollow Brook to Coveville to Jericho

The lake positions are listed as the highest upvalley location and ice position at farthest downvalley location during the stage

Table 2.2: Winooski Valley Lake Levels and Ice Positions

Stage	Winooski River	Huntington River	Little River	Mad River	Dog River	Stevens Branch
I	Ice Retreats to Valley Mouths	Lake Jerusalem to Southern Divide	Ice and Local Lakes	Lake Granville to Granville Gulf Divide	Lake Roxbury to Roxbury Divide	Lake Williamstown to Williamstown Divide
II	Ice Retreats to Jonesville	Lake Huntington to Hollow Brook Divide	Lake Winooski above Divide	Lake Winooski to Warren	Lake Winooski to South Northfield	Lake Winooski to Williamstown Divide
III	Ice Retreats to Richmond	Lake Huntington to Hollow Brook Divide	Lake Mansfield I above Divide	Lake Mansfield I to Moretown	Fluvial	Fluvial
IV	Ice Retreats to Green Mountain Front	Lake Mansfield II to Hollow Brook Divide	Lake Mansfield II to Stowe	Fluvial	Fluvial	Fluvial
V	Lake Coveville to Waterbury	Lake Coveville to Huntington	Lake Coveville to Moscow	Fluvial	Fluvial	Fluvial

The lake positions are cited as the farthest upvalley location and ice positions as farthest downvalley location during the stage.

Stage I Stage I lakes in the Winooski Basin formed separately in the presently north-draining Huntington River, Mad River, Dog River, and Stevens Branch Valleys (Figure 2.1). These lakes, bounded by ice to the north, were forced to drain through southern spillways that were at different elevations. During Stage I, the lakes expanded to the north, following the retreating ice margin. The south-draining Little River Valley was still occupied by ice. No river terraces formed in the main river valleys during Stage I because the lakes extended to the southern divides of each valley, but lacustrine and ice-contact sediments began to fill the valleys.

The lakes in the eastern Winooski Valley, named by Larsen (1972) for the town nearest the spillway, drained into the White River Valley and eventually into Lake Hitchcock, the proglacial lake that occupied the Connecticut River Valley. The highest of these lakes, Lake Granville in the Mad River Valley, flowed over a threshold at 430 m in the Granville Gulf and the lowest, Lake Williamstown in the Steven Branch Valley, emptied over a 279 m spillway north of the Williamstown Gulf. A previously unnamed Huntington Valley lake, suggested by Bryan (1995) as draining over the southern divide at an elevation of 460 m, would have flowed into Hollock Brook in the Champlain Valley. Following Larsen's criteria for naming Stage I lakes, the name Lake Jerusalem is suggested.

Stage II As the ice withdrew northwestward down the main Winooski Valley, the eastern lakes sequentially coalesced into Lake Winooski (Figure 2.2). Lake Winooski drained south through the 279 m spillway near Williamstown into the Connecticut River Valley. Larsen (1987a) contended that Lake Hitchcock drained when Lake Winooski was in existence based on the presence of longitudinal gravel bars south of the Williamstown spillway.

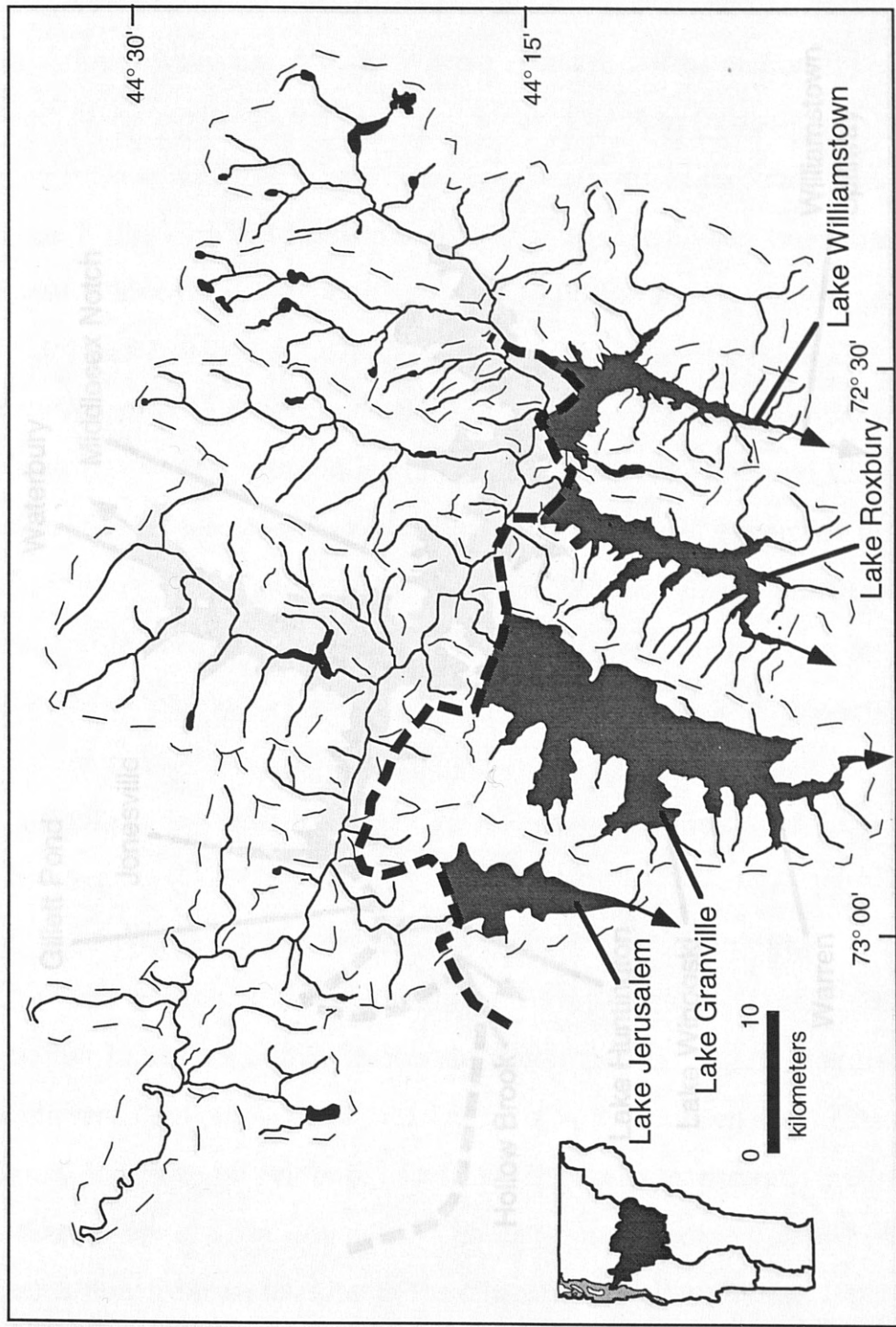


Figure 2.1: Extent of Stage I Lakes in the Winooski Drainage Basin. Proglacial lakes (shaded), controlled by southern spillways (arrows) and bounded by ice to the north (dashed line) formed in north-draining valleys during Stage I. The approximate ice margin is shown for the end of the stage. (After Larsen, 1987b and Valin, 1997). Base from USGS 1:250,000 Lake Champlain Sheet.

The elevation of the gravel bars is below the minimum projected elevation for Lake Hitchcock, implying that these fluvial features developed after this lake had disappeared.

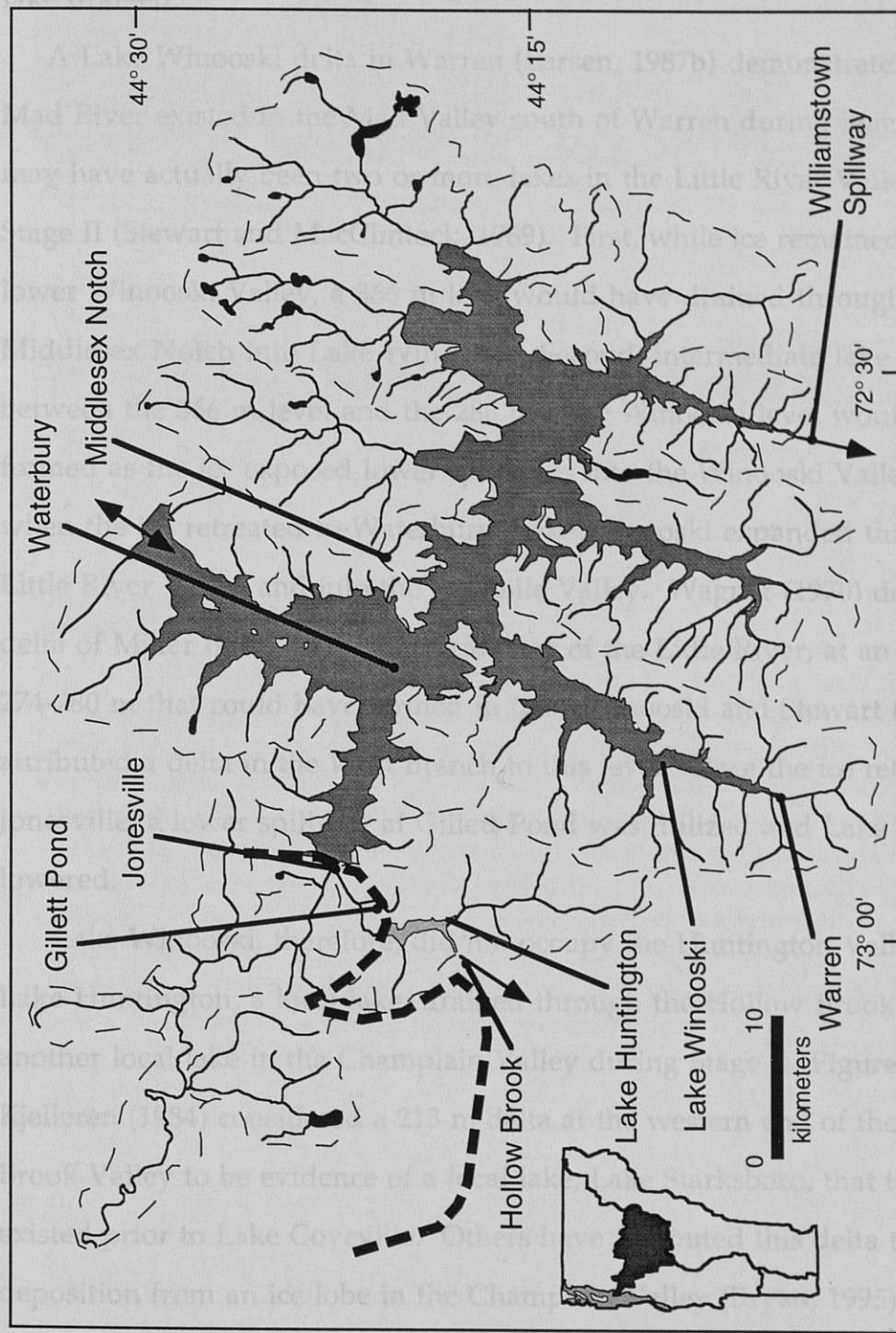


Figure 22: Extent of Stage II Lakes in the Winooski Drainage Basin. Lake Winooski, which drained over the Williamstown Spillway, expanded down the Winooski Valley during Stage II. Lake Huntington utilized the Hollow Brook Spillway. The approximate ice margin (dashed line) is shown for the end of the stage. (After Larsen, 1987b and Valin, 1997). Base from USGS 1:250,000 Lake Champlain Sheet.

The elevation of the gravel bars is below the minimum projected elevation for Lake Hitchcock, implying that these fluvial features developed after that lake drained.

A Lake Winooski delta in Warren (Larsen, 1987b) demonstrates that the Mad River existed in the Mad Valley south of Warren during Stage II. There may have actually been two or more lakes in the Little River Valley during Stage II (Stewart and MacClintock, 1969). First, while ice remained in the lower Winooski Valley, a 366 m lake would have drained through the Middlesex Notch into Lake Winooski. Second, intermediate lake levels between the 366 m level and the 280 m Lake Winooski level would have formed as the ice exposed lower spillways into the Winooski Valley. Finally, when the ice retreated to Waterbury, Lake Winooski expanded through the Little River Valley and into the Lamoille Valley. Wagner (1970) described a delta of Miller Brook, a western tributary of the Little River, at an elevation of 274-280 m that could have formed in Lake Winooski and Stewart (1961) attributed a delta in the West Branch to this level. Once the ice retreated to Jonesville, a lower spillway at Gillett Pond was utilized and Lake Winooski lowered.

Lake Winooski, therefore, did not occupy the Huntington Valley. Instead, Lake Huntington, a local lake, drained through the Hollow Brook Valley into another local lake in the Champlain Valley during Stage II (Figure 2.3). Kjelleren (1984) considered a 213 m delta at the western end of the Hollow Brook Valley to be evidence of a local lake, Lake Starksboro, that temporarily existed prior to Lake Coveville. Others have attributed this delta to deposition from an ice lobe in the Champlain Valley (Bryan, 1995) and to Lake Quaker Springs (Stewart and MacClintock, 1969).

Stage III: Larsen (1987b) named the lakes that drained through the

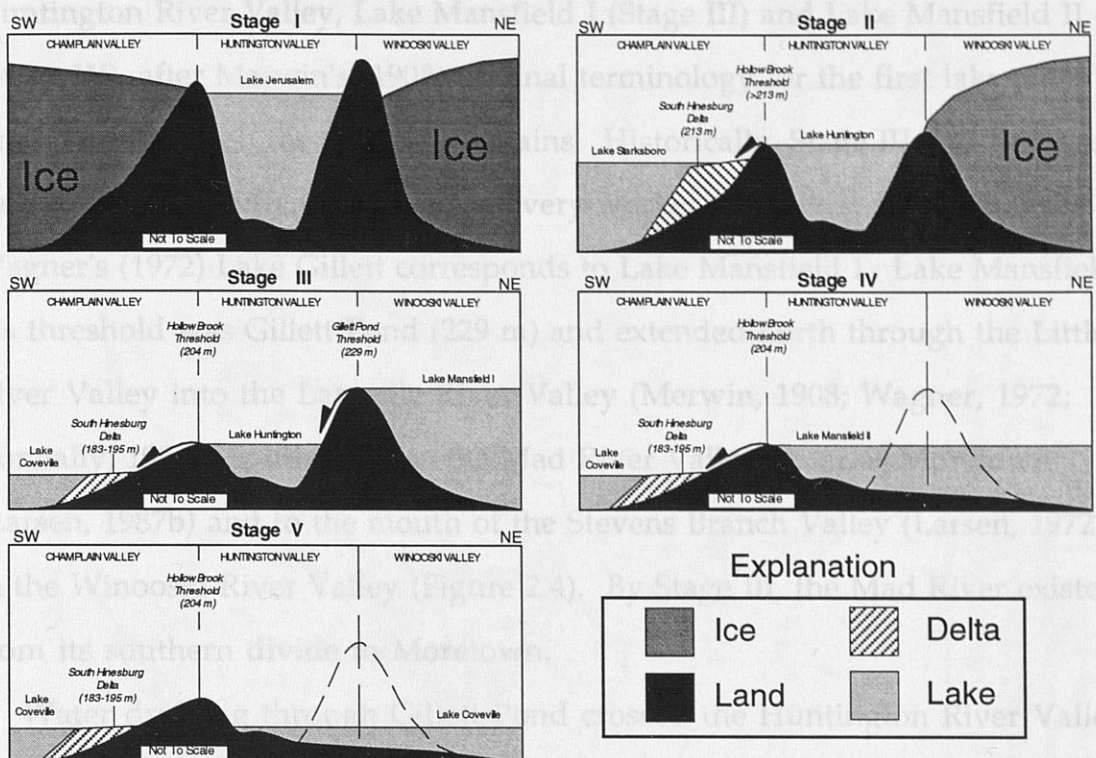


Figure 2.3: Schematic Cross Sections Through the Huntington Valley During Stages I-V. Stage I depicts Lake Jerusalem bounded by ice to the northeast and southwest; its spillway was the southern divide. By Stage II, ice had retreated north of Hollow Brook Valley and Lake Huntington first utilized the spillway there, draining into the local Lake Starksboro. When the Gillett Pond spillway was first free of ice at the beginning of Stage III, Lake Mansfield I emptied into Lake Huntington, and eventually into Lake Coveville in South Hinesburg. Lake Mansfield II extended through the Huntington Valley once the mouth of the Huntington River became ice-free (Stage IV). Finally at Stage V, the ice retreated past the Winooski River and Lake Coveville extended into the Winooski Valley.

threshold (204 m), before reaching the delta in South Hinesburg (figure 2.3).

Because it shares its spillway with later lakes, Lake Huntington has never

been independently documented.

There are other possible pathways for the Lake Mansfield I water to reach Hollow Brook. A remnant ice tongue, filling the present Huntington River Valley just west of Gillett Pond, must have existed during Stage III to

Stage III Larsen (1987b) named the lakes that drained through the Huntington River Valley, Lake Mansfield I (Stage III) and Lake Mansfield II (Stage IV), after Merwin's (1908) original terminology for the first lake to drain west through the Green Mountains. Historically, Stage III and IV lakes have been given different names by every worker (Table 2.1). For instance, Wagner's (1972) Lake Gillett corresponds to Lake Mansfield I. Lake Mansfield I's threshold was Gillett Pond (229 m) and extended north through the Little River Valley into the Lamoille River Valley (Merwin, 1908; Wagner, 1972; Connally, 1972), southeast into the Mad River Valley as far as Moretown (Larsen, 1987b) and to the mouth of the Stevens Branch Valley (Larsen, 1972) in the Winooski River Valley (Figure 2.4). By Stage III, the Mad River existed from its southern divide to Moretown.

Water draining through Gillett Pond crossed the Huntington River Valley and passed through Hollow Brook (threshold at 204 m) before entering the Champlain Valley in South Hinesburg. Since Lake Mansfield I eventually drained through the Hollow Brook Valley, it would be expected that some type of deposit would be present in the main Huntington Valley to link Gillett Pond to one of the deltas in South Hinesburg. As Lake Winooski lowered to the Gillett Pond threshold and during Stage III, the waters may have passed through Lake Huntington, controlled by the Hollow Brook threshold (204 m), before reaching the delta in South Hinesburg (Figure 2.3). Because it shares its spillway with later lakes, Lake Huntington has never been independently documented.

There are other possible pathways for the Lake Mansfield I water to reach Hollow Brook. A remnant ice tongue, filling the present Huntington River Valley just west of Gillett Pond, must have existed during Stage III to

maintain the Gillett threshold. It is possible that this ice extended south to near the Hollow Brook Valley, providing the waters with a supraglacial route

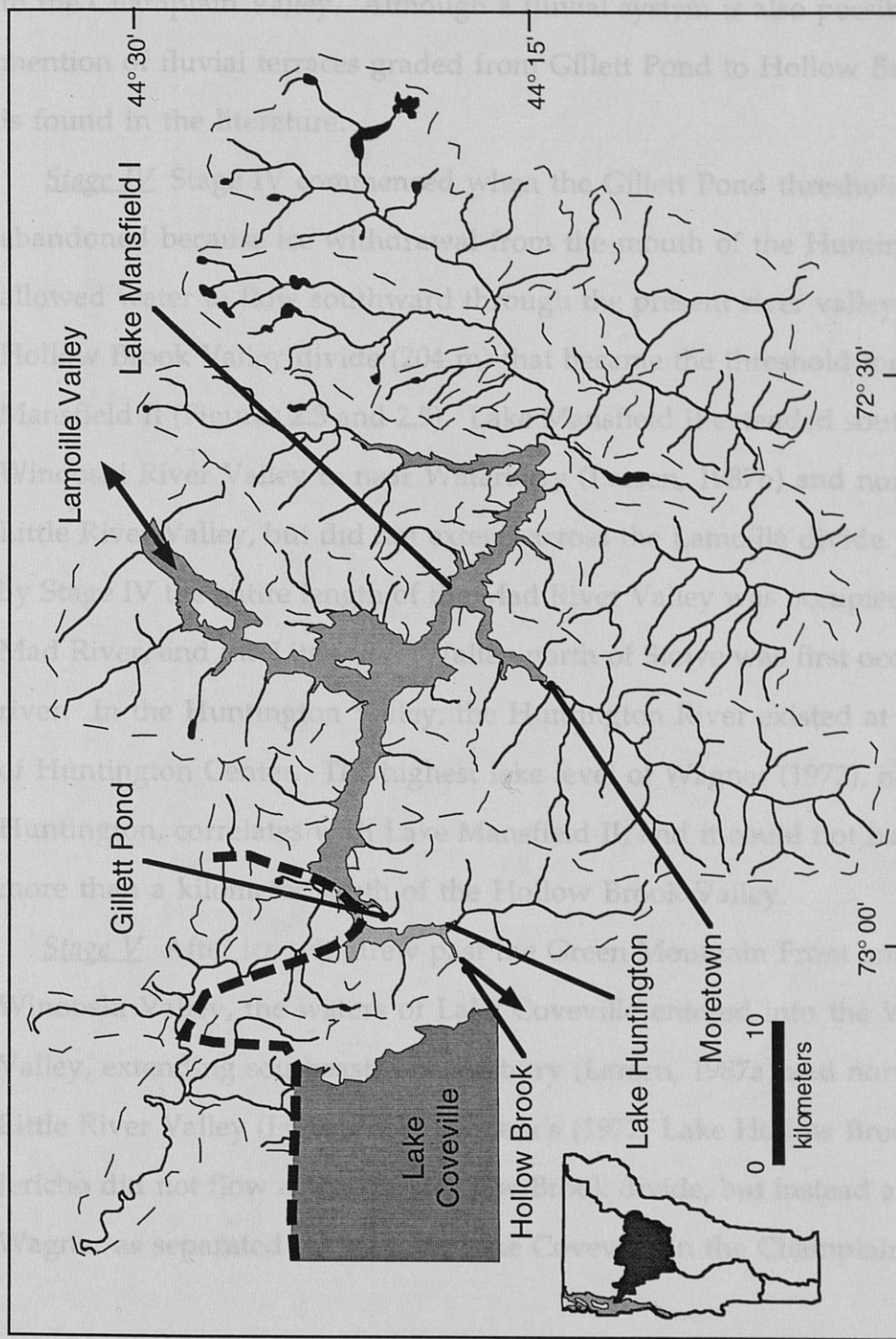


Figure 2.4: Extent of Stage III Lakes in the Winooski Drainage Basin. Lake Mansfield I drained into the Huntington Valley through the Gillett Pond spillway. The water in the Huntington Valley then drained through Hollow Brook into Lake Champlain. The approximate ice margin (dashed line) is shown for the end of the stage. (After Larsen, 1987b and Valin, 1997). Base from USGS 1:250,000 Lake Champlain Sheet.

maintain the Gillett threshold. It is possible that this ice extended south to near the Hollow Brook Valley, providing the waters with a supraglacial route to the Champlain Valley. Although a fluvial system is also possible, no mention of fluvial terraces graded from Gillett Pond to Hollow Brook Valley is found in the literature.

Stage IV Stage IV commenced when the Gillett Pond threshold was abandoned because ice withdrawal from the mouth of the Huntington River allowed water to flow southward through the present river valley to the Hollow Brook Valley divide (204 m) that became the threshold for Lake Mansfield II (Figures 2.3 and 2.5). Lake Mansfield II extended southeast in the Winooski River Valley to near Waterbury (Larsen, 1987b) and north into the Little River Valley, but did not extend across the Lamoille divide. Therefore, by Stage IV the entire length of the Mad River Valley was occupied by the Mad River, and the Little River Valley north of Stowe was first occupied by a river. In the Huntington Valley, the Huntington River existed at least south of Huntington Center. The highest lake level of Wagner (1972), named Lake Huntington, correlates with Lake Mansfield II, and it could not have extended more than a kilometer south of the Hollow Brook Valley.

Stage V After ice withdrew past the Green Mountain Front and out of the Winooski Valley, the waters of Lake Coveville entered into the Winooski Valley, extending southeast to Waterbury (Larsen, 1987a) and north into the Little River Valley (Figure 2.6). Wagner's (1972) Lake Hollow Brook and Lake Jericho did not flow across the Hollow Brook divide, but instead are shown by Wagner as separated by ice from Lake Coveville in the Champlain Valley.

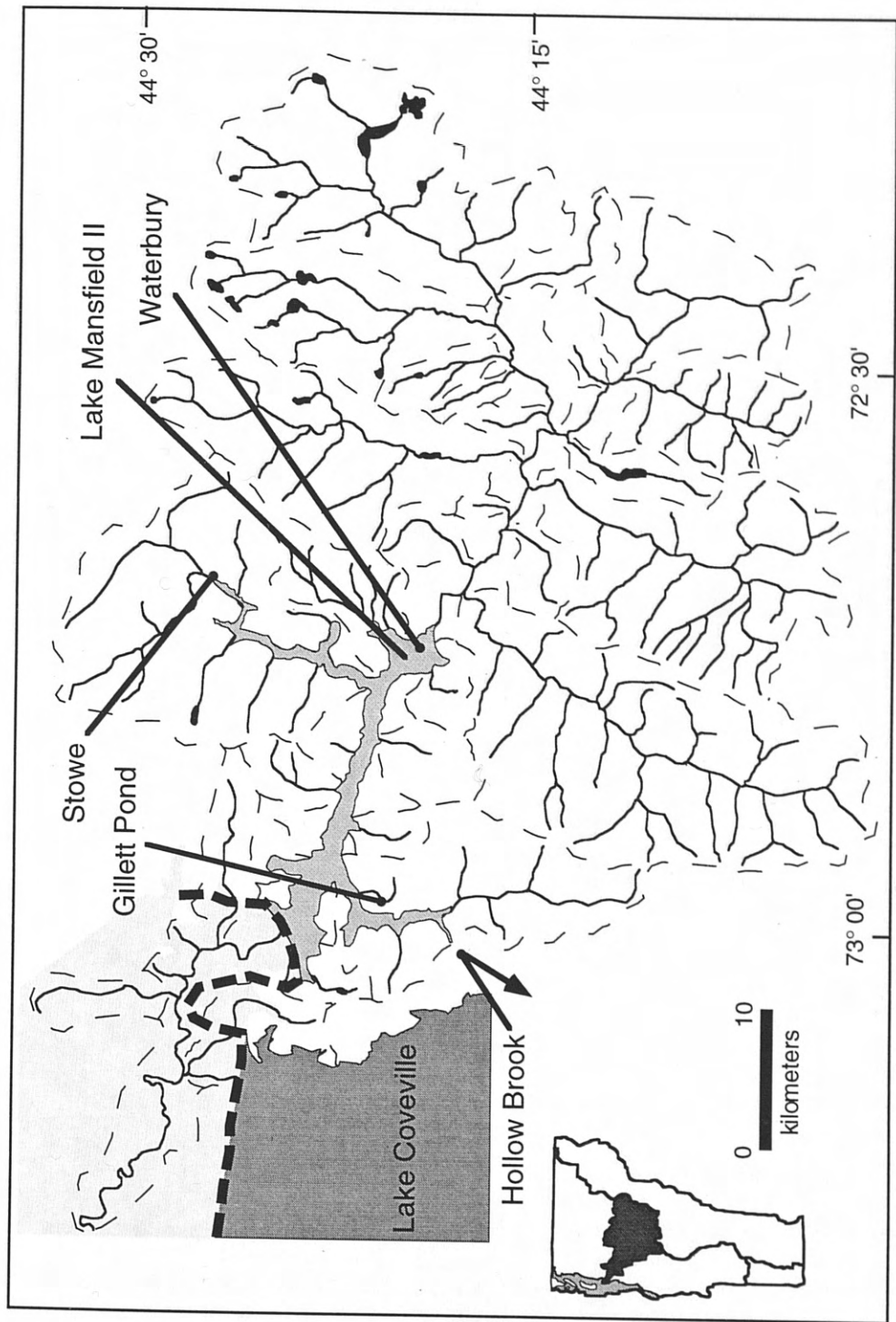


Figure 2.5: Extent of Stage IV Lakes in the Winooski Drainage Basin. The ice retreated past the Huntington Valley mouth, and Lake Mansfield II then drained through Hollow Brook. The approximate ice margin (dashed line) is shown for the end of the stage. (After Larsen, 1987b and Valin, 1997). Base from USGS 1:250,000 Lake Champlain Sheet.

Because the elevations of Lakes Hollow Brook and Jericho are similar to the elevation of Lake Champlain, they may have been part of the same sheet.

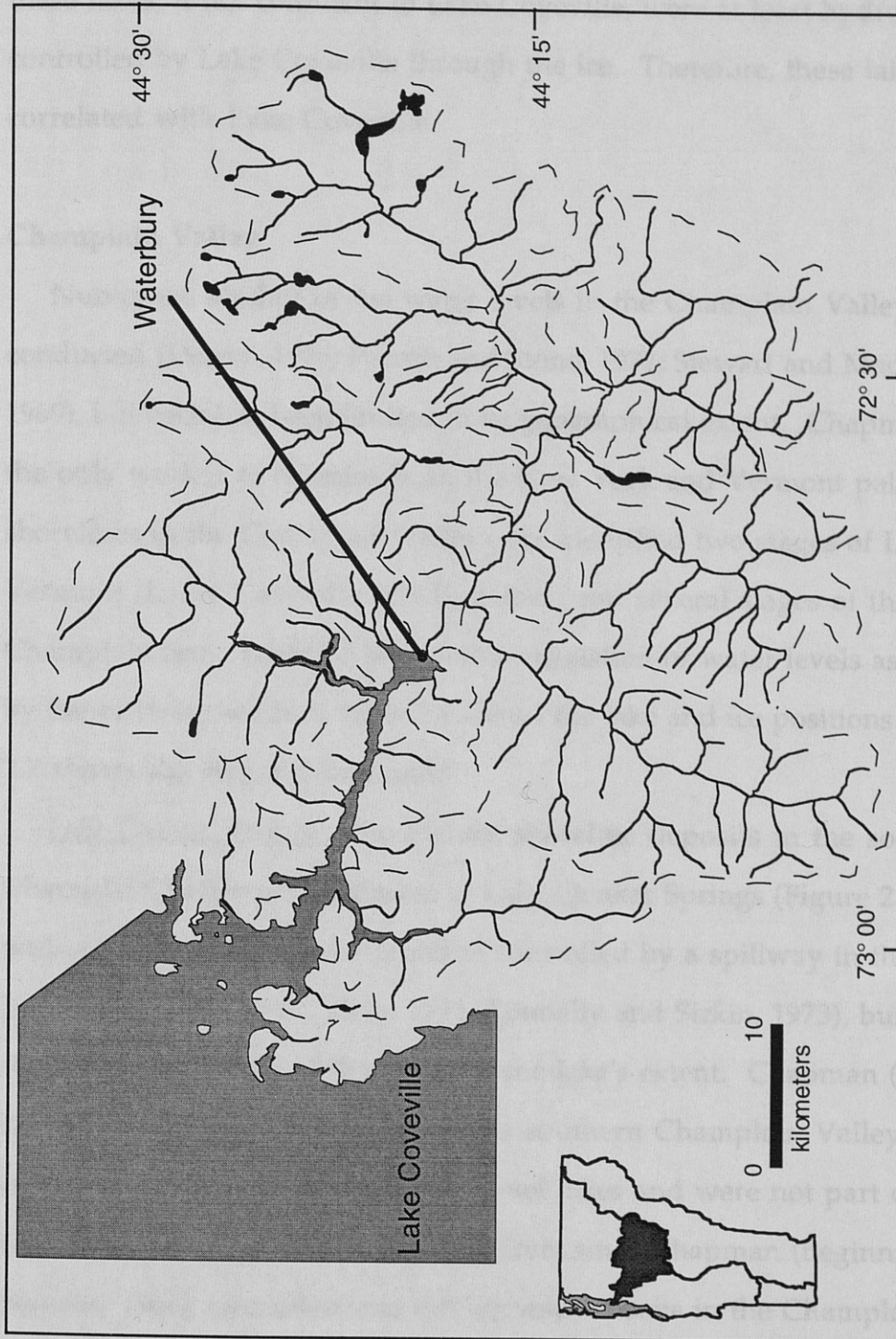


Figure 2.6: Extent of Stage V Lakes in the Winooski Drainage Basin. Once ice moved from the Green Mountain Front, Lake Coveville expanded into the Winooski Basin and the Hollow Brookspillway was abandoned. The approximate ice margin (dashed line) is shown for the end of the stage. (After Larsen, 1987b and Valin, 1997). Base from USGS 1:250,000 Lake Champlain Sheet.

Because the elevations of Lakes Hollow Brook and Jericho are similar to the elevation of Lake Coveville (Chapman, 1937) at the Green Mountain Front, these lakes, if not confluent to Lake Coveville, were at least hydrologically controlled by Lake Coveville through the ice. Therefore, these lakes are correlated with Lake Coveville.

Champlain Valley

Numerous studies of the water levels in the Champlain Valley have been conducted (Denny, 1974; Parrott and Stone, 1972; Stewart and MacClintock, 1969), but each has been limited in its geographical extent. Chapman (1937) is the only worker to examine both the New York and Vermont paleo-shorelines in the Champlain Valley. He identified two stages of Lake Vermont (Lakes Coveville and Fort Ann) and several stages of the Champlain Sea. Table 2.3 shows the correlation of water levels as identified by the different studies, Table 2.4 shows the lake and ice positions and Figure 2.7 shows the regional moraines.

Lake Quaker Springs The highest shoreline deposits in the southern Champlain Valley are attributed to Lake Quaker Springs (Figure 2.8), a lake with a northern limit near Brandon controlled by a spillway in the Hudson Valley (Connally and Calkin, 1972; Connally and Sirkin, 1973), but historically there has been some confusion as to the lake's extent. Chapman (1937) thought the highest shorelines in the southern Champlain Valley were constructed along individual, high-level lakes and were not part of the same regional lake. However, several workers since Chapman (beginning with Stewart, 1961) concluded that the highest deposits in the Champlain Valley were associated with an extensive lake, Lake Quaker Springs. Stewart and

Table 2.3: Champlain Valley Water Level Correlations

	Stewart and MacClintock, 1969	Connally and Sirkin, 1973	Denny, 1974	Clark and Karrow, 1984	DiSimone and LaFleur, 1985	This Study	Elevation *
High Local Lakes	Quaker Springs Stage	Lake Quaker Springs	-	-	Lake Quaker Springs	Lake Quaker Springs	-
Coveville Stage	Coveville Stage	Lake Coveville	Coveville Stage	-	Lake Coveville	Lake Coveville	Shoreline at 195 m at North Williston Hill
Fort Ann Stage	Fort Ann Stage	Fort Ann	Fort Ann Stage	Upper Fort Ann	Fort Ann I	Lake Fort Ann I	Delta at 152 m in Richmond
Fort Ann Stage	Fort Ann Stage	Fort Ann	Fort Ann Stage	Upper Fort Ann	Fort Ann II	Lake Fort Ann I	Delta at 152 m in Richmond
Fort Ann Stage	Fort Ann Stage	Fort Ann	Fort Ann Stage	Lower Fort Ann	Fort Ann III	Lake Fort Ann II	132 m in Richmond **
Upper Marine	Champlain Sea	Champlain Sea	Champlain Sea	Champlain Sea	Champlain Sea	Upper Marine	Delta at 104 m in Essex

* Elevations measured by Chapman (1937), except ** estimated from Clark and Karrow (1984).

Table 2.4: Champlain Valley Water Levels and Ice Positions

Water Level	Threshold	Ice Position	Winooski Valley Extent
Lake Quaker Springs	Across Hudson Divide	Brandon	
Lake Coveville	Across Hudson Divide	Lamoille Valley	Waterbury
Lake Fort Ann I	Fort Edward	International Border?	Richmond
Lake Fort Ann II	Fort Edward	Highland Front Moraine	Richmond
Upper Marine	Sea Level	St. Narcisse Moraine	Essex

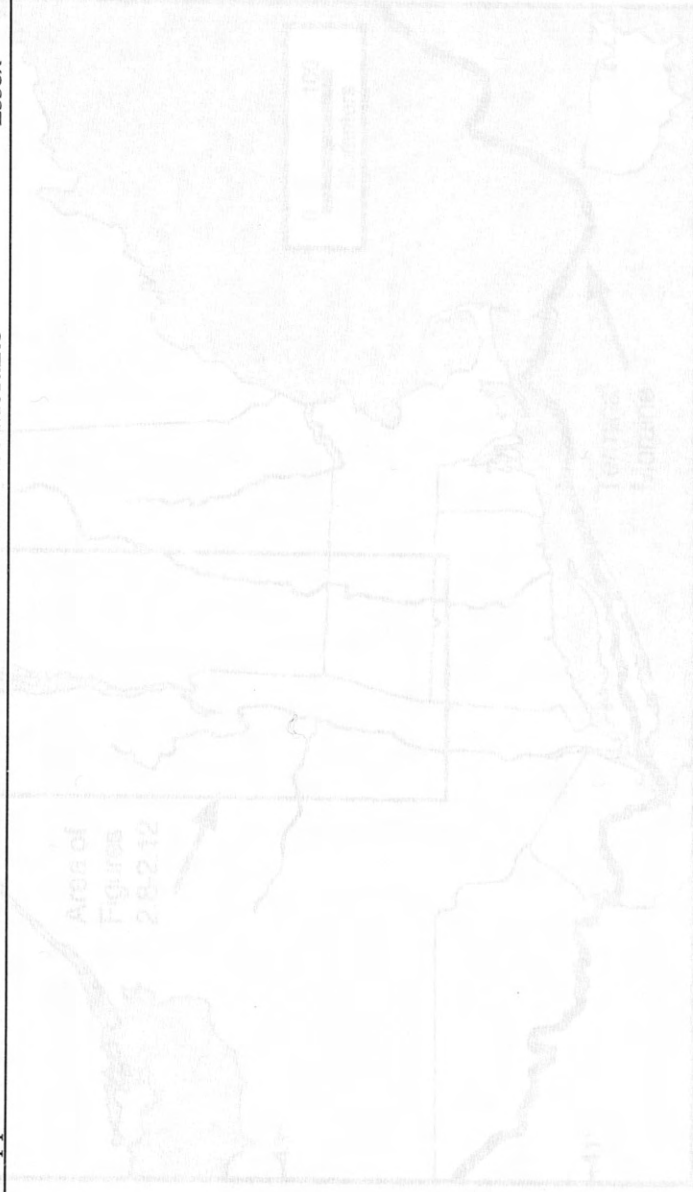


Figure 2.7. Location of Major Moraines in the Northeast. The Terrianal Mounain defines the basin margin of the Laurentide ice sheet about 18,000 yr B.P. The Highland Front Moraine marks the maximum extent Lake Fort Ann, 12,000 yr B.P., and the Saint-Narcisse Moraine delineates the highstand during the pre-lake phase of the Champlain Sea (11,700-10,800 yr B.P.).

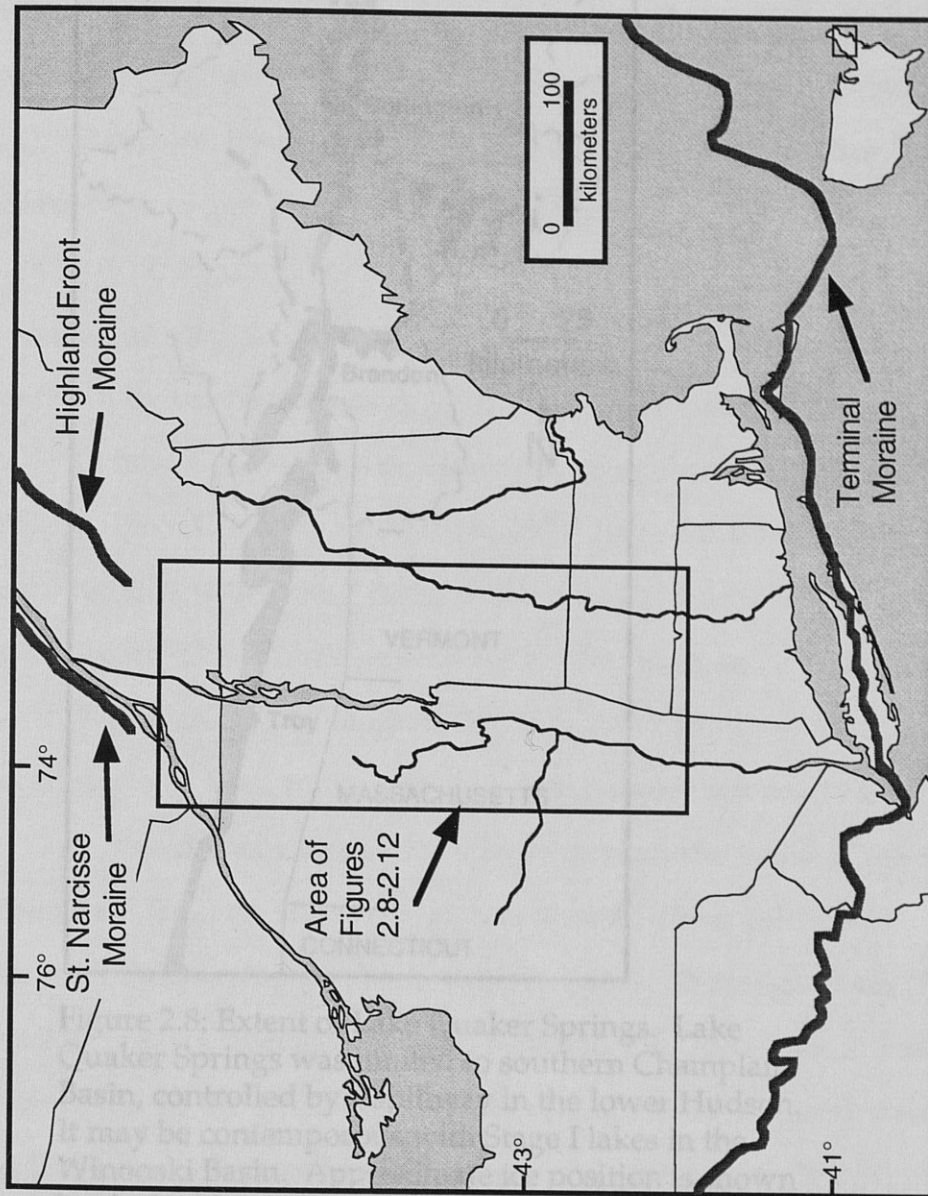
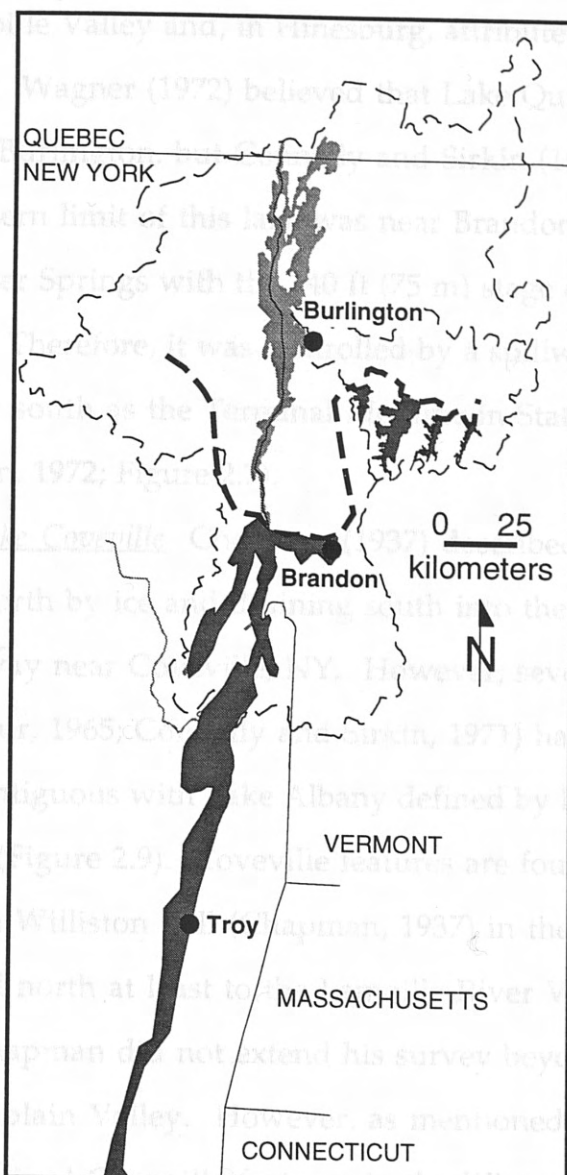


Figure 2.7: Location of Major Moraines in the Northeast. The Terminal Moraine delineates the maximum extent of the Laurentide ice sheet about 18,000 ^{14}C yr B.P. The Highland Front Moraine marks the northern extent Lake Fort Ann, 12,600 ^{14}C yr B.P., and the Saint Narcisse Moraine delineates the ice position during the Upper Marine Phase of the Champlain Sea (11,700-10,800 ^{14}C yr B.P.).

MacClintock (1969) described Lake Quaker Springs features as far north as the Lamoille Valley and, in Ciresburg, arranged a delta at 213 m to this lake level. Wagner (1972) believed that Lake Quaker Springs extended north to near Brandon, Vermont. Connally and Sirk (1973) later claimed that the northern limit of this lake was near Brandon. LaFleur (1965) correlated Lake Quaker Springs with the 190 ft (57 m) stage of Lake Albany (elevation in Troy, NY). Therefore, it was bounded by a spillway in the Hudson Valley, possibly as far south as the Bronx Kill in Staten Island, NY (Connally and Calkin, 1972; Figure 2.8).



Lake Coveville (Figure 2.9) has been placed Lake Coveville as rounded to the north by ice and flowing south into the Hudson Valley through a pathway near Coey Hill, NY. However, several workers since Chapman (e.g., LaFleur, 1965; Connally and Sirk, 1973) have considered Lake Coveville to be contiguous with Lake Albany defined by LaFleur (1965) as 180 ft (55 m) in Troy (Figure 2.9). Coveville features are found at an elevation of 195 m at North Williston (Chapman, 1937) in the Burlington area, and can be traced north at least to the lower Hudson Valley (Connally and Sirk, 1973). Chapman did not extend his survey beyond the walls of the main Champlain Valley; however, as mentioned before, other workers have incorporated Lake Coveville into the Champlain Drainage Basin (Figures 2.6 and 2.7).

Figure 2.8: Extent of Lake Quaker Springs. Lake Quaker Springs was limited to southern Champlain Basin, controlled by a spillway in the lower Hudson. It may be contemporaneous with Stage I lakes in the Winooski Basin. Approximate ice position is shown by dashed line. (After Connally and Sirk, 1973).

MacClintock (1969) described Lake Quaker Springs features as far north as the Lamoille Valley and, in Hinesburg, attributed a delta at 213 m to this lake level. Wagner (1972) believed that Lake Quaker Springs extended north to near Burlington, but Connally and Sirkin (1973) later claimed that the northern limit of this lake was near Brandon. LaFleur (1965) correlated Lake Quaker Springs with the 240 ft (75 m) stage of Lake Albany (elevation in Troy, NY). Therefore, it was controlled by a spillway in the Hudson Valley, possibly as far south as the Terminal Moraine in Staten Island, NY (Connally and Calkin, 1972; Figure 2.7).

Lake Coveville Chapman (1937) described Lake Coveville as bounded to the north by ice and draining south into the Hudson Valley through a spillway near Coveville, NY. However, several workers since Chapman (e.g., LaFleur, 1965; Connally and Sirkin, 1971) have considered Lake Coveville to be contiguous with Lake Albany defined by LaFleur (1965) as 180 ft (55 m) in Troy (Figure 2.9). Coveville features are found at an elevation of 195 m at North Williston Hill (Chapman, 1937) in the Burlington area, and can be traced north at least to the Lamoille River Valley (Connally and Sirkin, 1973).

Chapman did not extend his survey beyond the walls of the main Champlain Valley. However, as mentioned before, other workers have recognized Coveville features in the Winooski Drainage Basin (Figures 2.6 and 2.9). Lake Coveville (Stage V) reportedly extended southward to Huntington in the Huntington Valley (Wagner, 1972), northward to Stowe in the Little River Valley (Merwin, 1908), and eastward to Waterbury in the Winooski Valley (Larsen 1987a).

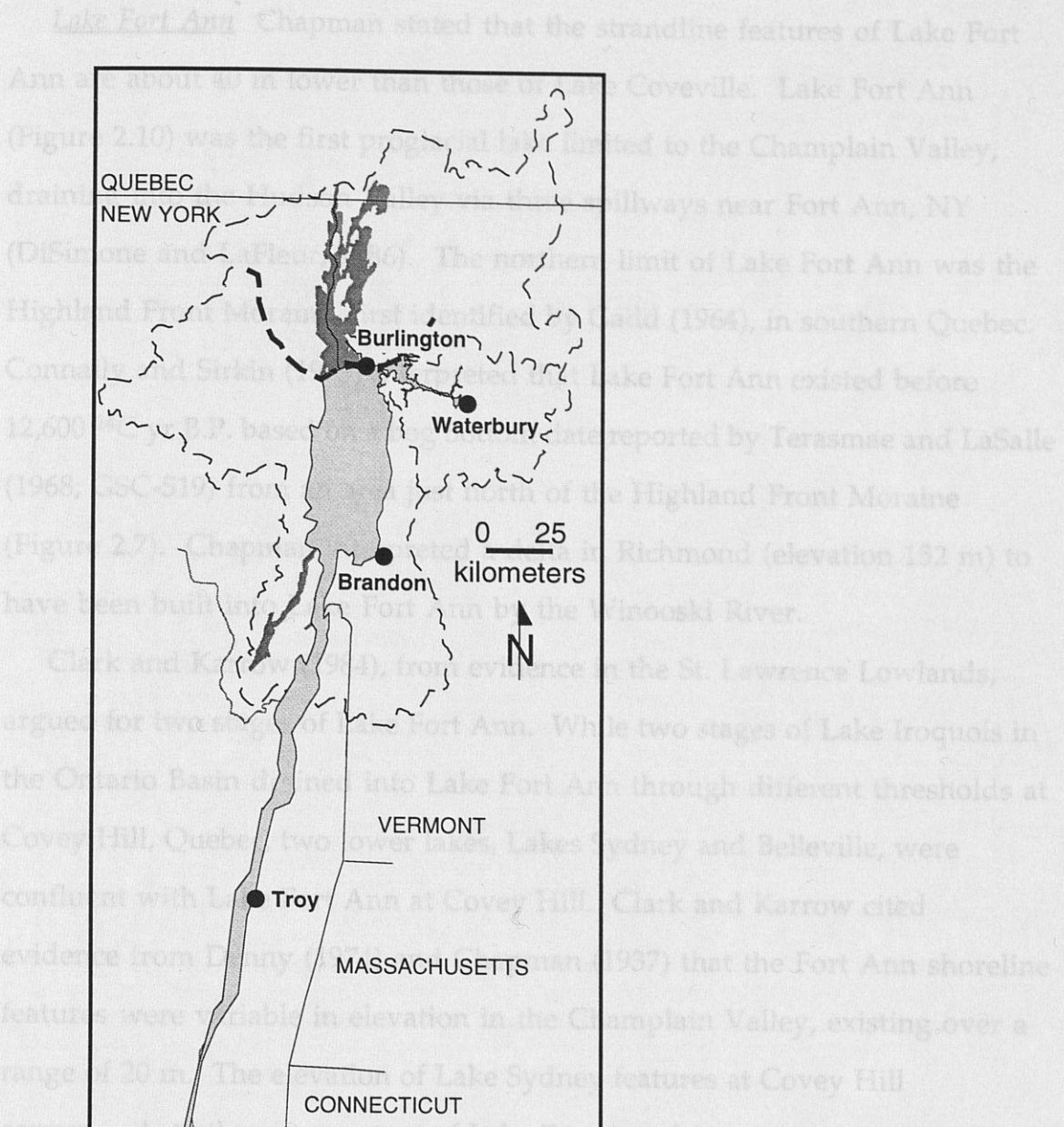


Figure 2.9: Extent of Lake Coveville. Lake Coveville was controlled by a spillway in the Hudson Valley south of Troy. Approximate ice position (dashed line) is shown during Stage V in the Winooski Basin. (After Lake Chapman, 1937 and Connally and Sirkin, 1973).

Lake Fort Ann Chapman stated that the strandline features of Lake Fort Ann are about 40 m lower than those of Lake Coveville. Lake Fort Ann (Figure 2.10) was the first proglacial lake limited to the Champlain Valley, draining into the Hudson Valley via three spillways near Fort Ann, NY (DiSimone and LaFleur, 1986). The northern limit of Lake Fort Ann was the Highland Front Moraine, first identified by Gadd (1964), in southern Quebec. Connally and Sirkin (1973) interpreted that Lake Fort Ann existed before 12,600 ^{14}C yr B.P. based on a bog bottom date reported by Terasmae and LaSalle (1968; GSC-519) from an area just north of the Highland Front Moraine (Figure 2.7). Chapman interpreted a delta in Richmond (elevation 152 m) to have been built into Lake Fort Ann by the Winooski River.

Clark and Karrow (1984), from evidence in the St. Lawrence Lowlands, argued for two stages of Lake Fort Ann. While two stages of Lake Iroquois in the Ontario Basin drained into Lake Fort Ann through different thresholds at Covey Hill, Quebec, two lower lakes, Lakes Sydney and Belleville, were confluent with Lake Fort Ann at Covey Hill. Clark and Karrow cited evidence from Denny (1974) and Chapman (1937) that the Fort Ann shoreline features were variable in elevation in the Champlain Valley, existing over a range of 20 m. The elevation of Lake Sydney features at Covey Hill corresponds to the upper extent of Lake Fort Ann features cited by Denny and Chapman and the elevation of Lake Belleville features corresponds with the lower limit of the features, implying that there were two distinct levels of Lake Fort Ann. The next highest shoreline examined by Clark and Karrow correlates with the highest extent of the Champlain Sea in both the Ontario and Champlain Basins.

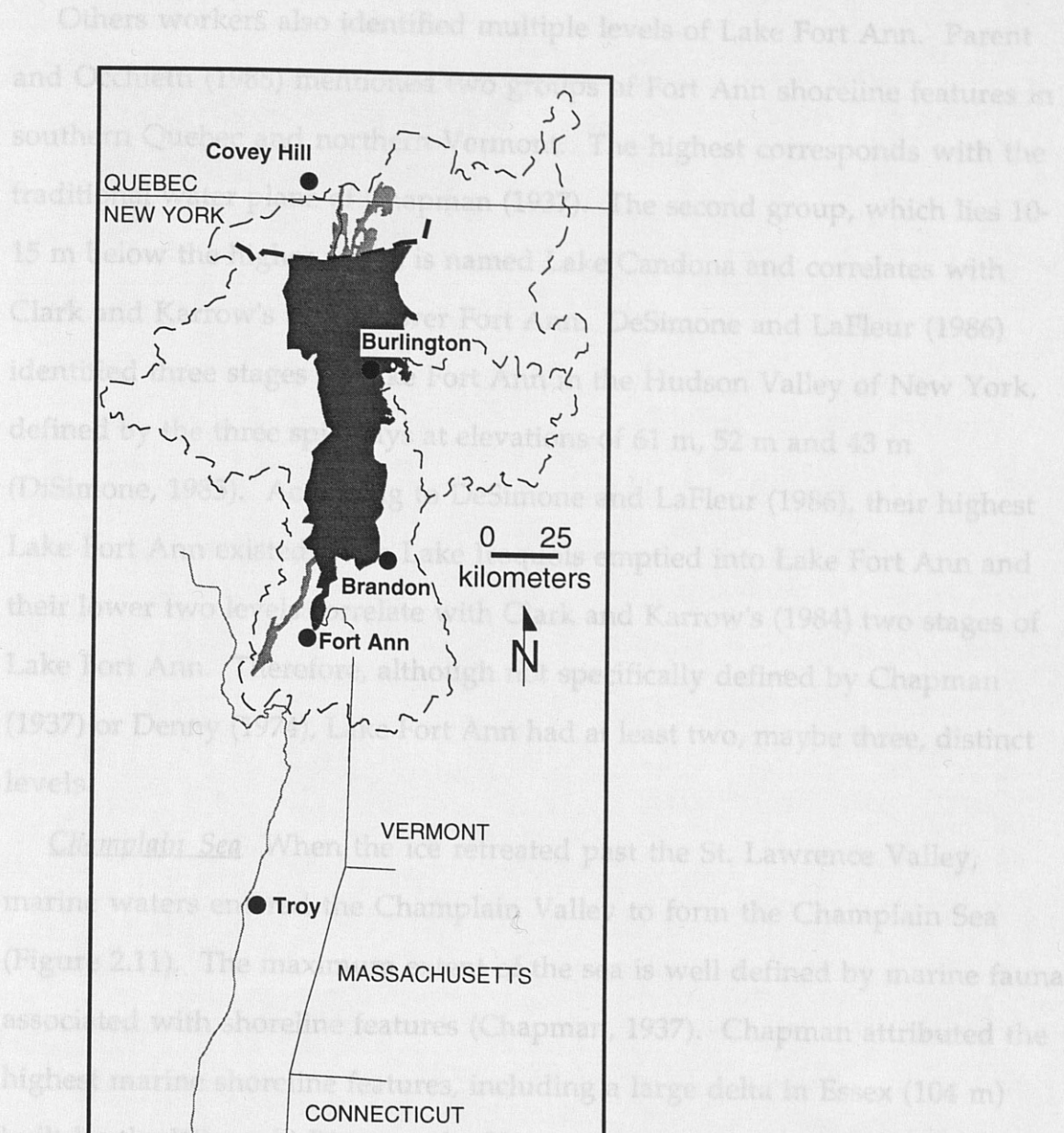


Figure 2.10: Extent of Lake Fort Ann I. Fort Ann I was the first lake to be controlled by a spillway within the Champlain Basin. It existed until the ice retreated past the international border at which point in time the lakes in the Ontario Basin became confluent with Champlain Basin waters. (After Chapman, 1937).

Others workers also identified multiple levels of Lake Fort Ann. Parent and Occhietti (1988) mentioned two groups of Fort Ann shoreline features in southern Quebec and northern Vermont. The highest corresponds with the traditional water plane of Chapman (1937). The second group, which lies 10-15 m below the higher plane, is named Lake Candona and correlates with Clark and Karrow's (1984) lower Fort Ann. DeSimone and LaFleur (1986) identified three stages of Lake Fort Ann in the Hudson Valley of New York, defined by the three spillways at elevations of 61 m, 52 m and 43 m (DiSimone, 1985). According to DeSimone and LaFleur (1986), their highest Lake Fort Ann existed when Lake Iroquois emptied into Lake Fort Ann and their lower two levels correlate with Clark and Karrow's (1984) two stages of Lake Fort Ann. Therefore, although not specifically defined by Chapman (1937) or Denny (1974), Lake Fort Ann had at least two, maybe three, distinct levels.

Champlain Sea When the ice retreated past the St. Lawrence Valley, marine waters entered the Champlain Valley to form the Champlain Sea (Figure 2.11). The maximum extent of the sea is well defined by marine fauna associated with shoreline features (Chapman, 1937). Chapman attributed the highest marine shoreline features, including a large delta in Essex (104 m) built by the Winooski River, to the Upper Marine stage of the Champlain Sea. Additional sets of water-line features were cut and deposited as the sea withdrew from the Champlain Valley.

Parent and Occhietti (1988) describe a three phase evolution of the Champlain Sea based on the timing of ice retreat. Phase I existed to the northeast of the Champlain Valley, in the mouth of the St. Lawrence, and was separated from Lake Fort Ann by ice. When the ice retreated from the

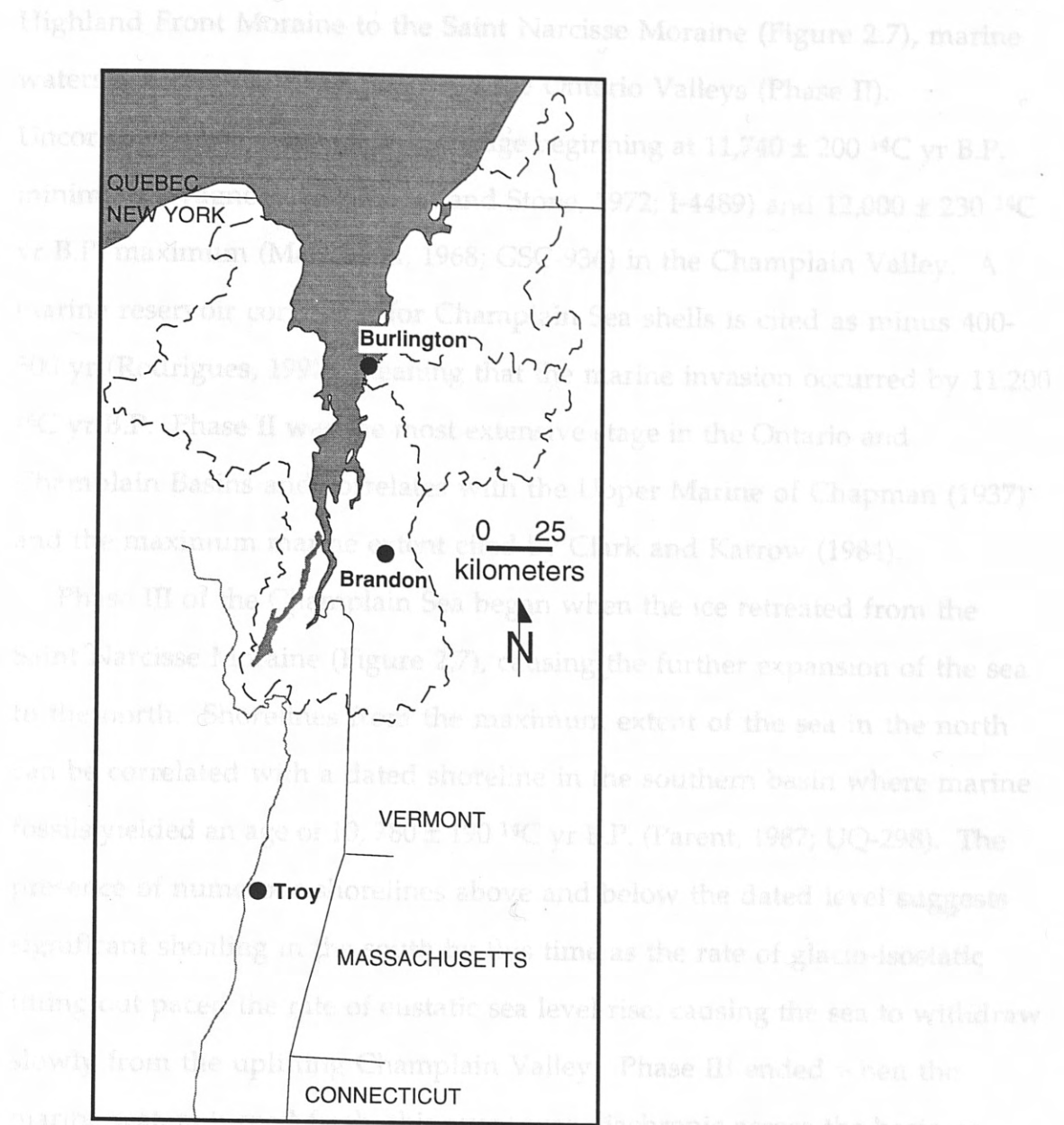


Figure 2.11: Extent of Upper Marine. The Upper Marine represents the farthest extent of Champlain Sea waters into the Champlain Basin. (After Chapman, 1937).

Lake Champlain Chapman noted that the marine interval ended when the present day threshold of the Richelieu River rose, due to glacio-isostatic rebound, above the level of the Champlain Sea. Lake Champlain's present

Highland Front Moraine to the Saint Narcisse Moraine (Figure 2.7), marine waters invaded the Champlain and the Ontario Valleys (Phase II). Uncorrected shell dates place this stage beginning at $11,740 \pm 200$ ^{14}C yr B.P. minimum (Wagner, 1972; Parrot and Stone, 1972; I-4489) and $12,000 \pm 230$ ^{14}C yr B.P. maximum (McDonald, 1968; GSC-936) in the Champlain Valley. A marine reservoir correction for Champlain Sea shells is cited as minus 400-500 yr (Rodrigues, 1992), meaning that the marine invasion occurred by $11,200$ ^{14}C yr B.P. Phase II was the most extensive stage in the Ontario and Champlain Basins and correlates with the Upper Marine of Chapman (1937) and the maximum marine extent cited by Clark and Karrow (1984).

Phase III of the Champlain Sea began when the ice retreated from the Saint Narcisse Moraine (Figure 2.7), causing the further expansion of the sea to the north. Shorelines from the maximum extent of the sea in the north can be correlated with a dated shoreline in the southern basin where marine fossils yielded an age of $10,780 \pm 190$ ^{14}C yr B.P. (Parent, 1987; UQ-298). The presence of numerous shorelines above and below the dated level suggests significant shoaling in the south by this time as the rate of glacio-isostatic tilting outpaced the rate of eustatic sea level rise, causing the sea to withdraw slowly from the uplifting Champlain Valley. Phase III ended when the marine waters turned fresh; this event was diachronic across the basin as evident by the numerous radiocarbon dates cited by Parent and Occhietti ranging from $10,300$ ^{14}C yr B.P. near Ottawa to $9,300$ ^{14}C yr B.P. near Quebec City.

Lake Champlain Chapman noted that the marine interval ended when the present day threshold of the Richelieu River rose, due to glacio-isostatic rebound, above the level of the Champlain Sea. Lake Champlain's present

average elevation is 29 m above sea level (Figure 2.12), but evidence suggests that today's elevation is higher than it was in the past (Chapman, 1937; Howard and Woods, 1976; Bay, 1991).

Geomorphic evidence in the south (Howard and Woods, 1976; Bay, 1991) and lack of deltas, has been attributed to a higher sea level (see Meeks, 1986).

Chapman (1937) described the southern end of the lake (from Whitehall to Port Henry, NY) as a drowned valley of a wandering river. Northeast of Port Henry, the drowned valley ends at a submerged delta, elevation 15 m above sea level. The lake bottom is 14 m below today's lake level. It was noted by Chapman that the southern lake has experienced significant shoreline regression. The northern lake also has experienced a regression, but it was of a lower magnitude. Recent work in Alburg (Astley, 1992) documents a transgression on the order of 8 m has occurred in the past 3,000-4,000 yrs. Differential uplift, where land to the north rises higher than the land to the south, is one of the only ways to have different magnitudes of level changes in the northern and southern parts of the lake.

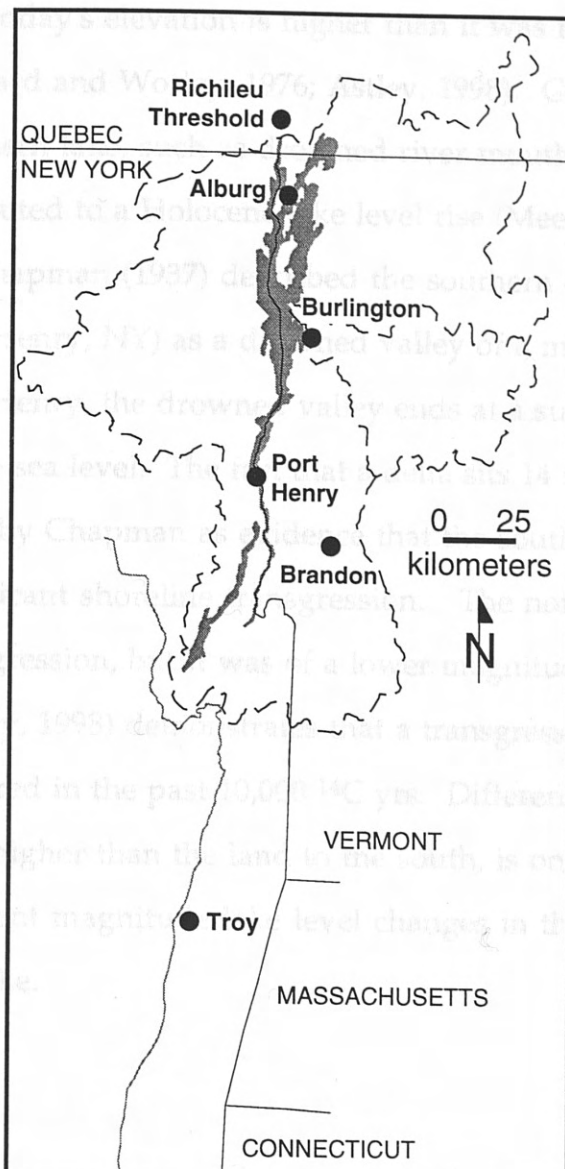


Figure 2.12: Extent of Lake Champlain. Drainage boundary after Vermont State Planning Office maps. Base map from Connally and Sirkin (1973).

average elevation is 29 m above sea level (Figure 2.12), but evidence suggests that today's elevation is higher than it was in the past (Chapman, 1937; Howard and Worley, 1976; Astley, 1998). Geomorphic evidence in the southern lake, such as drowned river mouths and lack of deltas, has been attributed to a Holocene lake level rise (Meeks, 1986).

Chapman (1937) described the southern end of the lake (from Whitehall to Port Henry, NY) as a drowned valley of a meandering river. Northeast of Port Henry, the drowned valley ends at a submerged delta, elevation 15 m above sea level. The fact that a delta sits 14 m below today's lake level was cited by Chapman as evidence that the southern lake has experienced significant shoreline transgression. The northern lake also has experienced a transgression, but it was of a lower magnitude. Recent work in Albion (Astley, 1998) demonstrates that a transgression on the order of 8 m has occurred in the past 10,000 ^{14}C yrs. Differential uplift, where land to the north rises higher than the land to the south, is one of the only ways to have different magnitude lake level changes in the northern and southern parts of the lake.

Summary

The deglacial record of the Winooski and Champlain Drainage Basins is one of lowering proglacial lake levels. Figures 2.13 and 2.14 illustrate the temporal and spatial relations of the water bodies occupying northern Vermont and surrounding areas. Due to the time-transgressive manner of ice retreat and lake histories, the histories of the southern and northern portions of the Champlain Basin are shown separately. In the Winooski Drainage Basin, the lakes lowered in five stages as the ice retreated northwestward down-valley and lower spillways progressively opened. As the lakes lowered, river incision was initiated. After the ice retreated from the Green Mountain Front, the lakes in the Winooski Valley were directly connected to the Champlain Valley. The mouth of the Winooski River migrated westward as the Champlain Valley lakes lowered and the sea invaded. Finally, Lake Champlain was established when the threshold at Richileu separated the basin from the ocean. Table 2.5 reports the timing and elevations of baselevel controls specific to the Winooski Valley.

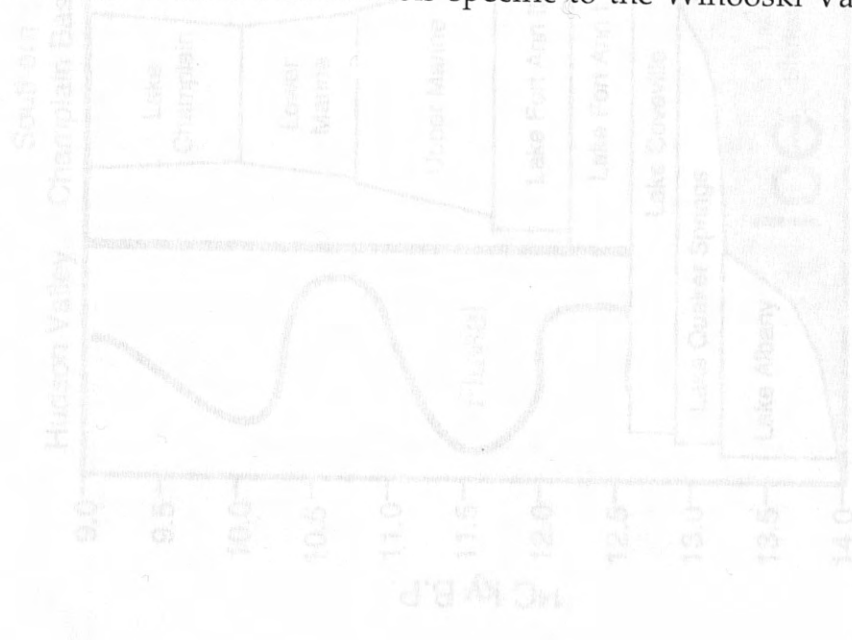


Figure 2.13: Correlation Diagram of Deglacial lake levels showing the spatial and temporal extent of proglacial lakes in the Southern Champlain Basin. Various lakes are presented in Table 2.5.

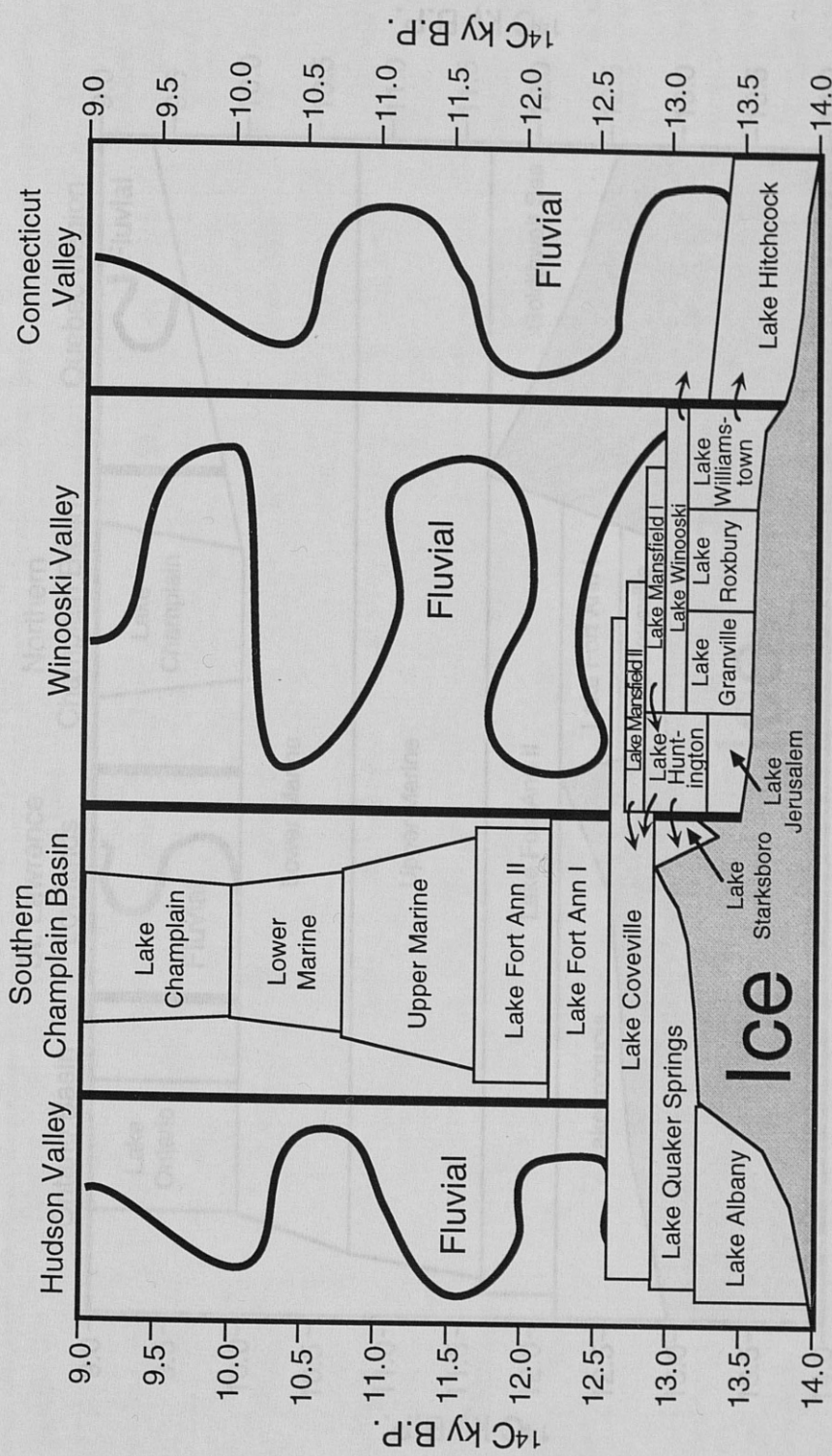


Figure 2.13: Correlation Diagram of Deglacial Events within the Southern Champlain Valley. Shown are the spatial and temporal extent of post-glacial water bodies in an approximate transect across the Southern Champlain Basin. Width of boxes indicate relative size of water bodies. Radiocarbon dates are presented in Table 2.5.

Table 2.14: Correlation Diagram of Deglacial Events within the Northern Champlain Valley

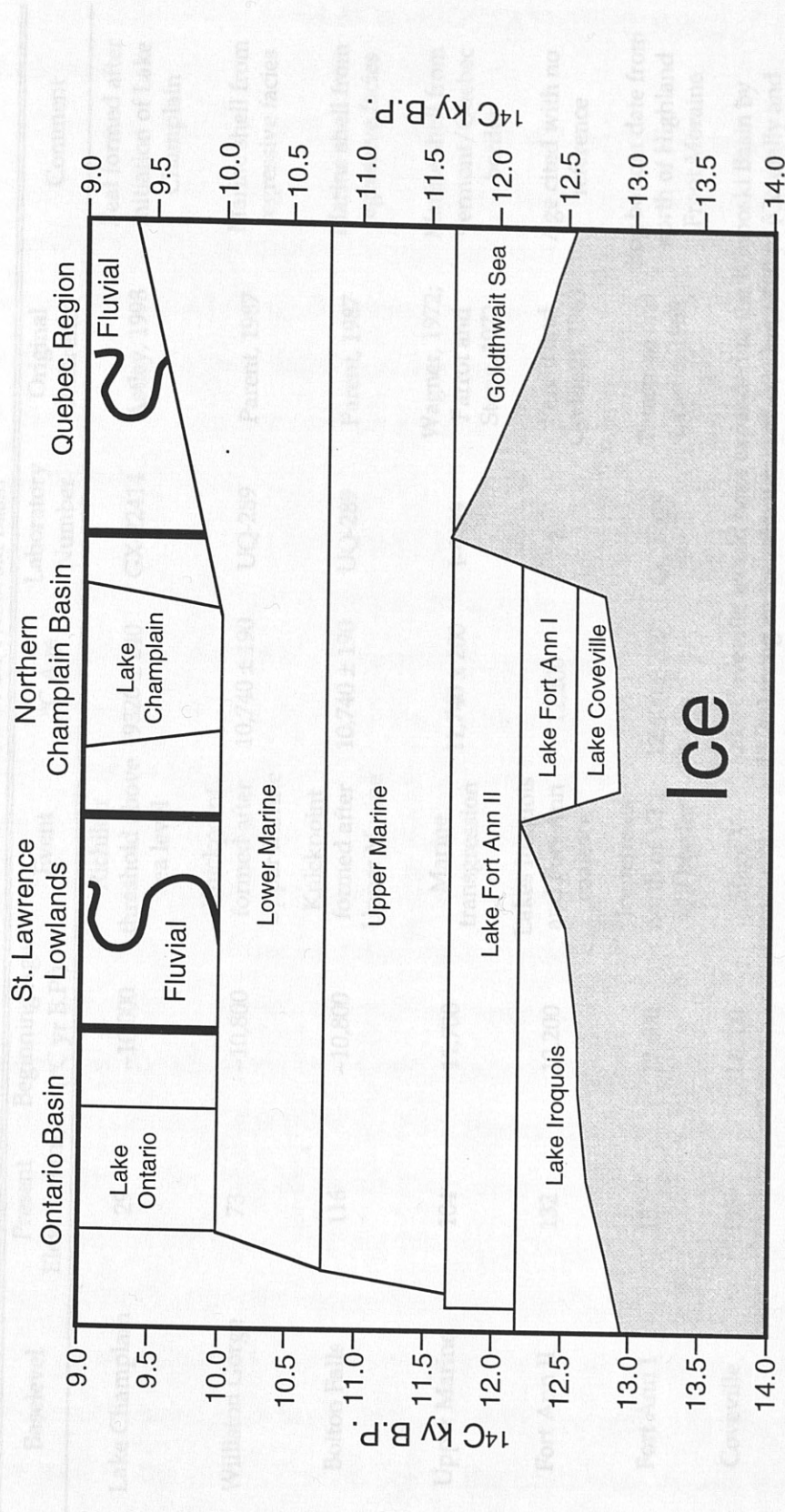


Figure 2.14: Correlation Diagram of Deglacial Events within the Northern Champlain Valley. Shown are the spatial and temporal extent of post-glacial water bodies in an approximate transect across the Northern Champlain Basin. Width of boxes indicate relative size of water bodies. Radiocarbon dates are presented in Table 2.5.

Table 2.5: Baselevel Controls in the Winooski Basin

Baselevel	Present Elevation (m)	Beginning Age (^{14}C yr B.P.)	Event	^{14}C Age	Laboratory Number	Original Reference	Comment
Lake Champlain	29	~10,000	Richileu threshold above sea level	9320 ± 240	GX-22414	Astley, 1998	Peat formed after initiation of Lake Champlain
Williston Gorge	73	~10,800	Knickpoint formed after Upper Marine	10,740 ± 190	UQ-289	Parent, 1987	Marine shell from regressive facies
Bolton Falls	116	~10,800	Knickpoint formed after Upper Marine	10,740 ± 190	UQ-289	Parent, 1987	Marine shell from regressive facies
Upper Marine	104	11,700	Marine transgression	11,740 ± 200	I-4489	Wagner, 1972; Parrot and Stone, 1972	Marine shell from Vermont/Quebec border
Fort Ann II	132	12,200	Lakes Iroquois and Fort Ann coalesce	12,200	?	Parent and Occhietti, 1988	Age cited with no reference
Fort Ann I	152	12,600	Ice retreats north of VT/ QE border	12,600 ± 200	GCS-519	Terasmae and LaSalle, 1968	Bog bottom date from north of Highland Front Moraine
Coveville	195	12,700	Stage V	Lake Coveville would have expanded to the Winooski Basin by 12,700 using an ice retreat rate of ~30 km / 100 yr (Connally and Sirkin, 1973). Using the same retreat rate in the Winooski Basin, deglaciation (Stages 1-4) would have taken ~200 years. With less of an ice front calving into the lakes, the retreat rate in the more mountainous Winooski Basin could have been slower. Therefore, the retreat rate is halved for the Winooski Basin and the time for deglaciation is equally divided so that each stage lasts 100 years.			
Mansfield II	204	12,800	Stage IV				
Mansfield I	229	12,900	Stage III				
Winooski	279	13,000	Stage II				

compensation index GLACIO-ISOSTATIC REBOUND the differential uplift

Background

Glacio-isostatic rebound is the result of land, once depressed under the weight of the ice sheet, rising to return to its original position when the load is removed. The additional weight of the ice on the crust is compensated isostatically; the mantle flows away from the region. Assuming that the crust remains rigid, a reasonable assumption over a small region, a given ice thickness will displace a column of mantle by an amount predicted by Archimedes Principle:

$$M_d = H_{ice} [\rho_{ice}/(\rho_m - \rho_{ice})]$$

where M_d is the height of displaced mantle, H_{ice} is the thickness of ice, and ρ_i and ρ_m are the densities of ice and mantle, respectively. However, the mantle is a viscous fluid and its response to the increasing thickness of ice will not be instantaneous or uniform over time. Therefore, in the ideal case where the mantle is in equilibrium with the ice load at the glacial maximum, M_d represents an upper limit, and can be defined as M_{dmax} .

The thickness of the ice (H_{ice}) is dependent on the distance from the center of the ice sheet. Ice reconstructions presented by Hughes (1987) show the Laurentide ice sheet centered over Hudson Bay, NNW of Vermont. At the glacial maximum, 18,000 ^{14}C yr B.P., the ice thickness decreased from about 4 km over Hudson Bay, to about 2 km over the Winooski Drainage Basin, and to 0 km at the terminus at Long Island. If H_{ice} equals 2 km, then M_{dmax} equals 720 m for northwestern Vermont (see Appendix A for calculations).

Ice flow indicators in northwestern Vermont point to a NW to SE flow direction (Stewart and MacClintock, 1970), implying that ice thickness increased to the NW. Thicker ice to the northwest means isostatic

compensation increased to the northwest, evidenced by the differential uplift of coeval features in Vermont (Chapman, 1937). To understand differential uplift, the uplift histories at two locations must be modeled.

Andrews (1968, 1970) presented a model, derived from published uplift curves from Arctic Canada, which predicts uplift at a location as a function of time using exponential growth. The amount of total potential uplift (U_t) after deglaciation will equal a percentage of M_{dmax} . At time t , the present uplift, U_p , or amount of uplift accomplished is defined by:

$$U_p = U_t (1 - e^{-kt})$$

where U_t is the total potential uplift, t is the time since uplift began, and k is the relaxation constant. The relaxation constant is a function of the mantle's viscosity that describes the "return" of the displaced mantle (Figure 2.15). Some authors describe the relaxation constant in terms of the relaxation time, τ , which equals $1/k$. Additionally, the relaxation constant is described by the half life, the time for half of the displaced mantle to return. The important concept to note is that because uplift is a result of an exponential decay of the displaced mantle, the rate of rebound decreases with time.

Differential uplift between two locations results from different uplift histories. Coeval shoreline features from a water body are often used to measure the differential uplift by measuring the gradient of the tilt plane. Features formed at one time are subsequently uplifted by different amounts because 1) uplift began later at one location, 2) one location was initially displaced more, or 3) a combination of 1) and 2). As shown in Figures 2.16 and 2.17, as long as two locations have the same initial displacement (scenarios a and b), the final gradient of the tilt plane will equal zero.

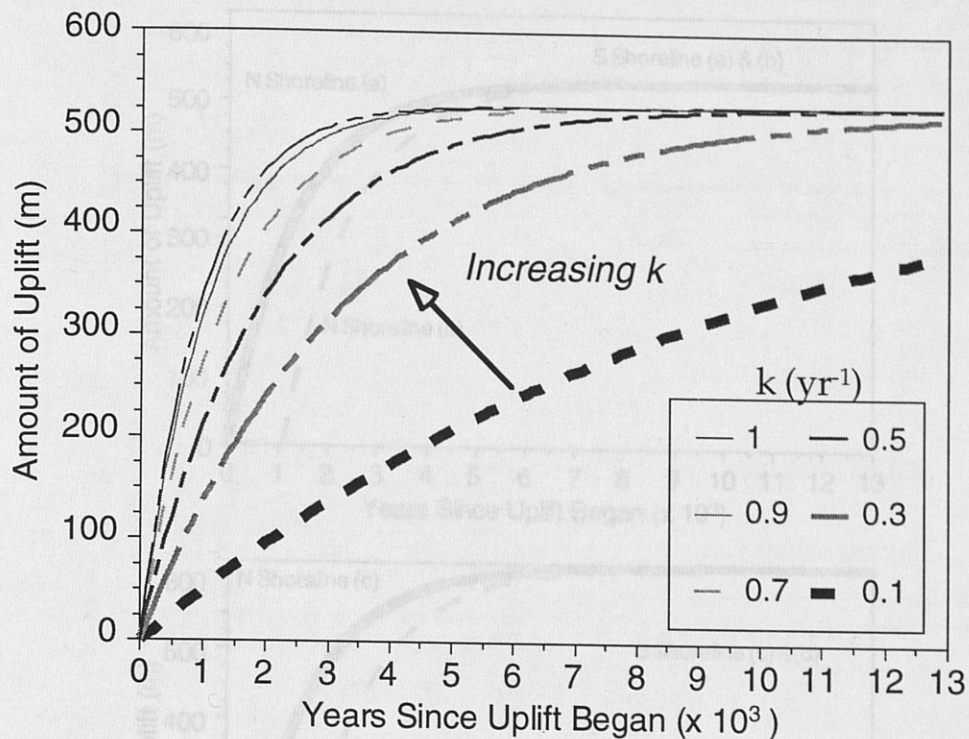


Figure 2.15: Graph of Effect of k on Rate of Rebound. The relaxation constant controls the rate of rebound; the higher the value, the faster uplift progresses. A value of approximately 0.7 yr^{-1} has been suggested for the Northeast (Barnhardt et al., 1995).

Figure 2.16: Graph of Different Rebound Scenarios. The amount of uplift is shown for the north and south shorelines of a lake for four different scenarios: a) Rebound begins at the same time in both north and south, and the amount of displacement is the same; b) Rebound is delayed by 1000 years in the north and the amount of initial displacement is the same; c) Rebound begins at the same time in both north and south, but the north is displaced by 50 meters more; d) Rebound is delayed and the north is initially displaced more.

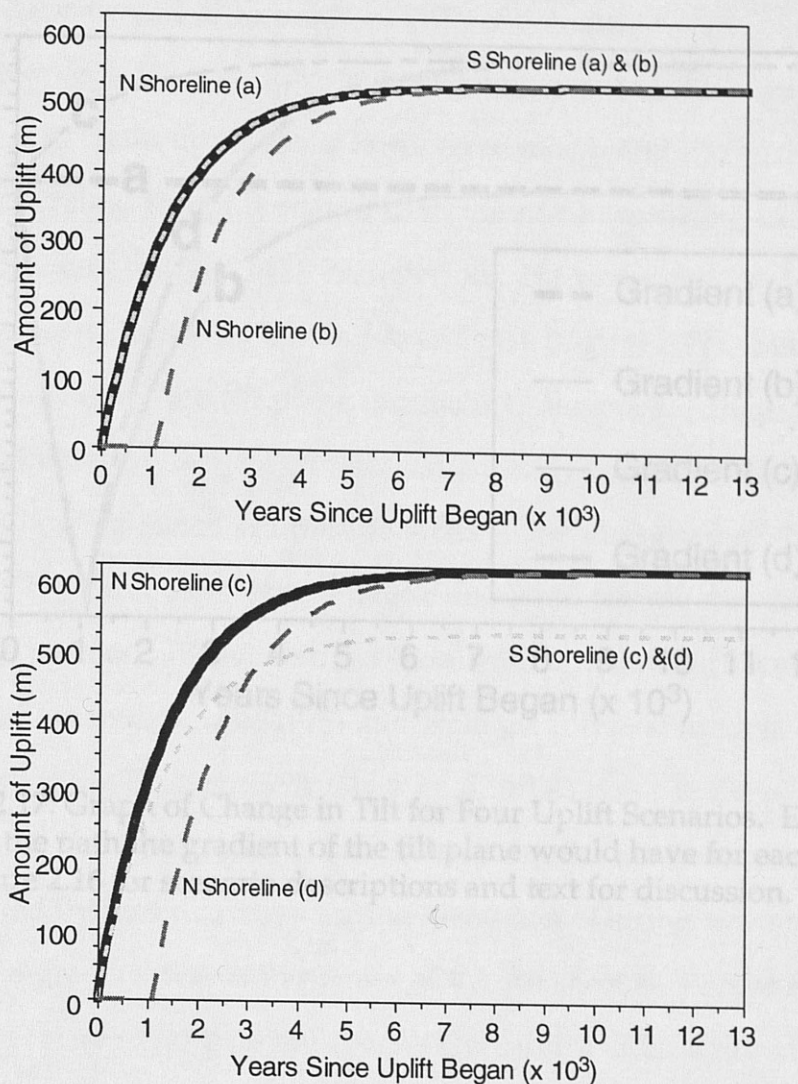


Figure 2.16: Graph of Different Rebound Scenarios. The amount of uplift is shown for the north and south shorelines of a lake for four different scenarios: a) Rebound begins at the same time in both north and south, and the amount of displacement is the same; b) Rebound is delayed by 1000 years in the north and the amount of initial displacement is the same; c) Rebound begins at the same time in both north and south, but the north is displaced by 50 meters more; d) Rebound is delayed and the north is initially displaced more.

Figure 2.16: Graph of Different Rebound Scenarios. The amount of uplift is shown for the north and south shorelines of a lake for four different scenarios: a) Rebound begins at the same time in both north and south, and the amount of displacement is the same; b) Rebound is delayed by 1000 years in the north and the amount of initial displacement is the same; c) Rebound begins at the same time in both north and south, but the north is displaced by 50 meters more; d) Rebound is delayed and the north is initially displaced more.

Therefore, the initial displacement must be greater in the north than the south (scenarios c and d) to produce differential uplift.

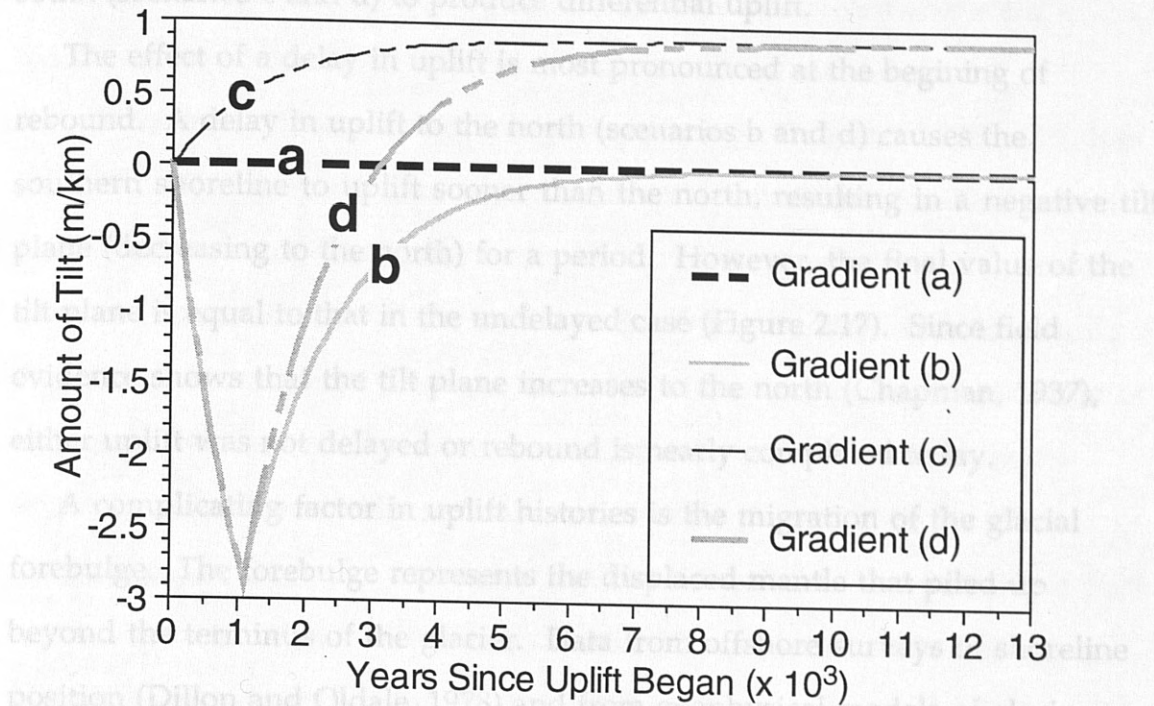


Figure 2.17: Graph of Change in Tilt for Four Uplift Scenarios. Each curve follows the path the gradient of the tilt plane would have for each scenario. See Figure 2.16 for scenario descriptions and text for discussion.

to be uplifted by tens of meters during glaciation. During rebound, the glacial forebulge migrates towards the center of the ice sheet as a series superposed on the uplift curve and then collapses. The land will be uplifted temporarily by a magnitude dependent on the forebulge amplitude at that point (several meters to tens of meters) and then lowered as it passes. The effect of the forebulge is most prominent in the relative sea level histories along the coast (Peltier, 1994), but has also been studied in inland lakes (Balco, 1997; Astley, 1998) and modeled for the Great Lakes Region (Clark et al., 1994). Based on the lake level curve for Lake Champlain, Astley (1998) suggests that the glacial forebulge passed through the region between 7500-5000 ¹⁴C yr B.P.

Therefore, the initial displacement must be greater in the north than the south (scenarios c and d) to produce differential uplift.

The effect of a delay in uplift is most pronounced at the begining of rebound. A delay in uplift to the north (scenarios b and d) causes the southern shoreline to uplift sooner than the north, resulting in a negative tilt plane (decreasing to the north) for a period. However, the final value of the tilt plane is equal to that in the undelayed case (Figure 2.17). Since field evidence shows that the tilt plane increases to the north (Chapman, 1937), either uplift was not delayed or rebound is nearly completed today.

A complicating factor in uplift histories is the migration of the glacial forebulge. The forebulge represents the displaced mantle that piled up beyond the terminus of the glacier. Data from offshore surveys of shoreline position (Dillon and Oldale, 1978) and from geophysical models of glacio-isostatic dynamics (Peltier, 1994; Clark et al., 1994) point to the presence of a peripheral glacial forebulge. Its presence causes the land beyond the ice sheet to be uplifted by tens of meters during glaciation. During rebound, the glacial forebulge migrates towards the center of the ice sheet as a wave superposed on the uplift curve and then collapses. The land will be uplifted temporarily by a magnitude dependent on the forebulge amplitude at that point (several meters to tens of meters) and then lowered as it passes. The effect of the forebulge is most prominent in the relative sea level histories along the coast (Peltier, 1994), but has also been studied in inland lakes (Balco, 1997; Astley, 1998) and modeled for the Great Lakes Region (Clark et al., 1994). Based on the lake level curve for Lake Champlain, Astley (1998) suggests that the glacial forebulge passed through the region between 7500-5000 ^{14}C yr B.P.

Northeast Rebound Studies

The glacio-isostatic rebound pattern has been interpreted across the Northeast from once-level water-line indicators, such as deltas and shorelines, for both coastal and inland regions (e.g., Chapman, 1937; Koteff et al., 1993). The orientation of the maximum tilt defines the direction toward the center of the ice sheet and necessarily varies across the region. I present the most recent studies for the region as they have the best altitudinal control. Table 2.6 is a summary of the gradient of the tilt plane, timing of initiation of tilting, and evidence for isostatic rebound from eastern New York to the Maine Coast as reported by several recent studies (Figure 2.18).

Eastern New York As mentioned earlier, the valleys in eastern New York north and south of the Adirondacks contained postglacial water bodies. Numerous wave-cut terraces, deltas and shorelines were formed in these lakes. Therefore, successful studies of isostatic rebound have been performed in the Hudson and Ontario Valleys.

LaFleur (1965) studied shorelines from three stages of Lake Albany in the Hudson Valley from Troy to the Hudson-Champlain divide. By plotting the shorelines on a N-S line, he found that the features of the highest Lake Albany stage had a gradient of 0.47 m/km and the features of the lower two stages both had gradients of 0.28 m/km. LaFleur correlated his lowest two stages of Lake Albany with Lakes Quaker Springs and Coveville in the Champlain Valley and proposed his slopes were lower than Chapman's (1937) slope of 0.95 m/km because of the presence of a hingeline in the latitude of Glens Falls. A hingeline is a theoretical line that separates two areas of different mantle dynamics. It was first proposed to explain the apparent vertical stability of the shorelines in the southern Great Lakes

Table 2.6: Summary of Glacio-isostatic Rebound Studies Across the Northeast

Reference	Clark and Karrow, 1984	Clark and Karrow, 1984	LaFleur, 1965	DiSimone and LaFleur, 1985	Chapman, 1937	Denny, 1974
Location on Figure 2.18	1	2	3a	3b	4a	4a
Region	Ontario Basin	St. Lawrence Lowlands	Hudson River	Hudson River	Champlain Basin	Champlain Basin
Direction*	N 20 E	N 0 E	N-S	N-S	N 14 W	N-S
Gradient	1.14 m/km	1.13 m/km	0.47 m/km	0.51 m/km	0.95 m/km	0.93 m/km
Water Plane	Lake Iroquois	Lake Iroquois	Lake Albany	Lake Albany	Upper Marine	Upper Marine
Rebound Begins**	Post-Lake Iroquois	Post-Lake Iroquois	Post-Lake Albany	Post-Lake Albany	Post-Upper Marine	-
Rebound Ends**	-	-	-	-	Still continuing?	-
Reference	Parent and Occhietti, 1988	Brakenridge et al., 1988	Koteff and Larsen, 1989	Koteff et al., 1993	Thompson et al., 1989	Barnhardt et al., 1995
Location on Figure 2.18	4b	4b	5	6	7	8
Region	Champlain Basin	Missisquoi River, Champlain Basin	Connecticut Valley	Coastal central New England	Coastal Maine	Western Gulf of Maine
Direction*	N 5 W-N 35 W	-	N 20.5 W-N 21 W	N 28.5 W	N 30 W-N 80 W	-
Gradient	1.0 m/km	-	0.9 m/km	0.85 m/km	0.5 m/km	-
Water Plane	Lake Fort Ann	-	Lake Hitchcock	Sea Level	Sea Level	Sea Level
Rebound Begins**	-	-	After 14,000 and before 13,300	After 14,000 and before 13,300	Before 13,000	Before 13,000
Rebound Ends**	-	By 8000	-	-	-	By 6000

Notes: * If a true direction were cited, the orientation is given; otherwise, the plane of projection is given.

** Ages are in radiocarbon years before present.

Region relative to the shorelines to the north. Geophysical models have since discounted the hingeline concept (Clark et al., 1994) and instead point to improper correlations as the explanation for the original hingeline idea.

The gradients measured for the lakes existing from Lake Albany to Lake

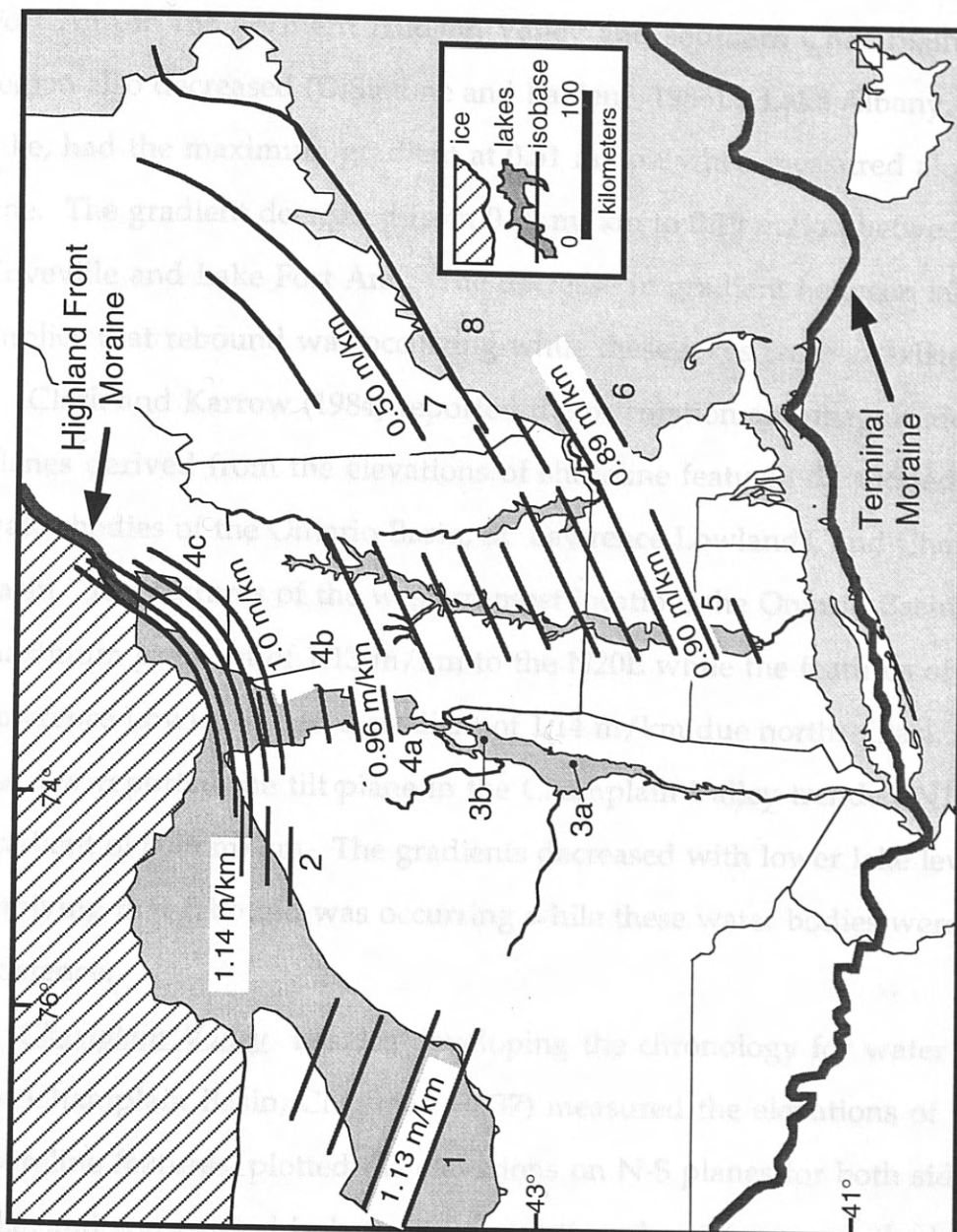


Figure 2.18 Location of Glacio-isostatic Rebound Studies in the Northeast. Orientation and gradient of isobases is shown with extent of water plane. Numbers refer to studies described in Table 2.6. (Modified from Balco, 1997)

coastal features. The gradient of the maximum tilt plane was 0.95 m/km, rising to the north at 110°W. By analyzing the gradient of the tilt planes,

Region relative to the shorelines to the north. Geophysical models have since discounted the hingeline concept (Clark et al., 1994) and instead point to improper correlations as the explanation for the original hingeline idea.

The gradients measured for the lakes existing from Lake Albany to Lake Fort Ann in the northern Hudson Valley and southern Champlain Valley region also decreased (DiSimone and LaFleur, 1986). Lake Albany, the oldest lake, had the maximum gradient at 0.51 m/km when measured along a N-S line. The gradient decreased from 0.30 m/km to 0.19 m/km between Lake Coveville and Lake Fort Ann. The decrease in gradient between lake levels implies that rebound was occurring while these lakes were in existence.

Clark and Karrow (1984) reported the orientation and magnitude of the tilt planes derived from the elevations of shoreline features developed in the water bodies of the Ontario Basin, St. Lawrence Lowlands, and Champlain Basin. The features of the western-most location, the Ontario Basin, had a maximum gradient of 1.13 m/km to the N20E while the features of the St. Lawrence Lowlands had a gradient of 1.14 m/km due north. Clark and Karrow reported the tilt plane in the Champlain Valley trended N12W with a gradient of 0.95 m/km. The gradients decreased with lower lake levels, implying that rebound was occurring while these water bodies were in existence.

Champlain Valley Besides developing the chronology for water bodies in the Champlain Basin, Chapman (1937) measured the elevations of the shoreline features, plotted the elevations on N-S planes for both sides of the lake, and constructed isobases by connecting elevations across the lake of coeval features. The gradient of the maximum tilt plane was 0.95 m/km, rising to the north at N14W. By analyzing the gradient of the tilt planes,

Chapman found that the Upper Marine, Fort Ann, and Coveville water planes were almost parallel and he interpreted this to mean that rebound began after the Upper Marine interval of the Champlain Sea. According to Chapman's interpretations, rebound would have started in the Champlain Valley at about 10,800 ^{14}C yr B.P. based on dates presented in Parent and Occhietti (1988).

However, Chapman acknowledged that uplift was occurring prior to and during the early development of Lake Coveville. In the more recent studies in New York mentioned above, the gradient of the tilt planes decreased with each successively lower lake level, beginning with Lake Albany. Therefore, it seems plausible that Chapman was unable to discern different gradients for his highest tilt planes because of poor elevation control and that uplift was occurring while the Champlain Valley was occupied with proglacial lakes.

Denny (1974), working in the northeast Adirondacks on the western margin of the northern Champlain Valley, also had difficulty measuring a gradient for the tilt planes. When measured along a N-S line, the Lake Fort Ann shorelines had a gradient of 0.85 m/km while the Upper Marine had a gradient of 0.93 m/km. These gradients must have an error of at least 0.08 m/km because the younger shoreline can not have a steeper inclination than the older shoreline. In addition, when measured along the true direction of tilt, reported by Denny as between N10W and N15W, the gradients will increase about 0.02-0.03 m/km. Therefore, while Denny's results are similar to Chapman's, they do not help to clear up the discrepancy of gradients decreasing in the Hudson Valley (LaFleur, 1965; DiSimone and LaFleur, 1985) for the same lake levels that have unchanging gradients in the Champlain Valley (Chapman, 1937).

Parent and Occhietti (1988) presented an isobase construction (Figure 2.18) for northern Vermont and southern Quebec compiled from previous sources, including Chapman (1937), McDonald (1968), Wagner (1972), and Parent (1987). The isobases trend from E-W in the west to NE-SW in the east. Their compilation is the only one to reflect the expected variable trend in isobases from east to west. The average gradient represented by the isobases is about 1.0 m/km and therefore the magnitude is consistent with the other studies in the area.

While these studies show that rebound began during deglaciation, none reported evidence of when rebound might have ended. Chapman (1937) suggested that uplift may still be occurring, but had no evidence to support his claim. The study of Brakenridge et al. (1988) on the Missisquoi River in the northern Champlain Basin found that the incision rate, initially high following deglaciation, decreased by 8000 ^{14}C yr B.P. They suggested that river incision was a response to vertical glacio-isostatic movements and concluded that rebound had ended by 8000 ^{14}C yr B.P. Therefore, rebound rates probably decreased in the Holocene and Brakenridge et al.'s conclusions can be tested in other rivers in the region.

Winooski Valley Larsen (1987b) used the tilt plane measured for the Connecticut Valley by Koteff and Larsen (1989) to predict the elevations of uplifted shoreline features of the lakes in the Winooski Drainage Basin. Using the elevation of the spillway for each lake as the starting point, Larsen constructed maps of where the shorelines would be if the area had been tilted N21W at 0.9 m/km. Larsen cited several instances where the projection adequately predicted the elevations of known shoreline features in the Winooski Valley and therefore believed that the tilt plane should be extended

westward from the Connecticut Valley to the Champlain Valley.

While the magnitude of the tilt plane is similar to that measured by Chapman (1937) in the Champlain Valley, the orientation differs by 7° . Larsen did not discuss this discrepancy, but in order for isobases to connect from the Champlain Valley to the Connecticut Valley, the orientation must change across central Vermont as illustrated by the isobases presented by Parent and Occhietti (1988) for southern Quebec and northern Vermont (Figure 2.18).

Connecticut Valley Koteff and Larsen (1989) presented an uplift plane for the Connecticut Valley based on topset-foreset contacts in deltas. They found that a single plane rising N20.5W-N21W at 0.9 m/km fit the elevations to within a meter of all the deltas built into the 245 km long Lake Hitchcock. The stability of the tilt plane over the entire distance of the lake was interpreted to mean that rebound did not begin until after Lake Hitchcock drained.

The threshold for Lake Hitchcock, a bedrock spillway in New Britain, CT, has long been regarded as stable during the entire time the lake existed. The present course of the Connecticut River passes through surficial material that presumably was incised during the drainage of Lake Hitchcock, implying that rebound was necessary to initiate drainage of Lake Hitchcock. Dated plant fragments from lacustrine bottom sediments north of the threshold, Windsor, CT, are $13,540 \pm 90$ ^{14}C yr B.P. (Beta 59094/CAMS #4875; Stone and Ashley, 1995). These fragments, stratigraphically associated with a delta that was built below the elevation of the Hitchcock threshold, represent post-Lake Hitchcock deposition. Stone and Ashley interpret that by $13,500$ ^{14}C yr B.P. Lake Hitchcock was draining because rebound had begun.

Central Coastal New England Koteff et al. (1993) studied glaciomarine deltas from northeastern Massachusetts to southwestern Maine. These deltas were deposited sequentially into the ocean at the margin of the ice sheet as the ice retreated northward through this region between 15,000 and 14,000 ^{14}C yr B.P. Koteff et al. measured the topset/foreset contacts of the deltas which were taken to represent eustatic sea level within a meter. Because the deltas described a single plane rising $\text{N}28.5\text{W} \pm 1.9^\circ$ at $0.85 \pm 0.02 \text{ m/km}$, two interpretations were made: 1) baselevel (eustatic sea level) remained nearly stable during this period; 2) differential uplift was delayed until after the deposition of all these features. Alternatively, the rate of eustatic sea-level rise equaled the rate of rebound and there was no net differential uplift during the deposition of the glacio-marine features.

Koteff et al. (1993) compared the stability, the magnitude, and the orientation to the tilt plane to the study of Koteff and Larsen (1989) and concluded that the style of uplift was similar in these two locations. Since the stability of the tilt plane in both studies was interpreted to mean delay of rebound and the timing of deglaciation was the same in both locations, Koteff et al. placed the beginning of differential rebound between 14,000 and 13,300 ^{14}C yr B.P. for the region. The date later proposed by Stone and Ashley (1995) of 13,500 ^{14}C yr B.P. for initiation in the Connecticut Valley fits the delay model as well and may be used to represent the timing of the initiation of differential rebound across the Northeast.

The magnitude and orientation of the tilt planes of Koteff et al. ($\text{N}28.5\text{W}$ at 0.85 m/km) and Koteff and Larsen ($\text{N}20.5\text{W}$ at 0.9 m/km) are very close. The difference in orientations was attributed to the expected variations based on position of the studies relative to the center of the ice sheet. The

difference in magnitude of the tilt plane, although not significant, could be explained by a lowering of sea level during the deposition of the later glaciomarine deltas or by variations in the lithosphere between the locations (Koteff et al., 1993).

Maine Thompson et al. (1989) presented the results of a comprehensive survey of glaciomarine deltas in Maine. The elevation of the topset-foreset contacts were surveyed and the stratigraphy of the deltas was described. The > 100 deltas included in the study were deposited at the margin of the Laurentide ice sheet, directly into the ocean, between 14,000 and 13,000 ^{14}C yr B.P. Because the land was isostatically depressed at deglaciation, the ocean transgressed into Maine following the retreating ice. The seaward deltas were deposited first, and later deltas were deposited progressively further inland. The farthest inland deltas represent the extent of the transgression. After that time, the rate of rebound exceeded the rate of sea level rise and the sea regressed.

During the regression, the shoreline passed over the deltas and fluvial or wave erosion modified many of the delta surfaces. Close examination of the stratigraphy and contacts was able to differentiate true topset-foreset contacts from those contacts where the foreset beds were truncated by later fluvial or marine sediments. The elevation of the topset-foreset contacts represents the relative sea level. However, due to the time-transgressive nature of ice retreat, deltas formed at the same relative sea level but at different times may not record the same amount of uplift, if uplift was occurring during ice retreat.

The orientation of reported isobases varies by 35° across Maine. Thompson et al. correlate the change in orientation with the direction of ice flow. Maximum uplift is parallel to the ice flow indicators, and the gradient

is 0.50 m/km across much of coastal Maine (Figure 2.18). Unlike Koteff et al. (1993), Thompson et al. did not conclude that the deltas were deposited during a stable sea level or that rebound began after the delta sequence was deposited. Therefore, the gradient of the deltas is a minimum of the total rebound, explaining why the magnitude is the lowest of all the Northeast. Since the transgression ended about 13,000 ^{14}C yr B.P., uplift was occurring by that time.

Barnhart et al. (1995) interpreted the uplift history of the coast by examining the relative sea level. They constructed their relative sea level curve for the western Gulf of Maine on the basis of 20 radiocarbon dates of flora and fauna recovered from vibracores and peat samples. By subtracting the relative sea level curve from the eustatic sea level curve of Fairbanks (1989), Barnhardt et al. derived an uplift curve for the area. The uplift curve flattened out after 6000 ^{14}C yr B.P., suggesting that rebound ended by that time. The uplift curve also showed a strong peak (magnitude ~ 25 m) between 11,000 and 10,500 ^{14}C yr B.P., corresponding to a relative sea level lowstand, that the authors interpreted as the passage of the glacial forebulge. Studies of the relative sea level in the St. Lawrence Estuary, Quebec (Dionne, 1988) have also found evidence of the glacial forebulge migration, and based on these results, Barnhardt et al. estimate the rate of forebulge migration to be between 7-11 km/100 yr.

Summary

CLIMATE HISTORY OF THE NORTHEAST

The previous studies of glacio-isostatic rebound in the Northeast establish: 1) the maximum gradient of the rebounded features is about 1 m/km; 2) the orientation of maximum rebound varies across the region, but generally it is to the northwest; 3) the date of initiation of rebound in the Connecticut Valley, 13,550 ^{14}C yr B.P., fits with the other regional data, implying that rebound was progressing during the deglaciation of the Winooski Drainage Basin; and 4) the rate of rebound decreased during the Holocene and has been low for at least the past several thousand years.

causes severe cyclonal storms
that may stagnate over an area. Redundant precipitation is an area. Along the
zonal flow, the two air masses meet, but since the contact length is not great
and the contrast between the air masses is less, the storms are not so severe and
move swiftly through the area (Lamb, 1995).

The path of the circumpolar vortex is controlled by areas of high pressure, anticyclones. Circulation around anticyclones is clockwise, a pattern which moves the frontal systems away from the high pressure area. Therefore, where high pressure dominates storm activity is deflected and the climate is rather dry because most large storms, including hurricanes, do not enter the region. Adjacent low pressure areas are inundated with the deflected storms and in areas dominated by low pressure, the frequency and magnitude of consecutive thunderstorms may increase due to surface heating. Therefore, where low pressure dominates, the climate is relatively wetter.

Seasonal variations in insolation or heating by the sun shift the latitudinal position of the circumpolar vortex. In the winter, it moves southward, subjecting New England to cold arctic air, and during the summer, it moves northward, bringing humid tropical air to the region. The

CLIMATE HISTORY OF THE NORTHEAST

Background

The climate of the Northeast is controlled by the circumpolar vortex, an upper air circulation pattern in which air flows from west to east (Lamb, 1995). It consists of two components, zonal flow (west to east) and meridional flow (north-south), which form a meandering pattern (Figure 2.19). The sinuosity of the circumpolar vortex controls the severity of the weather. Along the meridional flow, warm wet air is brought north and cool dry air is carried south. The collision of these air masses causes severe cyclonal storms that may stagnate, bringing abundant precipitation to an area. Along the zonal flow, the two air masses meet, but since the contact length is not great and the contrast between the air masses is less, the storms are not severe and move swiftly through the area (Lamb, 1995).

The path of the circumpolar vortex is controlled by areas of high pressure, anticyclones. Circulation around anticyclones is clockwise, a pattern which steers the frontal systems away from the high pressure area. Therefore, where high pressure dominates, storm activity is deflected and the climate is rather dry because most large storms, including hurricanes, do not enter the region. Adjacent low pressure areas are inundated with the deflected storms and in warm areas dominated by low pressure, the frequency and magnitude of convective thunderstorms may increase due to surface heating. Therefore, where low pressure dominates, the climate is relatively wetter.

Seasonal variations in insolation or heating by the sun shift the latitudinal position of the circumpolar vortex. In the winter, it moves southward, subjecting New England to cold arctic air, and during the summer, it moves northward, bringing humid tropical air to the region. The

long-term average position of the zonal component of the circumpolar vortex defines the temperature of a region, and where the zonal winds remain at a high latitude (northern hemisphere) for a period where the

zonal winds remain at a high latitude, the region will be cold. The amplitude of the meridional flow, frequency of the storms, and moving from the region.

Climate change, vegetation changes, and climate studies of these records. Climate changes by associating variations in the methods and conclusions of these studies are described below and the location and results

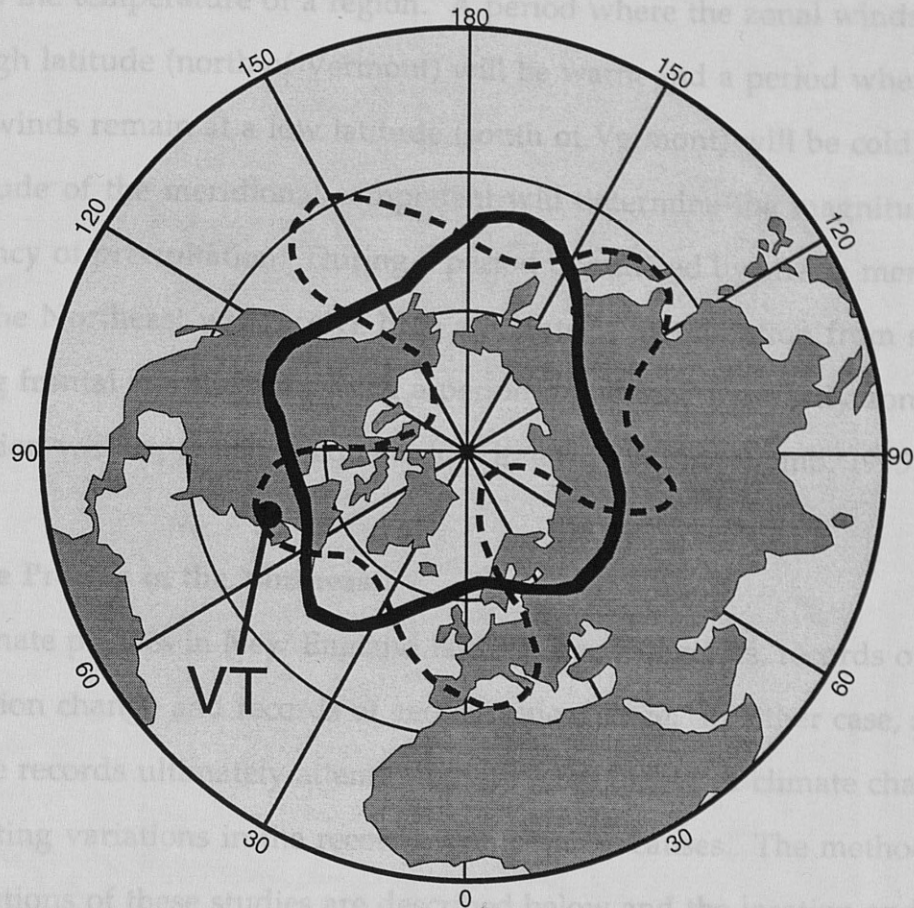


Figure 2.19: Upper Atmosphere Circulation Patterns. Two hypothetical paths for the circumpolar vortex are shown. The heavy solid line represents high-latitude zonal flow which would lead to a warm period with small, but frequent storms. The fine dashed line represents strong meridional flow which would bring long-lasting, severe storms to Vermont. The location of Vermont is shown for reference. (After Lamb, 1995).

foras where it is deposited in pond sediments. Macrofossils are presumed to be deposited directly from vegetation adjacent to the pond. Cores of pond sediments are extracted, macrofossils and other organic material are dated, and the pollen grains of different species are counted to construct the pollen record. The abundance of different species of pollen for a given horizon is used to deduce the vegetation in the region and the occurrence of

long term average position of the zonal component of the circumpolar vortex defines the temperature of a region. A period where the zonal winds remain at a high latitude (north of Vermont) will be warm and a period where the zonal winds remain at a low latitude (south of Vermont) will be cold. The amplitude of the meridional component will determine the magnitude and frequency of precipitation. During a period dominated by strong meridional flow, the Northeast will receive high amounts of precipitation from slow moving frontal storms, but during a period dominated by mostly zonal flow, the region will experience frequent, low intensity storms (Lamb, 1995).

Climate Proxies in the Northeast

Climate proxies in New England fall into two categories, records of vegetation change and records of geomorphic change. In either case, studies of these records ultimately attempt to define the timing of climate changes by associating variations in the records with climatic causes. The methods and assumptions of these studies are described below and the location and results of the studies are presented in Figures 2.20 and 2.21 respectively.

Pollen and Macrofossil Records Studies of pollen and macrofossils extracted from pond sediments are the most widely used climate proxy in New England. Pollen from trees and other plants is transported by wind to ponds where it is deposited in pond sediments. Macrofossils are presumed to be deposited directly from vegetation adjacent to the pond. Cores of pond sediments are extracted, macrofossils and other organic material are dated, and the pollen grains of different species are counted to construct the pollen record. The abundance of different species of pollen for a given horizon is used to deduce the vegetation in the region and the occurrence of

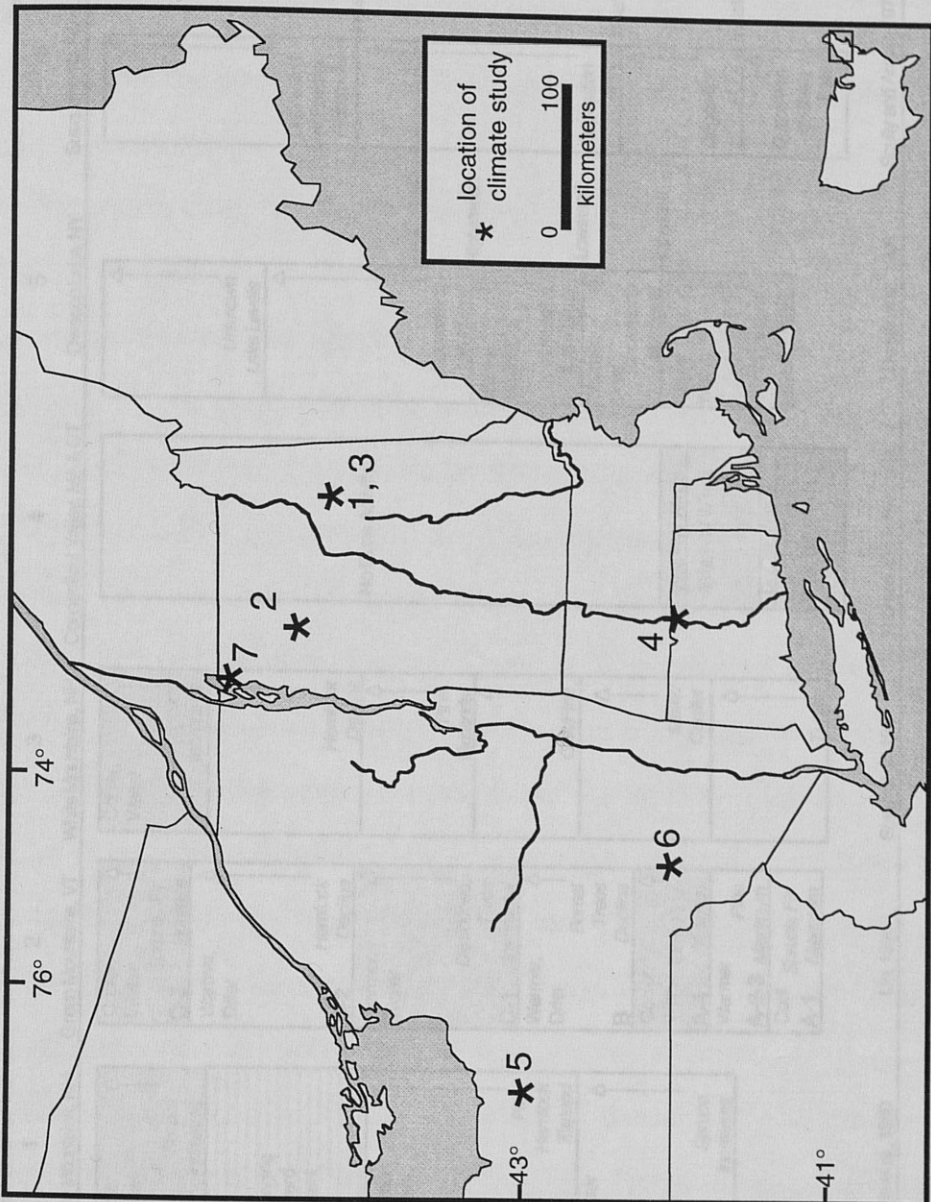


Figure 2.20: Location of Climate Studies in the Northeast. Number refer to studies described in the text and illustrated in Figure 2.21.

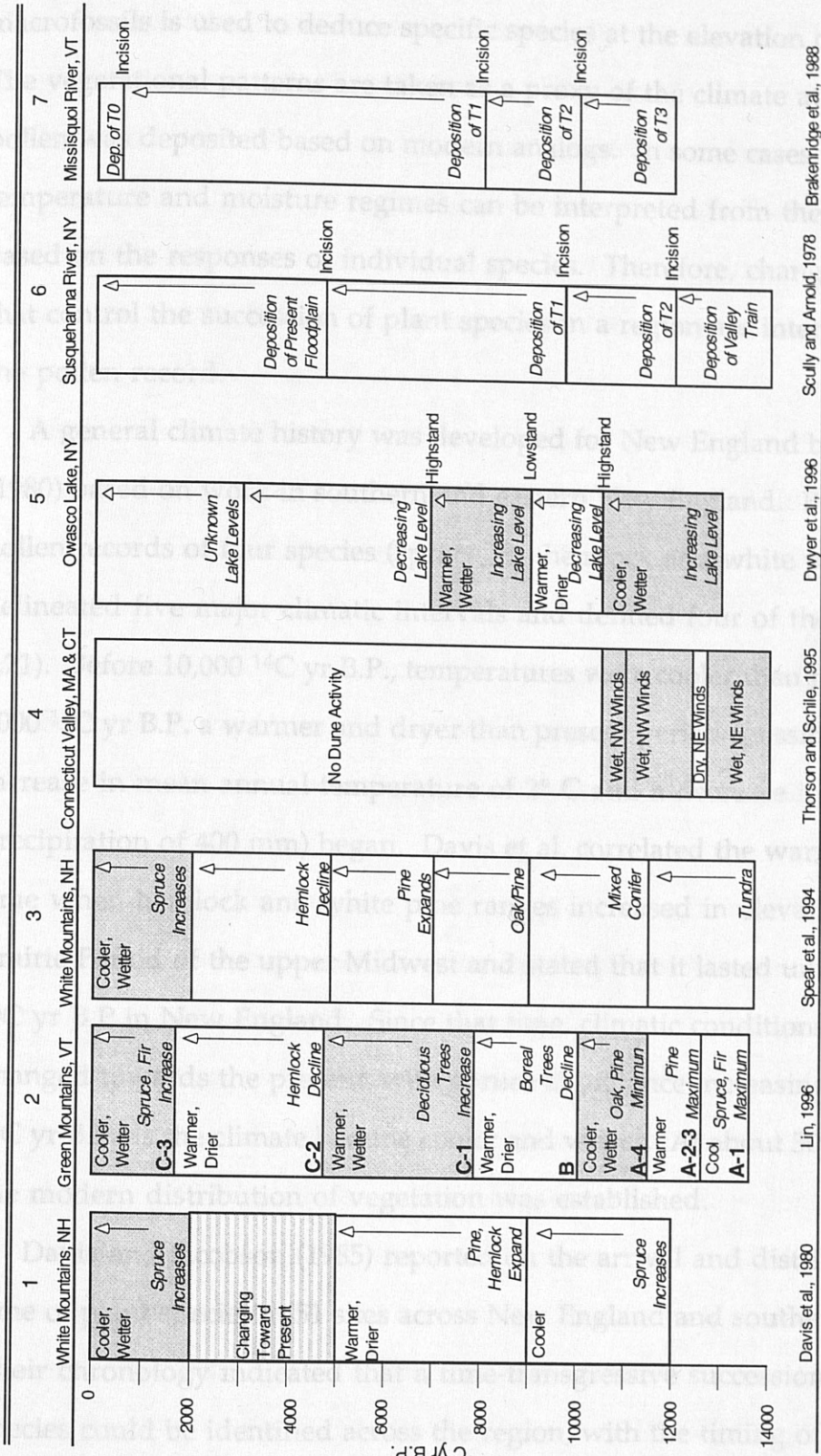


Figure 2.21: Results from Climate Studies Across the Northeast. Periods designated as wetter by the authors are greyed. Locations of the studies are shown on Figure 2.20. See text for descriptions.

macrofossils is used to deduce specific species at the elevation of the pond. The vegetational patterns are taken as a proxy of the climate at the time the pollen was deposited based on modern analogs. In some cases, past temperature and moisture regimes can be interpreted from the pollen records based on the responses of individual species. Therefore, changes in climate that control the succession of plant species in a region are interpreted from the pollen record.

A general climate history was developed for New England by Davis et al. (1980) based on work in southern and eastern New England. By analyzing the pollen records of four species (spruce, fir, hemlock and white pine), they delineated five major climatic intervals and defined four of them (Figure 2.21). Before 10,000 ^{14}C yr B.P., temperatures were cooler than present, and by 9000 ^{14}C yr B.P. a warmer and dryer than present period (possibly with an increase in mean annual temperature of 2° C and a decrease in mean annual precipitation of 400 mm) began. Davis et al. correlated the warmer period, a time when hemlock and white pine ranges increased in elevation, with the Prairie Period of the upper Midwest and stated that it lasted until at least 5000 ^{14}C yr B.P. in New England. Since that time, climatic conditions gradually changed towards the present, with spruce abundance increasing around 2000 ^{14}C yr B.P. as the climate became cooler and wetter. At about 500 ^{14}C yr B.P., the modern distribution of vegetation was established.

Davis and Jacobson (1985) reported on the arrival and distribution over time of plant species at 51 sites across New England and southern Quebec. Their chronology indicated that a time-transgressive succession of plants species could be identified across the region, with the timing of arrival and subsequent changes in species abundance dependent on factors such as

elevation and latitude. Therefore, although Davis et al. (1980) provide some insight into the climatic changes in New England since deglaciation, the work of Davis and Jacobson demonstrates that in order to address the timing of climate changes locally, site-specific studies are needed. Three sites in northeastern Vermont were included in Davis and Jacobson's study, but all three were poorly dated. The timing of climate changes in northwestern Vermont remained unstudied until Lin (1996).

Lin (1996) studied and dated the pollen stratigraphy of two ponds in the Green Mountains. Sterling Pond (elevation 917 m) is located at the northern edge of the Winooski Drainage Basin and Ritterbush Pond (elevation 317 m) is 25 km northeast of Sterling Pond. Because of its proximity to the Winnoski Drainage Basin and the similarity of its elevation to the headwater elevations for the rivers in the basin, the Sterling Pond pollen record represents the best proxy for climate changes affecting the rivers in the Winooski Drainage Basin.

Following the divisions made by previous workers in the Northeast, Lin defined seven pollen zones in the Sterling Pond core (Figure 2.21). The climate changes inferred from these pollen zones reflect an overall warming of temperatures as well as fluctuations in precipitation since deglaciation. Zone A-4 may represent the Younger-Dryas climate reversal, a period when the climate suddenly became colder and returned to near glacial conditions. Lin interpreted the oak and pine minimum during Zone A-4 to represent a cooler and moister climate than immediately prior, which is consistent with the return towards glacial conditions. Zones C-1 and C-2 correspond well with the timing of the mid-Holocene warming identified in the other regional studies.

In another interpretation of pollen stratigraphy, Spear et al. (1994) studied the pollen record of several ponds, both of high and low elevation, in the White Mountains of New Hampshire (Figure 2.21). Their climate interpretations were summarized in a qualitative diagram (Figure 2.22) which compared three factors (past temperature and precipitation, disturbances near today's treeline, and disturbances on lower slopes) relative to today's conditions. Although Spear et al.'s interpretations pertain specifically to New Hampshire, they may also be applicable to Vermont, at least in terms of the change in regimes from one dominated by the presence of the Laurentide ice to one periodically disturbed by hurricanes.

For the period from deglaciation to 8000 ^{14}C yr B.P., slope disturbances due to frost action, avalanches, and tree blow downs would have been more frequent. During this period, the valley slopes would have had a greater potential for failure and therefore could have delivered more sediment to the rivers. Spear et al. show with some uncertainty that the yearly precipitation was less than today's; however, with an increased sediment supply and a decreased discharge, there would be limited transportation of sediment in rivers.

In the time since 8.0 ^{14}C yr B.P., the most important change is in the frequency of tropical hurricanes. Spear et al. anticipated an increase of hurricanes to coincide with the waning northeastern cyclonic winds associated with the retreating Laurentide ice mass. Hurricanes, with their strong winds and heavy rainfall, could have also contributed to the sediment supply in rivers. Hurricane winds have the ability to down trees, exposing more soil to erosion, and a hurricane's rainfall would significantly increase river discharge, potentially transporting large volumes of sediment.

Other fluvial records: Several studies have used other records beside

glaciation to infer changes in climate in the Northeast. These studies have attempted to

determine the timing of climatic fluctuations over time that influence vegetation

and vegetation of the treeline. These studies have attempted to

infer changes in temperature and precipitation by level records

and correlation of pollen to determine paleowind

directions and summer temperatures, thereby showing deglaciation in

the White Mountains. The main surviving evidence recorded by the

fluvial features is the presence of dunes and talus slopes to define fire regimes.

Figure 2.22: This diagram compares a moist preglacial regime existing from

deglaciation to about 10,000 years ago with a dry postglacial regime existing from

about 10,000 to 12,400 years ago. The preglacial period was characterized by strong north-easterly winds

derived from the ice sheet, which caused extensive snow accumulation and development

of glaciogenic features such as talus slopes and dunes. During the postglacial period,

especially during the Holocene, there were fewer winds to keep the land moist and

extinctive agents such as fire, frost-action, and pathogens were more active. However, during

the dry postglacial period, there were more tropical hurricanes and snow cover from north-easterly winds.

The beginning of the Holocene (about 10,000 years ago) was a relatively cool period.

Establishment of vegetation began during this period, but it did not last long. The first

period of reworking of the landscape occurred during the early Holocene, but it was stabilized as

vegetation continued to grow. The landscape was again leveled again during the

beginning of the Holocene (about 10,000 years ago), but the most conditions of that period

Figure 2.22: Schematic Diagram of Changes in Conditions in the White Mountains. The diagram illustrates how disturbances could have changed since deglaciation. See text for discussion. (After Spear et al., 1994)

Finally, during the Holocene there were inactive until historic times when

Other Northeast Records Several studies have used other records beside pollen to interpret the climate changes since deglaciation in the Northeast. Rather than interpreting the temperature and moisture fluctuations over time that influence vegetation patterns, these other studies have attempted to infer changes in large scale atmospheric circulations from lake level records and orientation of eolian features.

Thorson and Schile (1995) used eolian features to determine paleowind directions and climatic regimes immediately following deglaciation in Connecticut River Valley. The dominant wind direction (as recorded by the eolian features) and types of dune activity were used to define five regimes (Figure 2.21). The two oldest regimes, a moist periglacial regime existing from deglaciation to 12,700 ^{14}C yr B.P. and a dry periglacial regime existing from 12,700 to 12,400 ^{14}C yr B.P., were dominated by strong northeasterly winds derived from the glacial anticyclone located above the Laurentide ice sheet. During the moist periglacial regime, there was no dune development. Presumably, summer cyclonic storms were able to keep the sand moist and prevented dune formation during times of no snow cover. However during the dry periglacial regime, dunes rapidly developed from northeasterly winds. The beginning of this regime coincides with the Bolling/Allerod period. Establishment of northwesterly winds, from 12,400-11,000 ^{14}C yr B.P., first caused a reworking of the older dune deposits, but dunes stabilized as vegetation colonized the valley. Sand transport increased again during the Younger Dryas (11,000-10,500 ^{14}C B.P.), but the moist conditions of that period inhibited dune growth. Instead, deposition of a mantle of eolian sand and silt occurred under high wind intensities for a time before ending abruptly. Finally, during the Holocene dunes were inactive until historic times when

agriculture and forestry practices were responsible for their reactivation.

The study by Dwyer et al. (1996), which examined the relative lake level of Owasco Lake in New York, used another climate proxy. In this study, sediment cores from the dry lake valley were dated and described to produce a relative lake level chronology (Figure 2.21). Highstands occurred at 10,500 ^{14}C yr B.P. and at 6900 ^{14}C yr B.P. and a lowstand occurred at 9000 ^{14}C yr B.P. The variations in lake level are interpreted to reflect different moisture balance situations. The highstands are attributed to increased precipitation and decreased evaporation during the Killarney-Younger Dryas cold interval (11,200-10,000 ^{14}C B.P.) and during the Hypsithermal (8500-5500 ^{14}C yr B.P.). The lowstand is attributed to the period of maximum summer solar insolation around 9000 ^{14}C yr B.P. which may have increased evaporation to lower lake level.

Dwyer et al. (1996) suggest their results support Forman et al.'s (1995) interpretation that changes in solar insolation caused latitudinal shifts in the circumpolar vortex during the Holocene. During the Hypsithermal the eastern United States would have experienced increased precipitation because the jet stream shifted to the north and the Bermuda high shifted to the northeast. Moist tropical air, responsible for carrying the precipitation to the Northeast, would have been able to enter the region. Despite the warmer temperatures, the additional precipitation could have caused an increase in Owasco Lake's level.

Summary

The diverse climatic data point to several widespread climatic changes. Prior to 12,400 ^{14}C yr B.P., the climate was strongly influenced by the Laurentide ice sheet and northeasterly winds brought cold, dry air to the Northeast. After that time, the anticyclone above the ice sheet waned, and west-northwesterly winds brought warmer, yet still cool air to the region until at least 11,000 ^{14}C yr B.P. Coinciding with the Younger Dryas period (11,000-10,500 ^{14}C yr B.P.), the air became cooler and precipitation increased in the Northeast. Between 10,500 and 9000 ^{14}C yr B.P., the climate was warmer and drier as the region was dominated by zonal flow located to the north. Then between 9000 and 8000 ^{14}C yr B.P., a period of increased precipitation and warmer temperatures developed when meridional flow dominated, lasting until about 5000 ^{14}C yr B.P. Next, the region became warmer and drier with a return to northern zonal flow. Since about 2000 ^{14}C yr B.P., the climate, under influence of meridional flow, has been colder and wetter.

(Peterson, 1984). Essentially, a river is either in equilibrium or else in a transitory state attempting to obtain equilibrium. A river will remain in equilibrium, being controlled by self-arresting feedback mechanisms, until a threshold is exceeded. Thresholds are points in time that separate periods of aggradation or degradation (Bull, 1991). At that time when the threshold is exceeded, the river will, through self-enhancing feedback mechanisms, adjust to the new conditions and obtain a new equilibrium by either raising or lowering its channel. Therefore, terraces are formed when thresholds are exceeded. In order to understand why thresholds are exceeded, a review of fluvial system dynamics and equilibrium concepts is presented.

RIVER TERRACES

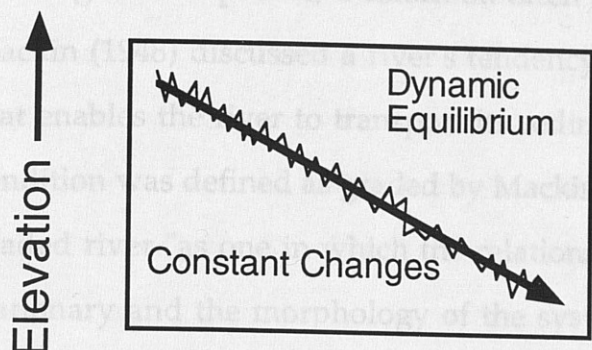
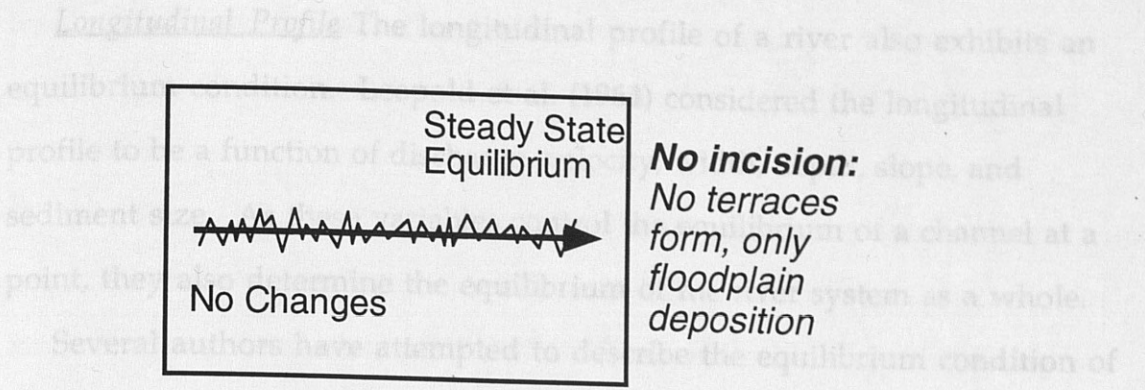
Conditions for Development of Terraces

Introduction River terrace formation is the result of floodplain abandonment by incision. A forcing, a input of energy into the river system, results in a change of the river dynamics that is accommodated by incision and the establishment of a new, lower floodplain. The forcing may either originate from changes in baselevel and tectonics that cause changes in the stream's potential energy or from changes in climate and human activity that produces changes in vegetation, water discharge, and sediment yield from hillslopes. As a dynamic system, some intrinsic threshold in the river system may need to be exceeded before incision and terrace formation can proceed.

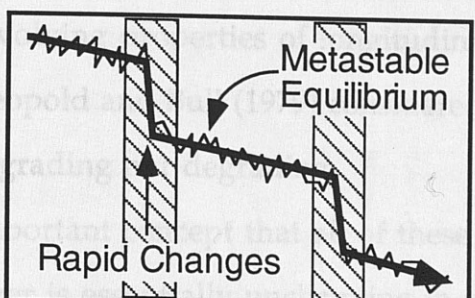
The formation of terraces requires degradation, a decrease in the channel elevation. Therefore, determining the reason for the channel elevation changes is important. Rivers are thought of as open systems which are controlled by self-arresting and self-enhancing feedback mechanisms (Knighton, 1984). Essentially, a river is either in equilibrium or else in a transitory state, attempting to obtain equilibrium. A river will remain in equilibrium, being controlled by self-arresting feedback mechanisms, until a threshold is exceeded. Thresholds are points in time that separate periods of aggradation or degradation (Bull, 1991). At that time when the threshold is reached, the river will, through self-enhancing feedback mechanisms, adjust to the new conditions and obtain a new equilibrium by either raising or lowering its channel. Therefore, terraces are formed when thresholds are exceeded. In order to understand why thresholds are exceeded, a review of fluvial system dynamics and equilibrium concepts is presented.

Fluvial Dynamics and Equilibrium Models of fluvial behavior were first developed through empirical analyses of factors affecting the fluvial morphology. Gilbert's (1880) original concepts of fluvial behavior, compiled from qualitative observations in the Henry Mountains of Utah, were the first to view the river as a system, where variables such as discharge, gradient, and sediment size were intimately related (Schumm, 1972). Gilbert's ideas laid the foundation for the later work of both geologists and engineers who used quantitative measurements from canals and rivers to develop the empirical relationships that are now widely accepted. For instance, Leopold and Maddock (1953) were able to show that at a given station, a river's width, depth, and velocity are related to its instantaneous discharge by power functions, a relationship described as the hydraulic geometry. Implicit in such a empirical relationship is the concept of equilibrium.

The hydraulic geometry represents either steady-state or dynamic equilibrium conditions. Steady-state equilibrium is the result of a fluctuation or oscillation about a mean equilibrium state (Figure 2.23). The mean annual discharge does not control the hydraulic geometry, but instead, floods with a return interval of about 2 years are responsible for the channel dimensions (Leopold and Wolman, 1957). In steady-state equilibrium, fluctuations may occur in the interdependent variables (width, depth, etc.), but the mean state of the system, the hydraulic geometry, remains constant. In dynamic equilibrium, the system constantly changes because incision is occurring, but the hydraulic geometry remains fairly constant.



No incision: No terraces form, only floodplain deposition



Constant incision: Either unpaired terraces or no terraces form, limited floodplain deposition

Time →

Periodic incision: Paired terraces form, floodplain deposition follows incision events

Figure 2.23: Types of Equilibria in River Systems. Equilibrium in rivers can be defined as steady-state, dynamic, or meta-stable, depending on the rate that the channel elevation changes. (Adapted from Knighton, 1985).

Longitudinal Profile The longitudinal profile of a river also exhibits an equilibrium condition. Leopold et al. (1964) considered the longitudinal profile to be a function of discharge, velocity, width, depth, slope, and sediment size. As these variables control the equilibrium of a channel at a point, they also determine the equilibrium of the river system as a whole.

Several authors have attempted to describe the equilibrium condition of the longitudinal profile, a condition often defined as "graded". For instance, Mackin (1948) discussed a river's tendency to achieve an equilibrium slope that enables the river to transport its sediment load; a river in such a condition was defined as graded by Mackin. Knox (1975, p. 92) defined a graded river "as one in which the relationship between processes and form is stationary and the morphology of the systems remains relatively constant" and an ungraded river "as (one) undergoing relatively rapid morphological change involving properties of longitudinal profiles and/or cross sections." Finally, Leopold and Bull (1979) considered a graded river as one that is neither aggrading nor degrading.

The important concept that all of these workers held in common is that a graded river is essentially unchanging in its longitudinal profile. However, the graded condition does not imply vertical stability. By Mackin's definition, it is conceivable for a river to maintain its grade while incising if the slope remains sufficient to transport the sediment load. Since Knox requires rapid adjustments for a river to be ungraded, gradual changes involving the longitudinal profile or cross section, such as a slowly incising river, would allow a river to remain graded. Knox associates a slow rate of change with a graded condition, but states that the ungraded condition may develop (p. 195) "after the cumulative effects of slowly changing environmental conditions

result in the breaking of a threshold of channel stability." Surpassing the threshold of channel stability leads to rapid adjustments and an ungraded condition. ~~resulting from climatic, tectonic, or human-use perturbations that affect~~ Leopold and Bull's (1979) definition is much narrower because they do not allow an incising river to be at grade; any changes in the channel elevation are characteristics of an ungraded river. Unlike Mackin, they do not equate slope with grade but instead believe that "changes in slope account for only a small part of the adjustment needed to achieve the balance necessary to transport the incoming load (p. 194; Leopold and Bull, 1979)." However, like Knox (1976), Leopold and Bull invoke exceeding thresholds as the cause of an ungraded river (p. 195): "the threshold of critical power is passed and the stream is not graded when the volume of load supplied is insufficient or is too large to be transported, and the channel bed aggrades or degrades."

~~Bull (1979) originally defined the threshold of critical power as the ratio of stream power to resisting power. Stream power is a measure of the energy available to transport material and is proportional to the discharge and slope of the river. Therefore, as either factor increases, the river is more capable of transporting sediment. Resisting power is a measure of the energy needed to transport the sediment delivered to the river and is proportional to the sediment size, sediment volume, and channel roughness. As any of these factors increase, the river will be less capable of transporting sediment.~~

If the threshold of critical power equals 1 (stream power = resisting power), the river will be in steady-state equilibrium, in the same sense it was with the hydraulic geometry, and the river is at grade by Leopold and Bull's definition. Although fluctuations may occur, the hydraulic variables adjust accordingly to transport the sediment supplied with the water available. However, Bull

(1991; p. 16) points out that a river "at the threshold of critical power or equilibrium may be highly susceptible to accelerated downcutting or alluviation resulting from climatic, tectonic, or human-use perturbations that affect discharges of water and bedload." Therefore, while this threshold represents the equilibrium condition, the stability of equilibrium is tenuous.

The ungraded condition occurs when the ratio of stream power to resisting power does not equal 1. If the ratio is less than 1 (stream power < resisting power), the river will aggrade because the load can not be transported. Rather than be transported through the system, the sediments will accumulate in the channel, raising the elevation of the channel. When the ratio is greater than 1 (stream power > resisting power), the river will incise because there is insufficient load. To compensate for the sediment deficit, the river will erode its bed and lower the elevation of the channel. In either case, once the channel establishes a new gradient where the stream power equals the resisting power, the river will return to steady-state equilibrium. Rivers in dynamic equilibrium are always ungraded.

If the self-enhancing feedback mechanisms responsible for returning the river to steady-state equilibrium change non-linearly with time, they represent a different type of equilibrium, meta-stable equilibrium (Figure 2.23; Knighton, 1984; Bull, 1991). In meta-stable equilibrium, once a threshold is exceeded in the dynamic system, the system adjusts to a new equilibrium state by rapid change. When the new equilibrium is established, the system returns to steady-state equilibrium. Therefore, if over time a river is in meta-stable equilibrium, it will be graded during the periods of steady-state equilibrium and ungraded during the intervening periods. These cycles will result in alternating periods of incision and floodplain aggradation and hence

terrace formation. The concept of meta-stable equilibrium satisfies all the definitions of grade previously described and provides a conceptual framework in which to consider terrace formation in Vermont.

Forcings There are no models that predict a river's response to changes and determine when the river will become ungraded. However by studying the river's aggradation and incision record, it is possible to determine when thresholds were exceeded and the mode of operation of the river changed. The next step, defining what caused the threshold to be exceeded, is accomplished by analyzing the variables in the threshold of critical power. For instance, consider the slope factor in the stream power. An increase in slope will cause an increase in the stream power and lead to incision while a decrease in slope will cause a decrease in the stream power and lead to aggradation. The magnitude and rate of the slope change is important in determining if a threshold was exceeded. Slope changes are the result of changes of the longitudinal profile and are triggered by changes in the relief of a basin due to baselevel, tectonic, and human forcings.

Baselevel is defined as the lowest elevation to which a river may erode. There are three types of baselevels: ultimate, basin-wide, and local. Ultimate baselevel is the elevation of eustatic sea level. Basin-wide baselevel is the elevation to which a basin-scale drainage network is graded and refers to the elevation of a lake or another river. A local baselevel, one contained within a drainage basin, is the elevation of a knickpoint. A bedrock knickpoint is often expressed as a waterfall and represents a sharp increase in the river's gradient.

An ultimate or basin-wide baselevel drop will initiate incision and knickpoint formation. The knickpoint will migrate upstream and diffuse at a rate determined by the erodibility of the river bed. Alluvium or other

unconsolidated sediments erode easily, and incision into these materials allows the knickpoint to proceed upstream unimpeded. Assuming homogenous material, the knickpoint will migrate a distance proportional to the amount of baselevel drop, with the amount of incision decreasing upstream. If the migrating knickpoint encounters resistant materials such as bedrock, the migration rate dramatically decreases and the knickpoint becomes the controlling baselevel for areas upstream.

Both tectonic and human forcings have the same affect as baselevel changes. Tectonic forcings are the result of vertical movements of the land which cause an increase or decrease of relief in the basin and change the river's slope. Aggradation will occur when the mouth rises relative to the headwaters and incision will occur when the headwaters rise relative to the river mouth. Humans also change the slope of the river by either lowering or raising the baselevel and by altering the sediment supply. The construction of a dam creates an artificially high baselevel and causes aggradation upstream, and channel modifications, such as channel straightening or channel dredging, create artificially low baselevels and cause incision upstream.

Knox (1975) viewed tectonic and baselevel forcings as low intensity and long duration processes which would not in themselves initiate an ungraded condition. With a constant uplift rate, the river would remain in steady-state (dynamic) equilibrium and the channel would constantly adjust to the changing gradient by altering its hydraulic geometry. For example, a meandering river would increase its sinosity to maintain a constant slope during uplift. Eustatic sea level changes, lake level changes, and knickpoint migration also normally occur at slow rates, allowing the river to make the

necessary adjustments to remain graded. Therefore, while changes in slope may make a river tend toward disequilibrium, the dynamic nature of the system may be able to absorb the forcing without crossing a threshold. Therefore, it is necessary to examine the other factors in the threshold of critical power to determine what causes a threshold to be exceeded.

The discharge factor (stream power) and the sediment supply and channel roughness factors (resisting power) are intimately related. They depend on the response of the drainage basin's hillslope subsystems to climate change and human activities. Climate change and human activities both affect the sediment yield and river discharge by altering vegetation patterns and hillslope stability. For instance, under a new climatic regime that may be characterized as wetter than the previous period, the discharge of the river could increase, thereby increasing the stream power and possibly causing incision. However, increases in the frequency and magnitude of storms may also cause the hillslopes to shed more sediments and in the end, increase the resisting power. The river-hillslope may easily adjust to climate changes without exceeding any thresholds if the frequency of bankful discharges does not increase. As previously mentioned, climate changes in the Northeast consist of more than a simple change in total precipitation. It is possible that Therefore, the nature of the climate change is an important factor in determining whether a threshold is exceeded.

Shifts in the upper atmospheric circulation patterns that Nevertheless over time, the vegetation stabilizes the slopes by increasing root mass and lowers the discharge by intercepting more rainfall and increasing evapotranspiration. The rate of response of the hillslope system is crucial to whether or not thresholds are exceeded.

According to Knox (1975), a river system will be stable or graded during a consistent climatic regime; once the climate regime changes, the river system will be unstable until it adjusts to the sediment yield and river discharge associated with the new dominant climate factors. Since channel morphology is controlled by the magnitude of moderate floods with ~ 2 year recurrence interval (Leopold and Wolman, 1957), a series of moderate to large floods, rather than a single flooding event, are needed for the channel to adjust to the new climatic conditions. Therefore, a climatic regime with an increase in the frequency and magnitude of storms is necessary for the stream power to increase, the threshold to be exceeded, and terraces to form.

Given that each basin is unique, each will have an individual response to the floods. The subsystems in the basin will all respond by varying degrees to a single storm; sediment or water will not be delivered to the river uniformly. The same storm may not affect all rivers in the same manner, but over time the net effect will be the same. Therefore, rivers' response to climate changes will likely appear synchronous across a region on longer time scales.

Terrace Classification

Terraces are classified according to the genesis of the floodplain and the rate of incision. Three types of river terraces (fill, fill-cut, and strath terraces) are recognized and can be separated into either depositional or erosional terraces (Figure 2.24). A fill terrace is a depositional terrace. If a river aggrades to fill its valley with alluvium (vertical accretion deposits) and then incises, a fill terrace will be formed. The surface of depositional terraces represents the highest extent of aggradation. Fill-cut and strath terraces are erosional

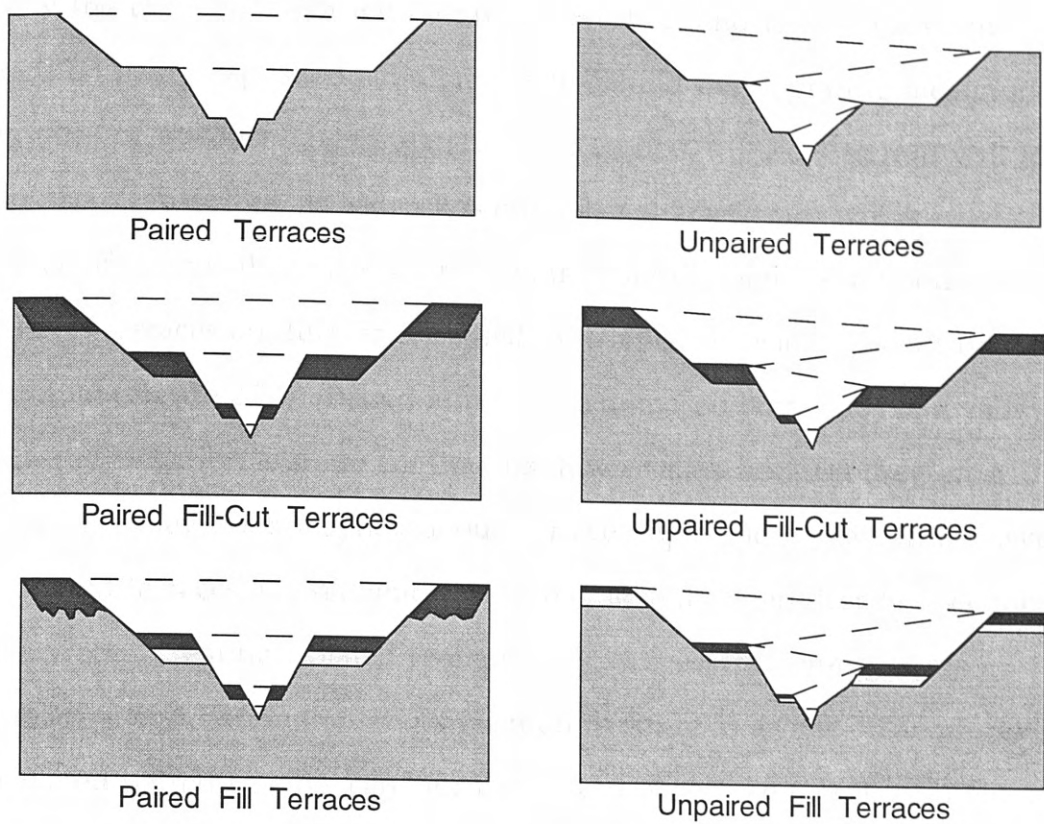


Figure 2.24: Types of River Terraces. Paired terraces are found on both sides of a valley at the same elevation. Unpaired terraces do not have an equivalent on the other side of the valley. Paired fill-cut terraces form during steady-state periods in meta-stable equilibrium while unpaired fill-cut terraces form during dynamic equilibrium. Both paired and unpaired fill terraces occur when aggradation temporarily becomes the dominant process.

terraces. Both develop when a river erodes laterally and cuts a planar surface below the channel, often with alluvium (vertical and lateral accretion deposits) being deposited simultaneously behind the migrating meanders. If alluvium or unconsolidated materials are eroded, a fill-cut terrace will form once the river incises. If bedrock is eroded, a strath terrace will form. The surface of erosional terraces represents the former height of a floodplain.

River terraces are further classified by whether incision was episodic or continual (Figure 2.24). Paired terraces are found on both sides of a valley at the same elevation and are continuous down valley because they once formed a valley floor, a synchronous surface. Episodic downcutting carves the paired terraces, subsequent lateral river activity often destroys sections of the terraces, creating isolated remnants. However, the remnants are correlative and define the river's position in space at a time. Therefore, correlated paired terraces can be used to reconstruct the river's gradient and represent a time marker in landscape development. Unpaired terraces do not have a correlative terrace on the other side of a valley because they are produced between periods of continuous incision and lateral channel migration (dynamic equilibrium). Presumably, the pauses in valley degradation occur independent of one another along a river. Since unpaired terraces are isolated surfaces that never formed a synchronous valley floor, they are inappropriate for reconstructing the river's gradient.

Development of both erosional and depositional terraces can be understood within the framework of meta-stable equilibrium. Fill-cut and strath terraces are interpreted to develop during periods of steady-state equilibrium, where the threshold of critical power equals 1, the river maintains an equilibrium profile, channel elevation does not change, and the

river migrates laterally. If the river erodes alluvium and builds a floodplain, a fill-cut terrace develops, and if the river bevels bedrock, a strath terrace forms. The thickness of the terrace deposits should not exceed the expected scouring depth of the river. Once a threshold is exceeded, the river will incise until a new level, one at which the threshold of critical power equals 1, is reached, and the river will once again be in steady-state equilibrium. Bull (1990) considered strath and fill-cut terraces to be primarily a tectonic landform.

Fill terraces are interpreted to develop between periods of steady-state or dynamic equilibrium, where stream power < resisting power. A change in river dynamics allows aggradation to occur in a previously equilibrated system. Aggradation will continue until a new level, one at which the threshold of critical power equals 1, is reached. The thickness of the deposits are not related to the present channel scouring depth because the mode of operation is different. Additionally, the terrace deposits may overlie an irregular surface because the river has not beveled the valley bottom. Bull (1990) considered fill terraces to be primarily a climatic landform.

Interpretation of Terrace Remnants as Related to Tilting

River terrace remnants have been utilized to document and measure active and recent tilting at the Mendicino triple junction of California (Merrits and Vincent, 1989; Merrits et al., 1994), the domal uplifts in the lower Mississippi River Valley, (Burnett and Schumm, 1983) and the Adirondack uplift in the Champlain Basin (Treadwell and Kneupfer, 1988). The river terrace surface is taken as a time marker that represents the gradient of the river at the time of formation. Once a terrace is formed (i.e., the river incises

and the surface no longer receives deposition), it becomes available to record vertical land movements. If the magnitude of uplift is constant across a region, the terrace gradient will remain constant. However, if there is differential uplift, such as in glacio-isostatic rebound, the terrace gradient will change over time. As tilting progresses, the river terrace is "warped" and the terrace gradient will increase or decrease by an amount equal to component of tilting in the direction of the river (Figure 2.25). By surveying river terrace elevations and plotting their longitudinal profiles, terrace gradients can be measured and taken as a means to quantify crustal tilting if an initial river profile, often the present river gradient, is assumed.

Interpretation of Terrace Remnants as Related to Environmental Changes

Comparisons of river terrace and pollen records (e.g., Brakenridge, 1980; Scully and Arnold, 1981; Knox, 1983; Arbogast and Johnson, 1994) show that the periods of incision or aggradation often occur coincident with the climate changes interpreted from the pollen records.

Brakenridge (1980) defined periods of floodplain stability (deposition) and instability (erosion) for the Pomme de Terre River in Missouri during the Holocene based on the distribution of 21 radiocarbon dates in six alluvial units. When the Pomme de Terre data were compared to alluvial chronologies from North America and Europe, Brakenridge found several intervals during the past 5000 ^{14}C yrs. where erosion was synchronous across the Northern Hemisphere. These episodes of erosion were also coincident with the advance of alpine glaciers. Brakenridge concluded that the increase in precipitation that lead to the advance of glaciers also caused widespread stream erosion. A strong meridional component of the circumpolar vortex

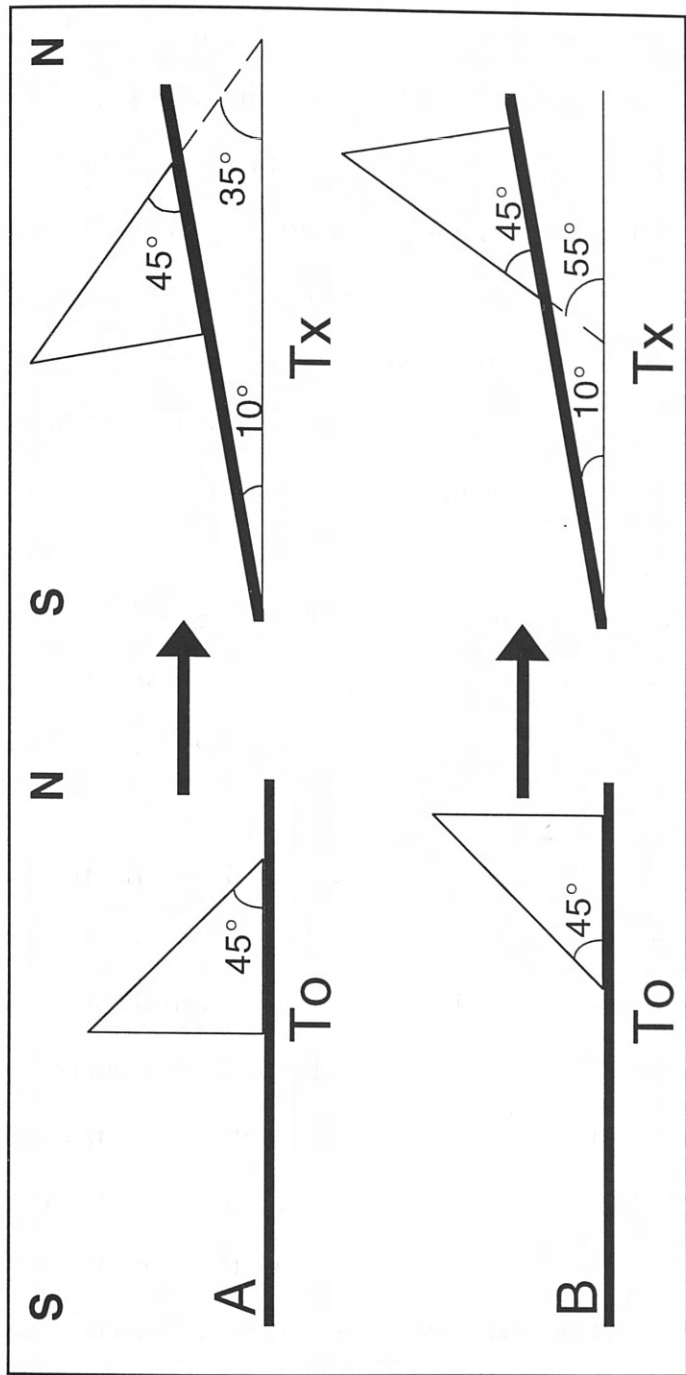


Figure 2.25: Effect of Glacio-isostatic Rebound on Terrace Gradients. Initial terrace/river gradient at T_0 is differentially tilted at T_X .
 A) A north-flowing stream's gradient will decrease.
 B) A south-flowing stream's gradient will increase. Knowing the initial gradient allows the tilt to be measured.

could create the cooler and wetter conditions necessary to cause glacial advances in the mountains and stream erosion in the lowlands. This is the same mechanism first proposed by Knox (1975) to explain climate-controlled periods of erosion.

Knox (1975) subdivided the Holocene into fluvial episodes beginning at 9800, 8500, 4600, and 2500 ^{14}C yr B.P. based on a statistical analysis of radiocarbon dates from alluvial deposits in the northern hemisphere mid latitudes. The logic behind these divisions was based on the premise that periods of alluviation should preserve organic matter whereas periods of stability or incision should contain little organic matter. Knox found that timing of his fluvial episodes was similar to that of climatic episodes proposed by Wendland and Bryson (1974), beginning at 10,030, 9300, 8490, 5060, and 2760 ^{14}C yr B.P. Therefore, it is reasonable to assume that terraces which formed at the same time as climate changes are probably formed because the new climatic regime changed the river dynamics.

Local Studies of River Terraces

The results of two local studies, one examining terrace tilting due to the recent doming of the Adirondacks and one examining river incision due to glacio-isostatic rebound, suggest that river terraces can be used to interpret crustal movements in the Champlain Basin. The terrace chronologies provided by these studies also present an opportunity to test the synchronicity of area terrace chronologies.

Treadwell and Knuepfer (1988) established a dated terrace chronology for the Ausable River, western Champlain Basin, and used their chronology to measure the recent tectonic tilt. The Adirondack Mountains are a NE-SW

trending domal structure that is believed to be actively uplifting (Barnett and Isachsen, 1980). The Ausable River flows northeast down the northeastern flank of the uplift and therefore is oriented parallel to the maximum tectonic tilt. Up to eight postglacial terraces of the Ausable River were surveyed and correlated along the river. The longitudinal profile of the terraces showed that the terraces diverged upstream from each other and from today's river profile. This is the expected result if the upstream reaches were uplifted higher than the downstream reaches, as would be the case in domal uplift for this river.

In addition to domal uplift, the Adirondacks have been uplifted due to glacio-isostatic rebound similar to the surrounding regions (i.e. Clark and Karrow, 1984). Chapman (1937) presented a glacio-isostatic uplift plane for the Champlain Valley based on the elevations of the shoreline features which formed in proglacial lakes following deglaciation. Treadwell and Knuepfer considered this plane to represent the tilt of the oldest terraces and calculated the expected glacio-isostatic tilt for the younger terraces based on an exponential decay model of glacio-isostatic rebound.

In order to measure the magnitude and rate of domal uplift, Treadwell and Knuepfer subtracted the calculated component of glacio-isostatic rebound for a terrace of a given age from today's river gradient to yield the amount and direction of tilting since each terrace formed. By using the ages of the terraces, long term average rates of tilting were calculated to be 0.05 mm/km per year, a result similar to the result obtained from geodetic surveys of 0.06 mm/km per year. Treadwell and Knuepfer concluded that post-glacial river terraces are sensitive to tectonic tilting.

In another local study, Brakenridge et al. (1988), studying a site along the

Missisquoi River in the northern Champlain Basin, delineated three terrace surfaces above the modern flood plain. The deposits of the terraces were distinguished by the soil development, grain size, and archeological materials. On the basis of 14 radiocarbon dates, Brakenridge et al. determined that T2 was deposited prior to 8000 ^{14}C yr B.P., T1 was deposited between 6400 and 500 ^{14}C yr B.P., and T0 was deposited since A. D. 1860. The highest terrace, T3, was not dated, but it was interpolated to be deposited around 10,000 ^{14}C yr B.P.

The history of this site is characterized by a period of rapid incision prior to 8000 ^{14}C yr B.P. and a period of slow, but episodic, lateral migration, paired floodplain construction, and valley widening since 8000 ^{14}C yr B.P. until European settlement. During historic times, incision followed by the deposition of T0 occurred. By plotting the distance of the radiocarbon samples from the present channel, Brakenridge et al. demonstrated that the lateral migration rate varied from 0-4 m/100 yr since 8000 ^{14}C yr B.P. A similar plot of elevation of the channel versus age showed that the average incision rate decreased by 8000 ^{14}C yr B.P. Both incision and lateral migration rates increased after European settlement.

Brakenridge et al. considered the decrease in incision rate at 8000 ^{14}C yr B.P. to be evidence that glacio-isostatic rebound had ended by that time, similar to a time frame proposed by Hutchison et al. (1981) based on an undeformed or horizontal unconformity in the sediments of nearby Lake George that was formed before 7000 ^{14}C yr B.P. Several lateral unconformities were present in T1, suggesting that the lateral migration of the channel was episodic; the distribution of the radiocarbon dates supports this interpretation. The change of land cover in the basin, from forest to agriculture, was cited by

Brakenridge et al. as a probable cause of increases in sedimentation and lateral migration during historic times.

Summary

Rivers are dynamic systems which exist in a steady state over time as long as the threshold of critical power is satisfied (stream power = resisting power). A river in steady-state equilibrium is also at grade. Over a longer time scale, the river is in meta-stable equilibrium if it periodically and episodically becomes ungraded. A river will become ungraded when forcings cause the stream power to increase or decrease relative to the resisting power. Paired strath and fill-cut terraces form during periods of steady-state equilibrium separated by periods of incision and fill terraces form between periods of steady-state or dynamic equilibrium. Unpaired terraces form during periods of dynamic equilibrium.

Several measurements were taken in order to define the river terrace surface. In general, downcut and cut edges of each terrace, as defined by the change in slope, and several intra-terrace points were measured along-profile lines. Ideally, a cross-section would be normal to the valley trend, but this is sufficient to measure the terrace elevation. However, the areal extent of the terraces is variable because of the past and present meandering patterns of the rivers. Therefore, several transects must be used to adequately sample the terraces at any one site.

All measurements were correlated either to established benchmarks or to prominent contour lines. When a benchmark was located nearby a location, it was surveyed. Later, the elevations of the survey data were adjusted to the

CHAPTER 3: METHODS AND DATA

My field work defined the position of river terraces in space through time. It involved surveying, trenching, and dating river terraces. In this chapter, I describe my three methods and present my results.

SURVEYING

Methods

Pentax total station survey equipment was used to provide the spatial control because elevations of terraces can be measured quickly, precisely and accurately. Elevations and X-Y coordinates (easting and northing) were measured for each point and recorded by a data collector connected to the total station. Each location was measured independently, with the first point given an arbitrary designation of 1000, 1000, 100 (northing, easting and elevation in meters). Surveyed elevations were later reconciled to known datums as described below.

Several measurements were taken in order to define the river terrace surface. In general, the inner and outer edges of each terrace, as defined by the breaks in slope, and several intra-terrace points were measured along profile lines. Ideally, a cross-valley profile, normal to the valley trend, would be sufficient to measure the terrace elevations. However, the areal extent of the terraces is variable because of the past and present meandering patterns of the rivers. Therefore, several survey lines were needed to adequately sample the terraces at any one site.

All measurements were correlated either to established benchmarks or to prominent contour lines. When a benchmark was located nearby a location, it was surveyed. Later, the elevations of the survey data were adjusted to the

elevation of the benchmark, with the elevations of the benchmarks taken either from USGS 7 1/2' quadrangles or from the United States Coastal and Geodetic Survey database. If no benchmarks were available, then the elevations were tied to a prominent contour line on the USGS 7 1/2' quadrangle. Usually, the chosen contour line lay on a wide terrace with little variation in elevation. Therefore, the accuracy of the final or "true" elevation differs by location, but for a given location, the relative elevations of terraces are internally consistent.

Terraces were surveyed along transects that best captured the terrace remnants, without respect to valley orientation. Therefore, the transect lines rarely were perpendicular or parallel to valley trend or even in a constant orientation. In order to standardize the survey data, the elevations were projected to a best fit plane along each survey line to construct the cross valley profiles. The cross valley profiles show the vertical relief and horizontal extent of terraces (Figure 3.1). Exaggerated ten times to accentuate the relief between terraces, the profiles also illustrate the relief of the terrace surface and the difficulty of assigning an average elevation to a given terrace.

The cross valley profiles are used to correlate the terraces between locations to construct the longitudinal profiles. The number of terraces, elevation above river, and relief between terraces were the main criteria used to correlate the terraces.

Longitudinal profiles of the terraces and the present river were constructed for each valley. Longitudinal profiles are used to measure the gradients of river terraces. Elevations of the river, taken from USGS 7 1/2' Quadrangles, and elevations of the terraces, compiled from the survey data and cross valley profiles, were projected onto a plane of the valley trend.

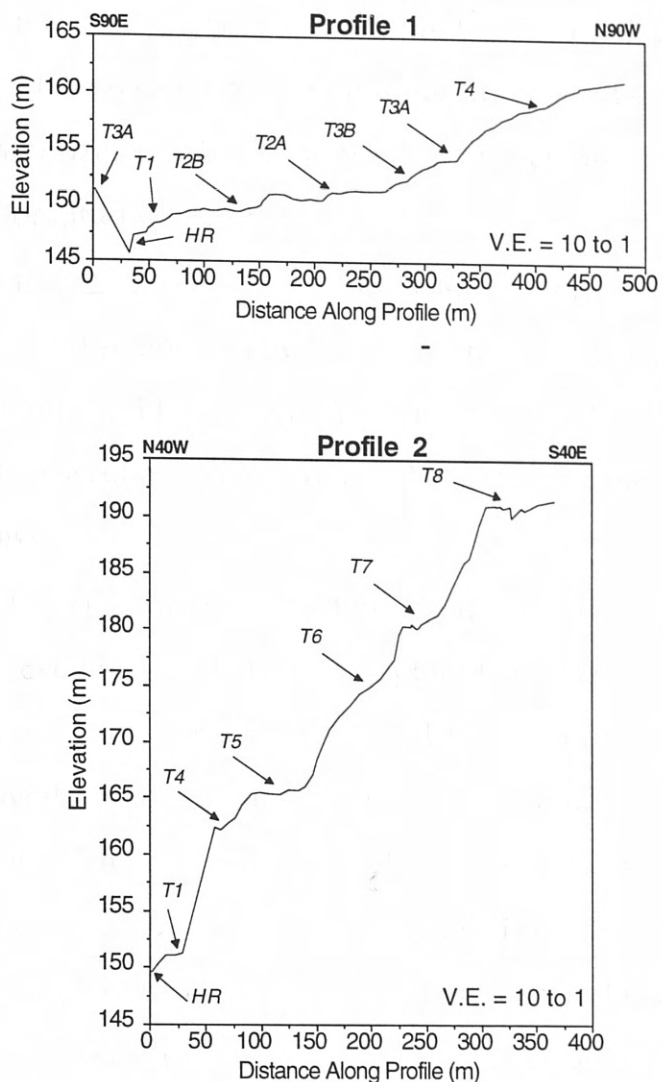


Figure 3.1: Examples of Cross-valley Profiles. Both profiles are from the Huntington Valley. Profile 1 shows a section of low-relief terraces that developed just downstream of the terraces in Profile 2.

Survey Data: Huntington River

Cross Valley Profiles Forty-five cross valley profiles were constructed from the 21 survey locations in the Huntington Valley (Figure 3.2). The survey data and profiles for all the locations are presented in Appendix B. Table 3.1 summarizes the data from the cross valley profiles and is used to generate the longitudinal profile.

Longitudinal Profiles The Huntington River longitudinal profile (Figure 3.3) consists of two segments (Figure 3.2). The longest segment trends N6W from the southern divide in Buels Gore north to the Moulthrop Property in Richmond. The second segment trends N61E from there to the Winooski River in Jonesville.

The longitudinal profile shows both the measured terrace elevations and the projected lake levels of Lake Huntington, Lake Mansfield II, and Lake Coveville. The highest terraces, T10 and T9, south of the Hollow Brook Valley are fluvial terraces grading into the lakes controlled by the Hollow Brook threshold. The elevations at Hollow Brook are minimas due to incision which likely occurred at the spillway. These highest terraces north of Hollow Brook are lacustrine shoreline deposits from the same lake levels. The first fluvial terrace to extend to the mouth of the Huntington Valley is T8, where it intersects the projected elevation of Lake Coveville.

Below T8 are a series of terraces that grade into the Winooski River in Jonesville. The elevations of T7 and T6 at the river's mouth are the interpolated elevations of fluvial terraces grading into Lakes Fort Ann I and II, respectively. T5 in Jonesville corresponds well with the interpolated elevation of fluvial terraces grading into the Upper Marine.

Table 3.1: Terrace and River Elevations for Huntington River Longitudinal Profile

Survey Location	Distance Upstream (km)	T10	T9	T8	T7	T6	T5	T4A	T3A	T2A	T1A	River
MOUTH	0.00		210.60	188.00	153.00	143.00						94.48
JON-2	0.38								108.17	104.21		
JON-1	0.59						126.57	122.43	108.81			
320	0.97											97.53
340	1.51											103.63
360	2.03											109.72
380	2.29											115.82
PAQ	2.53				176.72	170.66	137.14	133.22	129.92	125.21		118.49
400	2.64											121.91
PARO	2.80							138.73	136.06	129.08		
420	2.87											128.01
440	2.94											134.11
460	3.44											140.20
ALD2	3.82							158.81	153.89	151.07	147.05	
ALD1/3	4.05							161.10		152.17	149.53	145.86
480	4.21											146.30
ALD1-1	4.25			190.98	180.44	176.25	165.57	162.50				151.25
ALMO	4.27		209.53	191.10	180.68	175.10	165.93	162.12	158.70	155.11	151.75	
ROAD	4.38			191.46								
MOULA	4.48						166.84	162.80		157.81	154.20	
500	4.63											152.39
500	4.63											152.39
MOULB	4.96	217.98	206.36	192.49			171.65					
520	5.06											158.49
TOWR	5.37			192.65		182.06	172.64		167.66	164.17		
AUD1A	5.52							171.04	167.97	165.16	162.74	
AUD1B	5.74						173.49		170.79	167.33	165.26	163.89
540	5.86											164.58
AUD2/3	6.00						174.86	173.58		168.72		
560	6.80											170.68
HR2-1	7.55		206.35		191.98		183.55	181.21	180.29	177.30	176.40	
HR2-2	8.00	215.45	204.95		193.83							
580	8.08											176.78
600	8.89											182.87
620	9.95											188.97
HB	10.20	213.00	204.00	201.70	199.70	196.00						
640	10.72											195.06
660	11.21											201.16
SAAL	11.42	224.74	216.24	213.92	212.08	208.74			206.84	206.21		
680	12.44											207.25
700	13.24											213.35
HR4	13.93	238.86	231.57	227.86	226.52	220.99			218.57	216.56	214.30	
720	14.58											219.45
740	15.01											225.54
760	15.45											231.64
780	15.93											237.73
800	16.41											243.83
820	16.72											249.92
840	17.01											256.02
860	17.29											262.12
880	17.37											268.21
900	17.53											274.31
920	17.80											280.40
940	17.90											286.50
960	18.09											292.59
980	18.49											298.69
1000	18.85											304.79
1020	19.04											310.88
HR3	19.11	335.41	323.13							315.38		
1040	19.38											316.98
1060	19.81											323.07
1080	20.20											329.17
1200	21.39											365.74
1300	22.20											396.22
1400	22.92											426.70
1500	23.59											457.18
DIVIDE	23.64											460.23

Survey locations (ALMO) correspond to cross valley profiles and survey locations (640) correspond to river elevations from USGS 7.5' quadrangles. See Figure 3.2 for survey locations and Figure 3.3 for longitudinal profile.

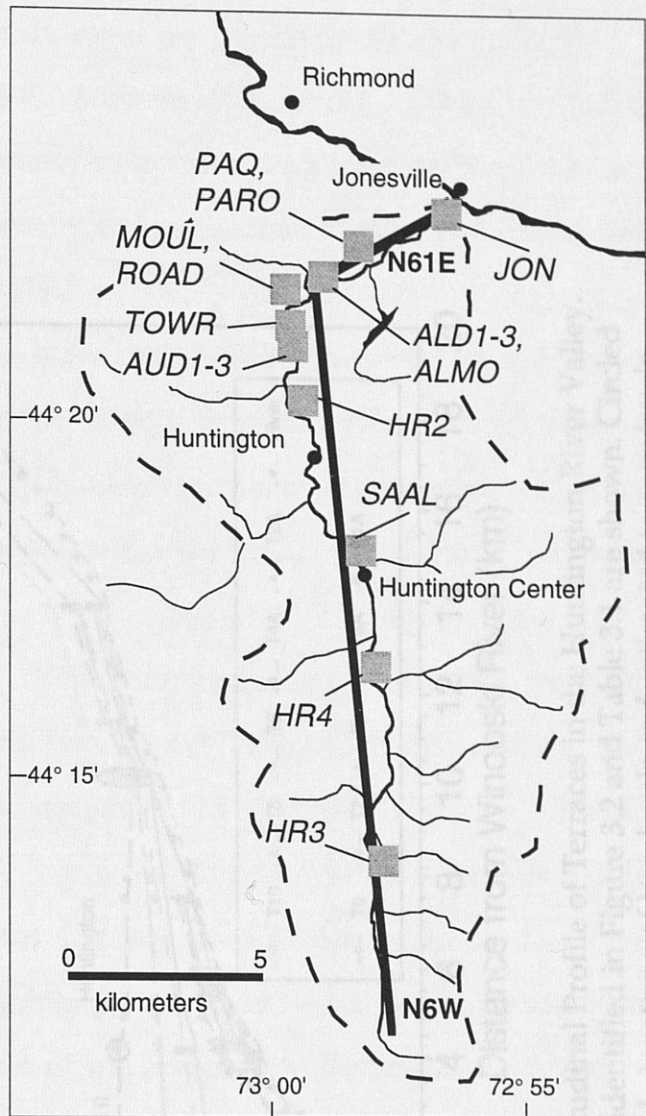


Figure 3.2: Map of Survey Locations and Longitudinal Profile in the Huntington River Basin. Base map from USGS 1:100,000 sheet.

The number of terraces at a location varied with position in the basin. At the farthest station upstream, HR3, four terrace levels were apparent and presumably represent different periods of formation throughout postglacial times. In contrast are the terraces found at the ADD survey locations. Several minor terraces are present, up to 12 levels are distinguishable. These minor terraces apparently merge upstream and they become nearly indistinguishable by HR2.

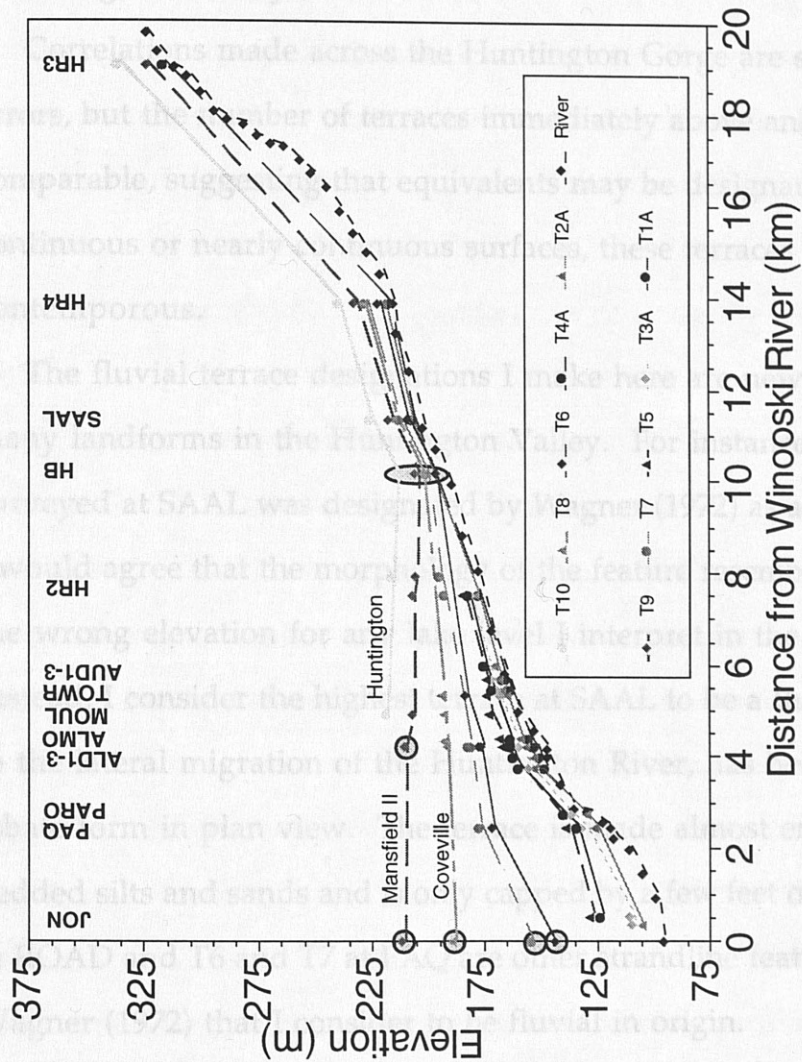


Figure 3.3: Longitudinal Profile of Terraces in the Huntington River Valley. Survey locations identified in Figure 3.2 and Table 3.1 are shown. Circled areas are projected elevations of baselevels and estimated terrace levels. See text for discussion.

The number of terraces at a location varied with position in the basin. At the farthest station upstream, HR3, four terrace levels were apparent and presumably represent different periods of formation throughout postglacial times. In contrast are the terraces found at the ALD survey locations. Several minor terraces are present, so up to 12 levels are distinguishable. These minor terraces apparently merge upstream and they become nearly undistinguishable by HR2.

Correlations made across the Huntington Gorge are subject to the most errors, but the number of terraces immediately above and below the gorge is comparable, suggesting that equivalents may be designated. If not once continuous or nearly continuous surfaces, these terraces may at least be contemporaneous.

The fluvial terrace designations I make here are new interpretations of many landforms in the Huntington Valley. For instance, the highest terrace I surveyed at SAAL was designated by Wagner (1972) as a delta of Brush Brook. I would agree that the morphology of the feature resembles a delta, but it is at the wrong elevation for any lake level I interpret in the Huntington Valley. Instead, I consider the highest terrace at SAAL to be a fluvial terrace that, due to the lateral migration of the Huntington River, has been carved into a lobate form in plan view. The terrace is made almost entirely of rhythmically bedded silts and sands and is only capped by a few feet of fluvial deposits. T8 at ROAD and T6 and T7 at PAQ are other strandline features designated by Wagner (1972) that I consider to be fluvial in origin.

almost coincident with the lowest terrace. I have designated the lowest terrace as T6, younger than T7, to account for the fact that it has been incised in the past 60 years.

Survey Data: Little River

Cross Valley Profiles Twenty-two cross valley profiles were constructed from the six surveys locations in the Little River Valley (Figure 3.4). The profiles and survey data are presented in Appendix C. Table 3.2 summarizes the data from the cross valley profiles and is used to generate the longitudinal profile.

Longitudinal Profile The Little River longitudinal profile (Figure 3.5) is a single line trending N30E from the Winooski River northwest of Waterbury to the northern divide northeast of Stowe (Figure 3.4). More than six kilometers of the profile is obscured by the presence of the Waterbury Dam. The dam was one of several built during the 1930's for flood control along the Winooski River and has impounded the river nearly to the Lake Coveville level.

Bathymetry maps were not located for Waterbury Reservoir, but a pre-dam USGS 15' quadrangle was. The difference between the current river profile and the old river profile on the longitudinal profile (taken from the 15' quadrangle) implies that significant river adjustments occurred since the dam was built. Although the old profile may be somewhat in error due to poor elevation control, it does reveal that upstream of the dam, the river has aggraded and immediately downstream of the dam, the river had incised. The aggradation at the north end of the reservoir has likely buried several terrace levels. Presently, the former T4 surface likely receives deposition during flooding events. In contrast, the old river profile below the dam is almost coincident with the lowest terrace. I have designated the lowest terrace as T0, younger than T1, to account for the fact that it has been incised in the past 60 years.

Table 3.2: Terrace and River Elevations for Little River Longitudinal Profile

Survey Location	Distance Upstream (km)	T9	T8	T7	T6	T5A	T5B	T4	T3	T2	T1	T0	River	Old River
Mouth	0.00	224.85	201.92	179.32									119.90	
LR2-5	0.16										128.93	124.96		
LR2-4	0.22							142.52			124.70	121.45		
LR2-3	0.59				156.03							125.64		
LR2-2	0.81					155.23								
400	0.85												121.95	
400	0.85													
LR2-1	0.98				157.50	155.77	148.44							121.95
LR1.3-8	1.20									130.86	130.03	126.23		
LR1.3-7	1.47					158.32		149.65				129.19	125.61	
LR1.3-4,5,6	1.64						156.98			135.41	131.59	129.22	128.54	
420	1.75												128.05	
LR1.3-3	1.89						158.07				133.14		129.35	
LR1.3-2	2.04				163.99	160.17	158.39				133.47		130.01	
420	2.08													
LR1.3-1	2.36							147.43			135.51	134.16		
440	2.36													134.15
LR1.2-1	2.64													
LR1.2-2	2.69									139.63	138.10	136.23		
LR1.1-3	2.73					161.07				140.19		136.93		
LR1.1-2	2.90						159.90		148.61	140.47	138.35			
LR1.1-1	3.00				164.69	161.40	160.40	154.78			139.39	138.22		
440	3.11											138.96	134.15	
LR7	3.19				164.97									
460	3.21												140.24	
480	3.22												146.34	
500	3.25												152.44	
520	3.27												158.54	
540	3.29												164.63	
560	3.31												170.73	
580	3.36												176.83	
Reservoir	3.40												179.70	
460	3.65													140.24
480	4.11													146.34
500	4.87													152.44
520	6.04													158.54
540	7.03													164.63
560	8.24													170.73
LR6	9.33				188.12	185.71	182.68	182.68	180.95				179.70	
580	9.81													176.83
600	10.09													
620	11.13												182.93	
600	11.45													189.02
620	11.57													
640	11.57													195.12
640	12.49													
LR3-2	12.57				207.76	205.72			198.11					
LR3-1	12.70					205.78			199.00				196.31	
660	14.15													201.22
Lake Mansfield II	14.32	234.44	211.52											
680	14.50													207.32
700	15.33													213.41
720	18.12													219.51
740	19.35													225.61
LR4	19.51	236.94	228.99	227.80	226.76									226.00
Divide	20.53	238.59												230.00

Survey locations (LR2-1) correspond to cross valley profiles and survey locations (640) correspond to river elevations from USGS 7.5' quadrangles. Old river is from USGS 15' quadrangle. See Figure 3.4 for survey locations and Figure 3.5 for longitudinal profile.

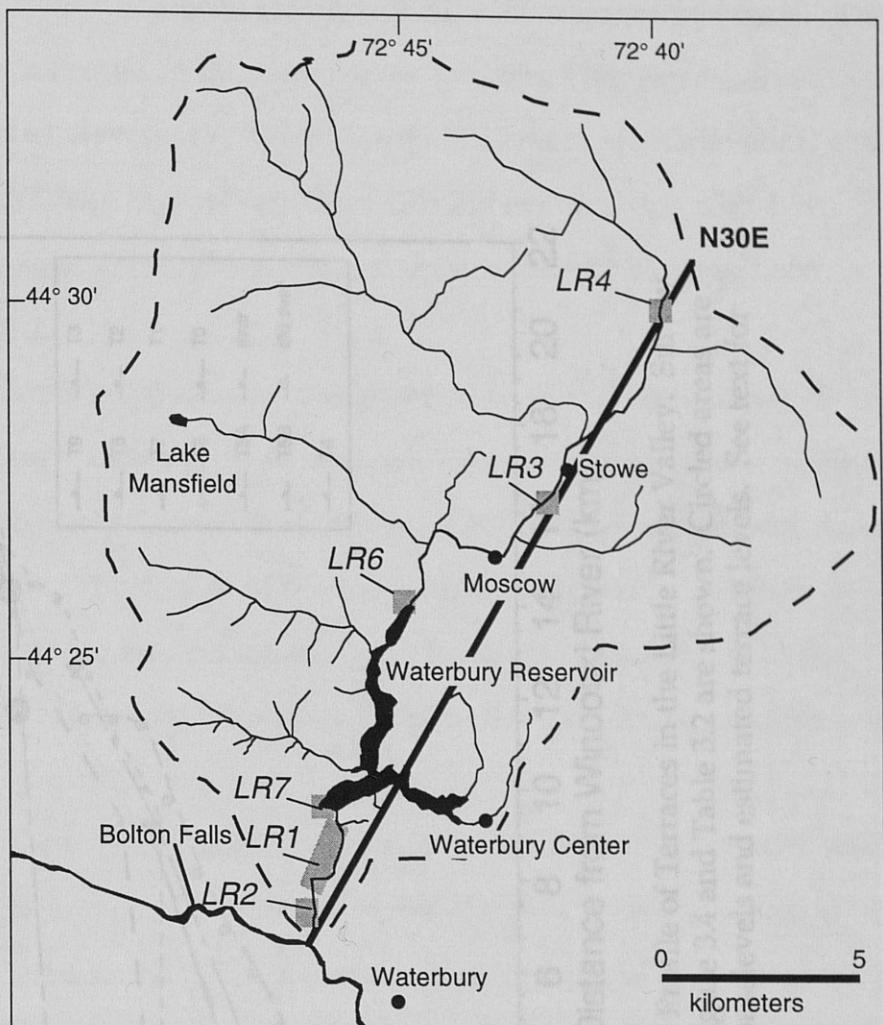


Figure 3.4: Map of Survey Locations and Longitudinal Profile Location in the Little River Basin. Base map from USGS 1:100,000 sheet.

The projected elevations of Lake Mansfield I, Lake Mansfield II, and Lake Coveville shown on the profile correlate well with measured terraces. The highest feature surveyed at the upper-most location, LR4, corresponds well with the projected elevation of Lake Mansfield I and is at an elevation well above the divide. The highest terrace at LR3 either correlates with Lake

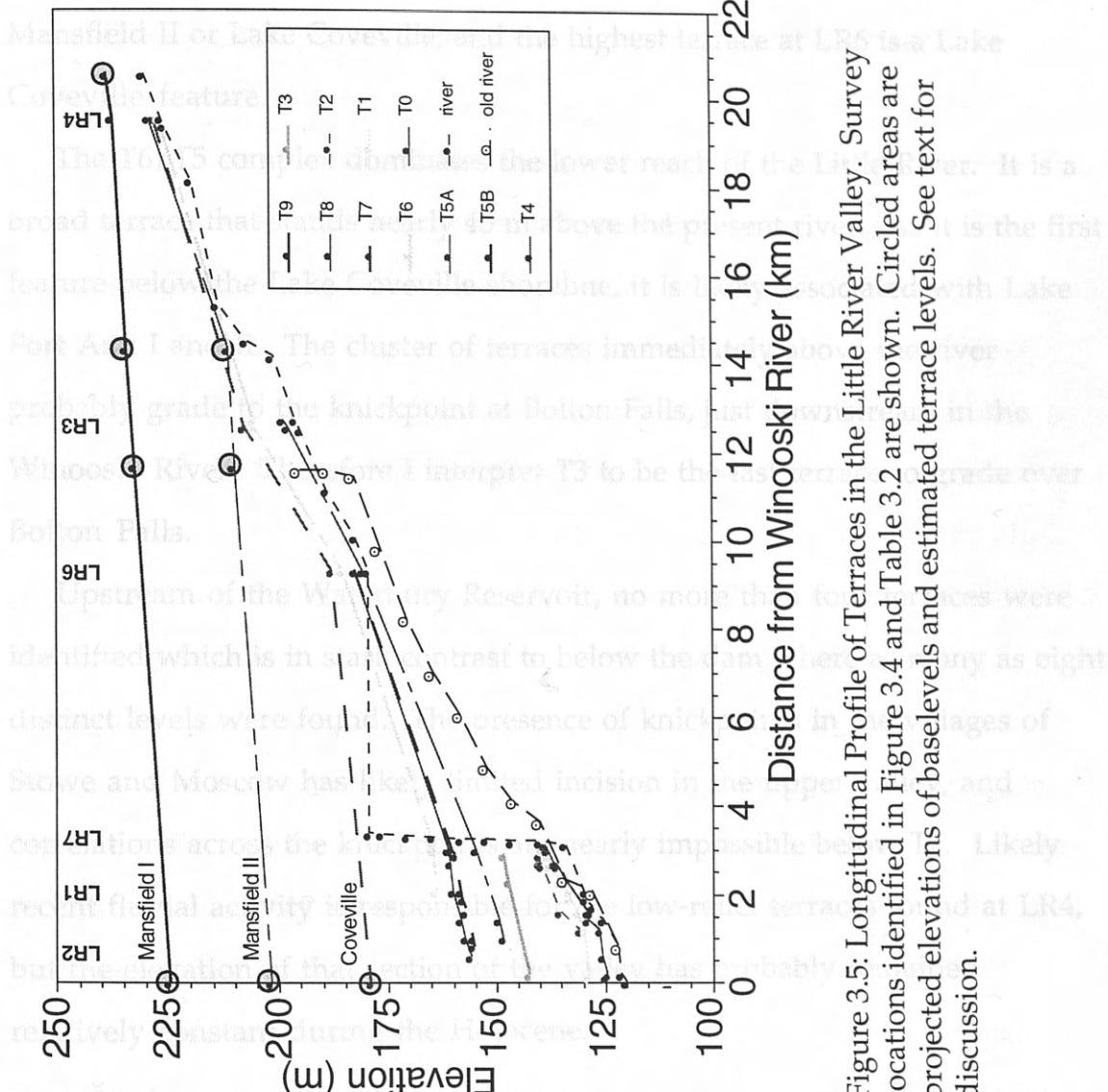


Figure 3.5: Longitudinal Profile of Terraces in the Little River Valley. Survey locations identified in Figure 3.4 and Table 3.2 are shown. Circled areas are projected elevations of baselevels and estimated terrace levels. See text for discussion.

The projected elevations of Lake Mansfield I, Lake Mansfield II, and Lake Coveville shown on the profile correlate well with measured terraces. The highest feature surveyed at the upper-most location, LR4, corresponds well with the projected elevation of Lake Mansfield I and is at an elevation well above the divide. The highest terrace at LR3 either correlates with Lake Mansfield II or Lake Coveville, and the highest terrace at LR6 is a Lake Coveville feature.

The T6/T5 complex dominates the lower reach of the Little River. It is a broad terrace that stands nearly 40 m above the present river. As it is the first feature below the Lake Coveville shoreline, it is likely associated with Lake Fort Ann I and II. The cluster of terraces immediately above the river probably grade to the knickpoint at Bolton Falls, just downstream in the Winooski River. Therefore I interpret T3 to be the last terrace to grade over Bolton Falls.

Upstream of the Waterbury Reservoir, no more than four terraces were identified which is in stark contrast to below the dam where as many as eight distinct levels were found. The presence of knickpoints in the villages of Stowe and Moscow has likely limited incision in the upper valley, and correlations across the knickpoints are nearly impossible below T7. Likely recent fluvial activity is responsible for the low-relief terraces found at LR4, but the elevation of that section of the valley has probably remained relatively constant during the Holocene.

As in the Huntington and Little River Valleys, the presence of knickpoints complicates the correlations of the lowest terraces. Vajin (1977) correlates terraces across the gorge in Moretown, but again, these correlations are "local time equivalents rather than continuous surface".

Survey Data: Mad River

The surveying of the Mad River was performed with Chris Valin, in conjunction with his Senior Theis research. The results, first presented in his thesis (Valin, 1997), are also presented here so that they may be compared with the results from the other valleys.

Cross Valley Profiles Sixteen cross valley profiles were plotted with the survey data from thirteen locations (Figure 3.6). The Mad River data are presented in Appendix D and in Valin (1997). Table 3.3 summarizes the data from the cross valley profiles and is used to generate the longitudinal profile.

Longitudinal Profiles The Mad River longitudinal profile consists of two segments (Figure 3.7). The first segment trends N10E from the southern divide in Granville north to the Irasville (Figure 3.6), and the second segment trends N40E from there to the Winooski River in Middlesex.

In contrast to the other studied valleys, most of the terraces in the Mad River Valley can be traced along the entire length. Two exceptions are T9 and T8. The highest terrace, T9, is only present in the town of Warren and presumably can be found south of there as well. It correlates with the shoreline elevation of Lake Winooski previously identified in Warren by Larsen (1987b) and is probably part of a delta complex. T8 can be traced from Warren to Moretown, where it grades into Lake Mansfield I.

Several of the lowest terraces were not surveyed closer to the mouth of the Mad River because of limited access to the river. As in the Huntington and Little River Valleys, the presence of knickpoints complicates the correlations of the lowest terraces. Valin (1997) correlated terraces across the gorge in Moretown, but again, these correlations represent time equivalents rather than continuous surfaces.

Table 3.3: Terrace and River Elevations for Mad River Longitudinal Profile

Survey Location	Upstream Distance (km)	T9	T8	T7	T6	T5	T4	T3	T2	T1	River
MR17	0.00			190.15	177.89	166.02	152.82		141.38		133.23
440	0.33										134.15
460	0.84										140.24
480	1.62										146.34
500, 520	1.85										161.00
540	3.21										164.63
MR13	4.20			203.41		187.09		173.35	170.50	168.86	166.84
MR14	5.88			205.04	198.54			179.32	174.81	172.34	170.28
560	7.34										170.73
580	7.42										176.83
MR15	8.30		212.28	207.67	203.39	199.00	195.22	193.06	191.28	190.52	188.00
600	8.48										
620	9.79										
MR12	10.18		214.32	210.64	206.22	201.12		193.66	192.05	190.61	190.00
640	11.56										191.50
MR18	11.66		216.09	212.30	207.55		201.29	197.69	196.34	195.34	193.00
660	13.06										201.22
680	15.30										207.32
MR10	15.84		232.36	230.09	226.71		219.19		213.60	212.54	210.00
700	16.42										213.41
MR7	18.48		238.72			229.15	226.27		222.40	221.41	219.00
720	18.48										219.51
MR5	19.54		243.90					230.38	228.60	226.87	225.51
740	20.14										225.61
760	20.76										231.71
780	21.79										237.80
800	22.85										243.90
MR8	23.02	291.65	263.32	259.84	258.30	257.05	254.56	252.67	251.81	249.08	247.00
MR4	23.75	292.68	266.00	262.90		260.06	257.47		254.68	253.05	250.00
820	24.07										253.00
840	24.40										256.10
860	24.82										262.20
880	24.94										268.29
900	25.56										274.39

Survey locations (MR4) correspond to cross valley profiles and survey locations (640) correspond to river elevations from USGS 7.5' quadrangles. See Figure 3.6 for survey locations and Figure 3.7 for longitudinal profile.

Figure 3.6: Map of Survey Locations and Longitudinal Profile in the Mad River Basin. Base map from USGS 1:100,000 sheet.

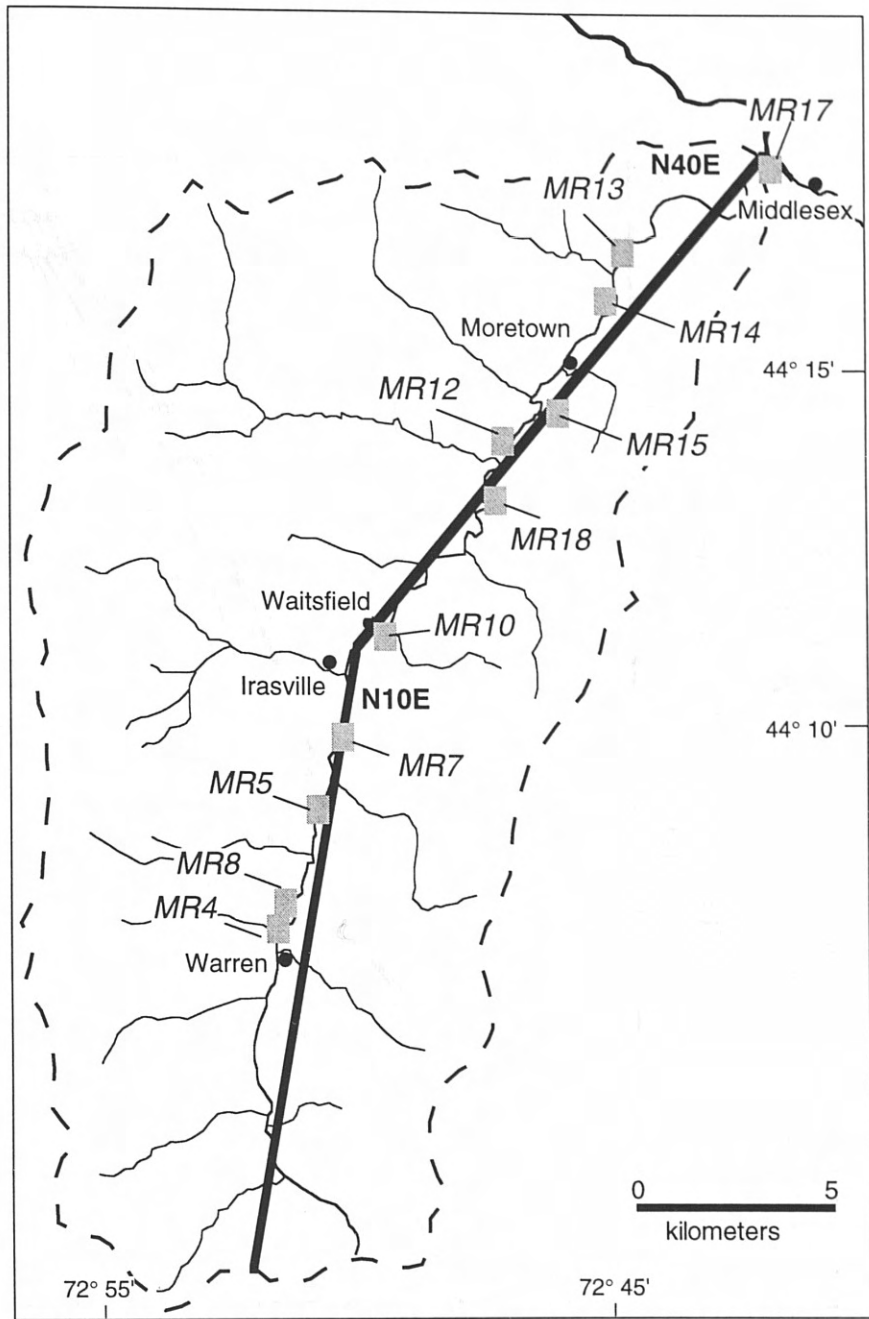


Figure 3.6: Map of Survey Locations and Longitudinal Profile in the Mad River Basin. Base map from USGS 1:100,000 sheet.

TRENCHING

Trench logs are important for interpreting the stratigraphy of the terrace deposits in order to classify the river system and river morphology. By understanding the system and morphology, interpretations of initial

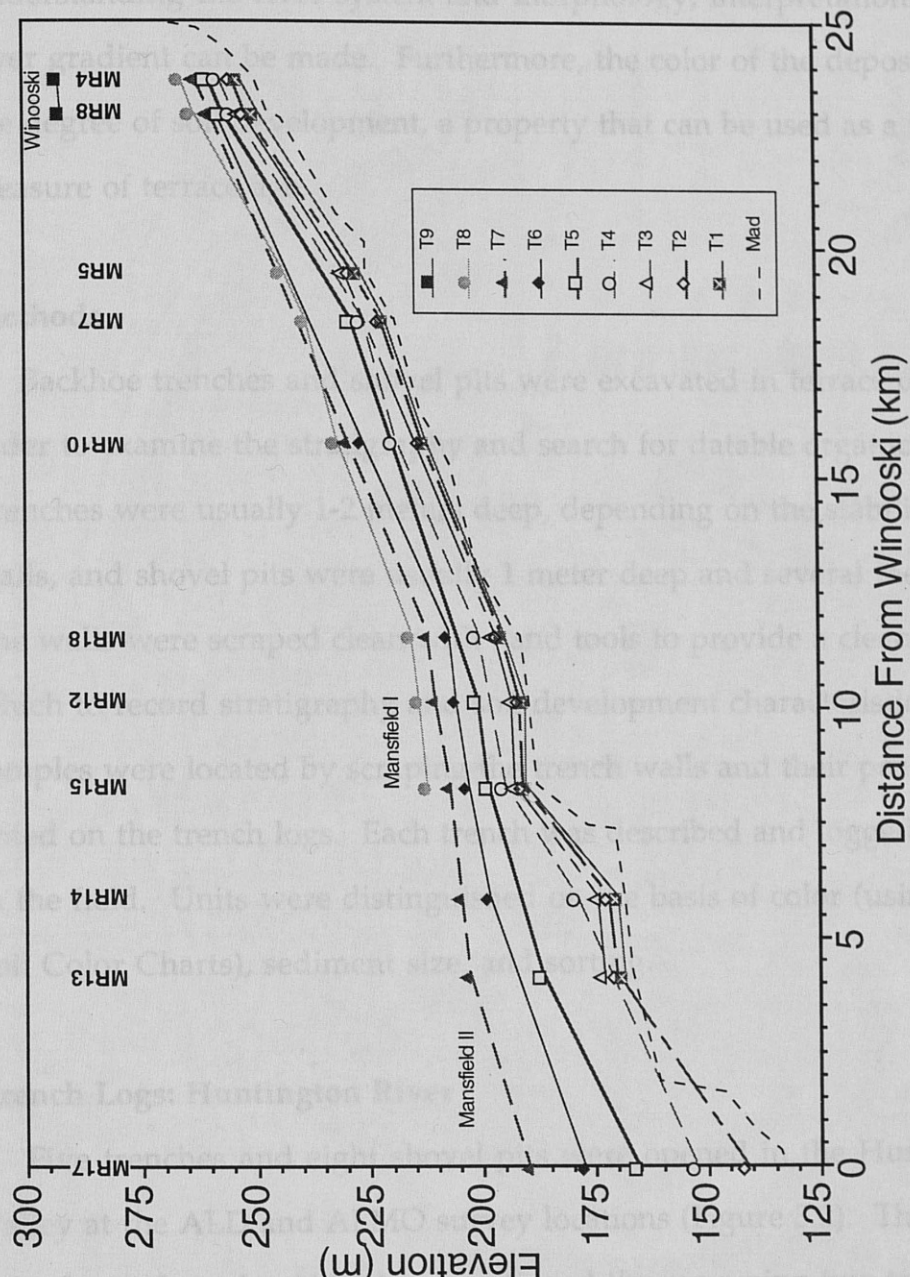


Figure 3.7: Longitudinal Profile of Terraces in the Mad River Valley. Survey locations identified in Figure 3.6 and Table 3.3 are shown. See text for discussion.

TRENCHING

Trench logs are important for interpreting the stratigraphy of the terrace deposits in order to classify the river system and river morphology. By understanding the river system and morphology, interpretations of initial river gradient can be made. Furthermore, the color of the deposits indicates the degree of soil development, a property that can be used as a relative measure of terrace age.

Methods

Backhoe trenches and shovel pits were excavated in terrace deposits in order to examine the stratigraphy and search for datable organic matter. Trenches were usually 1-2 meters deep, depending on the stability of the walls, and shovel pits were usually 1 meter deep and several meters wide. The walls were scraped clean with hand tools to provide a clean face from which to record stratigraphy and soil development characteristics. Charcoal samples were located by scraping the trench walls and their positions were noted on the trench logs. Each trench was described and logged individually in the field. Units were distinguished on the basis of color (using Munsell Soil Color Charts), sediment size, and sorting.

Trench Logs: Huntington River

Five trenches and eight shovel pits were opened in the Huntington River Valley at the ALD and ALMO survey locations (Figure 3.2). Three trenches were located on the Aldrich property and the remaining two trenches and all the shovel pits were on the Moulthrop property (Figure 3.8). With the assistance of the Geomorphology class, eight shovel pits were dug in October

1995. The trench log will be described in chronological order from oldest to youngest.

T8-Elevation 1211 m: The T8 pit is 1 m deep and contains four units

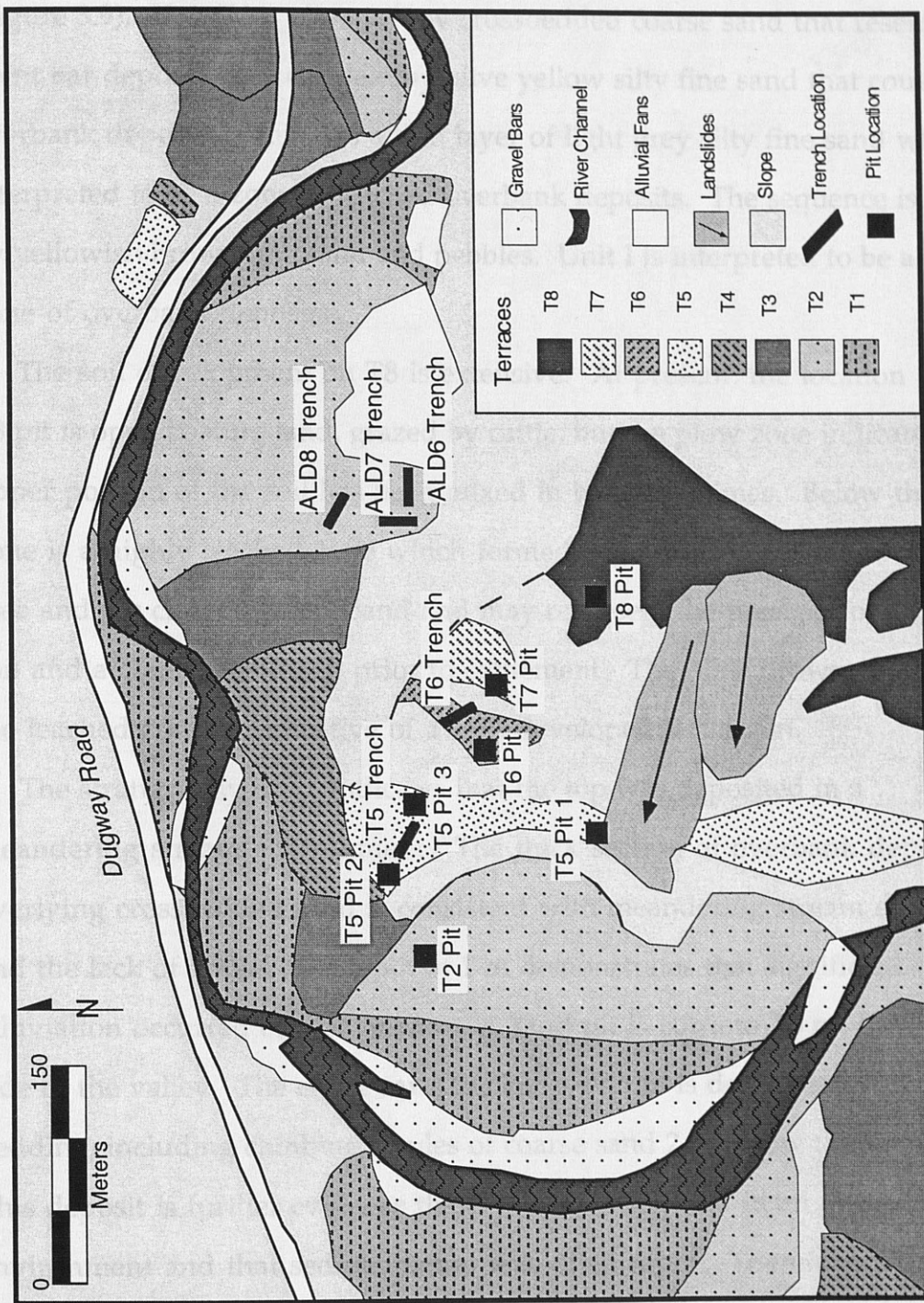


Figure 3.8: Location Map of Trenches and Pits in the Huntington Valley

1995. The trench logs will be described in chronological order from oldest to youngest.

T8-Elevation 191.1 m The T8 pit is 1 m deep and contains four units (Figure 3.9). Unit IV is olive yellow crossbedded coarse sand that resembles a point bar deposit. It is overlain by olive yellow silty fine sand that could be overbank deposits. Unit II is a thin layer of light grey silty fine sand which is interpreted to be a zone of leached overbank deposits. The sequence is capped by yellowish brown fine sand and pebbles. Unit I is interpreted to be a plowed zone of overbank deposits.

The soil development on T8 is extensive. At present, the location of the T8 pit is open pasture land, grazed by cattle, but the plow zone indicates the upper portion of the soil has been mixed in historical times. Below the plow zone is a highly leached zone which formed prior to the settlement of the area and the clearing of the land and may represent the presence of an acidic soil and a coniferous forest prior to settlement. The olive brown color below the leached zone is indicative of a well developed B-horizon.

The stratigraphy of T8 indicates that the top was deposited in a meandering stream environment. The thick section of overbank deposits overlying crossbedded sand is consistent with meandering stream deposits and the lack of gravel at a depth of 1 m demonstrates that significant alluviation occurred on this terrace. A sand pit is cut into T8 on the opposite side of the valley. The entire sand thickness of 5 m is dominated by cross bedding, including climbing ripples of coarse sand 2 m below the surface. This deposit is further evidence that T8 was constructed in an aggrading environment and that sedimentation was often rapid. Therefore, T8 was formed as a fill terrace.

T7-Elevation 180.0 m The T7 pit consists of three units (Figure 3.9). The lower unit is a thick deposit of channel gravel.

	Unit	Sediment	Color	Interpretation
T8	I	Fine Sand with Pebbles	Yellowish Brown 10YR 5/6	Plow Zone
	II	Silty Fine Sand	Light Grey 10YR 7/1	Leached Overbank Deposits
	III	Silty Fine Sand	Olive Yellow 2.5Y 6/6	Overbank Deposits
	IV	Cross Bedded Coarse Sand	Olive Yellow 2.5Y 6/6	Point Bar Deposits

	Unit	Sediment	Color	Interpretation
T7	I	Fine Sand with Pebbles	Dark Brown 10YR 3/3	Plow Zone
	II	Imbricated Gravels with Coarse Sand Matrix	N/A	Channel Deposits
	III	Silty Fine Sand	Pale Olive 5Y 6/4	Lacustrine Deposits

	Unit	Sediment	Color	Interpretation
T6	I	Silty Sand with Pebbles	Olive Brown 2.5Y 4/4	Plow Zone
	II	Pebbles in a Silty Sand Matrix	Yellowish Brown 10YR 5/8	Longitudinal Bar Deposits
	III	Coarse Sand and Imbricated Pebbles	N/A	Channel Deposits
	IV	Diamictite: Clayey Silt and Pebbles	Pale Olive 5Y 6/3	Glacial Till

Figure 3.9: T8-T6 Pits-Huntington River. See text for discussion.

T7-Elevation 180.5 m The T7 pit consists of three units (Figure 3.9). The lowest unit is a pale olive coarse sand that is interpreted to be glaciolacustrine deposits. A thick unit of clast supported imbricated gravels up to 10 cm and coarse sand overlies the basal sand. The orientation of the clasts indicates a down valley transport direction. This unit was deposited as channel gravels. The top unit is dark brown silty fine sand with random pebbles and represents a plowed zone of overbank deposits.

The presence of lacustrine sediments at this elevation in the valley demonstrates that significant valley filling occurred during the proglacial lake stages. The age of these sediments is probably Lake Mansfield II or Lake Coveville since Lake Mansfield II is the first lake to occupy this area and Lake Coveville is the last. The thick unit of channel gravels and the thin unit of overbank deposits are in contrast to the deposits of T8 and indicate a higher velocity fluvial regime was responsible for depositing T7. It is likely that the river which deposited T7 was a sediment-laden, high discharge braided stream. Since the channel gravels are cut into the lacustrine sediments, T7 is a fill-cut terrace.

T6-Elevation 175.1 A pit and a trench were opened on T6. Four units are present in the T6 pit (Figure 3.9). The lowest unit is a pale olive diamicton containing clayey silt supporting pebbles. Unit IV is interpreted to be glacial till. Unit III varies in thickness from 10-50 cm and consists of clast supported imbricated gravels with a coarse sand matrix. This unit was deposited as channel gravels and the orientation of the gravels indicates a downvalley transport direction. Unit II is a section of yellowish brown silty sand supporting pebbles up to 5 cm in diameter that forms an irregular contact with the unit below and a planar contact with the top unit. Unit II was

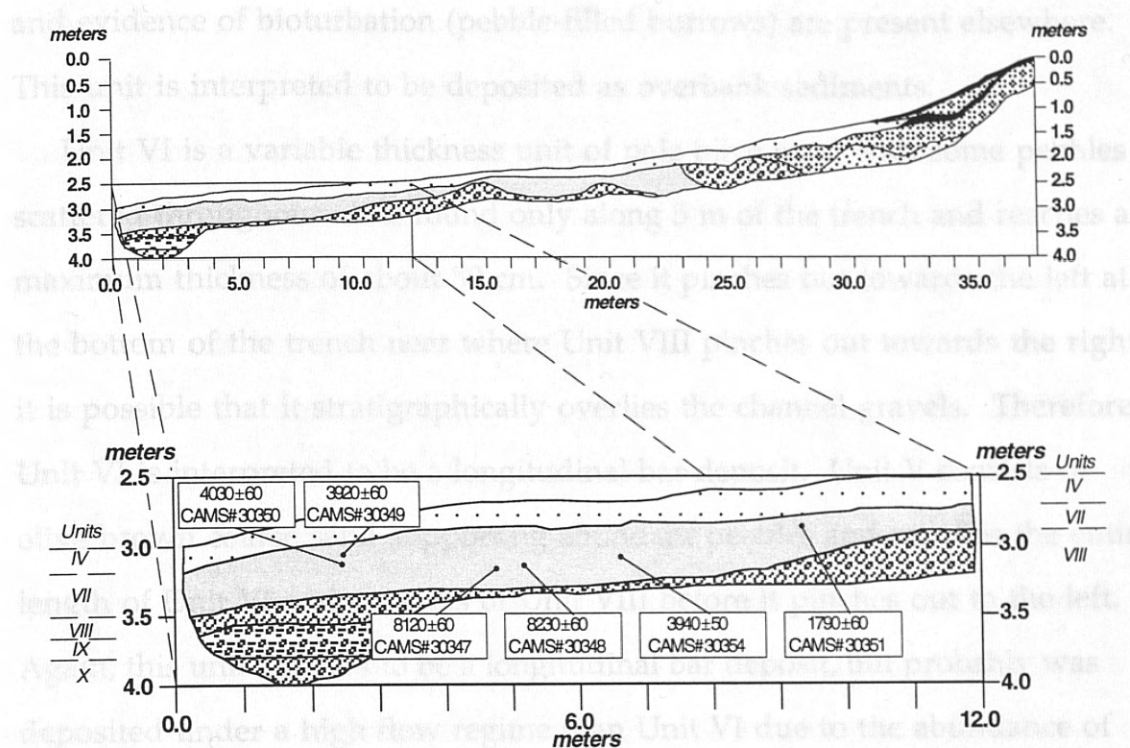
deposited as longitudinal bar deposits on top of the channel gravels. The uppermost 15 cm is olive brown fine sand with random pebbles and is interpreted to be a plowed zone of overbank deposits.

The 38 m long T6 trench was opened about 15 m downstream of the T6 pit. Six charcoal samples, collected from one end of the trench, were dated and are discussed in the Dating section. The stratigraphy of the T6 trench is similar to that of the T6 pit, but due to the length of the trench, several additional units were encountered and lateral variations in the units were observed (Figure 3.10).

Ten units are present in the T6 trench. Unit X is clast supported imbricated gravels with a matrix of coarse sand and is interpreted to be channel gravels. It is overlain by about 25 cm of an olive grey diamicton. This diamicton (Unit IX) is similar to the one found in the T6 pit, as it consists of a clayey silt matrix supporting pebbles, and it appears to have a horizontal layering, evident by the orientation of the clasts. Therefore, although the diamicton probably originated as glacial till, its stratigraphic position (above channel gravels) and its layering indicate that it has since been transported, most likely as a gravity flow, into the channel. It is possible that the river, eroding laterally into a bank of till, destabilized the till and caused it to flow into the channel. Consistent with this interpretation is the presence of more channel gravels, Unit VIII, immediately overlying the diamicton. Unit VIII is present along two thirds of the length of the trench, but briefly pinches out at 22 m where Unit VII extends down to the floor of the trench. Unit VII is a section of fining upwards olive brown fine sand and silt, often reddening towards the top. All of the charcoal samples were found within this unit, surrounded by the predominately massive fine sand;

Figure 3.10: T6 Trench - Huntington River. See text for discussion.

however, horizontal laminations are found in some locations, and mottling



T6 Trench - Huntington River

Unit	Pattern	Sediment	Color	Interpretation
I	■	Organic Layer	Reddish Black 2.5YR 3/1	Top Soil
II	□■■	Coarse Sand and Pebbles	Yellowish Brown 10YR 4/4	Colluvium
III	■■■	Organic Layer	Reddish Black 2.5YR 3/1	Buried Soil Horizon
IV	□□	Silty Sand and Pebbles	Dark Brown 10YR 3/3	Plow Zone
V	□■■	Pebbles with Coarse Sand Matrix	Olive Brown 2.5Y 4/4	Longitudinal Bar Deposit
VI	□■■	Coarse Sand and Pebbles	Pale Olive 5Y 6/3	Longitudinal Bar Deposit
VII	□□	Fining Upwards Fine Sand and Silt	Olive Brown 2.5Y 4/4	Overbank Deposits
VIII	□■■	Imbricated Gravels with Coarse Sand Matrix	N/A	Channel Gravels
IX	□■■	Diamicton	Olive Grey 5Y 5/2	Glacial Till Flow
X	□■■	Imbricated Gravels with Coarse Sand Matrix	N/A	Channel Gravels

Figure 3.10: T6 Trench - Huntington River. See text for discussion.

however, horizontal laminations are found in some locations, and mottling and evidence of bioturbation (pebble-filled burrows) are present elsewhere. This unit is interpreted to be deposited as overbank sediments.

Unit VI is a variable thickness unit of pale olive sand with some pebbles scattered throughout. It is found only along 5 m of the trench and reaches a maximum thickness of about 50 cm. Since it pinches out towards the left at the bottom of the trench near where Unit VIII pinches out towards the right, it is possible that it stratigraphically overlies the channel gravels. Therefore, Unit VI is interpreted to be a longitudinal bar deposit. Unit V consists of olive brown coarse sand supporting abundant pebbles and overlies the entire length of Unit VI and portions of Unit VIII before it pinches out to the left. Again, this unit appears to be a longitudinal bar deposit, but probably was deposited under a high flow regime than Unit VI due to the abundance of pebbles.

Unit IV is dark brown silty sand with random pebbles that forms the near-level terrace surface for most of the length of the trench; therefore, it probably represents a plowed zone of the units it overlies. It overlies the entire extent of Unit VII and portions of Units VIII and V, before pinching out to the right as it becomes covered. Unit III is a 10 cm thick reddish black organic layer that begins where Unit IV pinches out and extends to near the surface at the far right end of the trench. Because it is an organic layer, it is probably a soil horizon buried by Unit II. Unit II a chaotic mixture of yellowish brown coarse sand and pebbles. It only lies above the buried soil horizon and pinches out both up- and downslope; therefore it is interpreted to be a colluvial wedge with T7 as a source. Unit I is a 5 cm thick reddish black organic layer that has developed above the entire length of Unit II and overlies Unit III at the right

end of the trench. Because it is undisturbed, it formed since the colluvial wedge of Unit II was deposited and has never been plowed.

The pit and trench on T6 show the same characteristics as the T7 trench. The channel gravels of trench Units X and VIII and pit Unit III are identical to those in the T7 trench, and although the overbank deposits generally are thicker than those on T7, in places the overbank deposits are absent or are only represented by the plow zone. Therefore, like T7, T6 was probably deposited by a sediment-laden braided river. Glacial till probably underlies the river deposits. The full glacial till section (Unit IV) of the T6 pit was not uncovered or studied in detail; so, it is not known whether it represents a till flow into the river like trench Unit IX or *in situ* till. The bottom contact of Unit X was not exposed either, but from the interpretation that Unit IX is a till flow into the river, it follows that the river had incised vertically through till and was either flowing across bedrock and/or till. Therefore, T6 was deposited as a fill-cut terrace.

T5 -Elevation 165.9 Three shovelpits and one trench were opened on T5. Four units are found in the T5-1 pit (Figure 3.11). Unit IV, imbricated gravel with a coarse sand matrix, is interpreted to be channel deposits. It is overlain by three units of overbank deposits. Unit III is fining upwards olive grey fine sand that grades into the olive silty fine sand of Unit II. The top unit, Unit I, is light olive brown fine sand with evidence of burrowing and is interpreted to be a plowed zone of overbank deposits.

T5-2 pit (Figure 3.11) has four units. The lowest unit, Unit IV, is imbricated gravels with a coarse sand matrix and is interpreted to be channel gravel deposits. It is overlain by coarse sand and pebbles (Unit III) that were probably deposited at the edge of the channel, perhaps on the edge of a point

Figure 3.11: T5 Pits 1-3-Huntington River. See text for discussion.

bar. Unit II is an olive silty fine sand that likely represent the vertical

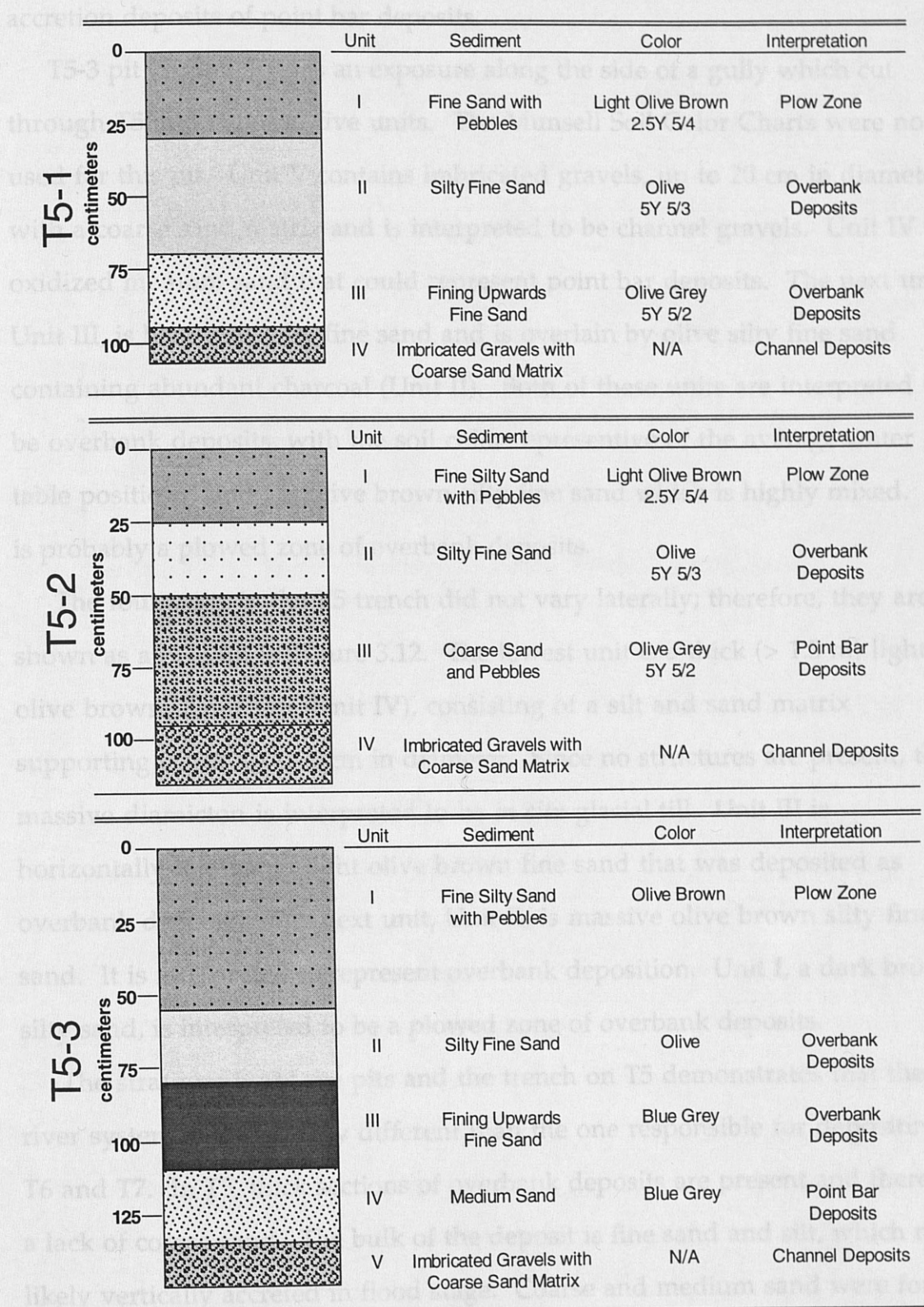


Figure 3.11: T5 Pits 1-3-Huntington River. See text for discussion.

bar. Unit II is an olive silty fine sand that likely represents the vertical accretion deposits of point bar deposits.

T5-3 pit (Figure 3.11) is an exposure along the side of a gully which cut through T5 and exposed five units. The Munsell Soil Color Charts were not used for this pit. Unit V contains imbricated gravels, up to 20 cm in diameter, with a coarse sand matrix and is interpreted to be channel gravels. Unit IV is oxidized medium sand that could represent point bar deposits. The next unit, Unit III, is blue-grey silty fine sand and is overlain by olive silty fine sand containing abundant charcoal (Unit II). Both of these units are interpreted to be overbank deposits, with the soil color representative of the average water table position. Unit I is olive brown silty fine sand which is highly mixed. It is probably a plowed zone of overbank deposits.

The four units in the T5 trench did not vary laterally; therefore, they are shown as a column in Figure 3.12. The lowest unit is a thick (> 1.5 m) light olive brown diamicton (Unit IV), consisting of a silt and sand matrix supporting clasts up to 5 cm in diameter. Since no structures are present, this massive diamicton is interpreted to be *in situ* glacial till. Unit III is horizontally laminated light olive brown fine sand that was deposited as overbank deposits. The next unit, Unit II, is massive olive brown silty fine sand. It is interpreted to represent overbank deposition. Unit I, a dark brown silty sand, is interpreted to be a plowed zone of overbank deposits.

The stratigraphy of the pits and the trench on T5 demonstrates that the river system is remarkably different than the one responsible for depositing T6 and T7. In T5, thick sections of overbank deposits are present and there is a lack of coarse sand. The bulk of the deposit is fine sand and silt, which most likely vertically accreted in flood stage. Coarse and medium sand were found

in two of the pits and suggest that there may have point bars occurring in

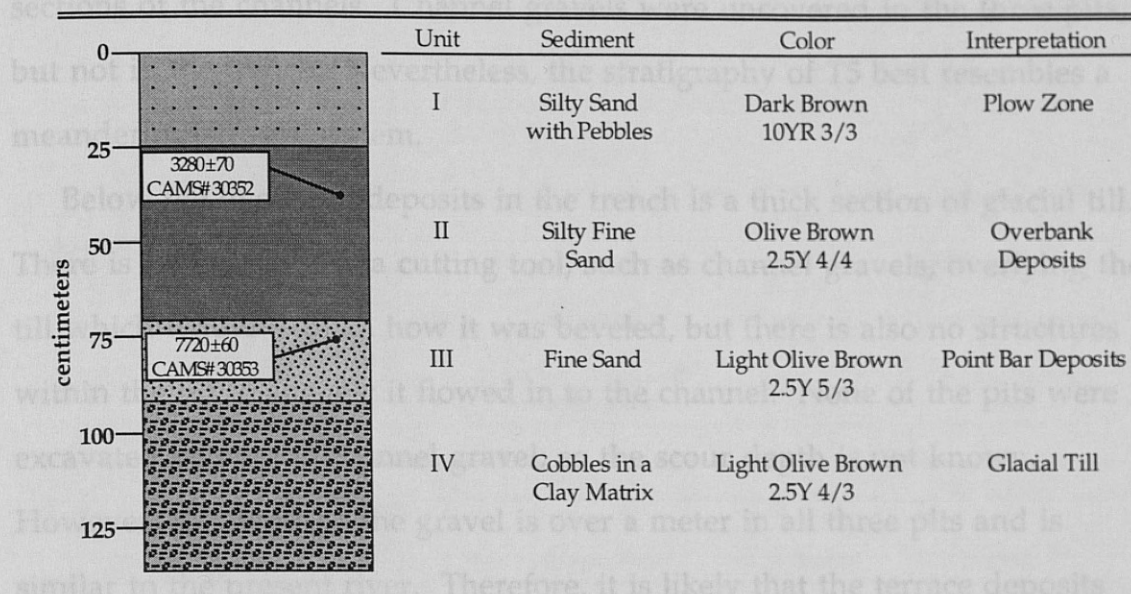


Figure 3.12: T5 Trench-Huntington River. See text for discussion.

another trench with the same elevation which implies that 15 is also a paired terrace.

T2 - Pit A - 152.2 m: Three trenches and one pit were opened in T2. Five units are found in the T2 pit (Figure 3.13). The lowest unit is imbricated gravels with a coarse sand matrix and is interpreted to be a channel deposit. The remaining units were deposited as overbank deposits. Unit IV, brown silty clay, grades into the fine olive sand of Unit III. Unit II is distinguished from Unit III by its color. It is dark yellowish brown fine sand and it grades into Unit I, light olive brown fine sand with coarse sand lenses. The shape of the lenses resembles furrows and a nail was found in Unit I; therefore, Unit I is interpreted to be a plowed zone of overbank deposits.

ALD-6 Trench: Two walls of the ALD-6 trench, located on perpendicular walls, were described. Wall 1 contains three units (Figure 3.13). The lowest unit is grey medium sand that is interpreted to be a point bar deposit. It is

in two of the pits and suggest that there may have point bars accreting in sections of the channels. Channel gravels were uncovered in the three pits, but not in the trench. Nevertheless, the stratigraphy of T5 best resembles a meandering stream system.

Below the overbank deposits in the trench is a thick section of glacial till. There is no evidence of a cutting tool, such as channel gravels, overlying the till which would explain how it was beveled, but there is also no structures within the till to suggest it flowed in to the channel. None of the pits were excavated below the channel gravel; so the scour depth is not known. However, the depth to the gravel is over a meter in all three pits and is similar to the present river. Therefore, it is likely that the terrace deposits were laid down as a fill-cut terrace. Immediately across the valley, there is another terrace with the same elevation which implies that T5 is also a paired terrace.

T2 -Elevation 152.2 m Three trenches and one pit were opened in T2. Five units are found in the T2 pit (Figure 3.13). The lowest unit is imbricated gravels with a coarse sand matrix and is interpreted to be a channel deposit. The remaining units were deposited as overbank deposits. Unit IV, brown silty clay, grades into the fine olive sand of Unit III. Unit II is distinguished from Unit III by its color. It is dark yellowish brown fine sand and it grades into Unit I, light olive brown fine sand with coarse sand lenses. The shape of the lenses resembles furrows and a nail was found in Unit I; therefore, Unit I is interpreted to be a plowed zone of overbank deposits.

ALD-6 Trench Two walls of the ALD-6 trench, located on perpendicular walls, were described. Wall 1 contains three units (Figure 3.13). The lowest unit is grey medium sand that is interpreted to be a point bar deposit. It is

overlain by grey silty fine sand (Unit II) and organic rich silty clay (Unit I).

Bottom

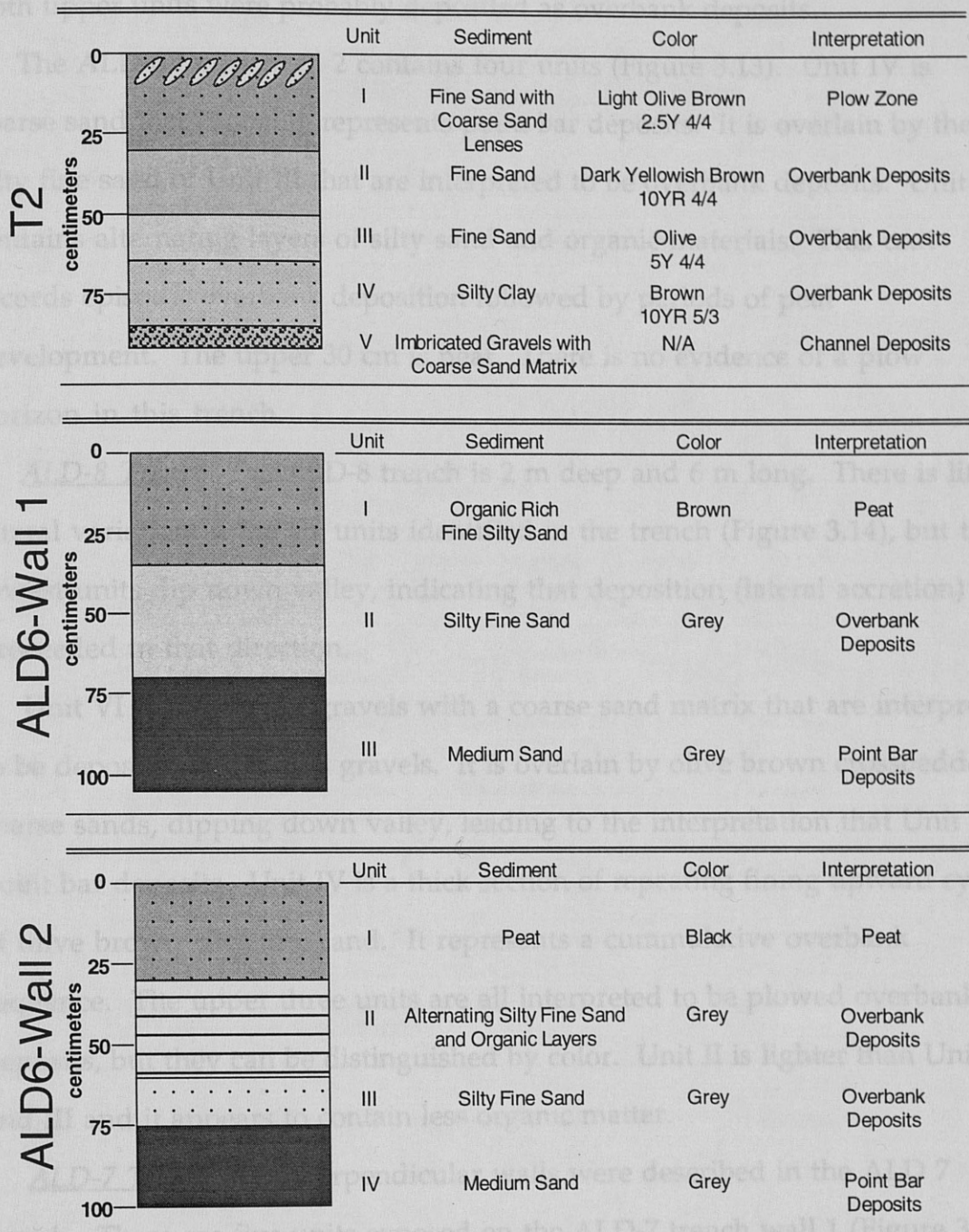


Figure 3.13: T2 Pit, ALD6-1, and ALD6-2-Huntington River. See text for discussion.

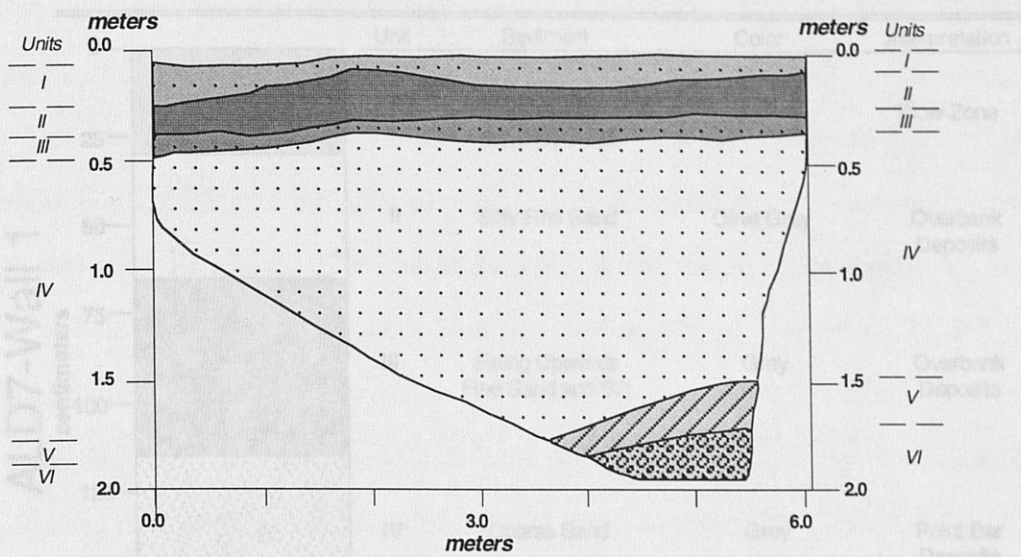
overlain by grey silty fine sand (Unit II) and organic rich silty clay (Unit I). Both upper units were probably deposited as overbank deposits.

The ALD-6 trench wall 2 contains four units (Figure 3.13). Unit IV is coarse sand that probably represents point bar deposits. It is overlain by the silty fine sand of Unit III that are interpreted to be overbank deposits. Unit II contains alternating layers of silty sand and organic materials. This unit records episodic overbank deposition followed by periods of peat development. The upper 30 cm is peat. There is no evidence of a plow horizon in this trench.

ALD-8 Trench The ALD-8 trench is 2 m deep and 6 m long. There is little lateral variation in the six units identified in the trench (Figure 3.14), but the lowest units dip down valley, indicating that deposition (lateral accretion) proceeded in that direction.

Unit VI is imbricated gravels with a coarse sand matrix that are interpreted to be deposited as channel gravels. It is overlain by olive brown crossbedded coarse sands, dipping down valley, leading to the interpretation that Unit V is point bar deposits. Unit IV is a thick section of repeating fining upward cycles of olive brown silty fine sand. It represents a cumulative overbank sequence. The upper three units are all interpreted to be plowed overbank deposits, but they can be distinguished by color. Unit II is lighter than Units I and III and it appears to contain less organic matter.

ALD-7 Trench Two perpendicular walls were described in the ALD 7 trench. There are five units exposed on the ALD-7 trench wall 1 (Figure 3.15). The lowest unit is imbricated gravels with a coarse sand matrix and is interpreted to be channel gravels. The next unit, Unit IV, is grey coarse sand that possibly was deposited as a point bar. It is overlain by a fining upward



ALD-8 Trench- Huntington River

Unit	Pattern	Sediment	Color	Interpretation
I	[dotted]	Fine Sand with Pebbles	Dark Yellowish Brown 10YR 3/3	Plow Zone
II	[solid dark gray]	Burrowed Silty Fine Sand	Dark Yellowish Brown 10YR 4/3	Plow Zone
III	[diagonal lines]	Coarse Sand and Pebbles	Dark Yellowish Brown 10YR 3/3	Plow Zone
IV	[white with dots]	Fining Upwards Silty Fine Sand	Olive Brown 2.5Y 4/4	Overbank Deposits
V	[diagonal lines]	Crossbedded Coarse Sand	Olive Brown 2.5Y 4/4	Point Bar Deposits
VI	[cross-hatch]	Imbricated Gravels with Coarse Sand Matrix	N/A	Channel Gravels

Figure 3.14: ALD-8 Trench-Huntington River. See text for discussion.

Figure 3.15: ALD-7 Trench Walls-Huntington River.
See text for discussion.

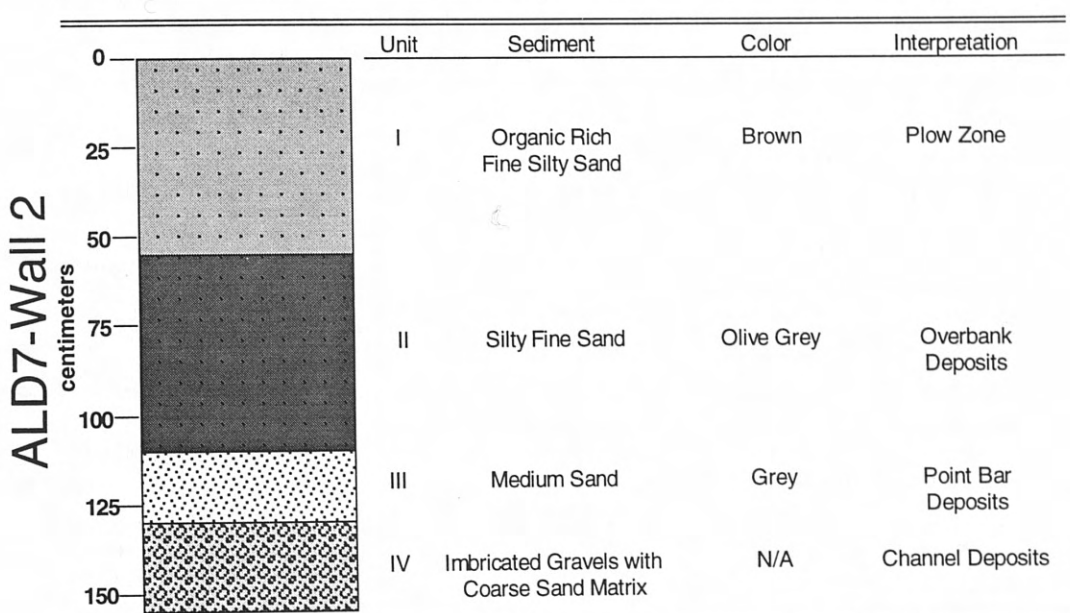
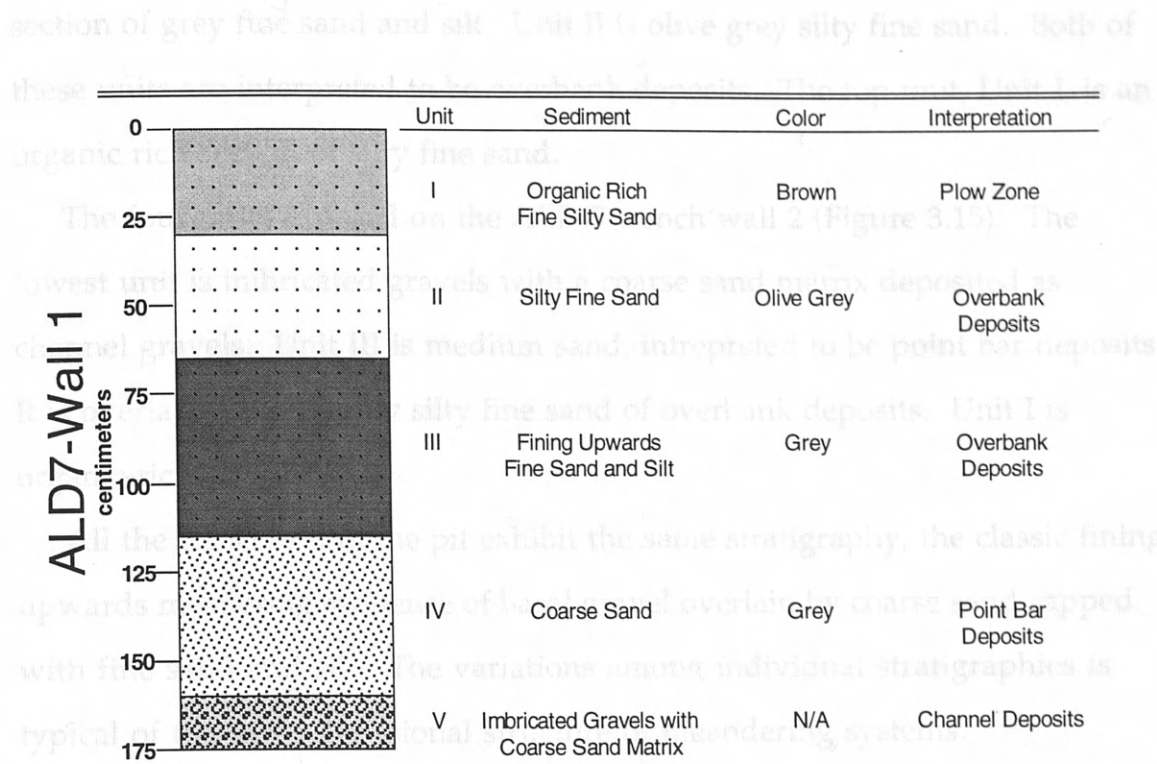


Figure 3.15: ALD-7 Trench Walls-Huntington River.
See text for discussion.

section of grey fine sand and silt. Unit II is olive grey silty fine sand. Both of these units are interpreted to be overbank deposits. The top unit, Unit I, is an organic rich section of silty fine sand.

The four units exposed on the ALD-7 trench wall 2 (Figure 3.15). The lowest unit is imbricated gravels with a coarse sand matrix deposited as channel gravels. Unit III is medium sand, interpreted to be point bar deposits. It is overlain by olive grey silty fine sand of overbank deposits. Unit I is organic-rich silty clay.

All the trenches and the pit exhibit the same stratigraphy, the classic fining upwards meandering sequence of basal gravel overlain by coarse sand capped with fine sand and silt. The variations among individual stratigraphies is typical of the three dimensional structure of meandering systems. Unit IV extends from meter 35 to the end of the trench and consists of imbricated cobbles in a coarse sand matrix. It distinguished from Unit V by the smaller cobbles, but also is interpreted to be channel deposits. The first 45 m of the trench expose Unit III, a 40 cm thick unit of coarse sand and gravel. It is overlain by two units which extend along the entire length of the trench. Unit II is 40 cm of olive brown silty sand and pebbles, interpreted to be vertically accreted overbank deposits and Unit I is a 15 cm thick dark yellow brown silty sand unit that represents a plowed zone or overbank deposits.

The fluvial deposits seen in the TB trench unconformably overlie lacustrine sands and silt. It is likely that the river eroded into the lacustrine deposits before the fluvial deposits were laid down. Therefore, the TB terrace is a fill-cut terrace. The lateral variations in the thickness of the gravels indicates there were multiple, small channels to carry the water. The fin-

Trench Logs: Mad River

Three backhoe trenches were opened in the Mad River Valley in the town of Warren (Figure 3.16). The trench logs will be described in order from oldest to youngest, beginning with the highest trench on T8.

T8-Elevation 263.3 m The T8 trench is 100 m long and contains several lateral variations (Figure 3.17). This trench was excavated to replace a water line on the property and in most places is less than 1.5 m deep. However, three deeper sections were dug to 2 m. In several locations the stratigraphy was obscured due to previous trenching. The lowest unit (Unit VI) is light grey fine sand and silt that is interpreted to be lacustrine deposits and is found only between meters 93-98 in the trench. Unit V is in the bottom of the other two deep excavations, meters 23-30 and meters 60-65. It is at least 1 m of imbricated cobbles that probably were deposited as channel gravels. Unit IV extends from meter 35 to the end of the trench and consists of imbricated cobbles in a coarse sand matrix. It distinguished from Unit V by the smaller clast size, but also is interpreted to be channel deposits. The first 45 m of the trench expose Unit III, a 40 cm thick unit of coarse sand and gravel. It is overlain by two units which extend along the entire length of the trench. Unit II is 40 cm of olive brown silty sand and pebbles, interpreted to be vertically accreted overbank deposits and Unit I is a 15 cm thick dark yellow brown silty sand unit that represents a plowed zone of overbank deposits.

The fluvial deposits seen in the T8 trench unconformably overlie lacustrine sands and silt. It is likely that the river eroded into the lacustrine deposits before the fluvial deposits were laid down. Therefore, the T8 terrace is a fill-cut terrace. The lateral variations in the thickness of the gravels indicates there were multiple, small channels to carry the water. The finer-

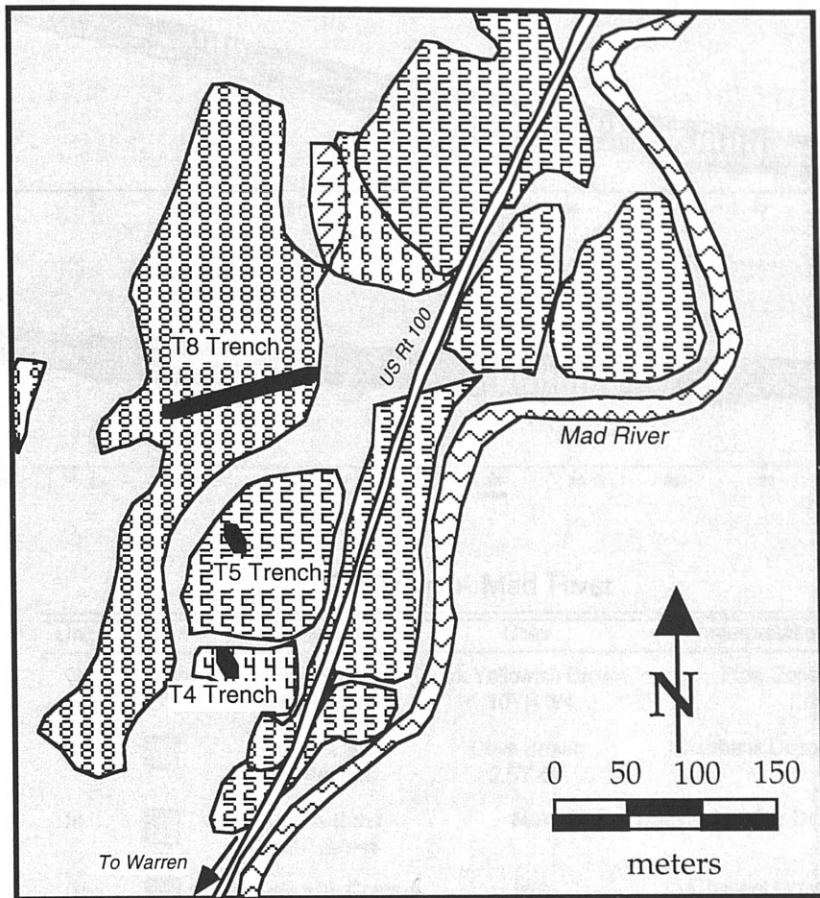
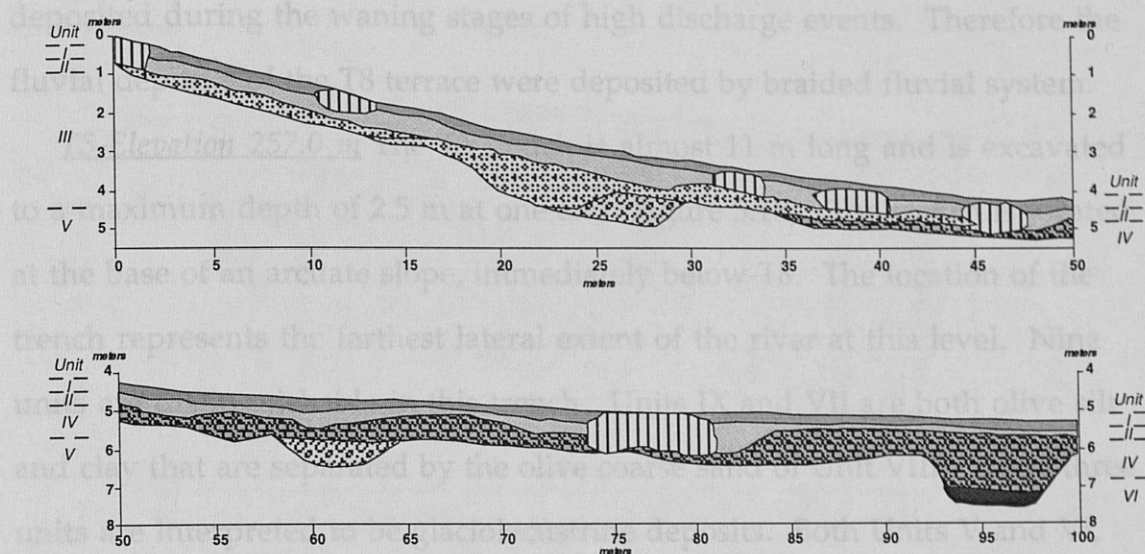


Figure 3.16: Location Map of Mad River Trenches. Trenches were opened at survey location MR8. See Figure 3.6 for location. Numbers in fill pattern refer to terrace numbers.

grained deposits toward the upper part of the sequence were probably

deposited during the waning stages of high discharge events. Therefore, the T8 terrace were deposited by braided fluvial systems.



T8 Trench- Mad River

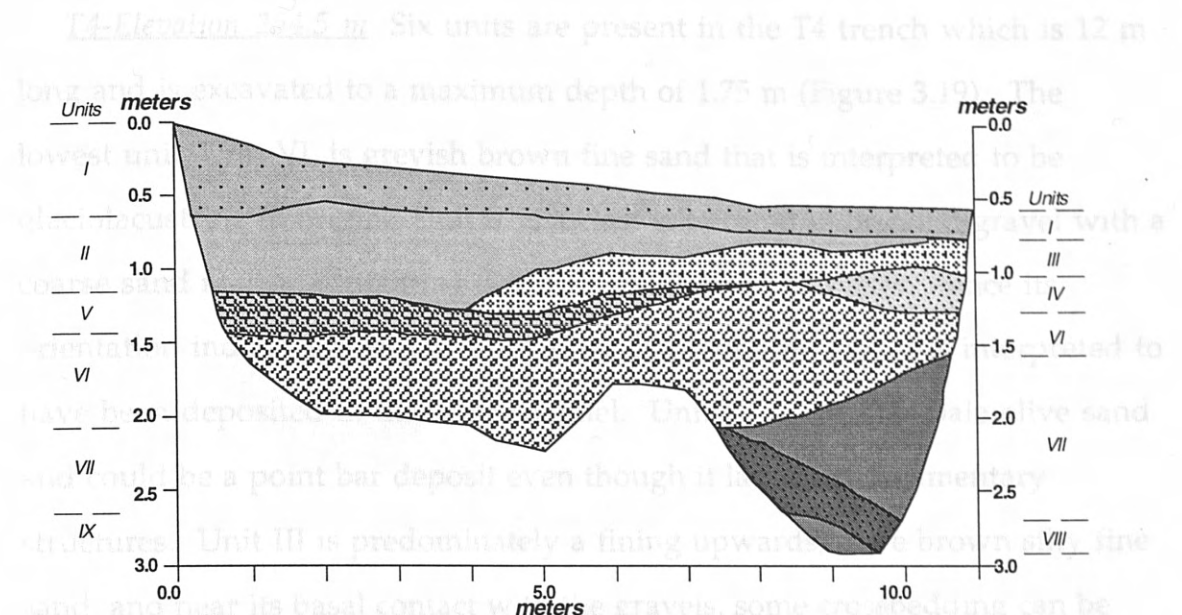
Unit	Pattern	Sediment	Color	Interpretation
I	■	Fine Sand with Pebbles	Dark Yellowish Brown 10YR 3/4	Plow Zone
II	□	Silty Fine Sand and Pebbles	Olive Brown 2.5Y 4/4	Overbank Deposits
III	▨	Coarse Sand and Pebbles	N/A	Longitudinal Bar Deposits
IV	▩	Gravels with Coarse Sand Matrix	N/A	Channel Gravels
V	▢	Imbricated Gravels with Coarse Sand Matrix	N/A	Channel Gravels
VI	■■■	Silts and Clays	Olive 5Y 5/4	Lacustrine Sediments
	■■■	Disturbed sediment due to previous trenching		

Figure 3.17: T8 Trench-Mad River. See text for discussion.

grained deposits toward the upper part of the sequence were probably deposited during the waning stages of high discharge events. Therefore the fluvial deposits of the T8 terrace were deposited by braided fluvial system.

T5-Elevation 257.0 m The T5 trench is almost 11 m long and is excavated to a maximum depth of 2.5 m at one end (Figure 3.18). The trench is located at the base of an arcuate slope, immediately below T8. The location of the trench represents the farthest lateral extent of the river at this level. Nine units are distinguishable in this trench. Units IX and VII are both olive silt and clay that are separated by the olive coarse sand of Unit VIII. These three units are interpreted to be glaciolacustrine deposits. Both Units V and VI, pebbles and gravels in a coarse sand matrix, are interpreted to be channel deposits, with Unit V deposited under a slightly lower flow regime. Unit IV is a coarse olive brown sand and Unit III is a coarse olive brown sand with pebbles. Charcoal pieces are found in both units. These sandy units could be longitudinal bar deposits. Unit II is a fining upwards, olive brown fine sand and probably was deposited as overbank material under waning flow conditions. Unit I is dark yellowish brown fine sand with random pebbles and is interpreted to be a plowed zone of overbank deposits.

The sedimentology of the T5 deposits suggests deposition by a braided river system. The abundance of coarse material as well as the lateral variations in unit thickness points toward a fluvial system which, by lacking the fine-grained sediment necessary for cohesive banks, flowed within wide, shallow channels. The lower-most gravels in the T5 trench, Units V and VI, cut into the lacustrine deposits below, indicating that it is a fill-cut terrace.



T5 Trench- Mad River

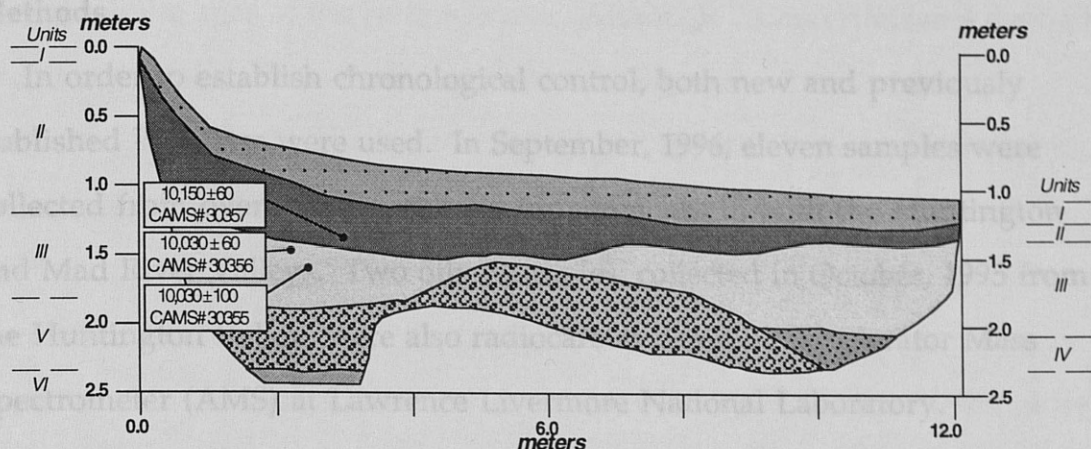
Unit	Pattern	Sediment	Color	Interpretation
I	[dotted]	Fine Sand with Pebbles	Dark Yellowish Brown 10YR 3/4	Plow Zone
II	[cross-hatched]	Burrowed Silty Fine Sand	Olive Brown 2.5Y 4/4	Overbank Deposits
III	[cross-hatched]	Coarse Sand and Pebbles	Olive Brown 2.5Y 4/4	Longitudinal Bar Deposits
IV	[cross-hatched]	Coarse Sand	Olive Brown 2.5Y 4/4	Longitudinal Bar Deposits
V	[cross-hatched]	Pebbles with Coarse Sand Matrix	N/A	Channel Gravels
VI	[cross-hatched]	Imbricated Gravels with Coarse Sand Matrix	N/A	Channel Gravels
VII	[solid dark grey]	Silts and Clays	Olive 5Y 5/4	Lacustrine Sediments
VIII	[solid black]	Coarse Sand	Olive 5Y 5/4	Lacustrine Sediments
IX	[solid black]	Silts and Clays	Olive 5Y 5/4	Lacustrine Sediments

Figure 3.18: T5 Trench-Mad River. See text for discussion.

T4-Elevation 254.5 m Six units are present in the T4 trench which is 12 m long and is excavated to a maximum depth of 1.75 m (Figure 3.19). The lowest unit, Unit VI, is greyish brown fine sand that is interpreted to be glaciolacustrine in origin. Unit V is a clast supported imbricated gravel with a coarse sand matrix, containing clasts up to 30 cm in diameter. Since its orientation indicates a down valley flow direction, the gravel is interpreted to have been deposited in the river channel. Unit IV is a coarse pale olive sand and could be a point bar deposit even though it lacks any sedimentary structures. Unit III is predominately a fining upwards, olive brown silty fine sand, and near its basal contact with the gravels, some crossbedding can be observed and charcoal can be found. Unit II also consists of fine sand and silt, but is distinguishable from Unit III by its redder color and burrows. Therefore, both of these units are interpreted to be overbank deposits, with Unit II exhibiting a well-developed B horizon. Unit I is dark brown fine sand with random pebbles and is interpreted to be a plowed zone.

As with the higher terraces, T4 is underlain by lacustrine deposits which again indicates that it is a fill-cut terrace, consisting of lateral accretion deposits laid down after the river incised. The stratigraphy of T4 is consistent with a meandering river deposit. Like T5, it is located at the inside of a meander bend and probably represents the farthest lateral extent of the river. The channel was probably abandoned due to a meander cutoff, but still received some overbank deposition during flood stage.

DATING



T4 Trench- Mad River

Unit	Pattern	Sediment	Color	Interpretation
I	■	Fine Sand with Pebbles	Dark Brown 10YR 3/3	Plow Zone
II	■	Burrowed Silty Fine Sand	Strong Brown 7.5YR 4/6	Overbank Deposits
III	□	Fining Upwards Silty Fine Sand	Olive Brown 2.5Y 4/3	Overbank Deposits
IV	■	Coarse Sand	Pale Olive 5Y 6/3	Point Bar Deposits
V	■	Imbricated Gravels with Coarse Sand Matrix	N/A	Channel Gravels
VI	■	Fine Sand	Greyish Brown 5Y 5/2	Lacustrine Sediments

Figure 3.19: T4 Trench-Mad River. See text for discussion.

organic matter.

The radiocarbon ages were converted to calibrated ages using the CALIB 3.03A program of Stuiver and Reimer (1993). Because the amount of ^{14}C in the atmosphere varies over time, the ^{14}C age must be calibrated to reflect calendar years. The CALIB program uses a data base of radiocarbon-dated tree rings to convert the ^{14}C ages to calibrated years.

Radiometric dating the organic material from the terrace deposits DATING

Methods the ages of the river terraces Although the river terraces deposits

In order to establish chronological control, both new and previously published ^{14}C dates were used. In September, 1996, eleven samples were collected from overbank deposits in four trenches in both the Huntington and Mad River Valleys. Two other samples, collected in October, 1995 from the Huntington Valley, were also radiocarbon dated by Accelerator Mass Spectrometer (AMS) at Lawrence Livermore National Laboratory.

As described above, charcoal samples were collected from the walls of the backhoe trenches for dating. The charcoal was found as isolated pieces in the overbank deposits at a depth of < 1 m and it was usually < 5 mm in diameter and subangular. The species of the charcoal was not identified.

Charcoal samples were brought to Lawrence Livermore National Laboratory in Livermore, California, and dated by AMS. The samples were cleaned using a series of acid (HCl) and base washes (NaOH) to remove any rootlets or humic and fulvic acids and then burned to produce CO_2 and other gases. The CO_2 was isolated using cryogenic techniques on a vacuum line and then was converted to graphite. The graphite was packed into targets and John Southon measured ^{14}C on the AMS. The radiocarbon ages were calculated assuming a $\delta^{13}\text{C}$ value of -25 per mil, appropriate for terrestrial organic matter.

The radiocarbon ages were converted to calibrated ages using the CALIB 3.0.3A program of Stuvier and Reimer (1993). Because the amount of ^{14}C in the atmosphere varies over time, the ^{14}C age must be calibrated to reflect sidereal years. The CALIB program uses a data base of radiocarbon-dated tree rings to convert the ^{14}C ages to calibrated years.

Radiometric dating the organic matter collected from the terrace deposits constrains the ages of the river terraces. Although the river terraces deposits are directly dated, these dates represent limiting ages. A river terrace is deposited, as a floodplain, both vertically and laterally over an extended time period. As a time-transgressive deposit, there is no single age for a terrace. Dating organic matter that was deposited along with the terrace deposits demonstrates that section of the terrace is at least that old, but there may be sections of the terrace that are either older or younger. Therefore, the oldest charcoal age provides a minimum age for the terrace formation and a minimum age for abandonment of the previous terrace.

There are two post-deposition mechanisms which can complicate the interpretation of radiocarbon ages: bioturbation and redeposition of the charcoal. Any time after deposition, young charcoal or other organic material may be stirred into the terrace by bioturbation. Unless there is a clear indication that the charcoal was deposited coevally with the deposits (i.e., charcoal is found within undisturbed cross beds), the age of the terrace must be considered a minimum. It is also possible that charcoal or wood stored within a terrace deposit may be subsequently eroded from the terrace, transported by the river, and redeposited downstream in a younger deposit. In this case, the organic matter would be older than the new terrace deposit. However, it seems unlikely that the small charcoal pieces would remain intact through two deposition cycles.

Table 3.4: Huntington River Basal Fan Radiocarbon Ages

Terrace	Sample	Laboratory #	Material	Depth (m)	¹⁴ C Age	Calibrated Date (yr B.P.)	1 Sigma Range (yr B.P.)	2 Sigma Range (yr B.P.)
T1	Ald 2-2*	GX-21329	Wood	4.00	< 100	62-0	128-0	238-0
T2	Ald 5-2*	CAMS# 22994	Wood	4.00	2500±60	2708-2402	2735-2363	2746-2352
T5	Af-45**	GX-20276	Wood	4.00	7835±105	8555	8713-8430	8981-8375
T5	Df-1**	CAMS# 20901	Wood	2.50	8530±100	9486	9531-9436	9819-9275
T5	Df-8**	CAMS# 20963	Wood	1.30	8060±60	8981	8993-8764	9194-8662

Note: Fan dates from *Zehfuss (1996), and **Church (1997). Calibrations by CALIB 3.0.3A (Stuiver and Reimer, 1993).

TERRACES

Note: Locations of radiocarbon samples for T0 and T5 are shown on Figures 3.10 and 3.14, respectively, and locations for T2-T4 are presented in Zehfuss (1996) and shown on Figure 3.7. Calibrations using ¹⁴C ages from Church and Stuiver, 1993.

Radiocarbon Dates: Huntington River

Previous studies of alluvial fans (Zehfuss, 1996; Church, 1997) have begun

to establish a chronology of landform development in the Huntington River

area. In this study, terrace deposits have

been sampled to obtain radiocarbon dates for these terraces on the basis of basal

samples. Two samples from T5

and two samples from T2

are from organic-rich layers, possibly

representing the fan surface and 1804

below the fan surface. These

samples have been present as a surface by

the time-transgressive nature of the fan that separates these two

terraces. The sample from T6 has an age of 2402 cal yr B.P. This surface

is interpreted to be at least 1804 m above the

fan surface. The sample from T2 just

above the fan surface is interpreted to be the time-transgressive

nature of the overbank deposits. In

addition, the sample, 0.33 m below the

fan surface, has an age of 9210 cal yr B.P.

All dates represent limiting ages. The samples could be from charcoal that

Table 3.5: Huntington River Terrace Radiocarbon Ages

Terrace	Sample#	CAMS#	Material	Depth (m)	¹⁴ C Age	Calibrated Date 1	Sigma Range 2	Sigma Range (yr B.P.)
T2	ALD4-8	30359	Wood	2.30	1800±80	1804, 1760	1871-1636	1946-1560
T2	ALD4-7	30358	Wood	3.60	1900±50	1830	1879-1751	1939-1710
T5	TW6	30352	Charcoal	0.33	3280±70	3471	3576-3400	3684-3359
T5	TW7	30353	Charcoal	0.75	7790±60	8424	8541-8407	8565-8367
T6	TW5	30351	Charcoal	0.28	1790±60	1706	1805-1615	1863-1542
T6	TW3	30349	Charcoal	0.32	3920±60	4404, 4361, 4358	4418-4263	4518-4150
T6	TW8	30354	Charcoal	0.55	3940±50	4408	4424-4295	4518-4232
T6	TW4	30350	Charcoal	0.36	4030±60	4512, 4473, 4449	4562-4416	4810-4354
T6	TW2	30348	Charcoal	0.46	8230±60	9210	9362-900	9380-8988
T6	TW1	30347	Charcoal	0.49	8120±60	8991	9189-8980	9240-8736

Note: Locations of radiocarbon samples for T6 and T5 are shown on Figures 3.10 and 3.14, respectively, and locations for T2 are presented in Zehfuss (1996) and shown on Figure 3.7. Calibration using CALIB 3.0.3A (Stuvier and Reimer, 1993).

Radiocarbon Dates: Huntington River

Previous studies of alluvial fans (Zehfuss, 1996; Church, 1997) have begun to establish a chronology of landform development in the Huntington River Valley. Limiting ages are assigned to three river terraces on the basis of basal dates from four alluvial fans (Table 3.4). For this study, terrace deposits have been directly dated (Table 3.5): six samples from T6, and two samples from T5 (Figures 3.10, 3.12). There are two additional basal fan samples from T2.

The two dates from T2 are from two different organic-rich layers, possibly paleosols, buried beneath an alluvial fan. The ages for these horizons are 1830 cal yr B.P. for the older horizon, 3.6 m below the fan surface and 1804-1760 cal yr B.P. for the younger horizon, 2.3 m below the fan surface. These ages constrain the age of T2 because T2 must have been present as a surface by 1830 cal yr B.P. to receive the deposition from the fan that separates these two horizons. When compared with the date of 2708-2402 cal yr B.P. (Zehfuss, 1996) from wood in point bar sands below a second fan built on T2 just upstream, it appears that these dates demonstrate the time-transgressive nature of river deposits. The age of this terrace is interpreted to be at least 2402 cal yr B.P.

The samples from T5 and T6 have a wide range of ages. The range of ages in T5 is 3471 cal yr B.P. for a sample 0.33 m below the surface to 8424 cal yr B.P. for a sample 0.75 m below the surface, at the base of the overbank deposits. In T6, the age range is even larger. The highest sample, 0.33 m below the surface, has an age of 1706 cal yr B.P., the lowest sample, 0.55 m below the surface, has an age of 4408 cal yr B.P., and the oldest sample, 0.46 m below the surface, has an age of 9210 cal yr B.P.

All dates represent limiting ages. The samples could be from charcoal that

was once sitting on the surface and subsequently was stirred in to the overbank deposits from biological activity. Therefore, the age of the oldest sample implies that the overbank deposits must be at least that old for the charcoal to have been deposited there. Charcoal deposition by the river is not necessarily implied for the oldest samples in this interpretation because the same processes could have introduced both the younger and older samples in the overbank deposits. However, the proper age relationship between the limiting ages of T5 and T6 does not eliminate the possibility that the oldest samples were deposited by the river. Although there is plenty of evidence of soil stirring (root cast, animal burrows), there are no sedimentary structures to prove deposition by the river.

Radiocarbon Dates: Mad River

The AMS dates presented here (Table 3.6), from a trench on T4 (Figure 3.19), are the first radiocarbon dates from the Mad River Valley. The three dates are from samples taken at about the same depth from overbank deposits in the same part of the trench. The ages are in close agreement, ranging from 11,837 to 11,138 cal yr B.P.

Although these may be samples that have been stirred in by biological activity, the similarity in age may point toward these samples being deposited directly by the river. However, there is no sedimentological evidence to support charcoal deposition by the river as the samples were removed from massive overbank deposits. Therefore, these dates must be considered limiting ages and are interpreted to mean that T4 had formed by 11,138 cal yr B.P.

CHAPTER 4: RESULTS AND CALCULATIONS

DATED TERRACE CHRONOLOGY

The dated terrace chronology is derived for each valley by combining the data from the dated terraces and alluvial fans (Tables 3.1-3.3) and the baselevel records (Table 2.5). The dated terrace chronology is carried to the other valleys as a baselevel record. The assumption that the processes responsible for terrace development in one valley may also have led to terrace development in another valley is discussed independently.

Mad River Valley

In the Mad River Valley terrace chronology, the data are ^{14}C yr. B.P. and the baselevel, terrace, and fan ages previously determined are ^{14}C yr. B.P., and the baselevels are correlated to the ^{14}C yr. B.P. terrace ages. The highest terraces, T10-T8, are correlated based on the assumption that they are at the highest baselevels in the lower part of the valley. Lakes Mad River, Washington, Mansfield II, and Coville, Lake Winooski, and Lake Mad River are expanded into the Winooski Drainage Basin. The baselevels for Lakes Fort Ann I and II are correlated with T7 and T6, respectively, based on the assumed mutuality of the baselevel and terrace records. In addition, the difference in elevation between Lakes Fort Ann I and II is used to estimate the baselevel for Lake Mad River.

Hunton River Valley

In the Hunton River Valley terrace chronology, the data are ^{14}C yr. B.P. and the baselevel, terrace, and fan ages previously determined are ^{14}C yr. B.P., and the baselevels are correlated to the ^{14}C yr. B.P. terrace ages. The highest terraces, T10-T8, are correlated based on the assumption that they are at the highest baselevels in the lower part of the valley. Lakes Mad River, Washington, Mansfield II, and Coville, Lake Winooski, and Lake Mad River are expanded into the Winooski Drainage Basin. The baselevels for Lakes Fort Ann I and II are correlated with T7 and T6, respectively, based on the assumed mutuality of the baselevel and terrace records. In addition, the difference in elevation between Lakes Fort Ann I and II is used to estimate the baselevel for Lake Mad River.

Table 3.6: Mad River Terrace Radiocarbon Ages

Terrace	Sample#	CAMS#	Material	Depth (m)	^{14}C Age	Calibrated Date (yr B.P.)	1 Sigma Range (yr B.P.)	2 Sigma Range (yr B.P.)
T5	TW12	30357	Charcoal	0.63	10150±80	11837	12069-11265	12238-11083
T5	TW10	30355	Charcoal	0.68	10030±100	11330, 11294, 11250, 11248, 11217, 11171, 11138	11830-11007	12097-11094
T5	TW11	30356	Charcoal	0.70	10030±60	11330, 11294, 11250, 11248, 11217, 11171, 11138	11730-11045	11970-111002

Note: Locations of radiocarbon samples are shown on Figure 3.25. Calibration using CALIB 3.0.3A (Stuvier and Reimer, 1993).

CHAPTER 4: RESULTS AND CALCULATIONS

DATED TERRACE CHRONOLOGY

The dated terrace chronologies are derived for each valley by combining the relative chronology presented in the longitudinal profiles (Figures 3.3, 3.5, and 3.7) with the limiting ages of terraces and alluvial fans (Tables 3.1-3.3) and the ages of dated baselevels (Table 2.5). The dated terrace chronology is best constrained for the Huntington Valley due to the abundance of dated landforms, but the terrace ages can be estimated for the other valleys as well. The Huntington River Valley chronology is carried to the other valleys as a first-order approach using the assumption that the processes responsible for the terraces in the Huntington may also have led to terrace development in the other valleys. The validity of this assumption is evaluated below where the chronology for each valley is discussed independently.

Terrace Chronology: Huntington River Valley

To construct the Huntington River Valley terrace chronology, the data are compiled in Table 4.1. The baselevel, terrace, and fan ages previously presented are assigned to the terraces correlated in the longitudinal profile.

Baselevel Ages The three highest terraces, T10-T8, are correlated based on the terrace elevations to the three highest baselevels in the lower part of the Huntington Valley, Lakes Huntington, Mansfield II, and Coveville. Lake Coveville is estimated to have expanded into the Winooski Drainage Basin by 12,700 ^{14}C yr B.P. and the other two baselevels are estimated each to span about 100 ^{14}C yrs (Table 2.5). Lakes Fort Ann I and II are correlated with T7 and T6, respectively, based on the assumed mutuality of the baselevel and terrace records. In addition, the difference in elevation between Lakes Fort

Tabel 4.1 Huntington River Terrace Chronology

Terrace	Baselevel	Baselevel Age (^{14}C ky B.P.)*	Fan/Terrace Age (^{14}C ky B.P.)†	Age (^{14}C ky B.P.)
T10	Lake Huntington	13.0-12.8	-	13.0-12.8
T9	Lake Mansfield II	12.8-12.7	-	12.8-12.7
T8	Lake Coveville	12.7-12.6	-	12.7-12.6
T7	Lake Fort Ann I	12.6-12.2	-	12.6-12.2
T6	Lake Fort Ann II	12.2-11.7	>8.2	12.2-11.7
T5	Upper Marine	<11.7	8.5-7.8	11.7-7.8
T4	Local Knickpoints	-	<7.8	7.8-5.2(?)
T3	Local Knickpoints	-	>2.5	5.2(?) - 2.5
T2	Local Knickpoints	-	2.5-1.8	2.5-0.2
T1	Local Knickpoints	-	<0.10	0.2-Today

* Dates from Table 2.5

† Dates from Tables 3.4 and 3.5

Ann I and II is relatively small and the amount of incision between T7 and T6 is small. T5 formed after Lake Fort Ann II. ~~ice chronology~~ the data are

Radiocarbon Ages Radiocarbon-dated deposits from T6, T5, T2, and T1 constrain the ages of those terraces. The age of >8200 ^{14}C yr B.P. for T6 is consistent with assigning T6 to Lake Fort Ann II. The oldest basal fan age and the terrace deposit age from T5 suggest that T5 was present by 8500 ^{14}C yr B.P. and limit the formation of T4 to after 7800 ^{14}C yr B.P. The basal fan age of 2500 ^{14}C yr B.P. from T2 implies that T3 was formed before then and the basal fan age of <100 ^{14}C yr B.P. points to T1 being of historic age.

Other Ages Presently there is no constraint on when T4/T3 incision took place. The estimated age of 5200 ^{14}C yr B.P. is simply the median age between the two limiting radiocarbon ages.

In the Huntington Valley mark the ending and beginning, respectively, of synchronous fan and terrace formation. Although there is no evidence to suggest that the Little River Valley responded to the same forcings which initiated landform development in the Huntington Valley before 7800 and after 2500 ^{14}C yr B.P., it is likely that the hillside, or river systems in the Little River Basin would have responded similarly as the forcings were regional in scale like eastward upwinds. The future use ages will be used to bracket the formation of T4-T5 in the Little River Valley. T1 is assumed to be formed during postglacial times and T2-T4 in the Huntington River Valley.

Terrace Chronology: Little River Valley

To construct the Little River Valley terrace chronology, the data are compiled in Table 4.2. The baselevel ages previously presented are assigned to the terraces correlated in the longitudinal profile. Since no radiocarbon dates were obtained from the Little River Valley, the Huntington River terrace chronology is used to assign the ages of the youngest terraces.

Baselevel Ages The highest three terraces in the Little River Valley (T9-T7) have been correlated with Lakes Mansfield I, Mansfield II, Coveville based on elevation. The next three terraces, T6 and T5A/B, are assigned to Lakes Fort Ann I and II. The age of T4 is interpreted as younger than Lake Fort Ann II.

Other Ages The lower limiting age of T5 and the upper limiting age of T2 in the Huntington Valley mark the ending and beginning respectively of synchronous fan and terrace formation. Although there is no evidence to suggest that the Little River Valley responded to the same forcings which initiated landform development in the Huntington Valley before 7800 and after 2500 ^{14}C yr B.P., it is likely that the hillslope and river systems in the Little River Basin would have responded similarly if the forcings were regional in scale, like climate changes. Therefore these ages are used to bracket the formation of T4-T2 in the Little River Valley. T1 is assumed to be formed during historical times as it was in the Huntington River Valley.

Table 4.2: Little River Terrace Chronology

Terrace	Baselevel	Baselevel Age (^{14}C ky B.P.)*	Age (^{14}C ky B.P.)
T9	Lake Mansfield I	12.9-12.8	12.9-12.8
T8	Lake Mansfield II	12.8-12.7	12.8-12.7
T7	Lake Coveville	12.7-12.6	12.7-12.6
T6	Lake Fort Ann I	12.6-12.2	12.6-12.2
T5A, 5B	Lake Fort Ann II	12.2-11.7	12.2-11.7
T4	Upper Marine	<11.7	11.7-7.8
T3	Local Knickpoints	-	7.8-2.5 ¥
T2	Local Knickpoints	-	2.5-0.2 ¥
T1	Local Knickpoints	-	0.2-Today ¥

* Dates from Table 2.5

¥ Dates extended from Huntington Valley, Table 4.1

assumed to represent base level and was formed between 12,600 and 11,700

^{14}C yr B.P.? T4 was formed sometime later.

Radiocarbon Ages: The T4 terrace is the only dated landform in the Mad River Valley. The limiting age of 10,100 ^{14}C yr B.P. is consistent with T4 being formed after 11,700 ^{14}C yr B.P.

Other Ages: The Huntington River Valley fan and terrace ages are again used to place limiting ages on the terraces after T5 in the Mad River based on the assumption that the same regional forcings caused terrace formation at the same time. Since the ages of post-baselevel terraces from the Huntington River Valley are extended to both the Mad and Little River terraces, both valleys appear to have identical chronologies during the Holocene. However, these chronologies are uncorroborated by radiocarbon ages and therefore, the similarity of terrace ages among the three valleys is an untested conclusion.

Terrace Chronology: Mad River Valley

Baselevel Ages The baselevels assigned to the Mad River Valley terraces are based on correlated elevations as in the other valleys (Table 4.3). Beginning with Lake Winooski and T9, the baselevels and terraces are correlated through Lake Fort Ann I. One difference between the Mad and the other valleys is no terrace is attributable to Lake Fort Ann II. As the Mad Valley is farther away from the Fort Ann shorelines and the amount of incision between the two levels is low, it is possible that the incision never propagated to the Mad River Valley. Therefore, T5 in the Mad River Valley is assumed to represent both levels and was formed between 12,600 and 11,700 ^{14}C yr B.P. T4 was formed sometime later.

Radiocarbon Ages The T4 terrace is the only dated landform in the Mad River Valley. The limiting age of 10,100 ^{14}C yr B.P. is consistent with T4 being formed after 11,700 ^{14}C yr B.P.

Other Ages The Huntington River Valley fan and terrace ages are again used to place limiting ages on the terraces after T5 in the Mad River based on the assumption that the same regional forcings caused terrace formation at the same time. Since the ages of post-baselevel terraces from the Huntington River Valley are extended to both the Mad and Little River terraces, both valleys appear to have identical chronologies during the Holocene. However, both chronologies are unconstrained by radiocarbon ages and therefore, the similarity of terrace ages among the three valleys is an untested correlation.

Table 4.3: Mad River Terrace Chronology

Terrace	Baselevel	Baselevel Age (^{14}C ky B.P.)*	Terrace Age (^{14}C ky B.P.)†	Age (^{14}C ky B.P.)
T9	Lake Winooski	13.0-12.9	-	13.0-12.9
T8	Lake Mansfield I	12.9-12.8	-	12.9-12.8
T7	Lake Mansfield II	12.8-12.7	-	12.8-12.7
T6	Lake Coveville	12.7-12.6	-	12.7-12.6
T5	Lake Fort Ann I	12.6-12.2	-	12.6-12.2
T5	Lake Fort Ann II	12.2-11.7	-	12.2-11.7
T4	Upper Marine	<11.7	10.1	11.7-10.1
T3	Local Knickpoints	-	-	7.8-2.5 ¥
T2	Local Knickpoints	-	-	2.5-0.2 ¥
T1	Local Knickpoints	-	-	0.2-Today ¥

* Dates from Table 2.5

† Dates from Tables 3.6

¥ Dates extended from Huntington Valley, Table 4.1

can be defined reasonably by a line. The present gradients are presented for both Huntington and Mad Rivers below.

The present terrace gradient has been deformed from its original gradient because river terraces are tilted with the rest of the land during glacio-isostatic rebound. Therefore to define the initial gradient of the river, the terrace gradients must be re-projected using previously published estimates of the magnitude and timing of tilting in the Champlain Basin. From the ages and present gradients of the terraces and the rate of glacio-isostatic rebound, an initial gradient can be estimated. As noted before, the Winooski Drainage basin lies between two areas where the gradient of the maximum tilt plane has been measured, the Champlain Valley (Chapman, 1937) and the Connecticut Valley (Kauf and Larson, 1989). The magnitude of the tilt plane increased through time as the rate of rebound decreased; therefore younger terraces were tilted less. I have tried to correct for glacio-isostatic tilting by using the exponential decay model I presented in Chapter 2 to determine the magnitude of tilting that would have occurred since the end of the time period

TERRACE GRADIENTS

The gradients of the terraces are calculated using the longitudinal profiles. Each river is divided into reaches based on the orientation of the profile, the location of knickpoints, and similar geomorphic criteria. A best-fit line is drawn through the plotted elevations of the terraces within a reach (Figure 4.1) and the slope of that line defines the present terrace gradient for that reach. The accuracy of the measured gradients for each reach depends on the number of survey locations within the reach; the line is better constrained with more survey locations. Each best-fit line had a correlation coefficient (R^2) value above 0.9, suggesting that gradient of the terraces within a reach can be defined reasonably by a line. The present gradients are presented for the Huntington and Mad Rivers below.

The present terrace gradient has been deformed from its original gradient because river terraces are tilted with the rest of the land during glacio-isostatic rebound. Therefore to define the initial gradient of the river, the terrace gradients must be retrodeformed using previously published estimates of the magnitude and timing of tilting in the Champlain Basin. From the ages and present gradients of the terraces and the rate of glacio-isostatic rebound, an initial gradient can be estimated. As noted before, the Winooski Drainage Basin lies between two areas where the gradient of the maximum tilt plane has been measured: the Champlain Valley (Chapman, 1937) and the Connecticut Valley (Koteff and Larsen, 1989). The magnitude of the tilt plane decreased through time as the rate of rebound decreased; therefore younger terraces were tilted less. I have tried to correct for glacio-isostatic tilting by using the exponential decay model I presented in Chapter 2 to determine the magnitude of tilting that would have occurred since the end of the time period

when a terrace was formed. The magnitude of tilting is reported for both the Chapman (1957) and Kotoff and Larsen (1989) tilt planes in the orientation of each reach. The tilting angle is calculated by subtracting the present gradient from the calculated gradient adding the present gradient to the gradient of the tilt plane.

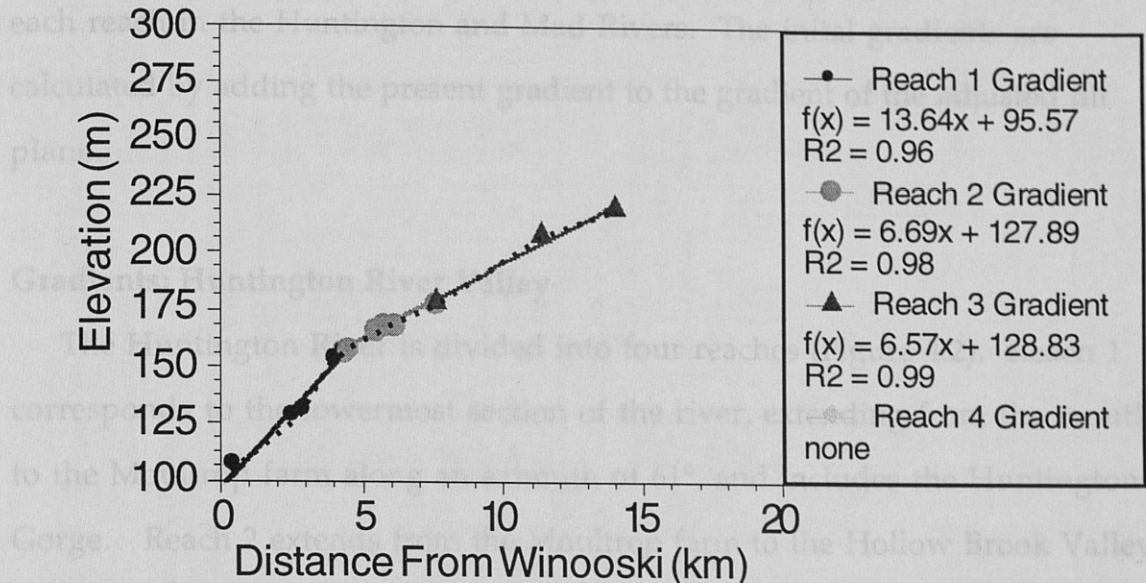


Figure 4.1: Example of Best-fit Lines for Terrace Elevations. Best-fit lines of terrace elevations are generated for each reach. The slope of the line is the terrace gradient. The dotted line is the terrace elevations from the longitudinal profile.

The Huntington Valley terrace gradients are reported in Table 4.4 and in Figure 4.3. The present river gradient is steeper in Reach 4. The river gradient in Reaches 2 and 3 is nearly identical. Since the formation of T10, the terrace gradients have progressively become steeper in Reaches 1, 2, and 4, while the gradient in Reach 3 has changed very little. When the gradients are plotted versus time (Figure 4.4), it appears that initially the gradient changed rapidly and although the gradient has continued increase toward the present, the rate of change is slower.

The shape of the curve in Figure 4.4 is similar to exponential decay and at first glance may appear to be a function of glacio-isostatic rebound. This premise can be tested by examining the corrected gradients. If the magnitude of the gradient change were similar to the magnitude of glacio-isostatic

when a terrace was formed. The magnitude of tilting is reported for both the Chapman (1937) and Koteff and Larsen (1989) tilt planes in the orientation of each reach in the Huntington and Mad Rivers. The initial gradients are calculated by adding the present gradient to the gradient of the adjusted tilt plane.

Gradients: Huntington River Valley

The Huntington River is divided into four reaches (Figure 4.2). Reach 1 corresponds to the lowermost section of the river, extending from the mouth to the Moulthrop farm along an azimuth of 61° , and includes the Huntington Gorge. Reach 2 extends from the Moulthrop farm to the Hollow Brook Valley along an azimuth of 354° . Reach 3 corresponds to the section from Hollow Brook to HR4, and Reach 4 continues from there to the HR3, comprising the steepest section of the river.

The Huntington Valley terrace gradients are reported in Table 4.4 and in Figure 4.3. The present river gradient is steepest in Reach 4. The river gradient in Reaches 2 and 3 is nearly identical. Since the formation of T10, the terrace gradients have progressively become steeper in Reaches 1, 2, and 4, while the gradient in Reach 3 has changed very little. When the gradients are plotted versus time (Figure 4.4), it appears that initially the gradient changed rapidly and although the gradient has continued increase toward the present, the rate of change is slower.

The shape of the curve in Figure 4.4 is similar to exponential decay and at first glance may appear to be a function of glacio-isostatic rebound. This premise can be tested by examining the corrected gradients. If the magnitude of the gradient change were similar to the magnitude of glacio-isostatic

Table 4.4: Huntington Valley Terrace Gradients

Terrace	Reach 1: N61E						Reach 2: N6W					
	Chapman (1937)			Koteff and Larsen (1989)			Chapman (1937)			Koteff and Larsen (1989)		
	Gradient (m/km)	Tilt Plane (m/km)	Initial Gradient (m/km)	Tilt Plane (m/km)	Initial Gradient (m/km)	Gradient (m/km)	Tilt Plane (m/km)	Initial Gradient (m/km)	Tilt Plane (m/km)	Initial Gradient (m/km)	Tilt Plane (m/km)	Initial Gradient (m/km)
10	-	-	-	-	-	-0.94	0.94	0.00	0.86	-0.08	-	-
9	-0.25	0.24	-0.01	0.12	-0.13	-0.67	0.92	0.25	0.84	0.17	-	-
8	0.70	0.21	0.91	0.11	0.81	1.77	0.82	2.59	0.75	2.52	-	-
7	6.68	0.19	6.87	0.09	6.77	3.01	0.71	3.72	0.65	3.66	-	-
6	8.06	0.14	8.20	0.07	8.13	3.33	0.53	3.86	0.49	3.82	-	-
5	10.53	0.10	10.63	0.05	10.58	5.21	0.37	5.58	0.33	5.54	-	-
4	11.82	0.00	11.82	0.00	11.82	5.98	0.01	5.99	0.01	5.99	0.01	5.99
3	13.21	0.00	13.21	0.00	13.21	6.47	0.01	6.48	0.01	6.48	0.01	6.48
2	13.64	0.00	13.64	0.00	13.64	6.69	0.00	6.69	0.00	6.69	0.00	6.69
1	-	-	-	-	-	7.46	0.00	7.46	0.00	7.46	0.00	7.46
River	14.30	0.00	14.30	0.00	14.30	6.92	0.00	6.92	0.00	6.92	0.00	6.92

Terrace	Reach 3: N6W						Reach 4: N6W					
	Chapman (1937)			Koteff and Larsen (1989)			Chapman (1937)			Koteff and Larsen (1989)		
	Gradient (m/km)	Tilt Plane (m/km)	Initial Gradient (m/km)	Tilt Plane (m/km)	Initial Gradient (m/km)	Gradient (m/km)	Tilt Plane (m/km)	Initial Gradient (m/km)	Tilt Plane (m/km)	Initial Gradient (m/km)	Tilt Plane (m/km)	Initial Gradient (m/km)
10	6.65	0.94	7.59	0.86	7.51	18.62	0.94	19.56	0.86	19.48	-	-
9	7.17	0.92	8.09	0.84	8.01	17.66	0.92	18.58	0.84	18.50	-	-
8	6.70	0.82	7.52	0.75	7.45	-	-	-	-	-	-	-
7	6.98	0.71	7.69	0.65	7.63	-	-	-	-	-	-	-
6	6.43	0.53	6.96	0.49	6.92	-	-	-	-	-	-	-
5	-	-	-	-	-	-	-	-	-	-	-	-
4	-	-	-	-	-	-	-	-	-	-	-	-
3	-	-	-	-	-	-	-	-	-	-	-	-
2	6.57	0.00	6.57	0.00	6.57	-	-	-	-	-	-	-
1	6.42	0.00	6.42	0.00	6.42	19.06	0.00	19.06	0.00	19.06	0.00	19.06
River	6.50	0.00	6.50	0.00	6.50	20.42	0.00	20.42	0.00	20.42	0.00	20.42

Notes: Gradient is measured for each terrace in each reach. Initial gradient is calculated for each terrace in each reach based on the magnitude of rebound at time of terrace formation in the direction of the reach using Chapman (1937) and Koteff and Larsen (1989) tilt planes (Table 2.6) and rebound model in Appendix A.

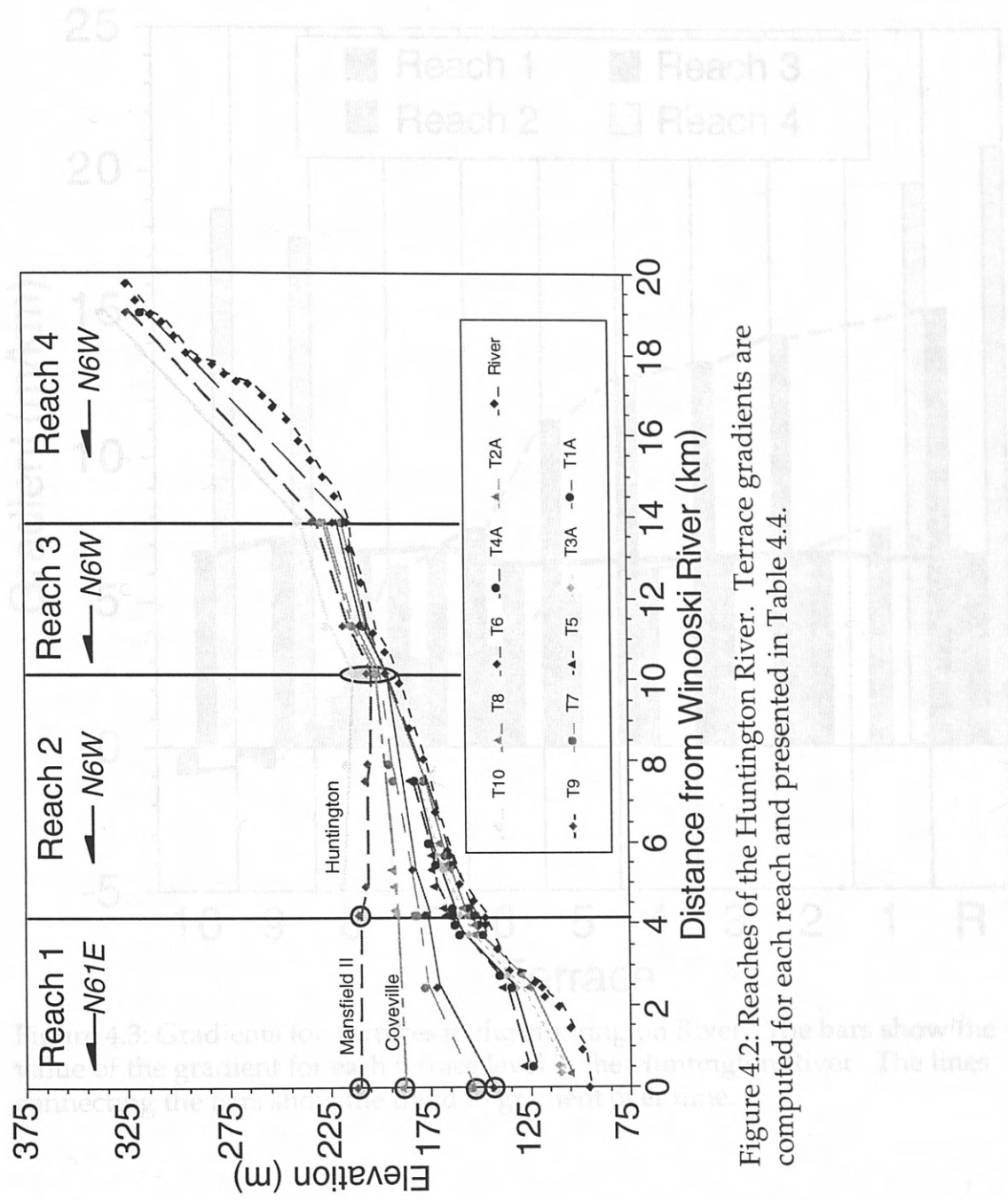


Figure 4.2: Reaches of the Huntington River. Terrace gradients are computed for each reach and presented in Table 4.4.

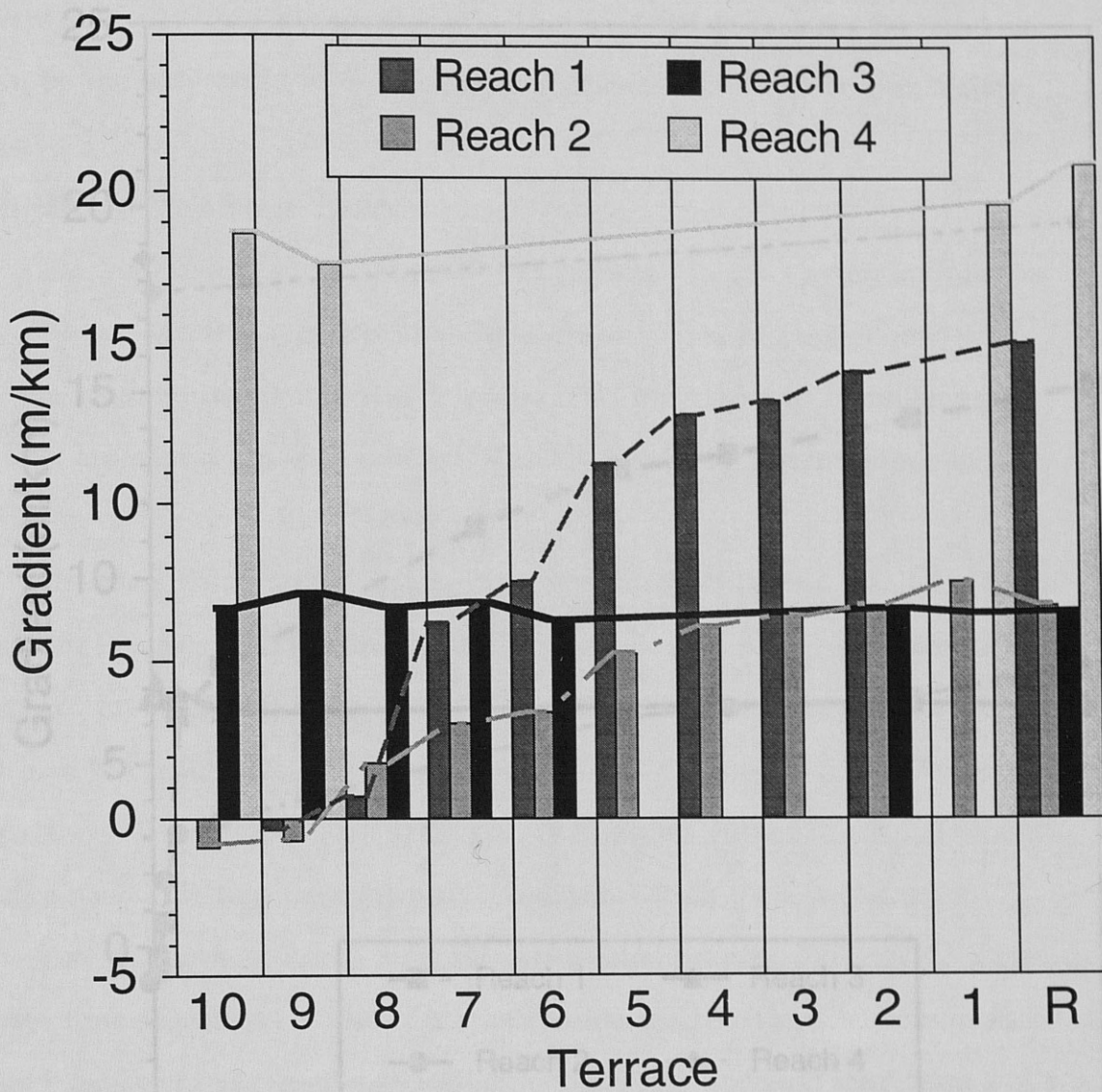


Figure 4.3: Gradients for Terraces in the Huntington River. The bars show the value of the gradient for each terrace level in the Huntington River. The lines connecting the bars show the trend in gradient over time.

Figure 4.4: Graph of Huntington River Terrace Gradient Versus Time. The gradients for each reach are plotted by their approximate age.

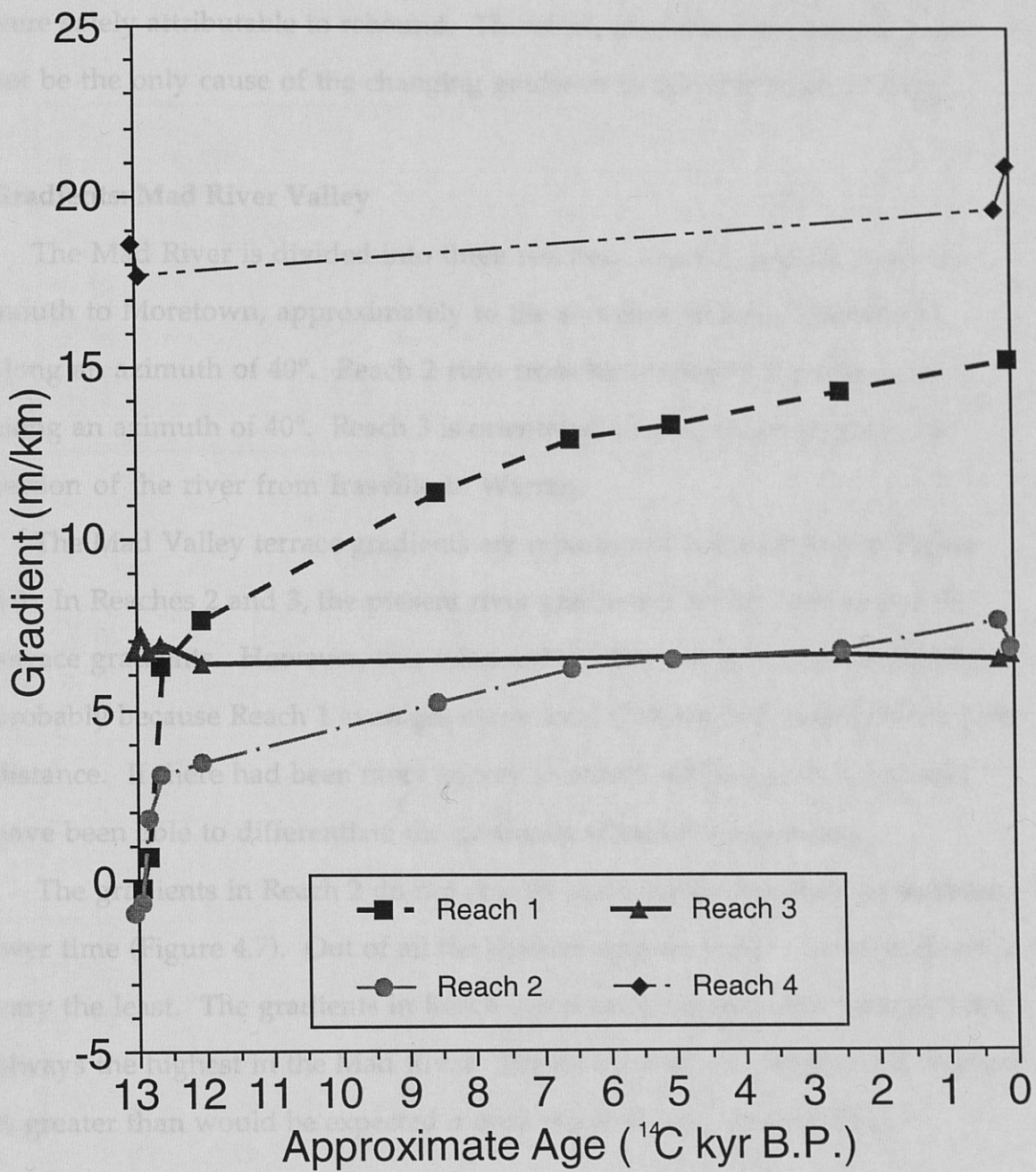


Figure 4.4: Graph of Huntington River Terrace Gradients Versus Time. The gradients for each reach are plotted by their approximate age.

rebound, then there might be a valid correlation. However, the change in gradient is often several times greater than would be expected if the change were solely attributable to rebound. Therefore, glacio-isostatic rebound can not be the only cause of the changing gradients in the Huntington Valley.

Gradients: Mad River Valley

The Mad River is divided into three reaches. Reach 1 extends from the mouth to Moretown, approximately to the shoreline of Lake Mansfield I, along an azimuth of 40° . Reach 2 runs from Moretown to Irasville, again along an azimuth of 40° . Reach 3 is orientated 10° and corresponds to the section of the river from Irasville to Warren.

The Mad Valley terrace gradients are reported in Table 4.5 and in Figure 4.6. In Reaches 2 and 3, the present river gradient is higher than any of the terrace gradients. However, this relationship does not hold true for Reach 1, probably because Reach 1 averages many local changes in gradient over a long distance. If there had been more survey locations within Reach 1, I would have been able to differentiate the gradients within these sections.

The gradients in Reach 2 do not change significantly, but they do increase over time (Figure 4.7). Out of all the studied reaches, the gradients in Reach 2 vary the least. The gradients in Reach 3 generally increase over time and are always the highest in the Mad River. For all the reaches, the gradient increase is greater than would be expected if only rebound were responsible.

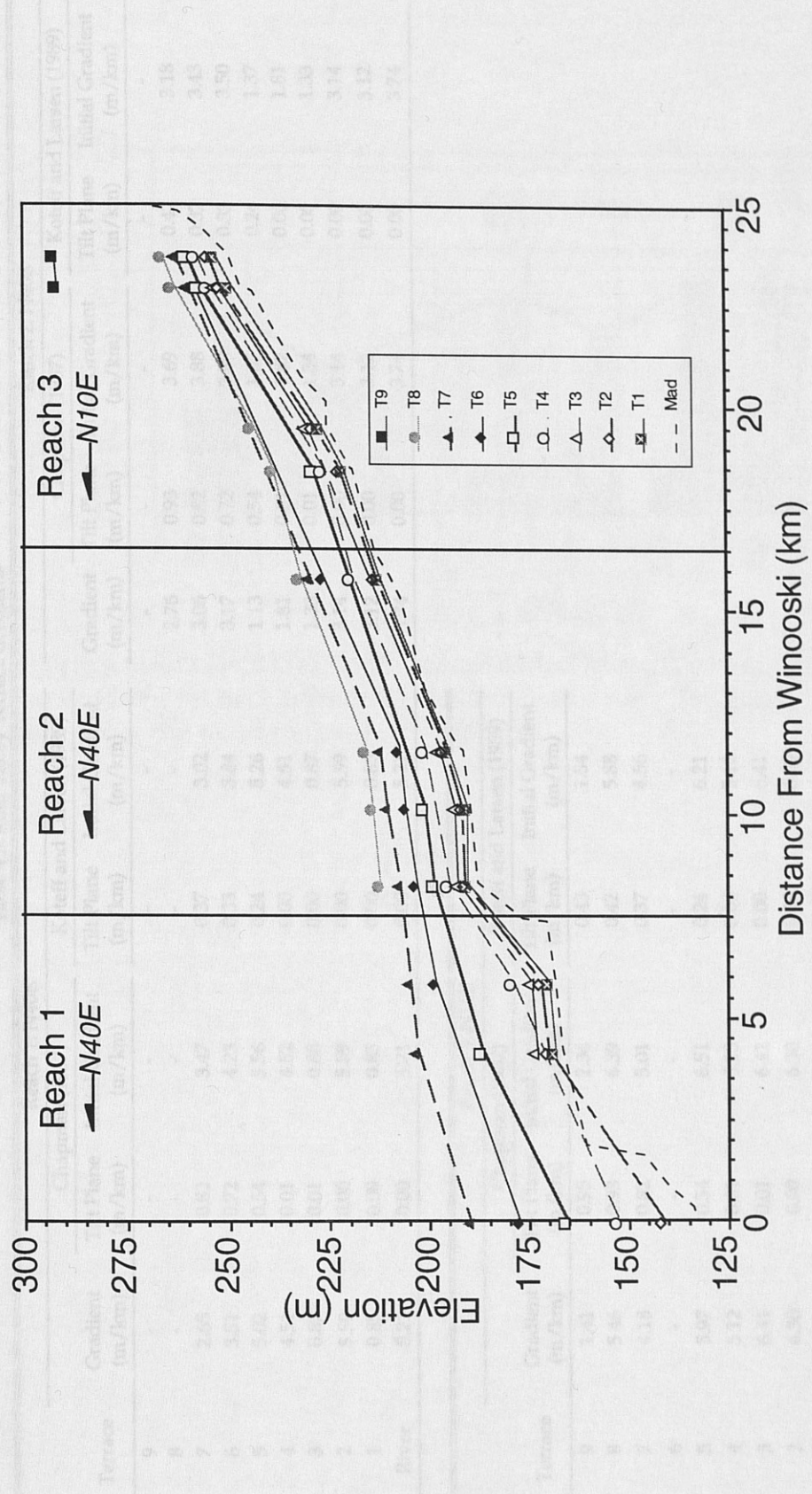


Figure 4.5: Reaches of the Mad River. The terrace gradients computed for each reach are presented in Table 4.5.

Table 4.5: Mad Valley Terrace Gradients

Terrace	Reach 1: N40E			Reach 2: N40E		
	Chapman (1937)		Koteff and Larsen (1989)	Chapman (1937)		Koteff and Larsen (1989)
	Gradient (m/km)	Tilt Plane (m/km)	Initial Gradient (m/km)	Tilt Plane (m/km)	Initial Gradient (m/km)	Tilt Plane (m/km)
9	-	-	-	-	-	-
8	-	-	-	-	-	-
7	2.65	0.82	3.47	0.37	3.02	2.76
6	3.51	0.72	4.23	0.33	3.84	3.06
5	5.02	0.54	5.56	0.24	5.26	3.17
4	4.51	0.01	4.52	0.00	4.51	0.72
3	0.87	0.01	0.88	0.00	0.87	0.54
2	5.59	0.00	5.59	0.00	5.59	1.13
1	0.85	0.00	0.85	0.00	0.85	1.81
River	5.21	0.00	5.21	0.00	5.21	0.01

Terrace	Reach 3: N10E			Reach 4: N10E		
	Chapman (1937)		Koteff and Larsen (1989)	Chapman (1937)		Koteff and Larsen (1989)
	Gradient (m/km)	Tilt Plane (m/km)	Initial Gradient (m/km)	Tilt Plane (m/km)	Initial Gradient (m/km)	Tilt Plane (m/km)
9	1.41	0.95	2.36	0.43	1.84	-
8	5.46	0.93	6.39	0.42	5.88	-
7	4.18	0.82	5.01	0.37	4.56	-
6	-	-	-	-	-	-
5	5.97	0.54	6.51	0.24	6.21	-
4	5.12	0.01	5.13	0.00	5.12	-
3	6.41	0.01	6.42	0.00	6.41	-
2	6.30	0.00	6.30	0.00	6.30	-
1	6.12	0.00	6.12	0.00	6.12	-
River	7.16	0.00	7.16	0.00	7.16	-

Notes: Gradient is measured for each terrace in each reach. Initial gradient is calculated for each terrace in each reach based on the magnitude of rebound at time of terrace formation in the direction of the reach using Chapman (1937) and Koteff and Larsen (1989) tilt planes (Table 2.6) and rebound model in Appendix A.

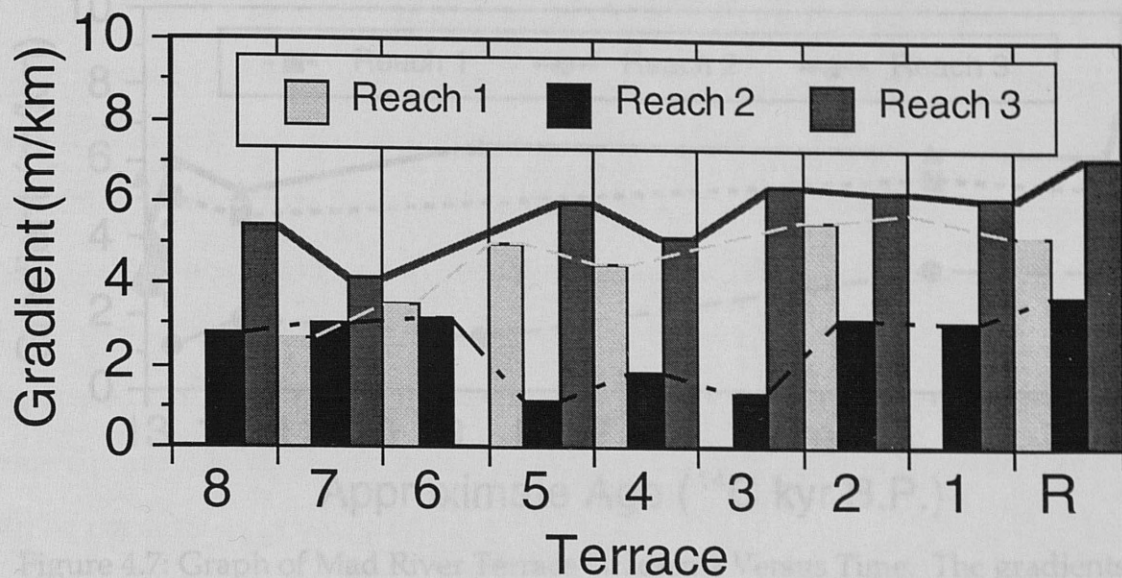


Figure 4.6: Gradients for Terraces in the Mad River. The bars show the value of the gradient for each terrace level in the Mad River. The lines connecting the bars show the trend in gradient over time.

CHAPTER 5: DISCUSSION

TERRACE GRADIENTS IN THE MAD RIVER DRAINAGE BASIN

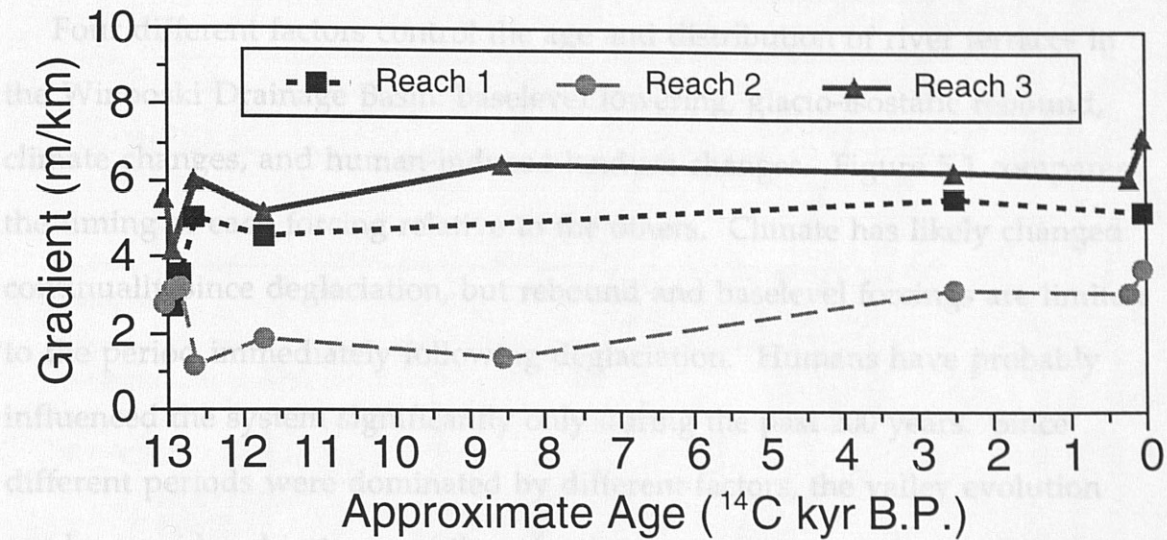


Figure 4.7: Graph of Mad River Terrace Gradients Versus Time. The gradients for each reach are plotted by their approximate age.

changes are several climate changes (Figure 5.1). Although tilting may have changed slightly the magnitude of present-day terrace gradients, it is an unlikely cause for incision because the baselevel changes associated with the lowering of proglacial lakes were gradual and essentially instantaneous as the lake withdrew and progressively lower spillways were exposed. The relatively slow rate of glacio-isostatic tilting, versus the instantaneous baselevel changes, and the low magnitude of glacio-isostatic tilting, versus the higher magnitude of changes in terrace gradients over time, both point to baselevel controlling the timing of incision. When the proglacial lakes existed in the Winooski Drainage Basin, they formed basin-wide baselevels for the tributary rivers. During the Champlain Sea interval, the Winooski River was controlled by the ultimate baselevel, the ocean. Once Lake Champlain formed, it became the basin-wide baselevel for all the rivers in the basin. Glacio-isostatic rebound was in part responsible for baselevel changes, but from the

CHAPTER 5: DISCUSSION

TERRACE FORMATION IN THE WINOOSKI DRAINAGE BASIN

Four different factors control the age and distribution of river terraces in the Winooski Drainage Basin: baselevel lowering, glacio-isostatic rebound, climate changes, and human-induced landuse changes. Figure 5.1 compares the timing of each forcing relative to the others. Climate has likely changed continually since deglaciation, but rebound and baselevel forcings are limited to the period immediately following deglaciation. Humans have probably influenced the system significantly only during the past 200 years. Since different periods were dominated by different factors, the valley evolution can be considered in terms of these forcings.

Rebound rates were the highest during the period of many baselevel changes and several climate changes (Figure 5.1). Although tilting may have changed slightly the magnitude of present-day terrace gradients, it is an unlikely cause for incision because the baselevel changes associated with the lowering of proglacial lakes were episodic and essentially instantaneous as ice withdrew and progressively lower spillways were exposed. The relatively slow rate of glacio-isostatic tilting, versus the instantaneous baselevel changes, and the low magnitude of glacio-isostatic tilting, versus the higher magnitude of changes in terrace gradients over time, both point to baselevel controlling the timing of incision. When the proglacial lakes existed in the Winooski Drainage Basin, they formed basin-wide baselevels for the tributary rivers. During the Champlain Sea interval, the Winooski River was controlled by the ultimate baselevel, the ocean. Once Lake Champlain formed, it became the basin-wide baselevel for all the rivers in its basin. Glacio-isostatic rebound was in part responsible for baselevel changes, but from the

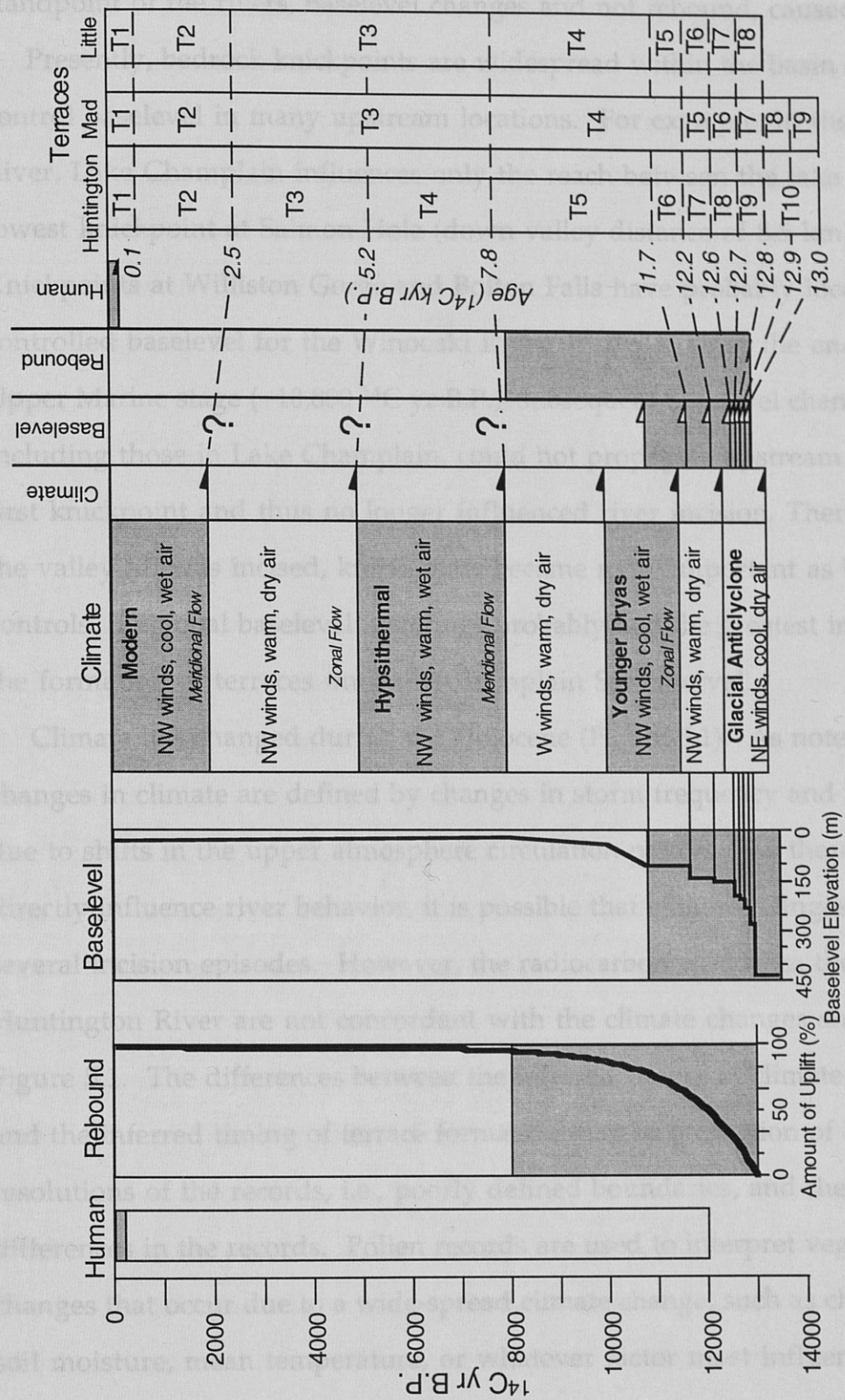


Figure 5.1: Comparison of Forcings on River Terrace Formation. Shown are the summary data compiled from the previous research and the terrace chronologies. Shaded areas represent periods when a forcing would be dominant. Arrows show interpreted correlations between forcings and terrace formation.

standpoint of the rivers, baselevel changes and not rebound, caused incision.

Presently, bedrock knickpoints are widespread within the basin and control baselevel in many upstream locations. For example, in the Winooski River, Lake Champlain influences only the reach between the lake and the lowest knickpoint at Salmon Hole (down-valley distance of 8.5 km). Knickpoints at Williston Gorge and Bolton Falls have probably locally controlled baselevel for the Winooski River upstream since the end of the Upper Marine stage (~10,800 ^{14}C yr B.P.); subsequent baselevel changes, including those in Lake Champlain, could not propagate upstream past the first knickpoint and thus no longer influenced river incision. Therefore, as the valley fill was incised, knickpoints became more important as baselevel controls. Regional baselevel lowerings probably had the greatest impact on the formation of terraces until the Champlain Sea interval.

Climate has changed during the Holocene (Figure 5.1). As noted earlier, changes in climate are defined by changes in storm frequency and intensity due to shifts in the upper atmosphere circulation pattern. As these changes directly influence river behavior, it is possible that climate changes triggered several incision episodes. However, the radiocarbon ages from the Huntington River are not concordant with the climate changes shown in Figure 5.1. The differences between the inferred timing of climate changes and the inferred timing of terrace formation may be a function of both the resolutions of the records, i.e., poorly defined boundaries, and the inherent differences in the records. Pollen records are used to interpret vegetation changes that occur due to a wide-spread climate change, such as changes in soil moisture, mean temperature, or whatever factor most influences the particular vegetation proxy. Subject to the same forcing, vegetation changes

may occur at a different time than terrace formation simply because the two different systems respond at different rates. The resolution of the climate and terrace records is such that this discrepancy can not be resolved.

The human influence is a potential factor since the first Native Americans settled northern New England after 11,000 ^{14}C yr B.P. (Bonnichsen et al., 1985). Native Americans living in the basin may have modified the land cover through the use of fire to keep open woodlands (Pyne, 1982). However, early human influence is probably minimal on a basin-wide scale, especially when compared to the Europeans. Therefore, significant human forcings are limited to the past 200 years.

GENERAL MODEL FOR VALLEY EVOLUTION

The valley evolution occurred in 5 stages (Figure 5.2). Each stage is time transgressive and is defined by periods when specific depositional and erosional processes occur. However, the general valley evolution consists of late glacial deposition followed by Holocene erosion. During the first two stages the valley is filled with sediments and during the last three stages the sediments are periodically and episodically eroded from the valley, leaving terraces.

Several modes of deposition during the first two stages produced the valley fill. Actively retreating lobes of the Laurentide ice sheet are responsible for Late Glacial Stage deposition. Till and ice-contact deposits that mantle the glacially scoured bedrock valley walls form the foundation of the valley fill. The Proglacial Lake Stage begins with the transition to lacustrine deposition and ends with the transition to fluvial deposition. Deep water deposits of rhythmically bedded silt and clay and shallow water deposits of fine to coarse

and gravel filled the valley. At the same time, glaciolacustrine sediments were deposited in the valley. Therefore, the highest terrace in the valley is composed of glaciolacustrine deposits.

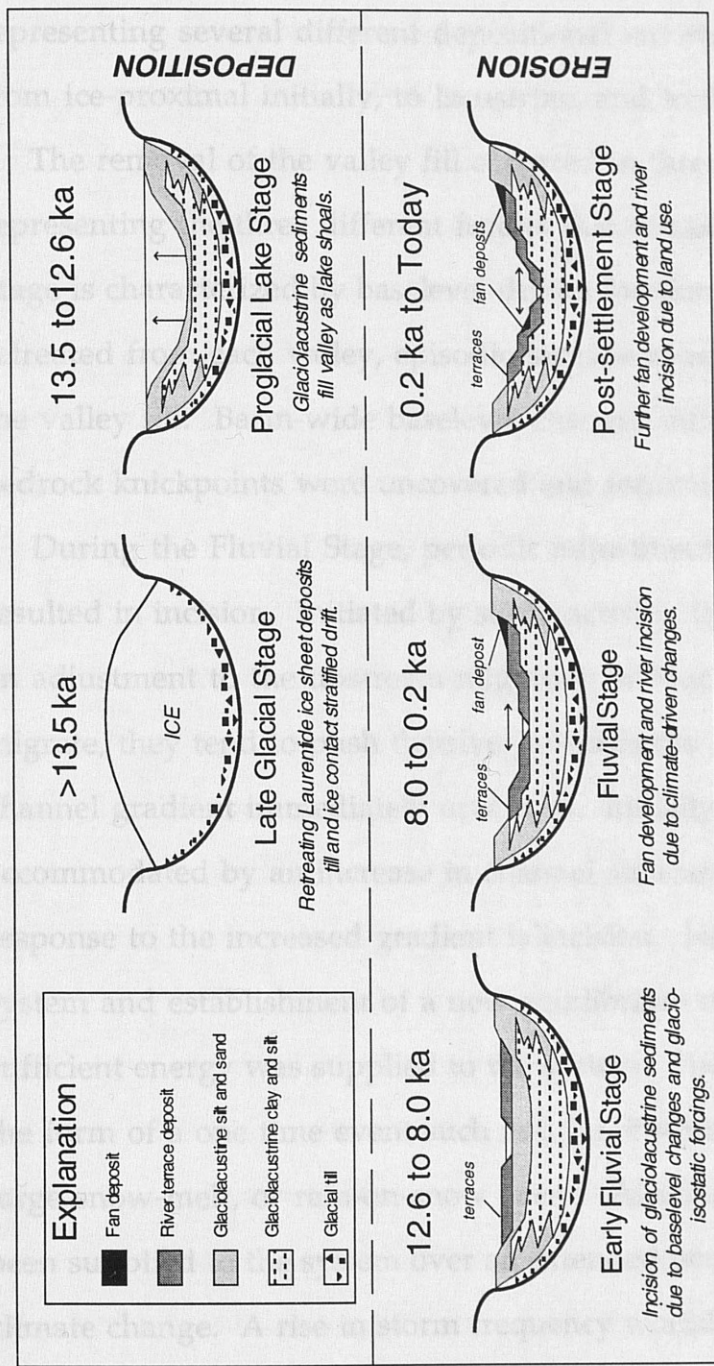


Figure 5.2: Schematic valley evolution. The evolution of the valley is represented by 5 stages. The Late Glacial and Proglacial Lake Stages are times of valley filling. Since Early fluvial times, incision has continually occurred. Ages are approximate, as the valley evolution is time-transgressive. (Modified from Church, 1997).

sand and gravel filled the valley. The highest extent of valley filling at a location occurred after the highest proglacial lake shoaled. At this point in time, fluvial processes capped the fill sequence with the first fluvial deposits. Therefore, the highest terrace in a valley is a composite fill terrace, representing several different depositional environments that may range from ice-proximal initially, to lacustrine, and to fluvial ultimately.

The removal of the valley fill occurred in three distinct stages, representing the three different factors that caused incision. The Early Fluvial Stage is characterized by baselevel-driven incision. As the proglacial lakes retreated from each valley, episodic incision removed significant portions of the valley fill. Basin-wide baselevel changes influenced the river until bedrock knickpoints were uncovered and formed the first local baselevels.

During the Fluvial Stage, periodic adjustments of fluvial behavior resulted in incision. Initiated by storm activity, incision occurred possibly as an adjustment to the upstream migration of knickpoints. As knickpoints migrate, they tend to push the river towards disequilibrium by steepening the channel gradient immediately upstream. Initially, the steeper gradient can be accommodated by an increase in channel sinuosity, but ultimately the likely response to the increased gradient is incision. However, adjustment of the system and establishment of a new equilibrium could only occur when sufficient energy was supplied to the system. The energy may have been in the form of a one time event such as a large storm, a local thunderstorm, a large snow-melt, or rain-on-snow event. Alternatively, the energy may have been supplied to the system over an extended period due to a large-scale climate change. A rise in storm frequency would increase the frequency of channel-modifying river discharges (Leopold and Wolman, 1957; Knox, 1975),

altering the river dynamics until the system, including the hillslopes, vegetation, and river, adjusted to the new precipitation/runoff conditions.

The Post-settlement Stage represents the historic period of valley evolution, a time when humans have been the dominant forcing. Beginning in the 1700's, Europeans settling the area cleared land for pastures and crops, deforesting up to 80% of Vermont (Meeks, 1986). The response of the hillslopes to deforestation is well documented. All of the alluvial fans trenched by Church (1997) and Zehfuss (1996) were capped by 0.5 to 4 m of post-settlement sediment, implying that European land use mobilized hillslope sediment and lead to fan aggradation (Bierman et al., 1997). The response of the lower Winooski River during deforestation is documented by aggradation and an increase in river migration rates during the early 1800's (Thomas, 1985) and by the progradation of the delta (Severson, 1991).

As forests returned to the region during the later half of the 1800's, landslides along tributaries in the lower Winooski River stabilized, evident by the age of trees growing on landslide scars (Baldwin et al., 1995; Bierman et al., 1997), the Winooski delta retreated (Severson, 1991), and the river incised the historic alluvium (Thomas, 1985). A similar river response, aggradation followed by incision, is reported for the lower Mississquoi River during historic times (Brakenridge et al., 1988). Therefore, since European settlement of the area, measurable hillslope and river activity coincided with changes in land use. If the amount of alluvial fan deposition is used as a proxy for the relative magnitude of hillslope activity and subsequent river activity, then river activity during historic times has been at least as great as during any time in the past 8500 ^{14}C yrs (Church, 1997; Bierman, et al., 1997).

GRADIENT

The gradient of the Huntington and Mad Rivers, represented by the present gradient of their terraces, changed since deglaciation (Figures 4.3 and 4.6). The valley evolution model provides the context in which to examine the mechanisms of gradient change and to propose possible longer term forcings on river gradients. The magnitude of gradient changes between terraces is significantly higher than would be expected if glacio-isostatic rebound were the only factor influencing river gradients. If the system were in steady-state equilibrium, then each incision event would return the system to its equilibrium gradient and the difference between today's gradient and the initial gradient would be the gradient of the glacio-isostatic tilt plane. Instead, terrace and therefore river gradients increase through time, punctuated by periods of temporary equilibrium that are represented by floodplain construction. Therefore, the river system is best described as being in meta-stable equilibrium. Meta-stable equilibrium implies that there is a larger, long-term forcing on the river's gradient in addition to the forcings identifiable on shorter time scales.

The increasing gradient with time of the Huntington and Mad Rivers is a direct result of the baselevel changes and knickpoint migration that dominated the Early Fluvial and Fluvial Stages. The close of the Proglacial Lake Stage marks the transition between lacustrine and fluvial processes. Initially, the river flowed atop the lacustrine fill terrace and the lake margin (the baselevel) was relatively close to the valley (if not within the valley). At this time, the river gradient was at its lowest in nearly every segment studied (Figures 4.3 and 4.6). As is shown schematically in Figure 5.3A, valley evolution during the Early Fluvial Stage is controlled by baselevel drops.

With each subsequent baselevel change, the lake margin moves down valley

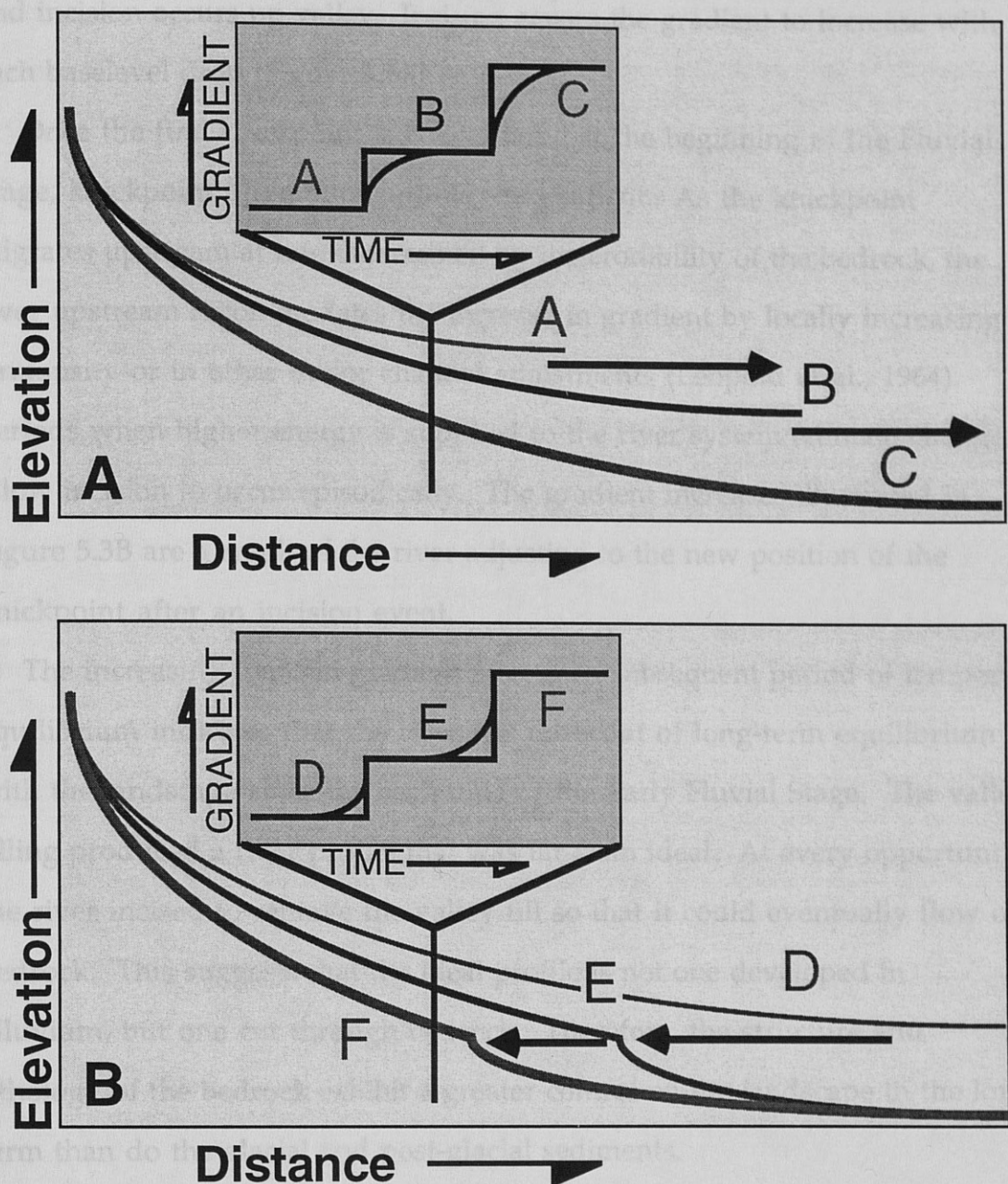


Figure 5.3: Schematic Graphs of Terrace Gradients over Time. The large graphs show the longitudinal profile of several terrace levels and the inset graphs show the change in gradient at a station. In A, the gradient increases over time due to baselevel changes. In B, the gradient increases over time due to upstream knickpoint migration. Once the knickpoint passes the station, the gradient will decrease.

With each subsequent baselevel change, the lake margin moves down valley and incision occurs up valley. Incision causes the gradient to increase with each baselevel drop (Figure 5.3A).

Once the first knickpoint is encountered at the beginning of the Fluvial Stage, knickpoint migration controls the gradient. As the knickpoint migrates upstream at rate determined by the erodibility of the bedrock, the river upstream accommodates the increase in gradient by locally increasing its sinuosity or in other minor channel adjustments (Leopold et al., 1964). Periods when higher energy is supplied to the river system (climate changes?) allow incision to occur episodically. The gradient increases illustrated in Figure 5.3B are a result of the river adjusting to the new position of the knickpoint after an incision event.

The increasing trend in gradient after each subsequent period of temporary equilibrium indicates that the river has been out of long-term equilibrium with the landscape since the beginning of the Early Fluvial Stage. The valley filling produced a river profile that was far from ideal. At every opportunity, the river incised to remove the valley fill so that it could eventually flow on bedrock. This suggests that the ideal profile is not one developed in alluvium, but one cut through bedrock. Therefore, the structure and lithology of the bedrock exhibit a greater control on the landscape in the long term than do the glacial and post-glacial sediments.

Even in the absence of the valley fill, the river profile would not be the smooth curve indicative of an ideal profile. There are multiple knickpoints presently exposed in each tributary as well as in the Winooski so that the valley floors of the tributaries lie at higher elevations than that of the main stem river. In order to achieve the ideal profile, the river requires not only

the removal of all of the valley fill, but also the removal of all bedrock knickpoints along its profile. Therefore, the initial fill terrace and fill-cut terraces that developed between periods of disequilibrium represent very transient steady-state equilibrium conditions. The entire system is moving towards strath development, with each fill-cut terrace signifying a step in the long-term meta-stable equilibrium. The alluvium-dominated system is moving toward a bedrock-controlled system.

Champlain and Adirondack

and Knuepfer (1988) imply that there are no formerly glaciated

IMPLICATIONS OF TERRACE GRADIENTS IN GLACIATED REGIONS

River gradients change between each temporary period of steady-state equilibrium in the Winooski Drainage Basin, making the present terrace gradients unreliable indicators of tectonic tilting. Not only is there no consistent initial gradient from which to calculate the tilt, but the magnitude of the gradient change over time (Tables 4.4 and 4.5) is significantly higher than the magnitude of glacio-isostatic rebound. This brings into question the results of Treadwell and Knuepfer (1988) and Brakenridge et al. (1988) which interpret crustal movements based on terrace gradients and river channel elevation, respectively, in the Champlain Basin.

Treadwell and Knuepfer (1988) calculated recent tilt rates of the Adirondack Mountains using the measured gradients of post-glacial fluvial terraces in the Ausable River Valley, Champlain Basin. The deglacial history of the Ausable Valley is similar to that of the Winooski Drainage Basin; proglacial lakes developed in the north-flowing valley before the baselevel was controlled by proglacial lakes in the Champlain Valley. By assuming that the initial terrace gradient equaled the present river gradient, Treadwell and Knuepfer were able to calculate tilt rates comparable to those measured from

repeated geodetic surveys.

If the Ausable Valley evolution was similar to that in the Winooski Drainage Basin, then the results of Treadwell and Knuepfer are fortuitous rather than indicative of any recent tilt. It is likely that initial terrace gradients were not similar to that of the present river and that the change in gradient that they attribute to recent tilting is in fact controlled by baselevel changes and fluvial adjustments associated with climate changes. Although Treadwell and Knuepfer (1988) imply that the terraces in formerly glaciated regions are sensitive to tectonic tilting, I would argue that one is not able to discern tilting from terrace gradients because the rivers' responses to longer term changes (metastable equilibrium) overpower the tectonic signal.

The conclusions of Brakenridge et al. (1988) are also questionable. Their study found that the long term incision rate of the Mississquoi River decreased by 8000 ^{14}C yr B.P. They attributed the incision to the river's adjustments associated with glacio-isostatic rebound and concluded that this reach of the river was no longer incising by 8000 ^{14}C yr B.P. because glacio-isostatic rebound had ended. The lake-level curves for Lake Champlain presented by Astley (1998) shows that tilting continued throughout the Holocene, decreasing to 0.046 m/km by 7500 ^{14}C yr B.P. and 0.029 m/km by 2000 ^{14}C yr B.P. The slow rate of tilt supports Brakenridge et al.'s assertion that rebound did not cause incision after 8000 ^{14}C yr B.P. However, it does not prove that the more rapid initial uplift associated with glacio-isostatic rebound directly caused incision.

Based on my interpretation of the Winooski Drainage Basin terrace record, I would argue that the decrease in incision rate is due to knickpoint formation and the fact that the incision rate decreased at about the same time

that the rate of rebound significantly decreased is only a coincidence. Like the rivers in the Winooski Basin, the studied reach of the Mississquoi River would have initially incised as a response to baselevel lowerings, in this case the regressing Champlain Sea. Despite baselevel rising more than 4 m between 10,000 and 8000 ^{14}C yr B.P., after the initiation of Lake Champlain (Astley, 1998), incision still occurred. While a rising baselevel during a period of incision strengthens the interpretation of Brakenridge et al. that vertical crustal movements were controlling incision, I suggest instead that incision proceeded because the post-glacial landscape was, and continues to be, out of equilibrium due to presence of glacial sediments. The rate of incision decreased when the downstream reach of the Mississquoi River encountered a resistant bedrock knickpoint at Highgate Falls.

In conclusion, glacio-isostatic and active tectonic movements do not appear to be discernible using river terraces as the indicator in the formerly glaciated Champlain Basin. The numerous baselevel lowerings caused the gradient to change so that initial river gradients can not be reliably inferred and once fill is removed, bedrock-dominated reaches control the gradient and long term incision rate. Therefore, it is unlikely that the studies of Treadwell and Knuefper (1988) and Brakenridge et al. (1988), which used initial gradients and long term incision rates, respectively, were able to indicate true crustal movements. All of the local studies of rivers, including my own, focused on higher-order reaches where rapid incision kept pace with baselevel changes to remove post-glacial fill. However, using higher-order reaches may introduce a sampling bias. Merritts and Vincent (1989) suggest that tectonic tilting is best recorded by first-order streams because they do not have sufficient stream power to respond to baselevel changes downstream. Perhaps any future

attempts at identifying and measuring tilting as recorded by rivers in the formerly glaciated Northeast should be centered on the low-order mountain streams. In addition, consider two end member cases. Activity in the fan's source area can be initiated at any time when the river undercuts the valley fill, leading to:

RELATIONSHIP BETWEEN ALLUVIAL FANS AND RIVER TERRACES

One question that has plagued the recent researchers in the Huntington Valley is: what controls the distribution of alluvial fans in space and through time? The oldest basal age obtained is approximately 8000 ^{14}C yr B.P. (Church, 1997) from a fan built on T5 while the youngest is < 100 ^{14}C yr B.P. (Zehfuss, 1996) from a fan built on T1. Fans are built on nearly every terrace below T5, but none have yet been found on the terraces above T5. The basal fan ages and the ages of terrace deposits are generally contemporary, suggesting that fan activity and terrace development occur during the same time periods rather than terraces predating the fans. Therefore, the same factors which lead to river incision, whether storms or human activities, might be responsible for initiation of fan activity.

In order to evaluate the assumption that river incision and fan deposition are triggered by the same factors, the question as to why there are no fans on terraces above T5 must be addressed. Not only are there no basal ages from alluvial fans in any other valleys to test if alluvial fan development occurred before 8000 ^{14}C yr B.P., but I did not observe any fans on the upper terraces (those formed during the Early Fluvial Stage). Were no fans deposited because there was not sufficient relief above the terraces for gullies to develop? Were the proper sediment types unavailable for transport? Were the transportation processes not occurring? Or has subsequent river action simply destroyed the older fans? Identifying what ultimately triggers fan deposition

may help in answering these questions.

In order to understand the mechanisms for the initiation of fan deposition, consider two end member cases. Activity in the fan's source area can be initiated at any time when the river undercuts the valley fill, leading to gully development on the hillslope (Case 1). Alternatively, activity in the source area may be the result of a change in the hillslope conditions, such as removal of groundcover by fire or humans or increase in overland flow from large precipitation events (Case 2). Fan deposition, however, will not occur unless there is a terrace upon which to build a fan. Therefore, if the river initiates gullying (Case 1), hillslope sediments may be carried into the river without any fan deposition. In Case 2, where the disturbance is from within the source area, fan deposition is almost certain, and the fan deposit will likely record all the erosion from the basin.

Headward erosion of the gullies will continue until the hillslope system reaches equilibrium. In Case 1, equilibrium may be reached before fan deposition while the river is still receiving the sediment or after significant amounts of sediment are carried away by the river. Therefore, while the initial pulse of fan deposition may be a significant portion of the present volume of the fan, it may represent only a fraction of total hillslope erosion in that drainage. The volume of initial fan deposition does not necessarily correspond with the magnitude of the initial disturbance and thus is evidence of activity, and a minimum limiting measure of activity, in the fan's drainage basin.

The sensitivity of a fan's drainage basin or source area to future disturbances was demonstrated in the studies by Church (1997) and Zehfuss (1996), especially in the case of historic land use. Subsequent to the initial fan

deposition, fan aggradation continued episodically throughout the Holocene. However, neither study provided a strong linkage of fan deposition to a specific disturbance except in the case of historic land use. Indeed, basal fan ages, representing the timing of fan preservation, cluster around periods of widespread climate changes (Bierman et al., 1997), but that fact does not mandate that the climate changes, by disturbing the drainage basin, directly initiated fan activity. It is just as likely that widespread climate changes, by causing an increase in river activity through incision or lateral channel migration, indirectly initiated or preserved fan activity. In either case, the proximity of the river channel to the fan basin ultimately controls fan preservation.

Another study has addressed the relationship between terraces and fans by examining fire and alluvial activity in Yellowstone National Park (Meyer et al., 1995). The abundance of radiocarbon dates (> 50) allowed Meyer et al. to define specific periods of fan formation and overbank deposition. They found that floodplain incision coincided with fan formation, occurring during dry periods punctuated by convective storms and fires. Periods of floodplain development and overbank deposition were usually characterized by a wetter climate and lacked significant fan activity. I mention this study as an example of the scope of investigation that is needed to discern the relationship between alluvial fans and terraces in Vermont.

In conclusion, the formation and preservation of alluvial fans and the formation of river terraces appear to be linked. The question remains if the linkage is one of mutual cause or one of cause and effect. Deciphering the mechanisms which trigger the formation of these landforms first requires identifying whether the alluvial fans develop independently of river terraces

or whether the river activity initiates fan activity and terracing allows fan preservation. A better alluvial fan chronology would not only help to define periods of fan formation, it would improve the terrace chronology since datable material is often found in the terrace deposits below alluvial fans.

waters from the valleys. Later, the baselevel of the valley has been lowered by base-level lowering until it reaches its present level. At the same time, river incision has modified the valley, and there have been changes. The river terrace chronology can form a base for the fan chronologies developed by other methods and can help to refine a more complete model of valley evolution.

The gradients of terrace fans are usually relatively low, and they are often very wide. Since the mechanisms of terrace formation are not well understood, interpretations caused a step-wise advance in the development of terrace theory. It appears to be in meta-stable equilibrium. The terrace fans are formed by the removal portion of valley fill which is removed by the river. Therefore, it seems likely that the terrace fans are formed by the river development in order to provide a smooth and even surface for the next checkpoints.

Since the river processes do not affect the terrace fans directly, the base-level decrease during the Holocene must be through the removal of the terrace components. There is an indirect relationship between the base-level decrease and the presence of glaciogenic debris. The base-level decrease may include a component of glaciogenic debris, but the amount of glaciogenic debris is much less and independent of the base-level decrease. Although base-level change is the result of the removal of the terrace components, the components did not directly cause the base-level decrease.

The river terrace history of the Winooski Valley

CHAPTER 6: CONCLUSIONS

Postglacial river terrace development in the Winooski Drainage Basin has been controlled by different forcings. The first fluvial terrace capped glaciolacustrine fill deposits and was associated with the withdrawal of lake waters from the valleys. Later, river incision was driven by proglacial lake baselevel lowerings until knickpoints developed in the river channels. Since that time, river incision has most likely coincided with large-scale climate changes. The river terrace chronologies are compatible with the deglacial chronologies developed by other workers and can be used to develop a five stage model of valley evolution.

The gradients of terraces have continued to increase with each incision event. Since the mechanisms of incision (baselevel lowerings, knickpoint migration) caused a step-wise increase in the gradients over time, the rivers appear to be in meta-stable equilibrium. Throughout their history, the rivers have removed portions of valley fill to expose bedrock knickpoints. Therefore, it seems likely that the river systems are moving toward strath development in order to produce a channel carved into bedrock, without knickpoints.

Since the river gradients of the Huntington and Mad Rivers continued to increase during the Holocene, they are inappropriate to study crustal movements. There is no baseline initial river gradient from which to compare present gradients of terraces. The present-day terrace gradients must include a component of glacio-isostatic tilting, but the magnitude of the tilting is much less and indecipherable from the overall gradient change. Although baselevel changes are associated with glacio-isostatic tilting, crustal movements did not directly cause river incision.

The river terraces and alluvial fans in the Huntington River Valley appear to have formed at similar times. Without additional radiocarbon dates, it is difficult to discern whether the mechanisms that initiated terrace formation directly caused alluvial fan development. Since datable organic material is often found within alluvial fan deposits and immediately below fans in the terrace deposits, further study of their mutual histories will better constrain landform development in the Winooski Drainage Basin.

Unpublished M.S. thesis, University of Vermont.

Balco, G. (1997). Postglacial land and lake levels: Moosehead Lake, Maine.

Unpublished Ph.D. thesis, University of Maine.

Baldwin, L., Church, A. B., Larsen, P. L. (1986). Geological Society of America Abstracts with Programs 27, Northeastern Section, A 73.

Barnett, S. C., and Jacobson, R. W. (1980). The regulation of Lake Champlain water level studies to the investigation of Aurorean Lake Champlain crustal movements. In "Conference on The Geology of the Lake Champlain Basin and Vicinity" (G. C. Denison, ed.), 5-11. Vermont Geological Society.

Bardgett, W. A., Goffeis, W. M., Kelley, J. R., and Kelly, J. T. (1994). Late Quaternary relative sea-level change in the western Gulf of Maine: Evidence for a migrating glacier. *Tectonophysics*, 23, A47-A54.

Bierman, P., Lira, A., Zeballos, L., Church, A. B., P. T. Sgroi, P., and Baldwin, L. (1993). Postglacial source and "fossil" lake recorders of Holocene landscape history. *GSA Special Paper* 318, 1-8.

Bonnechere, R., Jacobson, G. L. Jr., Davis, R. B., and Brum, H. W. Jr. (1981). The environmental setting for human colonization of northern New England and adjacent Canada in Late Pleistocene time. *Geological Society of America Special Paper* 177, 151-158.

BIBLIOGRAPHY

- Andrews, J. T. (1968). Postglacial rebound in Arctic Canada: similarity and prediction of uplift curves. Canadian Journal of Earth Sciences 5, 39-47.
- Andrews, J. T. (1970). A geomorphological study of post-glacial uplift with particular reference to Arctic Canada: London. Institute of British Geographers. 156 p.
- Astley, B. N. (1998). Holocene lake-level changes in Lake Champlain. Unpublished M.S. thesis, University of Vermont.
- Balco, G. (1997). Postglacial land and lake levels, Moosehead Lake, Maine. Unpublished Ph.D. thesis, University of Maine.
- Baldwin, L., Church, A. B., Larsen, P. L. (1995). Geological Society of America Abstracts with Programs 27, Northeastern Section, A-85.
- Barnett, S. G., and Isachsen, Y. W. (1980). The application of Lake Champlain water level studies to the investigation of Adirondack and Lake Champlain crustal movements. In, "Conference on The Geology of the Lake Champlain Basin and Vicinity" (J. C. Detenbeck, Ed.), 5-11. Vermont Geological Society.
- Barnhardt, W. A., Gehrels, W. R., Belknap, D. B., and Kelly, J. T. (1994). Late Quaternary relative sea level change in the western Gulf of Maine: Evidence for a migrating glacial forebulge. Geology 23, 317-320.
- Bierman, P., Lini, A., Zehfuss, P., Church, A., Davis, P. T., Southon, J., and Baldwin, L. (1997). Postglacial ponds and alluvial fans: recorders of Holocene landscape history. GSA Today 7, 10, 1-8.
- Bonnichsen, R., Jacobson, G. L. Jr., Davis, R. B., and Borns, H. W., Jr. (1985). The environmental setting for human colonization of northern New England and adjacent Canada in Late Pleistocene time. Geological Society of America Special Paper 197, 151-159.

- Brakenridge, G. R. (1980). Widespread episodes of stream erosion during the Holocene and their climatic causes. *Nature* 283, 655-656.
- Brakenridge, G. R., Thomas, P. A., Conkey, L. E., and Schiferle, J. C. (1988). Fluvial sedimentation in response to postglacial uplift and environmental change, Missisquoi River, Vermont. *Quaternary Research* 30, 190-203.
- Bryan, K. (1995). Deglaciation of southern Chittenden County and Northern Addison County, Vermont. Unpublished senior thesis, University of Vermont.
- Bull, W. B. (1991). *Geomorphic responses to climatic change*: New York. Oxford University Press. 326 p.
- Chapman, D. H. (1937). Late-Glacial and postglacial history of the Champlain Valley. *American Journal of Science*, 5th series 34, 89-124.
- Church, A. B. (1997). Fan deposits in northwestern Vermont: depositional activity and aggradation rates over the last 9,500 years. Unpublished M.S. thesis, University of Vermont.
- Clark, J. E., Hendriks, M., Timmermans, T. J., Struck, C., and Hilverda, K. J. (1994). Glacial isostatic deformation of the Great Lakes region. *Geological Society of America Bulletin* 106, 19-31.
- Clark, P., and Karrow, P. F. (1984). Late Pleistocene water bodies in the St. Lawrence Lowland, New York, and regional correlations. *Geological Society of America Bulletin*, 95, 805-813.
- Connally, G. G. (1972). Proglacial lakes in the Lamoille Valley, Vermont. In, "NEIGC Guidebook for Field Trips in Vermont" (Doolan, B. L., and Stanley, R. S., Eds.), 343-358. University of Vermont, Burlington, Vermont.

Connally, G. G., and Calkin, P. E. (1972). Woodfordian glacial history of the Champlain lowland, Burlington to Brandon, Vermont. In, "NEIGC Guidebook for Field Trips in Vermont" (Doolan, B. L., and Stanley, R. S., Eds.), 389-397. University of Vermont, Burlington, Vermont.

Connally, G. G., and Sirkin, L. A. (1973). Wisconsinian history of the Hudson-Champlain Lobe. In, "The Wisconsinian Stage" (Black, R. F., Goldthwait, R. P., and Willman, H. B., Eds.), 47-69. Geological Society of America Memoir 136.

Davis, M. B., Spear, R. W., and Shane, L. C. K. (1980). Holocene climate of New England. Quaternary Research 14, 240-250.

Davis, R. B., and Jacobson, G. L., Jr. (1985). Holocene climate of New England. Quaternary Research 23, 341-368.

Denny, C. S. (1974). Pleistocene geology of the northeast Adirondack region, New York. United States Geological Survey Professional Paper 786, 50 p.

DeSimone, D. J., and LaFleur, R. G. (1986). Glaciolacustine phases in the northern Hudson Lowland and correlatives in western Vermont. Northeastern Geology 8, 218-229.

Dillon, W. P., and Oldale, R. N. (1978). Late Quaternary sea-level curve: Reinterpretation based on glaciotectonic influence. Geology 6, 56-60.

Dionne, J. C. (1988). Holocene relative sea-level fluctuations in the St. Lawrence estuary, Quebec. Quaternary Research 29, 233-234.

Doll, C. G., Cady, W. M., Thompson, J. B., and Billings, M. P. (1961). Geologic map of Vermont. State of Vermont, Montpelier.

Dwyer, T. R., Mullins, H. T., and Good, S. C. (1996). Paleoclimatic implications of Holocene lake-level fluctuations, Owasco Lake, New York. Geology 24, 519-522.

- Fairbanks, R. G. (1989). A 17,000 year glacio-eustatic sea level record: Influence of glacial melting on the younger-Dryas event and deep ocean circulation. *Nature* 342, 637-642.
- Knox, J. C. (1983). *Response of Glaciers to Global Warming*. D. Reidel Publishing Co., Dordrecht, The Netherlands.
- Fairchild, H. L. (1916). Postglacial marine waters in Vermont. *Vermont State Geologist* 10th Report, 1-14.
- Gadd, N. R. (1964). Moraines in the Appalachian region of Quebec. *Geological Society of America Bulletin* 75, 1249-1254.
- Gilbert, G. K. (1880). Geology on the Henry Mountains. *United States Geological and Geographical Survey of the Rocky Mountains Region*.
- Hughes, T. (1987). Ice dynamics and deglaciation models when ice sheets collapsed. In, "North America and Adjacent Oceans During the Last Deglaciation, Geology of North America, K-3" (Ruddiman, W. F., and Wright, H. E., Jr., Eds.), 183-220. Geological Society of America, Boulder, Colorado.
- Howard, L. D., and Worley, I. A. (1976). Phytosociological, hydrological, and other ecological features at Colchester Bob, Vermont. In, "Proceedings of the Lake Champlain Environmental Conference, July 15, 1976" (Berberet, W. G., Ed.), 52-116. Institute for Man and Environment, Plattsburgh, New York.
- Hutchinson, D. R., Ferrebee, W. M., Knebel, H. J., Wold, R. J., and Isachsen, Y. M. (1981). The sedimentary framework of the southern basin of Lake George, New York. *Quaternary Research* 15, 44-61.
- Kjelleren, G. P. (1984). The source and deglacial implications of the Hollow Brook Delta: Champlain Valley, Vermont. Unpublished M.S. thesis, University of Connecticut.

Knighton, D. (1984). Fluvial Forms and Processes: Edward Arnold. London
218 p.

Knox, J. C. (1983). Responses of river systems to Holocene climates. In, "Late-Quaternary Environments of the United States, Volume 2: The Holocene" (Wright, H. E., Jr., Ed.), 26- 41. University of Minnesota Press, Minneapolis.

Koteff, C., and Larsen, F. D. (1989). Postglacial uplift in western New England: Geologic evidence for delayed rebound. In "Earthquakes at North Atlantic Passive Margins: Neotectonics and Postglacial Rebound" (Gregersen, S. and Basham, P. W., Eds.), 105-123. Kluwer Academic, Amsterdam.

Koteff, C., Robinson, G. R., Goldsmith, R., and Thompson, W. B. (1993). Delayed postglacial uplift and synglacial sea levels in coastal central New England. Quaternary Research 40, 46-54.

LaFleur, R. G. (1965). Glacial geology of the Troy, N.Y. Quadrangle. Map and Chart Series Number 7, New York State Museum and Science Service.

Lamb, H. H. (1995). Climate, History and the Modern World, Second edition: New York. Routledge. 433 p.

Larsen, F. D., (1972). Glacial history of central Vermont. In, "NEIGC Guidebook for Field Trips in Vermont" (Doolan, B. L., and Stanley, R. S., Eds.), 297-316. University of Vermont, Burlington, Vermont.

Larsen, F. D. (1987a). Glacial Lake Hitchcock in the valleys of the White and Ottauquechee Rivers, east-central Vermont. In, "NEIGC Guidebook for Field Trips in Vermont, Volume 2" (Westerman, D. S., Ed.) 30- 52. Norwich University, Northfield, Vermont.

Larsen, F. D. (1987b). History of glacial lakes in the Dog River Valley, central Vermont. In, "NEIGC Guidebook for Field Trips in Vermont, Volume 2" (Westerman, D. S., Ed.) 214-236. Norwich University, Northfield, Vermont.

- Leopold, L. B., and Bull, W. B. (1979). Base level, aggradation, and grade. *Proceedings of the American Philosophical Society* 123, 168-202.
- Leopold, L. B., and Maddock, T., Jr. (1953). The hydraulic geometry of stream channels and some physiographic implications. United States Geological Survey Professional Paper 252, 52 p.
- Leopold, L. B., and Wolman, M. G. (1957).
- Pawley, M. (1987). Late Pleistocene stratigraphy and events in the Adirondack Leopold, L. B., Wolman, M. G., and Miller, J. P. (1964). Fluvial processes in geomorphology: San Francisco. W. H. Freeman. 522 p.
- Lin, L. (1995). Environmental changes inferred from pollen analysis and ¹⁴C ages of pond sediments, Green Mountains, Vermont. Unpublished M.S. thesis, University of Vermont.
- McDonald, B. C. (1968). Deglaciation and differential postglacial rebound in the Appalachian region of southeastern Quebec. *Journal of Geology* 76, 664-667.
- Mackin, J. H. (1948). Concept of the graded river. *Geological Society of America Bulletin* 59, 463-512.
- Meeks, H. A. (1986). Vermont's land and resources: Shelburne, VT. The New England Press. 332 p.
- Merritts, D. J., and Vincent, K. R. (1989). Geomorphic response of coastal streams to low, intermediate, and high rates of uplift, Mendocino triple junction region, northern California, *Geological Society of America Bulletin* 101, 1373-1388.
- Merritts, D. J., Vincent, K. R., and Wohl, E. E. (1994). Long river profiles, tectonism, and eustacy: A guide to interpreting fluvial terraces, *Journal of Geophysical Research* 99, No. B7, 14,031-14,050.

Merwin, H. E. (1908). Some late Wisconsinan and post-Wisconsinan shore-lines of northwestern Vermont. *Vermont State Geologist* 6th Report, 113-138.

Meyer, G. A., Wells, S. G., and Jull, A. J. T. (1995). Fire and alluvial chronology in Yellowstone National Park: Climatic and intrinsic controls on Holocene geomorphic processes. *Geological Society of America Bulletin* 107, 1211-1230.

Parent, M. (1987). Late Pleistocene stratigraphy and events in the Asbestos-Valcourt region, southeastern Quebec. Unpublished Ph. D. thesis, University of Western Ontario, 320 p.

Parent, M., and Occhietti, S. (1988). Late Wisconsinan deglaciation and Champlain Sea invasion in the St. Lawrence Valley, Quebec. *Geographie physique et Quaternaire* 42, 215-246.

Parrott, W. R., and Stone, B. S. (1972). Strandline features and late Pleistocene chronology of northwestern Vermont. In, "NEIGC Guidebook for Field Trips in Vermont" (Doolan, B. L., and Stanley, R. S., Eds.), 359-376. University of Vermont, Burlington, Vermont.

Peltier, W. R. (1994). Ice age paleotopography. *Science* 265, 195-201.

Pyne, S. J. (1982). *Fire in America*: Princeton, New Jersey. Princeton University Press. 654 p.

Rodrigues, C. G. (1992). Successions of invertebrate microfossils and the late Quaternary deglaciation of the central St. Lawrence Lowland, Canada and United States. *Quaternary Science Reviews* 11, 503-534.

Schumm, S. A. (1972). *River morphology*: Stroudsburg, Pennsylvania. Dowden, Hutchinson & Ross, Inc. 429 p.

- Scully, R. W., and Arnold, R. W. (1981). Holocene alluvial stratigraphy in the Upper Susquehanna River basin, New York. *Quaternary Research* 15, 327-344.
- Severson, J. P. (1991). Patterns and causes of 19th and 20th century shoreline changes of the Winooski Delta. Unpublished M.S. thesis, University of Vermont.
- Spear, R. W., Davis, M. B., and Shane, L. C. K. (1994). Late Quaternary history of low- and mid-elevation vegetation in the White Mountains of New Hampshire. *Ecological Monographs* 64, 85-109.
- Stewart, D. P. (1961). The glacial geology of Vermont. *Vermont Geological Survey Bulletin* 19, 124 p.
- Stewart, D. P., and MacClintock, P. (1969). The surfical geology and Pleistocene history of Vermont. *Vermont Geological Survey Bulletin* 31, 251 p.
- Stewart, D. P., and MacClintock, P. (1970). Surfical geologic map of Vermont. Vermont Geological Survey.
- Stone, J. R., and Ashley, G. M. (1995). Timing and mechanisms of Glacial Lake Hitchcock drainage. *Geological Society of America Abstracts with Programs* 27, Northeastern Section, A-85.
- Terasmae J., and LaSalle, P. (1968). Notes on the late-glacial palynology and geochronology at St. Hilaire, Quebec. *Canadian Journal of Earth Sciences* 5, 249-257.
- Thomas, P. A. (1985). Archeological and geomorphic evaluation; M5000 (3) northern connector material supply/disposal area, Howe Farm flood plain: Burlington. University of Vermont, Department of Anthropology no. 54, 41 p.

Thompson, W. B., Crossen, K. J., Borns, W. H., and Anderson, B. G. (1989). "Neotectonics of Maine" 43-67. Maine Geological Survey.

Thorson, R. M., and Schile, C. A. (1995). Deglacial eolian regimes in New England. Geological Society of America Bulletin 107, 751-761.

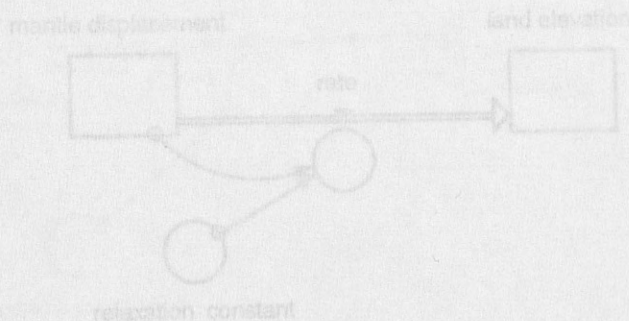
Treadwell, C. J., and Kneupfer, P. L. K. (1988). Deformation of Holocene river terrace profiles, northeast Adirondack Mountains, New York, Geological Society of America Abstracts with Programs 20, Northeastern Section, A-77.

Valin, C. C. G. (1997). A relative chronology of river terraces in the Mad River valley, northwestern Vermont. Unpublished senior research paper, University of Vermont.

Wagner, W. P. (1972). Ice margins and water levels in northwestern Vermont. In, "NEIGC Guidebook for Field Trips in Vermont" (Doolan, B. L., and Stanley, R. S., Eds.), 297-316. University of Vermont, Burlington, Vermont.

Zehfuss, P. H. (1996). Alluvial fans in Vermont as recorders of changes in sedimentation rates due to deforestation. Unpublished senior thesis, University of Vermont.

MODEL 2: REBOUND AT A LOCATION



APPENDIX A: STELLA MODEL

MODEL 2 DOCUMENTATION

mantle_displacement = rate * mantle_displacement(t - dt) + (-rate/t) * dt

INIT mantle_displacement = Md

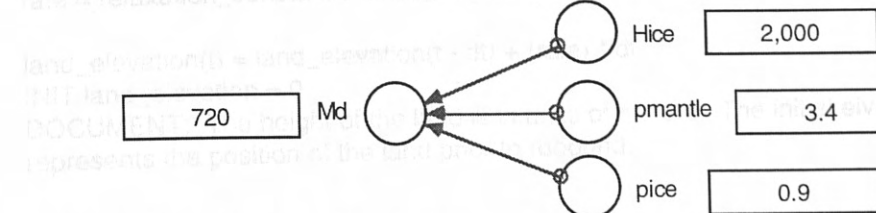
DOCUMENT: The initial mantle displacement is in meters and represents the amount of subsidence based on the ice load.

relaxation_constant = k/t²

DOCUMENT: The relaxation constant is dependent on the viscosity of the mantle. The value is based on the formula of the French (1972).

MODEL 1: MANTLE DISPLACEMENT

rate = relaxation_constant * Hice * pice / pmantle



MODEL 1 DOCUMENTATION

Hice = 2000

DOCUMENT: Ice thickness is in meters.

Md = Hice*(pice/(pmantle-pice))

DOCUMENT: Displaced mantle is in units of meters and represents the amount of mantle displaced by the ice load.

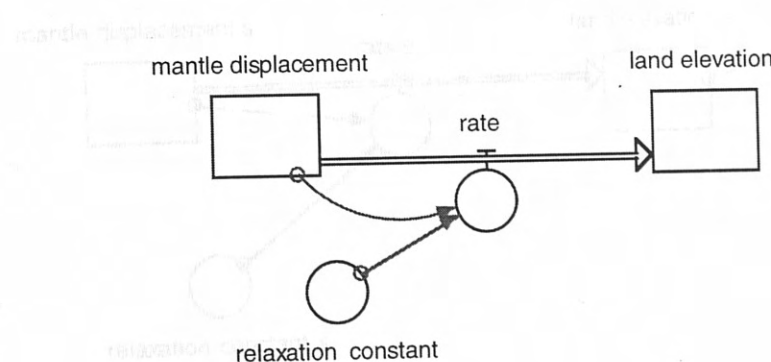
pice = 0.9

DOCUMENT: Density of ice is in g/cm^3

pmantle = 3.4

DOCUMENT: Density of mantle is in g/cm^3.

MODEL 2: REBOUND AT A LOCATION



MODEL 3 DOCUMENTATION

MODEL 2 DOCUMENTATION

mantle_displacement(t) = mantle_displacement(t - dt) + (- rate) * dt

INIT mantle_displacement = Md

DOCUMENT: The initial mantle displacement is in meters and represents the amount of subsidense based on the ice load.

relaxation_constant = .693

DOCUMENT: The relaxation constant is dependent on the viscosity of the mantle. Its value is based on the results of Barnhardt et al. (1995).

rate = relaxation_constant*mantle_displacement

land_elevation(t) = land_elevation(t - dt) + (rate) * dt

INIT land_elevation = 0

DOCUMENT: The height of the land is in units of meters. The initial elvation is 0 m and represents the position of the land prior to rebound.

tilt = land_elevation / s

DOCUMENT: The height of the land in units of meters. The initial elvation is 0 m and represents the position of the land prior to rebound.

mantle_displacement(t) = mantle_displacement(t - dt) + (- rate) * dt

INIT mantle_displacement = 0

DOCUMENT: The initial mantle displacement is in meters and represents the amount of subsidense based on the ice load.

mantle displacement n

rate n

land elevation n

DOCUMEN

rate n

land elevation s

DOCUMEN

rate s

land elevation s

DOCUMEN

rate s

relaxation constant s

MODEL 3 DOCUMENTATION

mantle_displacement_n(t) = mantle_displacement_n(t - dt) + (- rate_n) * dt

INIT mantle_displacement_n = Md+90

DOCUMENT: The initial mantle displacement is in meters and represents the amount of subsidense based on the ice load. An additional 90 m is added to produce the tilt of 0.9 m/km.

relaxation_constant_n = .693

DOCUMENT: The relaxation constant is dependent on the viscosity of the mantle. Its value is based on the results of Barnhardt et al. (1995).

uplift_delay = GRAPH(time)

DOCUMENT: The uplift delay will delay the beginning of uplift in the north using the graph. The value of the graph is set at zero for the length of time of the delay.

rate_n = mantle_displacement_n*relaxation_constant_n*uplift_delay

land_elevation_n(t) = land_elevation_n(t - dt) + (rate_n) * dt

INIT land_elevation_n = 0

DOCUMENT: The height of the land is in units of meters. The initial elvation is 0 m and represents the position of the land prior to rebound.

mantle_displacement_s(t) = mantle_displacement_s(t - dt) + (- rate_s) * dt

INIT mantle_displacement_s = Md

DOCUMENT: The initial mantle displacement is in meters and represents the amount of subsidense based onthe ice load.

relaxation_constant_s = .693

DOCUMENT: The relaxation constant is dependent on the viscosity of the mantle. Its value is based on the results of Barnhardt et al. (1995).

rate_s = mantle_displacement_s*relaxation_constant_s

land_elevation_s(t) = land_elevation_s(t - dt) + (rate_s) * dt

INIT land_elevation_s = 0

DOCUMENT: The height of the land is in units of meters. The initial elvation is 0 m and represents the position of the land prior to rebound.

tilt = (land_elevation_n-land_elevation_s)/distance

DOCUMENT: The tilt is measured in m/km.

distance = 100

DOCUMENT: The distance is the length between two points in the basin measured in kilometers.

APPENDIX B: HUNTINGTON RIVER DATA

Point Number	Latitude (m)	Longitude (m)	Elevation (m)	Aspect	Slope (%)	Point Description
HUNTINGTON RIVER SURVEY DATA						
1	1500.300	1000.000	100.000	20.000	± 0.20	TB
2	1500.300	950.000	100.000	20.000	± 0.20	TB
3	1500.300	900.000	100.000	20.000	± 0.20	TB
4	1500.300	850.000	100.000	20.000	± 0.20	TB
5	1500.300	800.000	100.000	20.000	± 0.20	TB
6	1500.300	750.000	100.000	20.000	± 0.20	TB
7	1500.300	700.000	100.000	20.000	± 0.20	TB
8	1500.300	650.000	100.000	20.000	± 0.20	TB
9	1500.300	600.000	100.000	20.000	± 0.20	TB
10	1500.300	550.000	100.000	20.000	± 0.20	TB
11	1500.300	500.000	100.000	20.000	± 0.20	TB
12	1500.300	450.000	100.000	20.000	± 0.20	TB
13	1500.300	400.000	100.000	20.000	± 0.20	TB
14	1500.300	350.000	100.000	20.000	± 0.20	TB
15	1500.300	300.000	100.000	20.000	± 0.20	TB
16	1500.300	250.000	100.000	20.000	± 0.20	TB
17	1500.300	200.000	100.000	20.000	± 0.20	TB
18	1500.300	150.000	100.000	20.000	± 0.20	TB
19	1500.300	100.000	100.000	20.000	± 0.20	TB
20	1500.300	50.000	100.000	20.000	± 0.20	TB
21	1500.300	0.000	100.000	20.000	± 0.20	TB
22	1500.300	-50.000	100.000	20.000	± 0.20	TB
23	1500.300	-100.000	100.000	20.000	± 0.20	TB
24	1500.300	-150.000	100.000	20.000	± 0.20	TB
25	1500.300	-200.000	100.000	20.000	± 0.20	TB
26	1500.300	-250.000	100.000	20.000	± 0.20	TB
27	1500.300	-300.000	100.000	20.000	± 0.20	TB
28	1500.300	-350.000	100.000	20.000	± 0.20	TB
29	1500.300	-400.000	100.000	20.000	± 0.20	TB
30	1500.300	-450.000	100.000	20.000	± 0.20	TB
31	1500.300	-500.000	100.000	20.000	± 0.20	TB
32	1500.300	-550.000	100.000	20.000	± 0.20	TB
33	1500.300	-600.000	100.000	20.000	± 0.20	TB
34	1500.300	-650.000	100.000	20.000	± 0.20	TB
35	1500.300	-700.000	100.000	20.000	± 0.20	TB
36	1500.300	-750.000	100.000	20.000	± 0.20	TB
37	1500.300	-800.000	100.000	20.000	± 0.20	TB
38	1500.300	-850.000	100.000	20.000	± 0.20	TB
39	1500.300	-900.000	100.000	20.000	± 0.20	TB
40	1500.300	-950.000	100.000	20.000	± 0.20	TB
41	1500.300	-1000.000	100.000	20.000	± 0.20	TB
42	1500.300	-1050.000	100.000	20.000	± 0.20	TB
43	1500.300	-1100.000	100.000	20.000	± 0.20	TB
44	1500.300	-1150.000	100.000	20.000	± 0.20	TB
45	1500.300	-1200.000	100.000	20.000	± 0.20	TB
46	1500.300	-1250.000	100.000	20.000	± 0.20	TB
47	1500.300	-1300.000	100.000	20.000	± 0.20	TB
48	1500.300	-1350.000	100.000	20.000	± 0.20	TB
49	1500.300	-1400.000	100.000	20.000	± 0.20	TB
50	1500.300	-1450.000	100.000	20.000	± 0.20	TB

The Huntington River survey data are presented in the following tables

beginning with the location closest to the mouth. See Figure 3.2 for survey locations.

Huntington River Location Jonesville							
Point Number	Northing (m)	Easting (m)	Measured Elevation (m)	Correction (m)	Final Elevation (m)	Error (m)	Point Description
1	1000.000	1000.000	100.000	26.75	126.75	± 0.20	T5
2	1000.000	1000.000	100.000	26.75	126.75	± 0.20	T5
3	978.450	956.800	100.231	26.75	126.98	± 0.20	T5
4	983.726	966.250	100.423	26.75	127.17	± 0.20	T5
5	990.198	978.182	100.164	26.75	126.91	± 0.20	T5
6	990.197	978.178	100.164	26.75	126.91	± 0.20	T5
7	997.497	990.248	100.044	26.75	126.79	± 0.20	T5
8	1035.983	980.856	99.700	26.75	126.45	± 0.20	T5
9	1027.147	985.592	99.774	26.75	126.52	± 0.20	T5
10	1016.763	993.368	99.611	26.75	126.36	± 0.20	T5
11	1006.859	998.930	99.888	26.75	126.64	± 0.20	T5
12	997.360	1001.950	99.981	26.75	126.73	± 0.20	SLOPE
13	995.498	1002.715	98.312	26.75	125.06	± 0.20	SLOPE
14	994.430	1004.543	97.235	26.75	123.98	± 0.20	SLOPE
15	988.377	1008.082	95.696	26.75	122.44	± 0.20	SLOPE
16	984.114	1025.677	95.745	26.75	122.49	± 0.20	ROAD
17	973.163	1042.916	95.650	26.75	122.40	± 0.20	ROAD
18	958.805	1052.116	95.594	26.75	122.34	± 0.20	ROAD
19	944.094	1057.020	94.949	26.75	121.70	± 0.20	ROAD
20	935.573	1044.270	95.953	26.75	122.70	± 0.20	T4
21	925.451	1045.924	95.438	26.75	122.19	± 0.20	T4
22	920.729	1047.085	93.672	26.75	120.42	± 0.20	SLOPE
23	916.247	1046.687	92.140	26.75	118.89	± 0.20	SLOPE
24	908.496	1046.669	89.672	26.75	116.42	± 0.20	SLOPE
25	899.326	1045.721	88.076	26.75	114.82	± 0.20	SLOPE
26	888.424	1045.895	86.318	26.75	113.07	± 0.20	SLOPE
27	870.203	1044.535	84.050	26.75	110.80	± 0.20	ROAD
28	846.092	1043.815	82.008	26.75	108.76	± 0.20	ROAD
29	828.768	1045.785	81.106	26.75	107.85	± 0.20	ROAD
30	944.062	1057.017	94.965	26.75	121.71	± 0.20	ROAD
31	870.952	1029.689	86.226	26.75	112.97	± 0.20	SLOPE
32	878.947	1026.391	87.782	26.75	114.53	± 0.20	SLOPE
33	874.292	1028.464	86.888	26.75	113.64	± 0.20	SLOPE
34	870.059	1030.568	85.821	26.75	112.57	± 0.20	SLOPE
35	863.509	1032.428	83.653	26.75	110.40	± 0.20	SLOPE
36	857.975	1036.089	82.114	26.75	108.86	± 0.20	SLOPE
37	788.909	1046.084	79.874	26.75	106.62	± 0.20	T3B
38	748.334	1045.904	79.821	26.75	106.57	± 0.20	T3B
39	688.021	1050.636	80.311	26.75	107.06	± 0.20	T3A
40	730.706	1160.523	77.912	26.75	104.66	± 0.20	T2A
41	828.656	1045.736	81.146	26.75	107.89	± 0.20	T3A
42	840.852	1171.110	81.419	26.75	108.17	± 0.20	T3A
43	832.445	1170.309	79.673	26.75	106.42	± 0.20	SLOPE
44	816.178	1168.732	78.544	26.75	105.29	± 0.20	T3B
45	786.774	1168.249	78.742	26.75	105.49	± 0.20	T3B
46	689.596	1169.555	77.261	26.75	104.01	± 0.20	SLOPE
47	663.653	1187.046	76.146	26.75	102.89	± 0.20	T2B
48	617.270	1215.041	75.620	26.75	102.37	± 0.20	T2B
49	531.830	1266.254	75.466	26.75	102.21	± 0.20	T2B
50	451.854	1314.925	74.651	26.75	101.40	± 0.20	T2B

Huntington River Location Jonesville							
Point Number	Northing (m)	Easting (m)	Measured Elevation (m)	Correction (m)	Final Elevation (m)	Error (m)	Point Description
51	730.674	1160.540	77.664	26.75	104.41	± 0.20	T2A
52	390.368	1377.920	76.070	26.75	102.82	± 0.20	T2B
53	368.125	1437.323	74.076	26.75	100.82	± 0.20	T2B
54	384.379	1492.180	73.391	26.75	100.14	± 0.20	T2B
Note: These elevations are tied to the Benchmark north of the Jonesville bridge							
6	877.325	1007.098	197.478	22.85	174.60	± 1.0	SLOPE
9	975.748	1014.046	198.980	22.85	173.33	± 1.0	SLOPE
10	975.757	1014.038	198.911	22.85	173.33	± 1.0	SLOPE
11	977.166	1021.294	195.561	22.85	172.60	± 1.0	SLOPE
12	975.242	1032.920	194.728	22.85	171.85	± 1.0	SLOPE
13	971.532	1036.422	193.942	22.85	171.08	± 1.0	T6
14	982.465	1048.162	193.414	22.85	170.53	± 1.0	T6
15	955.500	1050.560	193.550	22.85	170.41	± 1.0	T6
16	947.218	1056.016	193.148	22.85	170.27	± 1.0	T6
17	937.254	1062.817	192.362	22.85	169.23	± 1.0	SLOPE
18	952.227	1067.204	192.304	22.85	167.80	± 1.0	SLOPE
19	949.148	1067.822	193.167	22.85	167.29	± 1.0	T6
20	956.350	1073.207	194.250	22.85	167.38	± 1.0	T6
21	991.882	1013.105	198.477	22.85	176.59	± 1.0	SLOPE
22	993.761	994.709	198.454	22.85	175.57	± 1.0	T7
23	988.090	989.099	198.196	22.85	175.31	± 1.0	SLOPE
24	991.587	994.614	198.718	22.85	175.53	± 1.0	SLOPE
25	993.656	997.246	198.611	22.85	177.53	± 1.0	SLOPE
26	1000.717	997.866	198.366	22.85	187.88	± 1.0	SLOPE
27	1007.354	995.925	198.356	22.85	187.59	± 1.0	SLOPE
28	1016.200	939.566	197.936	22.85	167.75	± 1.0	SLOPE
29	1032.701	923.630	197.98	22.85	167.86	± 1.0	SLOPE
30	1047.885	917.429	198.18	22.85	168.20	± 1.0	SLOPE
31	1061.887	919.008	198.100	22.85	168.25	± 1.0	SLOPE
32	1078.712	895.655	198.15	22.85	165.66	± 1.0	ROAD
33	1086.467	891.659	198.15	22.85	165.84	± 1.0	ROAD
34	1097.456	879.923	198.15	22.85	161.05	± 1.0	ROAD
35	1097.460	879.930	198.15	22.85	161.15	± 1.0	ROAD
36	1110.329	861.747	198.134	22.85	160.23	± 1.0	ROAD
37	1111.095	860.568	198.048	22.85	160.09	± 1.0	ROAD
38	1115.513	846.914	198.047	22.85	158.10	± 1.0	ROAD
39	1122.078	828.107	198.051	22.85	154.95	± 1.0	ROAD
40	1130.500	809.875	198.017	22.85	152.93	± 1.0	ROAD
41	1134.413	798.941	198.016	22.85	150.93	± 1.0	ROAD
42	1136.821	788.276	198.034	22.85	148.15	± 1.0	ROAD
43	1146.645	769.219	198.054	22.85	145.95	± 1.0	ROAD
44	1159.651	749.230	198.061	22.85	141.06	± 1.0	ROAD
45	1183.032	702.659	198.063	22.85	137.52	± 1.0	ROAD
46	1113.645	729.760	198.047	22.85	135.96	± 1.0	T5
47	1100.242	750.051	198.065	22.85	137.50	± 1.0	T5
48	1079.445	764.495	198.039	22.85	130.96	± 1.0	SLOPE
49	1056.102	791.077	198.095	22.85	135.73	± 1.0	SLOPE
50	1048.339	791.041	198.073	22.85	133.90	± 1.0	SLOPE

Huntington River Location Paquette							
Point Number	Northing (m)	Easting (m)	Measured Elevation (m)	Correction (m)	Final Elevation (m)	Error (m)	Point Description
1	1000.000	1000.000	200.000	22.88	177.12	± 1.0	T7
2	1000.000	1000.000	200.000	22.88	177.12	± 1.0	T7
3	997.113	999.576	199.903	22.88	177.02	± 1.0	T7
4	991.898	998.346	199.697	22.88	176.81	± 1.0	T7
5	983.260	996.348	199.296	22.88	176.41	± 1.0	T7
6	975.403	994.092	198.867	22.88	175.98	± 1.0	T7
7	979.000	1002.773	198.557	22.88	175.67	± 1.0	SLOPE
8	977.325	1007.096	197.478	22.88	174.60	± 1.0	SLOPE
9	975.746	1014.046	196.209	22.88	173.33	± 1.0	SLOPE
10	975.757	1014.038	196.211	22.88	173.33	± 1.0	SLOPE
11	977.166	1021.298	195.681	22.88	172.80	± 1.0	SLOPE
12	975.242	1029.260	194.728	22.88	171.85	± 1.0	SLOPE
13	971.532	1036.492	193.942	22.88	171.06	± 1.0	T6
14	962.865	1043.152	193.414	22.88	170.53	± 1.0	T6
15	955.500	1050.535	193.350	22.88	170.47	± 1.0	T6
16	947.219	1056.913	193.148	22.88	170.27	± 1.0	T6
17	937.264	1062.837	192.162	22.88	169.28	± 1.0	SLOPE
18	932.227	1067.204	190.761	22.88	167.88	± 1.0	SLOPE
19	949.146	1047.672	193.167	22.88	170.28	± 1.0	T6
20	969.352	1028.901	194.260	22.88	171.38	± 1.0	T6
21	991.882	1013.103	198.477	22.88	175.59	± 1.0	SLOPE
22	993.761	994.703	199.454	22.88	176.57	± 1.0	T7
23	988.390	989.339	198.196	22.88	175.31	± 1.0	SLOPE
24	991.557	984.614	195.713	22.88	172.83	± 1.0	SLOPE
25	993.855	967.250	190.412	22.88	167.53	± 1.0	SLOPE
26	1000.717	957.859	190.263	22.88	167.38	± 1.0	SLOPE
27	1007.354	945.995	190.399	22.88	167.52	± 1.0	SLOPE
28	1018.200	932.556	190.610	22.88	167.73	± 1.0	SLOPE
29	1030.701	923.630	190.741	22.88	167.86	± 1.0	SLOPE
30	1047.395	917.429	191.080	22.88	168.20	± 1.0	SLOPE
31	1061.887	919.908	191.088	22.88	168.21	± 1.0	SLOPE
32	1076.712	903.656	188.566	22.88	165.68	± 1.0	ROAD
33	1086.467	891.658	186.246	22.88	163.36	± 1.0	ROAD
34	1097.466	879.323	184.532	22.88	161.65	± 1.0	ROAD
35	1097.460	879.330	184.533	22.88	161.65	± 1.0	ROAD
36	1110.032	861.781	183.114	22.88	160.23	± 1.0	ROAD
37	1111.085	860.666	182.968	22.88	160.09	± 1.0	ROAD
38	1115.513	846.914	180.987	22.88	158.10	± 1.0	ROAD
39	1122.078	828.107	177.830	22.88	154.95	± 1.0	ROAD
40	1130.000	809.878	174.917	22.88	152.03	± 1.0	ROAD
41	1134.443	798.041	173.216	22.88	150.33	± 1.0	ROAD
42	1136.821	789.576	172.030	22.88	149.15	± 1.0	ROAD
43	1146.643	769.216	168.531	22.88	145.65	± 1.0	ROAD
44	1158.651	740.230	163.941	22.88	141.06	± 1.0	ROAD
45	1163.012	702.659	160.406	22.88	137.52	± 1.0	ROAD
46	1113.845	729.760	159.841	22.88	136.96	± 1.0	T5
47	1100.222	742.941	160.385	22.88	137.50	± 1.0	T5
48	1079.445	764.446	159.839	22.88	136.96	± 1.0	T5
49	1056.102	791.177	158.608	22.88	135.73	± 1.0	SLOPE
50	1046.339	791.941	156.870	22.88	133.99	± 1.0	SLOPE

Huntington River Location Paquette							
Point Number	Northing (m)	Easting (m)	Measured Elevation (m)	Correction (m)	Final Elevation (m)	Error (m)	Point Description
51	1039.145	781.794	155.572	22.88	132.69	± 1.0	T4
52	1048.682	762.426	155.874	22.88	132.99	± 1.0	T4
53	1065.539	735.301	156.277	22.88	133.39	± 1.0	T4
54	1076.737	704.773	156.688	22.88	133.81	± 1.0	T4
55	1069.379	691.473	154.563	22.88	131.68	± 1.0	SLOPE
56	1059.943	679.442	153.101	22.88	130.22	± 1.0	T3
57	1037.629	697.172	152.669	22.88	129.79	± 1.0	T3
58	1027.518	713.428	151.917	22.88	129.03	± 1.0	T3
59	1027.546	734.254	151.027	22.88	128.14	± 1.0	SLOPE
60	1038.191	750.816	153.538	22.88	130.66	± 1.0	T3
61	1013.498	744.782	149.039	22.88	126.16	± 1.0	SLOPE
62	999.008	748.037	148.381	22.88	125.50	± 1.0	T2
63	996.424	763.069	148.295	22.88	125.41	± 1.0	T2
64	984.058	765.009	147.486	22.88	124.60	± 1.0	T2
65	975.193	761.448	141.372	22.88	118.49	± 1.0	RIVER
66	993.928	777.515	147.817	22.88	124.93	± 1.0	T2
67	1004.191	791.957	147.847	22.88	124.96	± 1.0	T2
68	1016.208	807.059	148.302	22.88	125.42	± 1.0	T2
69	992.213	749.555	148.493	22.88	125.61	± 1.0	T2

Note: These elevations are tied to a contour line (460 ft = 140.24 m) via PAQ1 Pt 44 = PARO Pt 3

21	1026.379	808.382	97.482	22.81	126.63	± 1.0	
22	1024.181	805.447	97.539	22.81	126.80	± 1.0	T3
23	1022.409	804.011	97.526	22.81	125.52	± 1.0	SLOPE
24	1020.718	803.472	95.529	22.82	126.10	± 1.0	SLOPE
25	1019.068	808.784	95.529	22.81	124.54	± 1.0	SLOPE
26	1016.690	807.313	95.639	22.81	124.24	± 1.0	SLOPE
27	1014.249	804.503	95.562	22.81	124.06	± 1.0	SLOPE
28	1009.157	807.068	91.181	22.81	129.39	± 1.0	T4
29	984.791	808.098	91.162	22.81	129.27	± 1.0	T4
30	982.496	805.545	90.687	22.81	128.76	± 1.0	T4
31	980.685	807.502	93.674	22.81	128.85	± 1.0	T4
32	900.435	871.416	97.529	22.81	136.70	± 1.0	T3
33	1017.302	828.748	97.529	22.81	123.47	± 1.0	SLOPE
34	1026.119	826.560	97.613	22.81	126.84	± 1.0	T3
35	1041.810	838.970	149.899	22.81	139.20	± 1.0	T4
36	1056.560	828.012	101.162	22.81	129.26	± 1.0	T4
37	1111.928	878.984	102.349	22.81	140.24	± 1.0	ROAD

Note: These elevations are tied to a contour line (460 ft = 140.24 m) via P137

Huntington River Location Paquette-Road							
Point Number	Northing (m)	Easting (m)	Measured Elevation (m)	Correction (m)	Final Elevation (m)	Error (m)	Point Description
1	1000.000	1000.000	100.000	38.21	138.21	± 1.0	T4
2	1000.000	1000.000	100.000	38.21	138.21	± 1.0	T4
3	1015.488	1030.425	102.847	38.21	141.06	± 1.0	ROAD
4	987.438	1010.502	98.657	38.21	136.87	± 1.0	SLOPE
5	1068.248	942.233	101.899	38.21	140.11	± 1.0	ROAD
6	1000.017	999.985	100.150	38.21	138.36	± 1.0	T4
7	1058.251	935.807	101.309	38.21	139.52	± 1.0	T4
8	1055.995	934.074	100.998	38.21	139.21	± 1.0	T4
9	1053.546	932.233	100.801	38.21	139.01	± 1.0	T4
10	1051.050	930.489	100.647	38.21	138.86	± 1.0	T4
11	1048.489	928.774	100.484	38.21	138.70	± 1.0	T4
12	1046.279	927.207	100.200	38.21	138.41	± 1.0	T4
13	1044.240	925.364	99.678	38.21	137.89	± 1.0	SLOPE
14	1041.745	923.520	98.950	38.21	137.16	± 1.0	SLOPE
15	1039.540	921.472	98.333	38.21	136.54	± 1.0	T3
16	1037.122	919.650	97.990	38.21	136.20	± 1.0	T3
17	1034.944	917.432	97.856	38.21	136.07	± 1.0	T3
18	1032.858	915.107	97.936	38.21	136.15	± 1.0	T3
19	1030.664	913.120	97.953	38.21	136.16	± 1.0	T3
20	1028.489	911.104	97.915	38.21	136.13	± 1.0	T3
21	1026.074	908.962	97.821	38.21	136.03	± 1.0	T3
22	1024.161	906.447	97.589	38.21	135.80	± 1.0	T3
23	1022.409	904.011	97.308	38.21	135.52	± 1.0	SLOPE
24	1020.719	901.472	96.889	38.21	135.10	± 1.0	SLOPE
25	1019.058	898.764	96.332	38.21	134.54	± 1.0	SLOPE
26	1015.890	897.313	96.030	38.21	134.24	± 1.0	SLOPE
27	1014.249	894.608	95.844	38.21	134.06	± 1.0	SLOPE
28	1000.167	867.098	91.183	38.21	129.39	± 1.0	T2
29	994.774	863.096	91.062	38.21	129.27	± 1.0	T2
30	992.965	860.546	90.583	38.21	128.79	± 1.0	T2
31	990.685	857.662	90.639	38.21	128.85	± 1.0	T2
32	1006.633	919.418	97.485	38.21	135.70	± 1.0	T3
33	1017.302	923.748	97.257	38.21	135.47	± 1.0	SLOPE
34	1026.119	926.580	97.630	38.21	135.84	± 1.0	T3
35	1041.610	932.070	100.085	38.21	138.30	± 1.0	T4
36	1056.580	938.012	101.046	38.21	139.26	± 1.0	T4
37	1116.336	876.964	102.033	38.21	140.24	± 1.0	ROAD

Note: These elevations are tied to a contour line (460 ft = 140.24 m) via Pt 37.

Huntington River Location Aldrich 2							
Point Number	Northing (m)	Easting (m)	Measured Elevation (m)	Correction (m)	Final Elevation (m)	Error (m)	Point Description
1	1000.000	1000.000	100.000	49.21	149.21	± 0.20	T2B
2	1000.000	1000.000	100.000	49.21	149.21	± 0.20	T2B
3	1016.963	977.196	102.409	49.21	151.62	± 0.20	T2A
4	1019.279	973.093	102.560	49.21	151.77	± 0.20	T2A
5	1016.815	969.554	102.639	49.21	151.85	± 0.20	T2A
6	1016.813	969.557	102.639	49.21	151.85	± 0.20	T2A
7	1012.200	967.123	102.753	49.21	151.97	± 0.20	T2A
8	1012.198	967.126	102.753	49.21	151.97	± 0.20	T2A
9	1010.468	972.385	102.398	49.21	151.61	± 0.20	T2A
10	1010.469	972.381	102.398	49.21	151.61	± 0.20	T2A
11	1012.999	972.332	102.418	49.21	151.63	± 0.20	T2A
12	1013.002	972.326	102.418	49.21	151.63	± 0.20	T2A
13	1015.024	974.179	102.417	49.21	151.63	± 0.20	T2A
14	1010.180	977.918	101.950	49.21	151.16	± 0.20	T2A
15	1007.945	979.440	101.475	49.21	150.69	± 0.20	T2A
16	1006.378	980.401	101.092	49.21	150.31	± 0.20	T2A
17	1006.375	980.408	101.092	49.21	150.31	± 0.20	T2A
18	999.945	972.728	100.626	49.21	149.84	± 0.20	T2B
19	994.218	967.220	100.402	49.21	149.62	± 0.20	T2B
20	989.438	959.009	100.593	49.21	149.81	± 0.20	T2B
21	987.342	950.420	100.782	49.21	150.00	± 0.20	T2B
22	984.425	944.806	100.819	49.21	150.03	± 0.20	T2B
23	984.427	944.814	100.819	49.21	150.03	± 0.20	T2B
24	980.914	946.367	100.718	49.21	149.93	± 0.20	T2B
25	978.016	947.378	100.383	49.21	149.60	± 0.20	T2B
26	978.814	953.097	100.308	49.21	149.52	± 0.20	T2B
27	984.874	966.268	100.219	49.21	149.43	± 0.20	T2B
28	984.878	966.279	100.219	49.21	149.43	± 0.20	T2B
29	978.484	957.990	100.276	49.21	149.49	± 0.20	T2B
30	976.394	958.170	99.854	49.21	149.07	± 0.20	SLOPE
31	974.980	958.806	99.550	49.21	148.76	± 0.20	SLOPE
32	972.102	958.741	99.150	49.21	148.36	± 0.20	SLOPE
33	970.449	964.046	98.773	49.21	147.99	± 0.20	T1A
34	970.382	970.646	98.664	49.21	147.88	± 0.20	T1A
35	970.901	979.399	98.560	49.21	147.77	± 0.20	T1A
36	971.844	984.783	98.541	49.21	147.76	± 0.20	T1A
37	974.181	993.387	98.441	49.21	147.65	± 0.20	T1A
38	977.180	1001.462	98.181	49.21	147.39	± 0.20	T1A
39	974.712	1003.075	97.923	49.21	147.14	± 0.20	T1A
40	971.366	1004.635	97.513	49.21	146.73	± 0.20	T1A
41	966.300	1008.294	97.427	49.21	146.64	± 0.20	T1A
42	959.728	1014.543	97.599	49.21	146.81	± 0.20	T1A
43	953.778	1021.151	97.773	49.21	146.99	± 0.20	T1A
44	953.769	1021.155	97.773	49.21	146.99	± 0.20	T1A
45	962.144	1028.180	97.565	49.21	146.78	± 0.20	T1A
46	969.973	1034.625	97.254	49.21	146.47	± 0.20	T1A
47	979.144	1040.000	97.177	49.21	146.39	± 0.20	T1A
48	988.727	1047.537	96.897	49.21	146.11	± 0.20	T1A
49	994.255	1050.497	96.706	49.21	145.92	± 0.20	T1A
50	954.665	1007.194	97.782	49.21	147.00	± 0.20	T1A

Huntington River Location Aldrich 2							
Point Number	Northing (m)	Easting (m)	Measured Elevation (m)	Correction (m)	Final Elevation (m)	Error (m)	Point Description
51	950.459	999.563	97.804	49.21	147.02	± 0.20	T1A
52	945.986	991.985	97.779	49.21	146.99	± 0.20	T1A
53	942.409	984.676	97.959	49.21	147.17	± 0.20	T1A
54	940.152	978.846	98.047	49.21	147.26	± 0.20	T1A
55	940.153	978.846	98.047	49.21	147.26	± 0.20	T1A
56	935.028	976.788	97.462	49.21	146.68	± 0.20	T1A
57	930.036	973.559	96.260	49.21	145.47	± 0.20	SLOPE
58	930.029	973.556	96.260	49.21	145.47	± 0.20	SLOPE
59	929.303	973.987	96.070	49.21	145.28	± 0.20	T1B
60	927.919	973.183	95.932	49.21	145.15	± 0.20	T1B
61	925.115	972.382	95.712	49.21	144.93	± 0.20	T1B
62	924.173	971.498	95.696	49.21	144.91	± 0.20	T1B
63	951.987	1072.159	98.470	49.21	147.68	± 0.20	T1A
64	933.910	1053.399	97.633	49.21	146.85	± 0.20	T1A
65	1036.265	946.179	102.687	49.21	151.90	± 0.20	T2A
66	1024.065	923.513	102.582	49.21	151.80	± 0.20	T2A
67	1018.041	923.624	102.299	49.21	151.51	± 0.20	T2A
68	1012.470	928.137	102.405	49.21	151.62	± 0.20	T2A
69	1000.354	935.349	102.733	49.21	151.95	± 0.20	T2A
70	1116.056	852.268	105.044	49.21	154.26	± 0.20	T3A
71	1110.413	861.935	104.643	49.21	153.86	± 0.20	T3A
72	1106.600	868.939	104.353	49.21	153.57	± 0.20	T3A
73	1101.896	874.753	103.997	49.21	153.21	± 0.20	SLOPE
74	1097.143	880.119	103.495	49.21	152.71	± 0.20	T3B
75	1091.775	885.771	103.441	49.21	152.65	± 0.20	T3B
76	1085.181	889.528	103.433	49.21	152.65	± 0.20	T3B
77	1082.344	892.330	103.333	49.21	152.55	± 0.20	T3B
78	1079.426	895.312	102.989	49.21	152.20	± 0.20	SLOPE
79	1077.053	897.608	102.390	49.21	151.60	± 0.20	T2A
80	1074.742	899.870	102.043	49.21	151.26	± 0.20	T2A
81	1071.520	903.342	101.716	49.21	150.93	± 0.20	T2A
82	1069.317	908.987	101.578	49.21	150.79	± 0.20	T2A
83	1069.320	908.984	101.577	49.21	150.79	± 0.20	T2A
84	1059.942	919.519	101.739	49.21	150.95	± 0.20	T2A
85	1055.846	924.679	101.717	49.21	150.93	± 0.20	T2A
86	1044.993	936.822	102.157	49.21	151.37	± 0.20	T2A
87	1042.108	939.854	102.227	49.21	151.44	± 0.20	T2A
88	1070.668	934.276	101.970	49.21	151.18	± 0.20	T2A
89	1093.148	932.940	102.127	49.21	151.34	± 0.20	T2A
90	1099.201	934.730	101.982	49.21	151.20	± 0.20	T2A
91	1104.072	944.354	101.436	49.21	150.65	± 0.20	T2A
92	1103.714	954.660	101.304	49.21	150.52	± 0.20	T2A
93	1103.481	965.705	101.243	49.21	150.46	± 0.20	T2A
94	1102.888	978.040	101.090	49.21	150.30	± 0.20	T2A
95	1102.126	990.688	101.139	49.21	150.35	± 0.20	T2A
96	1101.902	1004.008	100.873	49.21	150.09	± 0.20	T2A
97	1101.151	1020.544	100.694	49.21	149.91	± 0.20	T2B
98	1101.838	1033.682	100.965	49.21	150.18	± 0.20	T2A
99	1102.810	1048.993	101.481	49.21	150.69	± 0.20	T2A
100	1106.353	1064.784	101.229	49.21	150.44	± 0.20	T2A

Huntington River Location Aldrich 2							
Point Number	Northing (m)	Easting (m)	Measured Elevation (m)	Correction (m)	Final Elevation (m)	Error (m)	Point Description
101	1106.353	1064.842	101.228	49.21	150.44	± 0.20	T2A
102	1047.964	1139.048	109.155	49.21	158.37	± 0.20	T4A
103	1046.061	1140.600	109.151	49.21	158.36	± 0.20	T4A
104	1049.222	1140.557	109.073	49.21	158.29	± 0.20	T4A
105	1045.765	1142.394	109.041	49.21	158.25	± 0.20	T4A
106	1045.130	1141.078	109.131	49.21	158.34	± 0.20	T4A
107	1049.205	1137.442	109.055	49.21	158.27	± 0.20	T4A
108	1053.277	1134.248	106.864	49.21	156.08	± 0.20	SLOPE
109	1055.937	1130.702	103.845	49.21	153.06	± 0.20	SLOPE
110	1062.206	1127.222	100.910	49.21	150.12	± 0.20	T2A
111	1059.928	1094.121	100.961	49.21	150.17	± 0.20	T2A
112	1063.064	1080.716	100.367	49.21	149.58	± 0.20	T2B
113	1177.984	1050.514	110.250	49.21	159.46	± 0.20	T4A
114	1173.881	1046.010	110.138	49.21	159.35	± 0.20	T4A
115	1170.075	1035.063	110.731	49.21	159.95	± 0.20	T4A
116	1152.802	1021.178	110.193	49.21	159.41	± 0.20	T4A
117	1095.220	1052.881	100.990	49.21	150.20	± 0.20	T2A
118	1088.018	1041.809	101.219	49.21	150.43	± 0.20	T2A
119	1076.910	1034.552	101.680	49.21	150.89	± 0.20	T2A
120	1065.228	1031.379	101.989	49.21	151.20	± 0.20	T2A
121	1054.581	1028.392	101.839	49.21	151.05	± 0.20	T2A
122	1045.406	1022.364	101.713	49.21	150.93	± 0.20	T2A
123	1045.028	1012.589	102.053	49.21	151.27	± 0.20	T2A
Note: These elevations are tied to the Benchmark MAYOAZMK (160.75 m ± 0.05 m) on the bridge south of here via: ALD2 Pt 65 = ALD3 Pt 49; ALD3 Pt 48 = ALD1 Pt 1; ALD1 Pt 130 = ALMO Pt 87; ALMO Pt 87 = MOUL Pt 249; MOUL Pt 3 = TOM2 Pt 16; TOM2 Pt 3 = Benchmark							

25	1008.427	866.681	102.565	49.15	150.71	± 0.20	T2A
30	1008.707	858.681	102.561	49.15	150.71	± 0.20	T2A
31	1007.684	851.900	102.560	49.15	150.69	± 0.20	T2A
32	1008.591	844.790	102.453	49.15	150.59	± 0.20	T2A
33	1008.592	840.780	102.439	49.15	150.59	± 0.20	T2A
34	1008.268	834.635	102.962	49.15	151.73	± 0.20	T2A
35	1008.123	831.140	103.148	49.15	151.29	± 0.20	T2A
36	1008.084	824.743	103.026	49.15	151.17	± 0.20	T2A
37	1008.361	817.817	103.265	49.15	151.61	± 0.20	T2A
38	1008.369	830.125	103.310	49.15	151.65	± 0.20	T2A
39	1008.461	827.125	103.224	49.15	151.87	± 0.20	T2A
40	1008.294	780.412	103.226	49.15	151.27	± 0.20	T2A
41	1008.593	776.411	103.212	49.15	151.36	± 0.20	T2A
42	1008.800	773.14	103.270	49.15	151.42	± 0.20	T2A
43	1008.437	770.87	103.307	49.15	151.74	± 0.20	SLOPE
44	1007.351	774.911	103.238	49.15	152.08	± 0.20	T2B
45	1007.971	774.511	103.626	49.15	152.08	± 0.20	T2B
46	1008.208	769.948	104.070	49.15	152.92	± 0.20	T2B
47	1008.871	783.709	104.250	49.15	152.41	± 0.20	T2B

Huntington River Location Aldrich 1							
Point Number	Northing (m)	Easting (m)	Measured Elevation (m)	Correction (m)	Final Elevation (m)	Error (m)	Point Description
1	1000.000	1000.000	100.000	48.15	148.15	± 0.20	T1
2	1000.000	1000.000	100.000	48.15	148.15	± 0.20	T1
3	1005.394	1014.656	97.592	48.15	145.74	± 0.20	RIVER
4	1003.553	1011.742	99.178	48.15	147.32	± 0.20	T1
5	1006.449	1002.281	99.432	48.15	147.58	± 0.20	T1
6	1006.621	998.126	99.786	48.15	147.93	± 0.20	T1
7	1005.652	993.809	100.201	48.15	148.35	± 0.20	T1
8	1006.075	987.741	100.347	48.15	148.49	± 0.20	T1
9	1006.006	983.689	100.532	48.15	148.68	± 0.20	T1
10	1005.580	980.796	100.712	48.15	148.86	± 0.20	T1
11	1006.194	976.080	101.058	48.15	149.21	± 0.20	T2B
12	1006.759	968.070	101.123	48.15	149.27	± 0.20	T2B
13	1007.854	960.194	101.355	48.15	149.50	± 0.20	T2B
14	1007.229	951.948	101.442	48.15	149.59	± 0.20	T2B
15	1007.053	948.116	101.565	48.15	149.71	± 0.20	T2B
16	1007.490	943.200	101.440	48.15	149.59	± 0.20	T2B
17	1007.557	936.107	101.437	48.15	149.58	± 0.20	T2B
18	1008.008	929.105	101.593	48.15	149.74	± 0.20	T2B
19	1008.007	929.109	101.593	48.15	149.74	± 0.20	T2B
20	1008.081	919.860	101.386	48.15	149.53	± 0.20	T2B
21	1008.119	913.936	101.352	48.15	149.50	± 0.20	T2B
22	1007.450	908.215	101.679	48.15	149.83	± 0.20	T2B
23	1007.950	900.525	101.703	48.15	149.85	± 0.20	T2B
24	1007.350	897.048	101.937	48.15	150.08	± 0.20	T2B
25	1007.089	894.040	102.335	48.15	150.48	± 0.20	SLOPE
26	1007.255	889.026	102.847	48.15	150.99	± 0.20	SLOPE
27	1007.069	882.839	102.937	48.15	151.08	± 0.20	T2A
28	1007.734	874.654	102.832	48.15	150.98	± 0.20	T2A
29	1008.427	866.681	102.565	48.15	150.71	± 0.20	T2A
30	1008.707	858.884	102.468	48.15	150.61	± 0.20	T2A
31	1007.884	851.900	102.546	48.15	150.69	± 0.20	T2A
32	1008.591	844.790	102.450	48.15	150.60	± 0.20	T2A
33	1008.599	840.789	102.439	48.15	150.59	± 0.20	T2A
34	1008.268	834.636	102.962	48.15	151.11	± 0.20	T2A
35	1008.123	831.148	103.143	48.15	151.29	± 0.20	T2A
36	1008.084	824.149	103.026	48.15	151.17	± 0.20	T2A
37	1006.891	817.617	103.265	48.15	151.41	± 0.20	T2A
38	1006.869	810.288	103.300	48.15	151.45	± 0.20	T2A
39	1006.460	802.520	103.224	48.15	151.37	± 0.20	T2A
40	1005.294	794.410	103.226	48.15	151.37	± 0.20	T2A
41	1005.593	787.415	103.212	48.15	151.36	± 0.20	T2A
42	1006.930	783.182	103.276	48.15	151.42	± 0.20	T2A
43	1007.437	779.693	103.607	48.15	151.75	± 0.20	SLOPE
44	1007.371	774.511	103.938	48.15	152.08	± 0.20	T3B
45	1007.371	774.511	103.938	48.15	152.08	± 0.20	T3B
46	1008.200	769.040	104.073	48.15	152.22	± 0.20	T3B
47	1008.871	763.709	104.259	48.15	152.41	± 0.20	T3B

Huntington River Location Aldrich 1							
Point Number	Northing (m)	Easting (m)	Measured Elevation (m)	Correction (m)	Final Elevation (m)	Error (m)	Point Description
48	1009.141	759.919	104.625	48.15	152.77	± 0.20	T3B
49	1009.484	755.450	104.913	48.15	153.06	± 0.20	T3A
50	1009.744	750.314	105.234	48.15	153.38	± 0.20	T3A
51	1010.658	744.820	105.468	48.15	153.61	± 0.20	T3A
52	1010.732	740.027	105.690	48.15	153.84	± 0.20	T3A
53	1010.660	735.720	105.957	48.15	154.10	± 0.20	T3A
54	1009.988	728.700	106.062	48.15	154.21	± 0.20	T3A
55	1009.988	728.703	106.062	48.15	154.21	± 0.20	T3A
56	1010.474	718.454	106.168	48.15	154.32	± 0.20	T3A
57	1011.073	715.177	106.690	48.15	154.84	± 0.20	SLOPE
58	1009.750	710.121	107.250	48.15	155.40	± 0.20	SLOPE
59	1008.171	704.912	107.866	48.15	156.01	± 0.20	SLOPE
60	1007.637	699.438	108.289	48.15	156.44	± 0.20	SLOPE
61	1007.064	692.324	108.888	48.15	157.03	± 0.20	SLOPE
62	1005.724	684.357	109.209	48.15	157.36	± 0.20	T4
63	1002.762	677.264	109.649	48.15	157.80	± 0.20	T4
64	1001.361	669.675	110.028	48.15	158.18	± 0.20	T4
65	999.877	661.305	110.488	48.15	158.63	± 0.20	T4
66	999.188	650.961	110.664	48.15	158.81	± 0.20	T4
67	996.750	644.413	110.873	48.15	159.02	± 0.20	T4
68	994.623	637.601	110.977	48.15	159.12	± 0.20	T4
69	995.883	629.981	111.423	48.15	159.57	± 0.20	T4
70	995.883	630.029	111.421	48.15	159.57	± 0.20	T4
71	996.259	624.562	111.909	48.15	160.06	± 0.20	T4
72	995.998	617.837	112.446	48.15	160.59	± 0.20	T4
73	995.924	608.084	112.660	48.15	160.81	± 0.20	T4
74	1001.304	607.384	112.138	48.15	160.29	± 0.20	T4
75	1013.292	608.769	111.514	48.15	159.66	± 0.20	T4
76	1017.880	618.296	111.239	48.15	159.39	± 0.20	T4
77	1023.965	626.173	110.972	48.15	159.12	± 0.20	T4
78	1024.154	634.733	110.625	48.15	158.77	± 0.20	T4
79	1026.532	641.910	110.274	48.15	158.42	± 0.20	T4
80	1028.807	649.296	110.051	48.15	158.20	± 0.20	T4
81	1030.366	655.511	109.752	48.15	157.90	± 0.20	T4
82	1031.520	659.956	109.506	48.15	157.65	± 0.20	T4
83	1032.283	663.788	109.066	48.15	157.21	± 0.20	T4
84	1032.916	667.865	108.586	48.15	156.73	± 0.20	SLOPE
85	1033.819	673.204	107.910	48.15	156.06	± 0.20	SLOPE
86	1035.646	678.691	107.501	48.15	155.65	± 0.20	SLOPE
87	1037.659	685.806	107.243	48.15	155.39	± 0.20	T3A
88	1038.729	693.367	106.984	48.15	155.13	± 0.20	T3A
89	1041.255	702.747	106.679	48.15	154.83	± 0.20	T3A
90	1043.301	711.079	106.417	48.15	154.56	± 0.20	T3A
91	1044.535	719.303	106.243	48.15	154.39	± 0.20	T3A
92	1045.831	727.221	106.304	48.15	154.45	± 0.20	T3A
93	1047.144	734.928	106.018	48.15	154.17	± 0.20	T3A
94	1048.567	742.660	105.714	48.15	153.86	± 0.20	T3A

Huntington River Location Aldrich 1							
Point Number	Northing (m)	Easting (m)	Measured Elevation (m)	Correction (m)	Final Elevation (m)	Error (m)	Point Description
95	1050.059	748.911	105.363	48.15	153.51	± 0.20	SLOPE
96	1051.157	752.882	104.999	48.15	153.15	± 0.20	SLOPE
97	1052.908	756.747	104.768	48.15	152.91	± 0.20	T3B
98	1053.114	764.207	104.834	48.15	152.98	± 0.20	T3B
99	1054.111	769.875	104.551	48.15	152.70	± 0.20	T3B
100	1054.432	773.395	104.300	48.15	152.45	± 0.20	T3B
101	1054.782	784.930	103.675	48.15	151.82	± 0.20	T3B
102	1054.463	791.722	103.554	48.15	151.70	± 0.20	T3B
103	1053.559	800.464	103.651	48.15	151.80	± 0.20	T3B
104	1053.873	809.918	103.492	48.15	151.64	± 0.20	T2A
105	1053.322	820.993	103.500	48.15	151.65	± 0.20	T2A
106	1053.481	825.540	103.216	48.15	151.36	± 0.20	T2A
107	1054.187	829.655	103.177	48.15	151.32	± 0.20	T2A
108	1053.827	836.324	103.158	48.15	151.30	± 0.20	T2A
109	1053.797	845.914	103.336	48.15	151.48	± 0.20	T2A
110	1053.749	854.546	103.369	48.15	151.52	± 0.20	T2A
111	1051.996	863.598	103.383	48.15	151.53	± 0.20	T2A
112	1051.350	871.968	103.124	48.15	151.27	± 0.20	T2A
113	1050.336	876.938	102.843	48.15	150.99	± 0.20	T2A
114	1048.088	883.185	102.386	48.15	150.53	± 0.20	T2A
115	1048.155	889.302	102.172	48.15	150.32	± 0.20	T2A
116	1049.488	896.743	102.451	48.15	150.60	± 0.20	T2A
117	1049.707	903.866	102.613	48.15	150.76	± 0.20	T2A
118	1049.780	909.659	102.126	48.15	150.27	± 0.20	T2B
119	1049.586	913.917	101.686	48.15	149.83	± 0.20	T2B
120	1048.468	921.515	101.794	48.15	149.94	± 0.20	T2B
121	1048.456	932.227	101.840	48.15	149.99	± 0.20	T2B
122	1049.427	941.260	101.610	48.15	149.76	± 0.20	T2B
123	1049.902	947.503	101.364	48.15	149.51	± 0.20	T2B
124	1050.071	950.004	101.040	48.15	149.19	± 0.20	T2B
125	1050.874	953.378	100.659	48.15	148.81	± 0.20	T2B
126	1054.953	958.796	100.075	48.15	148.22	± 0.20	T2B
127	1060.628	964.240	99.638	48.15	147.79	± 0.20	T1
128	1068.282	970.190	97.830	48.15	145.98	± 0.20	RIVER
129	1011.902	1046.130	103.197	48.15	151.34	± 0.20	T2A
130	1004.724	566.021	113.239	48.15	161.39	± 0.20	T4
131	1078.689	550.138	101.499	48.15	149.65	± 0.20	RIVER
132	1072.133	551.052	102.232	48.15	150.38	± 0.20	RIVER
133	1063.605	551.313	103.080	48.15	151.23	± 0.20	T1
134	1054.314	553.799	103.059	48.15	151.21	± 0.20	T1
135	1047.542	555.756	103.181	48.15	151.33	± 0.20	T1
136	1010.006	563.624	113.392	48.15	161.54	± 0.20	T4
137	1003.080	548.058	114.316	48.15	162.46	± 0.20	T4
138	995.553	547.160	114.062	48.15	162.21	± 0.20	T4
139	987.730	547.292	114.692	48.15	162.84	± 0.20	T4
140	979.321	546.457	115.136	48.15	163.28	± 0.20	T4
141	973.585	543.414	115.516	48.15	163.66	± 0.20	SLOPE
142	967.673	543.146	116.275	48.15	164.42	± 0.20	SLOPE
143	957.246	541.816	117.333	48.15	165.48	± 0.20	SLOPE
144	955.672	553.084	117.371	48.15	165.52	± 0.20	T5

Huntington River Location Aldrich 1							
Point Number	Northing (m)	Easting (m)	Measured Elevation (m)	Correction (m)	Final Elevation (m)	Error (m)	Point Description
145	952.839	564.633	117.343	48.15	165.49	± 0.20	T5
146	950.739	575.373	117.245	48.15	165.39	± 0.20	T5
147	947.829	586.387	117.656	48.15	165.80	± 0.20	T5
148	946.932	598.144	117.603	48.15	165.75	± 0.20	T5
149	946.164	607.552	117.976	48.15	166.12	± 0.20	T5
150	944.243	614.164	118.985	48.15	167.13	± 0.20	SLOPE
151	943.015	619.711	120.349	48.15	168.50	± 0.20	SLOPE
152	941.151	625.137	121.674	48.15	169.82	± 0.20	SLOPE
153	938.175	631.248	123.090	48.15	171.24	± 0.20	SLOPE
154	931.888	638.063	124.222	48.15	172.37	± 0.20	SLOPE
155	925.181	645.218	125.273	48.15	173.42	± 0.20	SLOPE
156	919.052	650.809	126.259	48.15	174.41	± 0.20	SLOPE
157	912.014	657.832	126.838	48.15	174.98	± 0.20	T6
158	905.045	665.449	127.629	48.15	175.78	± 0.20	T6
159	900.022	671.528	128.661	48.15	176.81	± 0.20	T6
160	897.557	674.858	129.289	48.15	177.44	± 0.20	T6
161	897.691	676.760	130.351	48.15	178.50	± 0.20	SLOPE
162	896.835	682.344	132.177	48.15	180.32	± 0.20	SLOPE
163	896.799	682.354	132.184	48.15	180.33	± 0.20	T7
164	896.811	682.347	132.183	48.15	180.33	± 0.20	T7
170	895.032	679.154	131.502	48.15	179.65	± 0.20	SLOPE
171	891.115	679.707	132.294	48.15	180.44	± 0.20	T7
172	881.860	681.403	132.476	48.15	180.62	± 0.20	T7
173	872.339	683.416	132.464	48.15	180.61	± 0.20	T7
174	863.962	688.008	133.049	48.15	181.20	± 0.20	T7
175	858.456	690.633	133.264	48.15	181.41	± 0.20	T7
176	853.758	694.367	134.280	48.15	182.43	± 0.20	SLOPE
177	849.502	698.165	135.560	48.15	183.71	± 0.20	SLOPE
178	845.926	703.437	136.792	48.15	184.94	± 0.20	SLOPE
179	842.275	708.008	137.868	48.15	186.02	± 0.20	SLOPE
180	838.821	710.285	138.324	48.15	186.47	± 0.20	SLOPE
181	834.400	712.710	139.670	48.15	187.82	± 0.20	SLOPE
182	830.359	715.135	141.141	48.15	189.29	± 0.20	SLOPE
183	824.724	717.851	142.930	48.15	191.08	± 0.20	T8
184	819.093	721.951	142.990	48.15	191.14	± 0.20	T8
185	814.804	725.214	142.971	48.15	191.12	± 0.20	T8
186	807.061	712.210	142.867	48.15	191.01	± 0.20	T8
187	826.841	721.227	142.830	48.15	190.98	± 0.20	T8
188	827.691	732.709	142.856	48.15	191.00	± 0.20	T8
189	826.050	742.844	142.696	48.15	190.84	± 0.20	T8
190	820.312	746.939	142.883	48.15	191.03	± 0.20	T8
191	815.451	756.407	142.838	48.15	190.99	± 0.20	T8
192	808.834	772.391	143.178	48.15	191.33	± 0.20	T8
193	806.675	792.603	143.429	48.15	191.58	± 0.20	T8
194	823.499	770.283	142.512	48.15	190.66	± 0.20	T8
195	826.976	756.612	141.892	48.15	190.04	± 0.20	T8
196	892.185	692.543	132.272	48.15	180.42	± 0.20	T7
197	893.520	704.761	132.138	48.15	180.28	± 0.20	T7
198	903.023	713.943	132.094	48.15	180.24	± 0.20	T7
199	917.039	707.167	131.910	48.15	180.06	± 0.20	T7

Huntington River Location Aldrich 1							
Point Number	Northing (m)	Easting (m)	Measured Elevation (m)	Correction (m)	Final Elevation (m)	Error (m)	Point Description
Note: These elevations are tied to the Benchmark MAYOAZMK (160.75 m ± 0.05 m) on the bridge south of here via: ALD1 Pt 130 = ALMO Pt 87; ALMO Pt 87 = MOUL Pt 249; MOUL Pt 3 = TOM2 Pt 16; TOM2 Pt 3 = Benchmark							

4 932.717
 5 930.901 937.146
 6 930.027 937.146
 7 927.877 937.146
 8 924.701 937.146
 9 922.743 937.146
 10 920.987 937.146
 11 920.932 937.146
 12 927.681 937.146
 13 924.912 937.146
 14 922.081 937.146
 15 920.147 937.146
 16 924.291 937.146
 17 935.131 937.146
 18 923.464 937.146
 19 918.752 937.146
 20 901.221 937.146
 21 899.606 937.146
 22 898.347 937.146
 23 892.650 937.146
 24 892.847 937.146
 25 890.905 937.146
 26 885.789 937.146
 27 886.297 937.146
 28 881.476 937.146
 29 884.038 937.146
 30 874.487 937.146
 31 892.922 937.146
 32 900.321 937.146
 33 910.391 937.146
 34 933.912 937.146
 35 937.952 937.146
 36 945.202 937.146
 37 951.152 937.146
 38 954.627 937.146
 39 958.852 937.146
 40 958.272 937.146
 41 952.892 937.146
 42 951.442 937.146
 43 977.240 937.146
 44 971.280 937.146
 45 974.994 937.146
 46 976.694 937.146
 47 979.105 937.146
 48 935.329 937.146
 49 1020.050 937.146
 50 892.662 937.146

Huntington River Location Aldrich 3							
Point Number	Northing (m)	Easting (m)	Measured Elevation (m)	Correction (m)	Final Elevation (m)	Error (m)	Point Description
1	1000.000	1000.000	100.000	51.31	151.31	± 0.20	T2A
2	1000.000	1000.000	100.000	51.31	151.31	± 0.20	T2A
3	983.367	968.029	94.840	51.31	146.15	± 0.20	RIVER
4	982.717	966.343	95.979	51.31	147.29	± 0.20	T1
5	980.901	963.065	96.130	51.31	147.44	± 0.20	T1
6	980.027	961.546	96.469	51.31	147.78	± 0.20	T1
7	977.877	957.147	96.880	51.31	148.19	± 0.20	T2B
8	974.709	950.645	97.065	51.31	148.37	± 0.20	T2B
9	972.746	945.380	97.107	51.31	148.41	± 0.20	T2B
10	970.567	940.744	97.221	51.31	148.53	± 0.20	T2B
11	969.582	938.129	97.438	51.31	148.75	± 0.20	SLOPE
12	967.691	933.725	97.853	51.31	149.16	± 0.20	SLOPE
13	964.912	929.178	98.191	51.31	149.50	± 0.20	T2B
14	959.081	918.287	97.908	51.31	149.22	± 0.20	T2B
15	953.447	903.420	97.952	51.31	149.26	± 0.20	T2B
16	944.291	886.991	98.137	51.31	149.44	± 0.20	T2B
17	935.151	867.530	97.833	51.31	149.14	± 0.20	T2B
18	923.464	844.629	98.022	51.31	149.33	± 0.20	T2B
19	913.756	816.490	98.393	51.31	149.70	± 0.20	T2B
20	901.221	786.413	98.620	51.31	149.93	± 0.20	T2B
21	893.658	769.282	99.052	51.31	150.36	± 0.20	SLOPE
22	893.347	765.955	99.308	51.31	150.62	± 0.20	SLOPE
23	892.650	760.343	99.637	51.31	150.94	± 0.20	SLOPE
24	892.644	760.345	99.637	51.31	150.94	± 0.20	SLOPE
25	890.905	752.941	99.548	51.31	150.86	± 0.20	T2A
26	888.789	743.501	99.620	51.31	150.93	± 0.20	T2A
27	886.297	730.171	100.270	51.31	151.58	± 0.20	T2A
28	861.176	820.939	101.867	51.31	153.17	± 0.20	FAN
29	864.638	827.797	101.365	51.31	152.67	± 0.20	FAN
30	875.467	835.967	99.930	51.31	151.24	± 0.20	FAN
31	892.222	850.310	98.806	51.31	150.11	± 0.20	FAN
32	900.321	862.109	98.350	51.31	149.66	± 0.20	T2B
33	910.338	876.099	98.061	51.31	149.37	± 0.20	T2B
34	932.459	907.651	97.634	51.31	148.94	± 0.20	T2B
35	937.988	915.743	97.664	51.31	148.97	± 0.20	T2B
36	945.565	925.423	97.712	51.31	149.02	± 0.20	T2B
37	951.936	932.602	97.864	51.31	149.17	± 0.20	T2B
38	954.627	936.627	97.704	51.31	149.01	± 0.20	SLOPE
39	956.859	940.285	97.497	51.31	148.80	± 0.20	SLOPE
40	959.393	943.920	97.137	51.31	148.44	± 0.20	SLOPE
41	962.696	948.100	97.040	51.31	148.35	± 0.20	T2B
42	967.449	954.208	97.021	51.31	148.33	± 0.20	T2B
43	971.248	959.494	96.889	51.31	148.20	± 0.20	SLOPE
44	971.250	959.498	96.887	51.31	148.19	± 0.20	SLOPE
45	974.596	964.649	96.546	51.31	147.85	± 0.20	SLOPE
46	976.694	968.411	96.060	51.31	147.37	± 0.20	T1
47	979.105	971.250	94.735	51.31	146.04	± 0.20	RIVER
48	935.329	956.931	96.840	51.31	148.15	± 0.20	T2B
49	1020.050	1017.850	100.594	51.31	151.90	± 0.20	T2A
50	990.665	1015.463	100.618	51.31	151.93	± 0.20	T2A

Huntington River Location Aldrich 3							
Point Number	Northing (m)	Easting (m)	Measured Elevation (m)	Correction (m)	Final Elevation (m)	Error (m)	Point Description
51	988.914	1020.959	100.616	51.31	151.92	± 0.20	T2A
52	988.912	1020.962	100.616	51.31	151.92	± 0.20	ROAD
53	1015.116	1037.690	101.005	51.31	152.31	± 0.20	ROAD
54	1008.295	1030.196	101.153	51.31	152.46	± 0.20	ROAD
55	1008.992	1016.178	101.028	51.31	152.34	± 0.20	ROAD
56	1015.590	1016.837	100.855	51.31	152.16	± 0.20	ROAD
57	1018.910	1003.246	100.614	51.31	151.92	± 0.20	ROAD
58	1011.796	1001.949	100.959	51.31	152.27	± 0.20	ROAD

Note: These elevations are tied to the Benchmark MAYOAZMK (160.75 m ± 0.05 m) on the bridge south of here via: ALD3 Pt 48 = ALD1 Pt 1; ALD1 Pt 130 = ALMO Pt 87; ALMO Pt 87 = MOUL Pt 249; MOUL Pt 3 = TOM2 Pt 16; TOM2 Pt 3 = Benchmark

59	985.501	1023.205	100.616	51.31	151.92	± 0.20	T3
60	981.858	1015.264	100.504	56.01	156.51	± 0.20	T3
65	985.026	1028.120	101.295	56.01	157.31	± 0.20	SLOPE
67	985.190	1026.719	102.776	56.01	159.78	± 0.20	SLOPE
68	986.110	1042.958	103.024	56.01	170.03	± 0.20	SLOPE
69	987.533	1052.669	105.095	56.01	172.01	± 0.20	SLOPE
70	990.170	1062.805	107.573	56.01	174.58	± 0.20	SLOPE
21	990.373	1082.852	107.576	56.01	172.169	± 0.20	SLOPE
22	981.544	1071.570	106.475	56.01	174.74	± 0.20	T6
23	982.063	1073.324	106.577	56.01	174.62	± 0.20	T6
24	989.807	1073.507	109.387	56.01	175.40	± 0.20	T6
25	985.842	1078.697	109.721	56.01	175.78	± 0.20	T6
26	1005.657	1078.723	108.916	56.01	174.83	± 0.20	T6
27	1004.567	1086.582	109.450	56.01	175.47	± 0.20	T6
28	1002.893	1092.281	110.110	56.01	176.12	± 0.20	SLOPE
29	1000.949	1098.141	111.214	56.01	179.24	± 0.20	SLOPE
30	1000.249	1098.149	111.214	56.01	179.24	± 0.20	SLOPE
31	989.748	1095.165	111.735	56.01	177.74	± 0.20	T7
32	980.751	1097.357	114.289	56.01	180.27	± 0.20	T7
33	978.378	1107.217	114.729	56.01	180.74	± 0.20	T7
34	987.440	1111.980	114.853	56.01	180.86	± 0.20	T7
35	987.416	1111.987	114.854	56.01	180.86	± 0.20	T7
36	976.206	1110.523	114.912	56.01	180.93	± 0.20	T7
37	976.206	1110.523	114.913	56.01	180.93	± 0.20	T7
38	987.702	1125.187	118.026	56.01	174.02	± 0.20	SLOPE
39	977.725	1125.189	118.048	56.01	174.02	± 0.20	SLOPE
40	976.014	1127.247	121.398	56.01	187.41	± 0.20	SLOPE
41	926.141	1141.897	125.073	56.01	181.08	± 0.20	T4
42	911.073	1148.170	125.082	56.01	181.09	± 0.20	T4
43	917.260	1148.804	125.152	56.01	181.18	± 0.20	T4
44	1000.110	984.874	99.508	56.01	185.51	± 0.20	T5
45	971.043	990.519	98.377	56.01	181.38	± 0.20	SLOPE
46	9705.811	974.781	98.419	56.01	182.23	± 0.20	T4
47	1105.581	967.514	96.287	56.01	182.26	± 0.20	T4
48	1105.429	963.729	95.852	56.01	181.86	± 0.20	T4
49	1105.584	951.026	95.145	56.01	181.15	± 0.20	SLOPE
50	1175.923	958.210	94.141	56.01	180.87	± 0.20	SLOPE

Huntington River Location Aldrich-Moultrip							
Point Number	Northing (m)	Easting (m)	Measured Elevation (m)	Correction (m)	Final Elevation (m)	Error (m)	Point Description
1	1000.000	1000.000	100.000	66.01	166.01	± 0.20	T5
2	1000.000	1000.000	100.000	66.01	166.01	± 0.20	T5
3	1070.833	979.843	99.368	66.01	165.38	± 0.20	T5
4	1065.883	987.753	99.425	66.01	165.43	± 0.20	T5
5	1064.237	994.816	99.330	66.01	165.34	± 0.20	T5
6	1058.278	1000.930	99.460	66.01	165.47	± 0.20	T5
7	1051.638	1013.071	99.852	66.01	165.86	± 0.20	T5
8	1049.074	1019.324	99.838	66.01	165.85	± 0.20	T5
9	1043.023	1027.450	99.990	66.01	166.00	± 0.20	T5
10	1032.830	1026.135	100.091	66.01	166.10	± 0.20	T5
11	1023.186	1026.843	100.211	66.01	166.22	± 0.20	T5
12	1014.268	1025.786	100.434	66.01	166.44	± 0.20	T5
13	1005.920	1023.983	100.511	66.01	166.52	± 0.20	T5
14	992.904	1015.990	100.362	66.01	166.37	± 0.20	T5
15	981.886	1016.264	100.504	66.01	166.51	± 0.20	T5
16	985.026	1028.120	101.798	66.01	167.81	± 0.20	SLOPE
17	985.196	1034.713	102.775	66.01	168.78	± 0.20	SLOPE
18	986.110	1042.358	104.024	66.01	170.03	± 0.20	SLOPE
19	987.357	1052.869	105.996	66.01	172.01	± 0.20	SLOPE
20	990.173	1062.805	107.575	66.01	173.58	± 0.20	SLOPE
21	990.173	1062.812	107.576	66.01	173.59	± 0.20	SLOPE
22	991.644	1071.373	108.735	66.01	174.74	± 0.20	T6
23	982.033	1073.364	108.877	66.01	174.89	± 0.20	T6
24	989.537	1079.982	109.387	66.01	175.40	± 0.20	T6
25	995.512	1078.697	109.171	66.01	175.18	± 0.20	T6
26	1005.837	1078.723	108.916	66.01	174.93	± 0.20	T6
27	1004.567	1086.862	109.460	66.01	175.47	± 0.20	T6
28	1002.894	1092.291	110.110	66.01	176.12	± 0.20	SLOPE
29	1000.949	1098.141	111.214	66.01	177.22	± 0.20	SLOPE
30	1000.949	1098.149	111.215	66.01	177.22	± 0.20	SLOPE
31	989.749	1095.161	111.735	66.01	177.74	± 0.20	SLOPE
32	980.767	1097.357	114.259	66.01	180.27	± 0.20	T7
33	978.976	1107.217	114.729	66.01	180.74	± 0.20	T7
34	987.420	1111.986	114.653	66.01	180.66	± 0.20	T7
35	987.416	1111.997	114.654	66.01	180.66	± 0.20	T7
36	978.208	1110.325	114.872	66.01	180.88	± 0.20	T7
37	978.206	1110.333	114.873	66.01	180.88	± 0.20	T7
38	957.722	1125.597	118.009	66.01	184.02	± 0.20	SLOPE
39	957.725	1125.589	118.008	66.01	184.02	± 0.20	SLOPE
40	925.011	1129.247	121.396	66.01	187.41	± 0.20	SLOPE
41	928.141	1141.897	125.073	66.01	191.08	± 0.20	T8
42	913.013	1143.170	125.082	66.01	191.09	± 0.20	T8
43	917.360	1146.604	125.122	66.01	191.13	± 0.20	T8
44	1060.810	964.874	99.505	66.01	165.51	± 0.20	T5
45	1112.045	990.519	95.377	66.01	161.39	± 0.20	SLOPE
46	1105.814	974.761	96.219	66.01	162.23	± 0.20	T4
47	1105.381	967.514	96.267	66.01	162.28	± 0.20	T4
48	1105.479	963.723	95.852	66.01	161.86	± 0.20	T4
49	1105.654	961.025	95.145	66.01	161.15	± 0.20	SLOPE
50	1105.823	958.210	94.566	66.01	160.57	± 0.20	SLOPE

Huntington River Location Aldrich-Moulthrop							
Point Number	Northing (m)	Easting (m)	Measured Elevation (m)	Correction (m)	Final Elevation (m)	Error (m)	Point Description
51	1106.434	955.988	93.796	66.01	159.81	± 0.20	SLOPE
52	1107.346	955.264	93.471	66.01	159.48	± 0.20	SLOPE
53	1108.039	952.629	93.072	66.01	159.08	± 0.20	T3A
54	1108.438	948.697	92.873	66.01	158.88	± 0.20	T3A
55	1108.493	944.072	92.734	66.01	158.74	± 0.20	T3A
56	1108.161	940.973	92.375	66.01	158.38	± 0.20	SLOPE
57	1108.140	940.984	92.378	66.01	158.39	± 0.20	SLOPE
58	1107.896	937.568	91.876	66.01	157.89	± 0.20	SLOPE
59	1108.478	934.588	91.590	66.01	157.60	± 0.20	T3B
60	1108.273	930.777	91.502	66.01	157.51	± 0.20	T3B
61	1108.850	927.541	91.508	66.01	157.52	± 0.20	T3B
62	1109.815	923.484	91.444	66.01	157.45	± 0.20	T3B
63	1110.380	918.489	91.291	66.01	157.30	± 0.20	T3B
64	1111.242	915.466	91.155	66.01	157.16	± 0.20	T3B
65	1103.933	911.764	91.392	66.01	157.40	± 0.20	T3B
66	1104.621	909.483	91.174	66.01	157.18	± 0.20	T3B
67	1105.664	907.968	90.902	66.01	156.91	± 0.20	SLOPE
68	1106.896	906.034	90.686	66.01	156.70	± 0.20	SLOPE
69	1106.906	906.020	90.686	66.01	156.70	± 0.20	SLOPE
70	1107.472	904.673	90.520	66.01	156.53	± 0.20	SLOPE
71	1108.097	903.202	90.414	66.01	156.42	± 0.20	T2A
72	1108.762	900.557	90.293	66.01	156.30	± 0.20	T2A
73	1109.371	896.580	90.362	66.01	156.37	± 0.20	T2A
74	1109.153	892.781	90.207	66.01	156.22	± 0.20	T2A
75	1109.604	888.213	89.971	66.01	155.98	± 0.20	T2A
76	1110.672	884.949	89.624	66.01	155.63	± 0.20	T2B
77	1089.764	916.678	91.638	66.01	157.65	± 0.20	T3B
78	1087.495	916.776	91.401	66.01	157.41	± 0.20	T3B
79	1084.420	917.041	91.042	66.01	157.05	± 0.20	SLOPE
80	1083.860	915.558	90.508	66.01	156.52	± 0.20	SLOPE
81	1081.310	914.109	89.451	66.01	155.46	± 0.20	T2B
82	1079.094	913.236	88.898	66.01	154.91	± 0.20	T2B
83	1075.576	911.347	88.569	66.01	154.58	± 0.20	T2B
84	1053.227	908.049	88.514	66.01	154.52	± 0.20	T2B
85	1032.619	906.670	88.755	66.01	154.76	± 0.20	T2B
86	1032.619	906.672	88.755	66.01	154.76	± 0.20	T2B
87	946.599	903.313	89.211	66.01	155.22	± 0.20	T2B
88	996.145	1001.997	99.790	66.01	165.80	± 0.20	T5
89	994.506	998.021	98.264	66.01	164.27	± 0.20	SLOPE
90	993.263	996.414	96.894	66.01	162.90	± 0.20	SLOPE
91	992.626	994.585	95.834	66.01	161.84	± 0.20	SLOPE
92	991.066	992.848	94.482	66.01	160.49	± 0.20	SLOPE
93	989.955	989.678	93.165	66.01	159.17	± 0.20	SLOPE
94	988.034	983.966	92.494	66.01	158.50	± 0.20	T3A
95	984.022	979.138	92.429	66.01	158.44	± 0.20	T3A
96	972.571	977.829	92.549	66.01	158.56	± 0.20	T3A
97	967.373	971.802	92.240	66.01	158.25	± 0.20	SLOPE
98	962.981	966.822	91.810	66.01	157.82	± 0.20	SLOPE
99	959.798	963.636	91.119	66.01	157.13	± 0.20	SLOPE
100	955.217	958.649	90.538	66.01	156.55	± 0.20	SLOPE

Huntington River Location Aldrich-Moulthrop							
Point Number	Northing (m)	Easting (m)	Measured Elevation (m)	Correction (m)	Final Elevation (m)	Error (m)	Point Description
101	951.215	952.375	90.095	66.01	156.10	± 0.20	T2A
102	948.160	945.877	89.461	66.01	155.47	± 0.20	T2A
103	937.856	937.321	89.143	66.01	155.15	± 0.20	T2A
104	926.831	933.937	89.368	66.01	155.38	± 0.20	T2A
105	916.510	931.979	89.977	66.01	155.99	± 0.20	T2A
106	901.659	931.712	89.774	66.01	155.78	± 0.20	T2A
107	887.807	927.853	89.759	66.01	155.77	± 0.20	T2A
108	875.779	932.286	89.784	66.01	155.79	± 0.20	T2A
109	864.985	936.961	90.270	66.01	156.28	± 0.20	T2A
110	838.182	921.283	89.608	66.01	155.62	± 0.20	T2B
111	822.705	921.884	89.351	66.01	155.36	± 0.20	T2B
112	807.248	922.171	89.061	66.01	155.07	± 0.20	T2B
113	792.814	923.442	88.884	66.01	154.89	± 0.20	T2B
114	777.773	924.508	88.848	66.01	154.86	± 0.20	T2B
115	758.007	931.157	89.174	66.01	155.18	± 0.20	T2B
116	774.557	911.146	88.368	66.01	154.38	± 0.20	T2B
117	788.658	906.120	88.430	66.01	154.44	± 0.20	T2B
118	797.238	899.184	88.374	66.01	154.38	± 0.20	T2B
119	808.351	893.868	88.365	66.01	154.37	± 0.20	T2B
120	819.259	886.118	88.426	66.01	154.44	± 0.20	T2B
121	830.551	873.667	88.328	66.01	154.34	± 0.20	T2B
122	841.797	865.570	88.390	66.01	154.40	± 0.20	T2B
123	855.802	866.036	88.212	66.01	154.22	± 0.20	T2B
124	867.845	865.923	88.197	66.01	154.21	± 0.20	T2B
125	880.810	866.954	87.932	66.01	153.94	± 0.20	T1
126	896.431	867.699	87.788	66.01	153.80	± 0.20	T1
127	914.677	872.143	87.476	66.01	153.48	± 0.20	T1
128	933.567	876.524	88.001	66.01	154.01	± 0.20	T1
129	944.461	876.916	88.097	66.01	154.11	± 0.20	SLOPE
130	944.040	874.324	87.747	66.01	153.76	± 0.20	T1
131	943.942	872.714	87.400	66.01	153.41	± 0.20	T1
132	944.038	871.331	86.721	66.01	152.73	± 0.20	T1
133	943.687	869.870	86.001	66.01	152.01	± 0.20	T0
134	943.806	867.442	85.672	66.01	151.68	± 0.20	T0
135	942.655	861.259	86.032	66.01	152.04	± 0.20	T0
136	954.804	853.040	86.154	66.01	152.16	± 0.20	T0
137	966.740	847.292	86.135	66.01	152.14	± 0.20	T0
138	976.452	853.456	86.084	66.01	152.09	± 0.20	T0
139	987.599	850.578	85.907	66.01	151.92	± 0.20	T0
140	997.183	846.581	85.955	66.01	151.96	± 0.20	T0
141	1013.152	845.897	85.907	66.01	151.92	± 0.20	T0
142	1021.070	837.401	85.844	66.01	151.85	± 0.20	T0
143	1023.199	825.213	85.914	66.01	151.92	± 0.20	T0
144	1027.523	820.836	85.356	66.01	151.36	± 0.20	T0
145	1031.426	816.846	85.322	66.01	151.33	± 0.20	T0
146	1034.248	814.246	85.023	66.01	151.03	± 0.20	T0
147	1042.649	805.463	85.614	66.01	151.62	± 0.20	T0
148	1055.838	791.356	85.574	66.01	151.58	± 0.20	T0
149	1063.052	783.765	85.108	66.01	151.12	± 0.20	T0
150	1070.035	778.336	84.641	66.01	150.65	± 0.20	RIVER

Huntington River Location Aldrich-Moulthrop							
Point Number	Northing (m)	Easting (m)	Measured Elevation (m)	Correction (m)	Final Elevation (m)	Error (m)	Point Description
151	1018.819	770.384	85.338	66.01	151.35	± 0.20	T0
152	1013.007	781.540	85.461	66.01	151.47	± 0.20	T0
153	1004.820	798.111	85.786	66.01	151.79	± 0.20	T0
154	998.609	809.211	85.877	66.01	151.89	± 0.20	T0
155	985.132	821.252	86.131	66.01	152.14	± 0.20	T0
156	980.390	831.377	86.322	66.01	152.33	± 0.20	T1
157	960.311	829.421	86.454	66.01	152.46	± 0.20	T1
158	966.268	745.806	86.695	66.01	152.70	± 0.20	T1
159	967.083	736.020	86.592	66.01	152.60	± 0.20	T1
160	968.056	724.442	86.953	66.01	152.96	± 0.20	T1
161	969.018	714.403	86.772	66.01	152.78	± 0.20	T1
162	970.856	701.553	86.851	66.01	152.86	± 0.20	T1
163	972.075	689.095	86.863	66.01	152.87	± 0.20	T1
164	975.633	662.462	87.000	66.01	153.01	± 0.20	T1
165	978.400	650.303	87.066	66.01	153.08	± 0.20	T1
166	979.269	640.766	87.108	66.01	153.12	± 0.20	T1
167	980.938	628.929	87.133	66.01	153.14	± 0.20	T1
168	983.085	618.115	86.911	66.01	152.92	± 0.20	T1
169	983.086	618.104	86.911	66.01	152.92	± 0.20	T1
170	983.353	600.762	87.046	66.01	153.06	± 0.20	T1
171	987.302	586.737	87.006	66.01	153.02	± 0.20	T1
172	988.155	574.109	87.064	66.01	153.07	± 0.20	T1
173	990.671	564.303	87.231	66.01	153.24	± 0.20	T1
174	990.768	556.321	87.693	66.01	153.70	± 0.20	T1
175	863.663	726.542	87.228	66.01	153.24	± 0.20	T1
176	857.707	713.141	87.003	66.01	153.01	± 0.20	T1
177	851.218	699.401	87.678	66.01	153.69	± 0.20	T1
178	783.117	648.446	95.047	66.01	161.06	± 0.20	T4A

Note: These elevations are tied to the Benchmark MAYOAZMK (160.75 m ± 0.05 m) on the bridge south of here via: ALMO Pt 87 = MOUL Pt 249; MOUL Pt 3 = TOM2 Pt 16; TOM2 Pt 3 = Benchmark

32	1228.307	805.978	77.65	191.31	± 0.20	T8
33	1254.415	887.017	77.65	191.55	± 0.20	T8
34	1281.602	863.148	77.65	191.35	± 0.20	T8
35	1302.132	854.856	77.65	191.60	± 0.20	T8
36	1324.860	874.131	77.65	191.61	± 0.20	T8
37	1360.761	861.136	77.65	191.41	± 0.20	T8
38	1381.910	859.511	77.65	191.49	± 0.20	T8
39	1186.415	819.874	77.65	191.12	± 0.20	ROAD
40	1203.250	873.917	77.65	191.80	± 0.20	ROAD
41	1209.871	832.634	77.65	191.80	± 0.20	ROAD
42	1242.928	849.240	77.65	191.93	± 0.20	ROAD
43	1238.342	808.952	77.65	191.60	± 0.20	ROAD
44	1277.533	750.802	77.65	191.75	± 0.20	ROAD
45	1284.106	762.806	77.65	191.94	± 0.20	ROAD
46	1331.543	715.970	77.65	191.84	± 0.20	ROAD
47	1337.250	730.988	77.65	191.94	± 0.20	ROAD
48	1325.487	731.579	77.65	191.88	± 0.20	ROAD
49	1272.781	607.502	77.65	191.82	± 0.20	T8
50	1241.867	872.277	77.65	191.38	± 0.20	T8

Huntington River Location Road							
Point Number	Northing (m)	Easting (m)	Measured Elevation (m)	Correction (m)	Final Elevation (m)	Error (m)	Point Description
1	1000.000	1000.000	100.000	77.65	177.65	± 0.20	ROAD
2	1000.000	1000.000	100.000	77.65	177.65	± 0.20	ROAD
3	865.534	1112.620	90.364	77.65	168.01	± 0.20	ROAD
4	880.304	1102.070	91.033	77.65	168.68	± 0.20	ROAD
5	876.439	1096.421	90.830	77.65	168.48	± 0.20	ROAD
6	918.276	1061.379	93.833	77.65	171.48	± 0.20	ROAD
7	923.775	1065.580	93.781	77.65	171.43	± 0.20	ROAD
8	953.364	1031.535	96.244	77.65	173.89	± 0.20	ROAD
9	958.624	1035.888	96.215	77.65	173.86	± 0.20	ROAD
10	980.324	1012.048	98.544	77.65	176.19	± 0.20	ROAD
11	984.695	1017.771	98.351	77.65	176.00	± 0.20	ROAD
12	1003.308	1007.562	99.844	77.65	177.49	± 0.20	ROAD
13	1034.156	993.723	102.687	77.65	180.33	± 0.20	ROAD
14	1030.103	988.087	102.723	77.65	180.37	± 0.20	ROAD
15	1072.748	969.384	106.794	77.65	184.44	± 0.20	ROAD
16	1075.086	975.868	106.788	77.65	184.44	± 0.20	ROAD
17	1109.670	961.122	110.041	77.65	187.69	± 0.20	ROAD
18	1106.027	955.303	110.016	77.65	187.66	± 0.20	ROAD
19	1130.836	943.593	112.068	77.65	189.72	± 0.20	ROAD
20	1134.158	949.306	112.190	77.65	189.84	± 0.20	ROAD
21	1148.997	940.761	113.386	77.65	191.03	± 0.20	ROAD
22	1163.455	929.929	114.148	77.65	191.80	± 0.20	ROAD
23	1022.867	1026.485	113.970	77.65	191.62	± 0.20	T8
24	1170.057	925.832	114.190	77.65	191.84	± 0.20	T8
25	1170.163	925.987	114.165	77.65	191.81	± 0.20	T8
26	1000.018	999.992	99.879	77.65	177.53	± 0.20	T8
27	1172.018	936.865	113.621	77.65	191.27	± 0.20	T8
28	1180.704	986.197	113.818	77.65	191.47	± 0.20	T8
29	1182.903	998.015	113.709	77.65	191.36	± 0.20	T8
30	1185.983	1013.536	113.609	77.65	191.26	± 0.20	T8
31	1203.639	914.877	113.407	77.65	191.05	± 0.20	T8
32	1228.307	906.078	113.563	77.65	191.21	± 0.20	T8
33	1254.415	897.017	113.906	77.65	191.55	± 0.20	T8
34	1281.602	890.133	113.904	77.65	191.55	± 0.20	T8
35	1302.132	882.566	113.855	77.65	191.50	± 0.20	T8
36	1324.880	874.131	113.959	77.65	191.61	± 0.20	T8
37	1360.761	861.483	113.765	77.65	191.41	± 0.20	T8
38	1381.918	859.514	113.842	77.65	191.49	± 0.20	T8
39	1166.415	918.574	113.774	77.65	191.42	± 0.20	ROAD
40	1203.256	877.973	114.151	77.65	191.80	± 0.20	ROAD
41	1208.677	882.404	114.255	77.65	191.90	± 0.20	ROAD
42	1242.928	842.349	114.283	77.65	191.93	± 0.20	ROAD
43	1236.642	838.952	114.253	77.65	191.90	± 0.20	ROAD
44	1277.636	790.302	114.106	77.65	191.75	± 0.20	ROAD
45	1283.104	794.306	114.295	77.65	191.94	± 0.20	ROAD
46	1331.547	735.070	114.292	77.65	191.94	± 0.20	ROAD
47	1331.550	735.066	114.292	77.65	191.94	± 0.20	ROAD
48	1325.487	731.579	114.244	77.65	191.89	± 0.20	ROAD
49	1272.761	697.502	113.673	77.65	191.32	± 0.20	T8
50	1241.887	672.377	113.731	77.65	191.38	± 0.20	T8

Huntington River Location Road							
Point Number	Northing (m)	Easting (m)	Measured Elevation (m)	Correction (m)	Final Elevation (m)	Error (m)	Point Description
51	1207.724	652.277	113.408	77.65	191.06	± 0.20	T8
52	1165.119	709.298	113.624	77.65	191.27	± 0.20	T8
53	1176.277	754.476	114.007	77.65	191.66	± 0.20	T8
54	1176.277	754.478	114.007	77.65	191.66	± 0.20	T8
55	1164.282	800.327	114.049	77.65	191.70	± 0.20	T8
56	1091.372	780.215	113.924	77.65	191.57	± 0.20	T8
57	1059.284	822.233	114.404	77.65	192.05	± 0.20	T8
58	1083.350	843.552	113.846	77.65	191.49	± 0.20	T8
59	1106.760	863.953	114.120	77.65	191.77	± 0.20	T8
60	1147.029	856.433	113.874	77.65	191.52	± 0.20	T8
Note: These elevations are tied to the Benchmark MAYOAZMK (160.75 m ± 0.05 m) on the bridge south of here via: ROAD Pt 3 = TOM2 Pt 16; TOM2 Pt 3 = Benchmark							

14	1132.217	821.300	101.113	± 0.20	194.43	± 0.20	T9
15	1140.658	831.938	100.873	± 0.20	187.56	± 0.20	T9
16	1143.604	841.988	100.605	± 0.20	183.87	± 0.20	T9
17	1148.777	955.639	100.553	± 0.20	183.66	± 0.20	T8
18	1150.137	986.461	100.457	± 0.20	183.52	± 0.20	SLOPE
19	1059.311	985.924	100.271	± 0.20	182.34	± 0.20	T4
20	1149.550	968.598	99.895	± 0.20	182.78	± 0.20	T4
21	1149.916	964.529	99.420	± 0.20	182.36	± 0.20	T4
22	1149.272	878.518	99.144	± 0.20	182.11	± 0.20	T4
23	1149.854	987.964	99.054	± 0.20	182.02	± 0.20	T4
24	1144.822	989.136	98.869	± 0.20	181.86	± 0.20	T4
25	1106.481	1058.240	98.416	± 0.20	182.17	± 0.20	T4
26	1130.125	1019.505	98.346	± 0.20	182.31	± 0.20	T4
27	1129.579	1029.400	98.250	± 0.20	182.85	± 0.20	T4
28	1149.820	1038.193	98.147	± 0.20	183.00	± 0.20	T4
29	1118.381	1039.177	97.911	± 0.20	183.00	± 0.20	T4
30	1150.867	1037.891	98.016	± 0.20	182.86	± 0.20	T4
31	+104.935	1035.145	98.014	± 0.20	182.78	± 0.20	T4
32	1100.858	1056.268	98.193	± 0.20	182.44	± 0.20	T4
33	1085.980	1057.208	98.087	± 0.20	181.75	± 0.20	SLOPE
34	1082.150	1048.931	98.284	± 0.20	181.26	± 0.20	T4B
35	1092.161	1041.919	98.284	± 0.20	181.25	± 0.20	T4B
36	1080.500	1057.143	98.724	± 0.20	180.99	± 0.20	T4B
37	1070.050	1071.729	98.180	± 0.20	181.32	± 0.20	T4B
38	1072.786	1085.154	98.086	± 0.20	181.54	± 0.20	T4B
39	1773.555	1094.968	98.148	± 0.20	181.16	± 0.20	T4B
40	1068.701	1048.428	97.519	± 0.20	180.79	± 0.20	T4A
41	1055.751	1117.316	97.269	± 0.20	180.64	± 0.20	T4A
42	1082.033	1129.327	97.552	± 0.20	180.51	± 0.20	T4A
43	1058.758	1141.985	97.299	± 0.20	180.20	± 0.20	T4A
44	1050.672	1149.582	96.921	± 0.20	180.99	± 0.20	T4A
45	1053.646	1185.452	97.681	± 0.20	180.55	± 0.20	T4A
46	1048.100	1176.418	97.853	± 0.20	180.33	± 0.20	T4A
47	1043.121	1186.548	97.974	± 0.20	180.31	± 0.20	T4A
48	1038.421	1186.814	97.251	± 0.20	180.22	± 0.20	T4A
49	1033.703	1207.672	97.220	± 0.20	180.24	± 0.20	T4A
50	1024.241	1217.939	97.181	± 0.20	180.15	± 0.20	T4A

Huntington River Location Moultrip							
Point Number	Northing (m)	Easting (m)	Measured Elevation (m)	Correction (m)	Final Elevation (m)	Error (m)	Point Description
1	1000.000	1000.000	100.000	62.97	162.97	± 0.20	T4
2	1000.000	1000.000	100.000	62.97	162.97	± 0.20	T4
3	1099.345	844.941	105.046	62.97	168.01	± 0.20	ROAD
4	1140.138	868.293	104.248	62.97	167.21	± 0.20	T5
5	1139.422	871.006	103.905	62.97	166.87	± 0.20	T5
6	1137.373	876.116	103.319	62.97	166.29	± 0.20	T5A
7	1137.375	876.114	103.319	62.97	166.29	± 0.20	T5A
8	1135.939	883.177	102.751	62.97	165.72	± 0.20	T5A
9	1134.318	891.269	102.509	62.97	165.48	± 0.20	T5A
10	1134.088	897.440	102.263	62.97	165.23	± 0.20	T5
11	1134.069	902.782	101.859	62.97	164.83	± 0.20	T5
12	1135.762	911.761	101.535	62.97	164.50	± 0.20	T5
13	1137.218	921.304	101.170	62.97	164.14	± 0.20	T5
14	1137.225	921.300	101.170	62.97	164.14	± 0.20	T5
15	1140.655	931.933	100.913	62.97	163.88	± 0.20	T5
16	1143.604	941.989	100.905	62.97	163.87	± 0.20	T5
17	1148.777	955.530	100.693	62.97	163.66	± 0.20	T5
18	1149.017	960.361	100.557	62.97	163.52	± 0.20	SLOPE
19	1149.311	965.094	100.271	62.97	163.24	± 0.20	T4
20	1149.550	969.596	99.815	62.97	162.78	± 0.20	T4
21	1149.311	974.329	99.420	62.97	162.39	± 0.20	T4
22	1149.272	978.515	99.141	62.97	162.11	± 0.20	T4
23	1146.834	987.964	99.054	62.97	162.02	± 0.20	T4
24	1141.832	998.136	98.896	62.97	161.86	± 0.20	T4
25	1136.461	1008.240	99.208	62.97	162.17	± 0.20	T4
26	1130.126	1019.505	99.346	62.97	162.31	± 0.20	T4
27	1123.579	1029.406	99.683	62.97	162.65	± 0.20	T4
28	1118.229	1039.193	100.033	62.97	163.00	± 0.20	T4
29	1118.181	1039.177	100.033	62.97	163.00	± 0.20	T4
30	1110.881	1047.591	100.015	62.97	162.98	± 0.20	T4
31	1104.935	1051.745	99.818	62.97	162.79	± 0.20	T4
32	1100.558	1054.201	99.468	62.97	162.44	± 0.20	T4
33	1095.985	1057.209	98.887	62.97	161.85	± 0.20	SLOPE
34	1092.159	1059.918	98.284	62.97	161.25	± 0.20	T4B
35	1092.160	1059.919	98.284	62.97	161.25	± 0.20	T4B
36	1080.399	1067.609	98.024	62.97	160.99	± 0.20	T4B
37	1080.080	1071.729	98.150	62.97	161.12	± 0.20	T4B
38	1076.788	1083.154	98.068	62.97	161.04	± 0.20	T4B
39	1073.533	1094.363	98.129	62.97	161.10	± 0.20	T4B
40	1068.701	1105.426	97.819	62.97	160.79	± 0.20	T3A
41	1065.752	1117.315	97.669	62.97	160.64	± 0.20	T3A
42	1062.933	1129.327	97.542	62.97	160.51	± 0.20	T3A
43	1059.758	1141.085	97.229	62.97	160.20	± 0.20	T3A
44	1058.672	1153.469	96.921	62.97	159.89	± 0.20	T3B
45	1053.698	1165.482	96.681	62.97	159.65	± 0.20	T3B
46	1048.138	1176.418	96.963	62.97	159.93	± 0.20	T3B
47	1043.121	1186.449	97.374	62.97	160.34	± 0.20	T3A
48	1038.421	1196.614	97.251	62.97	160.22	± 0.20	T3A
49	1033.703	1207.672	97.276	62.97	160.24	± 0.20	T3A
50	1029.241	1217.939	97.180	62.97	160.15	± 0.20	T3A

Huntington River Location Moultrip							
Point Number	Northing (m)	Easting (m)	Measured Elevation (m)	Correction (m)	Final Elevation (m)	Error (m)	Point Description
51	1025.109	1229.476	97.006	62.97	159.97	± 0.20	T3A
52	1009.738	1232.471	96.948	62.97	159.92	± 0.20	T3B
53	999.054	1235.061	96.911	62.97	159.88	± 0.20	T3B
54	984.475	1233.999	96.993	62.97	159.96	± 0.20	SLOPE
55	983.721	1223.309	97.069	62.97	160.04	± 0.20	T3A
56	983.910	1218.809	97.256	62.97	160.22	± 0.20	T3A
57	983.617	1214.273	97.499	62.97	160.47	± 0.20	T3A
58	983.450	1207.457	97.710	62.97	160.68	± 0.20	T3A
59	982.179	1196.137	97.594	62.97	160.56	± 0.20	T3A
60	982.079	1196.236	97.569	62.97	160.54	± 0.20	T3A
61	981.754	1184.980	97.585	62.97	160.55	± 0.20	T3A
62	981.304	1173.432	97.683	62.97	160.65	± 0.20	T3A
63	980.692	1161.892	97.526	62.97	160.49	± 0.20	T3A
64	980.257	1150.473	97.461	62.97	160.43	± 0.20	T3A
65	979.946	1144.472	97.475	62.97	160.44	± 0.20	T3A
66	980.021	1139.966	97.638	62.97	160.61	± 0.20	T3A
67	979.904	1135.186	97.817	62.97	160.78	± 0.20	T3A
68	979.900	1135.186	97.817	62.97	160.78	± 0.20	T3A
69	978.922	1119.068	97.567	62.97	160.53	± 0.20	T3A
70	978.416	1107.855	97.485	62.97	160.45	± 0.20	T3A
71	977.838	1096.570	97.468	62.97	160.43	± 0.20	T3A
72	977.869	1096.596	97.465	62.97	160.43	± 0.20	T3A
73	977.266	1090.487	97.613	62.97	160.58	± 0.20	T3A
74	976.995	1083.963	97.887	62.97	160.85	± 0.20	SLOPE
75	976.476	1076.373	98.307	62.97	161.27	± 0.20	T4B
76	976.323	1068.694	98.716	62.97	161.68	± 0.20	T4B
77	975.727	1062.047	98.877	62.97	161.84	± 0.20	T4B
78	974.983	1050.948	98.866	62.97	161.83	± 0.20	T4B
79	973.654	1041.693	98.820	62.97	161.79	± 0.20	T4B
80	971.792	1028.908	98.835	62.97	161.80	± 0.20	T4B
81	971.792	1028.908	98.834	62.97	161.80	± 0.20	T4B
82	978.159	1020.576	98.531	62.97	161.50	± 0.20	T4B
83	983.348	1014.213	98.668	62.97	161.64	± 0.20	T4B
84	983.344	1014.217	98.668	62.97	161.63	± 0.20	T4B
85	986.696	1010.183	98.813	62.97	161.78	± 0.20	T4B
86	989.765	1007.140	99.187	62.97	162.15	± 0.20	T4
87	992.748	1003.414	99.628	62.97	162.59	± 0.20	T4
88	999.789	990.316	99.957	62.97	162.92	± 0.20	T4
89	999.789	990.298	99.957	62.97	162.92	± 0.20	T4
90	1001.226	982.701	99.855	62.97	162.82	± 0.20	T4
91	1002.609	977.496	100.231	62.97	163.20	± 0.20	T4
92	1003.778	971.050	100.525	62.97	163.49	± 0.20	T4
93	1005.880	959.464	100.450	62.97	163.42	± 0.20	T4
94	1008.766	946.512	100.096	62.97	163.06	± 0.20	T4
95	1010.367	940.380	100.192	62.97	163.16	± 0.20	T4
96	1013.885	928.492	100.062	62.97	163.03	± 0.20	T4
97	1014.948	916.878	100.242	62.97	163.21	± 0.20	T4
98	1015.405	905.192	100.503	62.97	163.47	± 0.20	T4
99	1017.410	892.867	100.918	62.97	163.89	± 0.20	T5
100	1018.161	879.041	102.375	62.97	165.34	± 0.20	T5A

Huntington River Location Moultrip							
Point Number	Northing (m)	Easting (m)	Measured Elevation (m)	Correction (m)	Final Elevation (m)	Error (m)	Point Description
101	1017.582	871.160	102.393	62.97	165.36	± 0.20	T5A
102	1017.213	868.711	102.115	62.97	165.08	± 0.20	T5
103	1015.807	857.615	101.792	62.97	164.76	± 0.20	T5
104	1015.812	845.934	101.551	62.97	164.52	± 0.20	T5
105	1014.536	835.008	101.771	62.97	164.74	± 0.20	T5
106	1012.541	825.169	102.069	62.97	165.04	± 0.20	T5
107	1011.350	812.260	102.307	62.97	165.27	± 0.20	T5A
108	1004.611	770.558	107.780	62.97	170.75	± 0.20	APEX
109	1024.476	786.736	103.570	62.97	166.54	± 0.20	T5
110	1036.284	793.462	103.172	62.97	166.14	± 0.20	T5A
111	1045.601	797.926	103.525	62.97	166.49	± 0.20	T5
112	1045.582	798.011	103.524	62.97	166.49	± 0.20	T5
113	1056.085	803.420	103.836	62.97	166.80	± 0.20	T5
114	1067.375	812.188	103.909	62.97	166.88	± 0.20	T5
115	1077.340	819.287	104.046	62.97	167.01	± 0.20	T5
116	1086.864	826.746	104.191	62.97	167.16	± 0.20	T5
117	1094.447	834.891	104.280	62.97	167.25	± 0.20	T5
118	1098.557	845.652	105.018	62.97	167.98	± 0.20	ROAD
119	1070.981	839.823	103.224	62.97	166.19	± 0.20	T5A
120	1048.572	844.810	102.420	62.97	165.39	± 0.20	T5A
121	1026.460	850.681	101.890	62.97	164.86	± 0.20	T5
122	1004.595	855.447	101.599	62.97	164.57	± 0.20	T5
123	983.440	858.821	101.485	62.97	164.45	± 0.20	T5
124	961.972	864.825	101.416	62.97	164.38	± 0.20	T5
125	940.509	871.364	101.381	62.97	164.35	± 0.20	T5
126	940.510	871.367	101.381	62.97	164.35	± 0.20	T5
127	990.965	1047.945	98.680	62.97	161.65	± 0.20	T4B
128	973.833	1042.073	98.816	62.97	161.78	± 0.20	T4B
129	957.666	1041.194	98.595	62.97	161.56	± 0.20	T4B
130	950.612	1041.797	97.885	62.97	160.85	± 0.20	SLOPE
131	950.611	1041.799	97.885	62.97	160.85	± 0.20	SLOPE
132	941.803	1041.906	96.895	62.97	159.86	± 0.20	T3B
133	934.750	1041.400	95.710	62.97	158.68	± 0.20	SLOPE
134	925.171	1047.860	94.913	62.97	157.88	± 0.20	T2A
135	912.761	1042.977	94.870	62.97	157.84	± 0.20	T2A
136	891.600	1043.083	94.709	62.97	157.68	± 0.20	T2A
137	874.409	1043.500	94.839	62.97	157.81	± 0.20	T2A
138	853.761	1043.603	94.527	62.97	157.49	± 0.20	T2A
139	836.696	1044.063	95.156	62.97	158.12	± 0.20	SLOPE
140	817.163	1042.935	94.253	62.97	157.22	± 0.20	T2B
141	800.100	1042.885	94.478	62.97	157.44	± 0.20	T2B
142	790.991	1042.977	94.066	62.97	157.03	± 0.20	T2B
143	774.826	1042.971	94.203	62.97	157.17	± 0.20	T2B
144	759.345	1043.397	94.492	62.97	157.46	± 0.20	T2B
145	742.908	1042.516	94.282	62.97	157.25	± 0.20	T2B
146	742.907	1042.517	94.282	62.97	157.25	± 0.20	T2B
147	736.350	1042.597	93.739	62.97	156.71	± 0.20	T1
148	728.677	1042.374	94.021	62.97	156.99	± 0.20	T2B
149	724.457	1042.862	94.078	62.97	157.04	± 0.20	T2B
150	729.123	1059.205	93.970	62.97	156.94	± 0.20	T2B

Huntington River Location Moultrip							
Point Number	Northing (m)	Easting (m)	Measured Elevation (m)	Correction (m)	Final Elevation (m)	Error (m)	Point Description
151	736.426	1078.846	94.544	62.97	157.51	± 0.20	T2A
152	741.356	1099.032	94.508	62.97	157.47	± 0.20	T2B
153	744.890	1114.859	94.248	62.97	157.21	± 0.20	T2B
154	745.790	1120.315	94.006	62.97	156.97	± 0.20	T2B
155	746.573	1125.527	93.863	62.97	156.83	± 0.20	T2B
156	750.030	1145.876	93.874	62.97	156.84	± 0.20	T2B
157	753.656	1165.684	93.846	62.97	156.81	± 0.20	T2B
158	753.634	1165.698	93.846	62.97	156.81	± 0.20	T2B
159	757.294	1186.731	93.942	62.97	156.91	± 0.20	T2B
160	761.508	1208.274	93.966	62.97	156.93	± 0.20	T2B
161	767.033	1228.714	93.803	62.97	156.77	± 0.20	T2B
162	775.346	1247.349	93.722	62.97	156.69	± 0.20	T2B
163	779.814	1254.514	93.677	62.97	156.64	± 0.20	T2B
164	784.545	1260.633	93.179	62.97	156.15	± 0.20	T2B
165	790.819	1268.007	92.903	62.97	155.87	± 0.20	T1
166	795.175	1273.671	92.790	62.97	155.76	± 0.20	T1
167	800.780	1280.603	93.008	62.97	155.98	± 0.20	T1
168	806.087	1288.724	93.465	62.97	156.43	± 0.20	T1
169	811.157	1297.665	93.753	62.97	156.72	± 0.20	T1
170	821.252	1328.870	92.668	62.97	155.63	± 0.20	T1
171	855.569	1335.791	92.884	62.97	155.85	± 0.20	T1
172	875.043	1340.056	92.868	62.97	155.83	± 0.20	T1
173	875.036	1340.075	92.868	62.97	155.83	± 0.20	T1
174	893.789	1343.583	92.798	62.97	155.77	± 0.20	T1
175	865.333	1336.456	92.918	62.97	155.89	± 0.20	T1
176	866.388	1331.952	92.973	62.97	155.94	± 0.20	T1
177	866.795	1326.636	93.304	62.97	156.27	± 0.20	T1
178	865.435	1320.619	93.813	62.97	156.78	± 0.20	SLOPE
179	863.926	1309.231	93.898	62.97	156.86	± 0.20	T2B
180	868.562	1299.090	94.258	62.97	157.22	± 0.20	T2B
181	872.487	1289.472	94.440	62.97	157.41	± 0.20	T2B
182	874.561	1281.173	94.491	62.97	157.46	± 0.20	T2B
183	876.230	1276.673	94.680	62.97	157.65	± 0.20	T2A
184	878.329	1271.398	94.881	62.97	157.85	± 0.20	T2A
185	888.611	1268.530	94.954	62.97	157.92	± 0.20	T2A
186	900.338	1264.271	94.974	62.97	157.94	± 0.20	T2A
187	914.381	1250.291	94.715	62.97	157.68	± 0.20	T2A
188	914.377	1250.302	94.709	62.97	157.68	± 0.20	T2A
189	922.856	1242.617	94.538	62.97	157.50	± 0.20	T2A
190	925.123	1237.519	94.826	62.97	157.79	± 0.20	T2A
191	927.113	1231.717	95.454	62.97	158.42	± 0.20	SLOPE
192	929.914	1223.760	96.356	62.97	159.32	± 0.20	T3B
193	933.384	1217.890	96.564	62.97	159.53	± 0.20	T3B
194	937.759	1210.759	96.463	62.97	159.43	± 0.20	T3B
195	942.133	1204.744	96.472	62.97	159.44	± 0.20	T3B
196	944.696	1200.458	96.940	62.97	159.91	± 0.20	T3B
197	947.348	1193.384	97.410	62.97	160.38	± 0.20	T3A
198	950.853	1180.492	97.665	62.97	160.63	± 0.20	T3A
199	955.609	1160.206	97.654	62.97	160.62	± 0.20	T3A
200	962.396	1140.860	97.791	62.97	160.76	± 0.20	T3A

Huntington River Location Moultrip							
Point Number	Northing (m)	Easting (m)	Measured Elevation (m)	Correction (m)	Final Elevation (m)	Error (m)	Point Description
201	714.748	1229.075	93.472	62.97	156.44	± 0.20	T2B
202	704.513	1205.953	93.346	62.97	156.31	± 0.20	T2B
203	696.522	1162.033	93.478	62.97	156.44	± 0.20	T2B
204	692.305	1142.483	93.572	62.97	156.54	± 0.20	T2B
205	689.125	1216.970	93.107	62.97	156.07	± 0.20	T2B
206	674.562	1226.689	93.395	62.97	156.36	± 0.20	T2B
207	656.034	1240.388	93.418	62.97	156.38	± 0.20	T2B
208	647.221	1246.573	93.531	62.97	156.50	± 0.20	T2B
209	642.625	1249.643	95.287	62.97	158.25	± 0.20	SLOPE
210	638.344	1252.777	97.519	62.97	160.49	± 0.20	T3A
211	630.479	1257.356	100.600	62.97	163.57	± 0.20	SLOPE
212	630.416	1257.306	100.600	62.97	163.57	± 0.20	SLOPE
213	619.797	1265.508	103.541	62.97	166.51	± 0.20	T5
214	613.501	1270.867	106.613	62.97	169.58	± 0.20	SLOPE
215	609.225	1274.726	108.419	62.97	171.39	± 0.20	T5
216	590.906	1267.039	108.776	62.97	171.74	± 0.20	T5
217	630.652	1296.418	108.841	62.97	171.81	± 0.20	T5
218	593.799	1318.900	115.703	62.97	178.67	± 0.20	SLOPE
219	531.213	1331.766	124.587	62.97	187.55	± 0.20	SLOPE
220	500.326	1336.154	129.337	62.97	192.30	± 0.20	T8
221	449.386	1292.082	128.652	62.97	191.62	± 0.20	T8
222	425.200	1281.229	128.887	62.97	191.85	± 0.20	T8
223	359.551	1280.897	129.821	62.97	192.79	± 0.20	T8
224	338.460	1286.903	130.940	62.97	193.91	± 0.20	T8
225	393.172	1366.423	143.064	62.97	206.03	± 0.20	T9
226	411.415	1378.268	143.644	62.97	206.61	± 0.20	T9
227	426.575	1384.720	143.478	62.97	206.44	± 0.20	T9
228	426.591	1384.751	143.444	62.97	206.41	± 0.20	T9
229	479.727	1429.558	143.154	62.97	206.12	± 0.20	T9
230	479.891	1429.762	143.565	62.97	206.53	± 0.20	T9
231	477.283	1454.836	147.642	62.97	210.61	± 0.20	SLOPE
232	498.314	1508.740	155.012	62.97	217.98	± 0.20	T10
233	690.501	1023.347	91.839	62.97	154.81	± 0.20	T1
234	703.465	1054.699	91.816	62.97	154.78	± 0.20	T1
235	715.800	1131.971	91.485	62.97	154.45	± 0.20	T1
236	718.938	1164.331	91.369	62.97	154.34	± 0.20	T1
237	722.916	1182.001	91.430	62.97	154.40	± 0.20	T1
238	715.289	1222.774	91.077	62.97	154.04	± 0.20	T1
239	715.110	1260.393	91.078	62.97	154.05	± 0.20	T1
240	717.950	1280.414	90.966	62.97	153.93	± 0.20	T1
241	723.656	1294.935	90.652	62.97	153.62	± 0.20	T1
242	731.039	1304.645	90.662	62.97	153.63	± 0.20	T1
243	780.545	1276.017	93.388	62.97	156.35	± 0.20	T2A
244	777.541	1277.784	92.572	62.97	155.54	± 0.20	T2A
245	770.703	1284.453	92.848	62.97	155.81	± 0.20	T2A
246	759.778	1293.988	92.588	62.97	155.55	± 0.20	T2A
247	1078.778	1369.562	92.868	62.97	155.83	± 0.20	T2A
248	1237.138	1340.721	92.224	62.97	155.19	± 0.20	T2A
249	1236.956	1340.670	92.253	62.97	155.22	± 0.20	T2A

Note: These elevations are tied to the Benchmark MAYOAZMK (160.75 m ± 0.05 m) on the bridge

Huntington River Location Moultrip							
Point Number	Northing (m)	Easting (m)	Measured Elevation (m)	Correction (m)	Final Elevation (m)	Error (m)	Point Description
south of here via: MOUL Pt 3 = TOM2 Pt 16; TOM2 Pt 3 = Benchmark							
2	1000.000	1000.000	156.22	± 0.20	156.22		T2A
3	723.621	692.987	162.86	± 0.20	162.86		T4
4	899.982	922.976	155.27	± 0.20	155.27		T2A
5	-17.586	751.763	171.20	± 0.20	171.20		T5
6	-76.942	754.384	172.97	± 0.20	172.97		T5
7	299.501	652.086	155.03	± 0.20	155.03		T2A
8	337.008	666.937	157.86	± 0.20	157.86		T2A

Note: These elevations are tied to the Benchmark MAYDAZM (180.75 m ± 0.05 m) on the ocean.

south of here via: MOUL Pt 3 = TOM2 Pt 16; TOM2 Pt 3 = Benchmark

Huntington River Location Moulthrop-Tower							
Point Number	Northing (m)	Easting (m)	Measured Elevation (m)	Correction (m)	Final Elevation (m)	Error (m)	Point Description
1	1000.000	1000.000	100.000	55.22	155.22	± 0.20	T2A
2	1000.000	1000.000	100.000	55.22	155.22	± 0.20	T2A
3	723.031	690.997	107.736	55.22	162.96	± 0.20	T4
4	999.982	999.980	100.051	55.22	155.27	± 0.20	T2A
5	-17.599	731.793	116.008	55.22	171.23	± 0.20	T5
6	-75.242	754.894	117.754	55.22	172.97	± 0.20	T5
7	296.501	662.086	102.814	55.22	158.03	± 0.20	T2A
8	297.958	668.937	102.639	55.22	157.86	± 0.20	T2A

Note: These elevations are tied to the Benchmark MAYOAZMK (160.75 m ± 0.05 m) on the bridge south of here via: MOTO Pt1 = MOUL Pt 249; MOUL Pt 3 = TOM2 Pt 16; TOM2 Pt 3 = Benchmark

14	1650.917	693.92	99.01862	72.78	164.81	± 0.20	ROAD
15	1650.532	897.32	99.18454	72.78	163.95	± 0.20	ROAD
16	1695.7	806.901	99.23146	72.78	168.01	± 0.20	ROAD
17	1677.094	648.579	99.26211	72.78	167.04	± 0.20	ROAD
18	1746.112	1651.3	99.36746	72.78	161.95	± 0.20	ROAD
19	1781.203	1016.7	99.41771	72.78	162.81	± 0.20	ROAD
20	982.042	7824.89	102.76202	72.78	167.84	± 0.20	ROAD
21	1048.588	987.84	99.49801	72.78	167.79	± 0.20	ROAD

Note: These elevations are tied to the Benchmark MAYOAZMK (160.75 m ± 0.05 m) on the bridge north of here via: TCM2 Pt 9 = Benchmark

Huntington River Location Tower-Moultrap 2							
Point Number	Northing (m)	Easting (m)	Measured Elevation (m)	Correction (m)	Final Elevation (m)	Error (m)	Point Description
1	1000	1000	100	72.78	172.78	± 0.20	T5
2	1000	1000	100	72.78	172.78	± 0.20	T5
3	1433.327	936.634	87.9692	72.78	160.75	± 0.20	ROAD
4	1483.523	931.125	89.61542	72.78	162.40	± 0.20	ROAD
5	1532.541	925.512	90.82258	72.78	163.60	± 0.20	ROAD
6	1532.515	925.515	90.82304	72.78	163.60	± 0.20	ROAD
7	1532.265	918.724	90.98021	72.78	163.76	± 0.20	ROAD
8	1574.178	914.957	92.06385	72.78	164.84	± 0.20	ROAD
9	1574.642	921.908	91.97252	72.78	164.75	± 0.20	ROAD
10	1648.398	918.615	92.04746	72.78	164.83	± 0.20	ROAD
11	1649.753	918.637	92.03113	72.78	164.81	± 0.20	ROAD
12	1649.759	918.636	92.03105	72.78	164.81	± 0.20	ROAD
13	1710.029	909.411	92.00081	72.78	164.78	± 0.20	ROAD
14	1850.917	898.2	93.01982	72.78	165.80	± 0.20	ROAD
15	1853.532	897.32	93.16454	72.78	165.95	± 0.20	ROAD
16	1895.13	886.301	95.23166	72.78	168.01	± 0.20	ROAD
17	1877.034	895.679	94.2621	72.78	167.04	± 0.20	ROAD
18	1746.112	1051.3	89.06746	72.78	161.85	± 0.20	ROAD
19	1781.883	1016.7	90.02771	72.78	162.81	± 0.20	ROAD
20	982.0442	1034.89	100.76292	72.78	173.54	± 0.20	ROAD
21	1048.388	961.635	94.95318	72.78	167.73	± 0.20	ROAD

Note: These elevations are tied to the Benchmark MAYOAZMK (160.75 m ± 0.05 m) on the bridge
north of here via: TOM2 Pt 3 = Benchmark

Huntington River Location Tower-Moultrap 1							
Point Number	Northing (m)	Easting (m)	Measured Elevation (m)	Correction (m)	Final Elevation (m)	Error (m)	Point Description
1	1000.000	1000.000	100.000	72.71	172.71	± 0.20	T5
2	1000.000	1000.000	100.000	72.71	172.71	± 0.20	T5
3	1054.849	971.606	95.007	72.71	167.71	± 0.20	ROAD
4	1053.639	974.036	95.303	72.71	168.01	± 0.20	ROAD
5	1048.663	978.863	95.420	72.71	168.13	± 0.20	ROAD
6	1051.210	965.448	94.999	72.71	167.71	± 0.20	ROAD
7	1049.493	967.493	95.283	72.71	167.99	± 0.20	ROAD
8	1045.823	973.255	95.422	72.71	168.13	± 0.20	ROAD
9	1022.005	961.247	95.515	72.71	168.22	± 0.20	ROAD
10	1025.636	955.282	95.361	72.71	168.07	± 0.20	ROAD
11	1064.393	974.839	95.262	72.71	167.97	± 0.20	ROAD
12	1104.409	990.666	94.249	72.71	166.96	± 0.20	ROAD
13	1105.088	1005.099	94.594	72.71	167.30	± 0.20	ROAD
14	1105.082	1005.098	94.594	72.71	167.30	± 0.20	ROAD
15	1092.620	1008.549	94.974	72.71	167.68	± 0.20	ROAD
16	1092.606	1008.548	94.972	72.71	167.68	± 0.20	ROAD
17	1092.117	999.792	94.930	72.71	167.64	± 0.20	ROAD
18	1023.720	1021.061	99.093	72.71	171.80	± 0.20	ROAD
19	1018.277	1015.989	99.234	72.71	171.94	± 0.20	ROAD
20	976.400	1025.641	100.153	72.71	172.86	± 0.20	ROAD
21	978.601	1031.151	100.119	72.71	172.83	± 0.20	ROAD
22	979.378	1033.449	100.733	72.71	173.44	± 0.20	ROAD
23	903.066	1056.294	101.473	72.71	174.18	± 0.20	ROAD
24	901.540	1050.300	101.380	72.71	174.09	± 0.20	ROAD
25	900.369	1048.003	101.448	72.71	174.15	± 0.20	ROAD
26	1090.824	1003.811	95.008	72.71	167.72	± 0.20	ROAD
27	1122.809	1000.697	93.597	72.71	166.30	± 0.20	ROAD
28	1148.676	991.915	92.023	72.71	164.73	± 0.20	ROAD
29	1149.221	998.568	92.172	72.71	164.88	± 0.20	ROAD
30	1196.813	991.235	91.130	72.71	163.84	± 0.20	ROAD
31	1192.792	984.465	91.236	72.71	163.94	± 0.20	ROAD
32	1252.140	975.796	88.412	72.71	161.12	± 0.20	ROAD
33	1253.021	982.473	88.397	72.71	161.10	± 0.20	ROAD
34	1302.469	976.291	86.599	72.71	159.31	± 0.20	ROAD
35	1375.288	970.830	86.407	72.71	159.11	± 0.20	ROAD
36	1487.217	967.924	89.689	72.71	162.40	± 0.20	ROAD

Note: These elevations are tied to the Benchmark MAYOAZMK (160.75 m ± 0.05 m) on the bridge
north of here via: TOMO PT 36 = TOM2 PT 4; TOM2 PT 3 = Benchmark

Huntington River Location Tower							
Point Number	Northing (m)	Easting (m)	Measured Elevation (m)	Correction (m)	Final Elevation (m)	Error (m)	Point Description
1	1000	1000	100	72.49	172.49	± 0.20	T5
2	1000	1000	100	72.49	172.49	± 0.20	T5
3	1114.4345	1246.325	119.81005	72.49	192.30	± 0.20	T8
4	1114.44	1246.321	119.80998	72.49	192.30	± 0.20	T8
5	1138.8782	1254.368	120.06378	72.49	192.55	± 0.20	T8
6	1098.645	1243.73	120.95359	72.49	193.44	± 0.20	T8
7	1097.0752	1230.98	116.71252	72.49	189.20	± 0.20	SLOPE
8	1095.9694	1224.635	114.48704	72.49	186.98	± 0.20	T7
9	1092.9499	1214.424	111.30938	72.49	183.80	± 0.20	SLOPE
10	1055.9145	1214.233	110.99476	72.49	183.48	± 0.20	SLOPE
11	1052.1896	1230.827	112.37795	72.49	184.87	± 0.20	SLOPE
12	1049.5922	1203.136	110.22661	72.49	182.72	± 0.20	SLOPE
13	1046.9759	1196.55	109.74143	72.49	182.23	± 0.20	T6
14	1044.9518	1189.462	109.29692	72.49	181.79	± 0.20	T6
15	1042.3929	1180.625	109.09309	72.49	181.58	± 0.20	T6
16	1040.2129	1171.467	109.14157	72.49	181.63	± 0.20	T6
17	1038.9786	1162.375	108.51387	72.49	181.00	± 0.20	SLOPE
18	1037.131	1153.173	107.63028	72.49	180.12	± 0.20	SLOPE
19	1035.1317	1144.359	106.80357	72.49	179.29	± 0.20	SLOPE
20	1033.109	1135.376	105.36391	72.49	177.85	± 0.20	SLOPE
21	1031.2207	1126.525	103.86516	72.49	176.35	± 0.20	SLOPE
22	1029.6439	1119.648	102.49341	72.49	174.98	± 0.20	SLOPE
23	1029.1057	1116.966	101.78074	72.49	174.27	± 0.20	SLOPE
24	1027.9912	1113.355	101.26388	72.49	173.75	± 0.20	SLOPE
25	1025.6944	1105.536	100.94474	72.49	173.43	± 0.20	SLOPE
26	1023.1584	1097.282	100.52876	72.49	173.02	± 0.20	SLOPE
27	1020.7365	1088.555	100.21063	72.49	172.70	± 0.20	T5
28	1018.5556	1079.984	100.0717	72.49	172.56	± 0.20	T5
29	1016.173	1071.194	100.25246	72.49	172.74	± 0.20	T5
30	1013.7864	1062.387	100.14939	72.49	172.64	± 0.20	T5
31	1011.2595	1053.501	100.01398	72.49	172.50	± 0.20	T5
32	1008.7228	1044.33	99.56753	72.49	172.06	± 0.20	T5
33	1006.5281	1035.376	99.99692	72.49	172.49	± 0.20	T5
34	1004.3996	1026.92	100.00008	72.49	172.49	± 0.20	T5
35	1002.6123	1017.537	100.08608	72.49	172.57	± 0.20	T5
36	1000.7174	1008.462	100.34429	72.49	172.83	± 0.20	T5
37	1000.7162	1008.448	100.34374	72.49	172.83	± 0.20	T5
38	749.00773	1225.159	115.38699	72.49	187.88	± 0.20	T7
39	749.03004	1225.139	115.38562	72.49	187.87	± 0.20	T7
40	762.7404	1213.338	113.93312	72.49	186.42	± 0.20	SLOPE
41	776.77976	1201.626	112.50767	72.49	185.00	± 0.20	SLOPE
42	789.76146	1189.91	111.01757	72.49	183.51	± 0.20	SLOPE
43	801.68965	1177.518	110.20241	72.49	182.69	± 0.20	T6
44	815.93374	1167.178	109.9366	72.49	182.43	± 0.20	T6
45	829.8382	1156.373	109.58936	72.49	182.08	± 0.20	T6
46	843.54419	1145.063	108.7762	72.49	181.26	± 0.20	SLOPE
47	856.00482	1132.275	107.2414	72.49	179.73	± 0.20	SLOPE
48	869.09947	1120.281	105.24299	72.49	177.73	± 0.20	SLOPE
49	882.29363	1107.937	103.66516	72.49	176.15	± 0.20	SLOPE
50	882.2929	1107.937	103.66518	72.49	176.15	± 0.20	SLOPE

Huntington River Location Tower							
Point Number	Northing (m)	Easting (m)	Measured Elevation (m)	Correction (m)	Final Elevation (m)	Error (m)	Point Description
51	896.18341	1095.911	102.90894	72.49	175.40	± 0.20	SLOPE
52	909.24982	1083.681	102.03	72.49	174.52	± 0.20	SLOPE
53	917.92195	1068.136	101.41419	72.49	173.90	± 0.20	SLOPE
54	868.17107	1075.393	103.18007	72.49	175.67	± 0.20	SLOPE
55	868.26402	1075.34	103.17783	72.49	175.67	± 0.20	SLOPE
56	898.17197	1054.924	101.34783	72.49	173.84	± 0.20	SLOPE
57	913.54145	1045.501	100.91947	72.49	173.41	± 0.20	SLOPE
58	929.22035	1036.224	100.24129	72.49	172.73	± 0.20	T5
59	944.63092	1027.784	100.3614	72.49	172.85	± 0.20	T5
60	960.80982	1019.798	100.33782	72.49	172.83	± 0.20	T5
61	976.16632	1011.804	100.44135	72.49	172.93	± 0.20	T5
62	991.90705	1003.997	100.24635	72.49	172.73	± 0.20	T5
63	998.4796	985.5344	99.14549	72.49	171.63	± 0.20	SLOPE
64	998.40906	980.6605	99.14768	72.49	171.64	± 0.20	SLOPE
65	998.00119	977.7621	98.47916	72.49	170.97	± 0.20	SLOPE
66	999.05377	970.3482	96.41408	72.49	168.90	± 0.20	SLOPE
67	1000.1499	966.3953	95.7498	72.49	168.24	± 0.20	T3
68	1002.7565	961.5315	95.78337	72.49	168.27	± 0.20	T3
69	1042.6948	960.1245	95.24549	72.49	167.73	± 0.20	T3
70	1050.8585	955.9946	94.87939	72.49	167.37	± 0.20	T3
71	1063.5613	950.1566	94.95173	72.49	167.44	± 0.20	T3
72	1071.9966	946.6091	94.65428	72.49	167.14	± 0.20	T3
73	1076.0996	953.46	95.11172	72.49	167.60	± 0.20	T3
74	1069.2213	945.8508	94.51926	72.49	167.01	± 0.20	SLOPE
75	1077.7962	942.4397	93.78716	72.49	166.28	± 0.20	SLOPE
76	1085.3122	938.7252	93.08459	72.49	165.57	± 0.20	SLOPE
77	1092.9068	934.215	92.24335	72.49	164.73	± 0.20	SLOPE
78	1101.043	929.8495	91.54632	72.49	164.03	± 0.20	T2
79	1108.1328	927.3492	91.49688	72.49	163.99	± 0.20	T2
80	1134.7361	916.4736	91.10077	72.49	163.59	± 0.20	T2
81	1125.4853	871.017	91.48427	72.49	163.97	± 0.20	T2
82	1124.3464	840.5971	92.00304	72.49	164.49	± 0.20	T2
83	1123.0857	829.9551	92.03241	72.49	164.52	± 0.20	T2
84	1102.0476	839.6029	91.82053	72.49	164.31	± 0.20	T2
85	1097.8211	837.0015	91.41	72.49	163.90	± 0.20	T2
86	1091.7764	832.6849	90.51441	72.49	163.00	± 0.20	T2
87	1085.9608	828.4545	90.13133	72.49	162.62	± 0.20	T2
88	1079.8053	824.2515	90.14763	72.49	162.64	± 0.20	T2
89	1062.9902	815.2024	90.9119	72.49	163.40	± 0.20	T2
90	1055.8067	812.8665	91.09506	72.49	163.58	± 0.20	T2
91	1049.1722	813.3412	91.13216	72.49	163.62	± 0.20	T2
92	1007.4193	812.44	91.16254	72.49	163.65	± 0.20	T2
93	994.56802	810.3098	90.76569	72.49	163.25	± 0.20	T2
94	981.36576	807.3572	89.8763	72.49	162.36	± 0.20	T2
95	969.35172	804.8414	90.44417	72.49	162.93	± 0.20	T2
96	957.38519	801.431	90.84199	72.49	163.33	± 0.20	T2
97	944.70035	798.2429	91.19627	72.49	163.68	± 0.20	T2
98	933.2093	794.7103	90.98809	72.49	163.48	± 0.20	T2
99	933.20806	794.7065	90.98793	72.49	163.48	± 0.20	T2
100	921.53879	790.703	90.92395	72.49	163.41	± 0.20	T2

Huntington River Location Tower							
Point Number	Northing (m)	Easting (m)	Measured Elevation (m)	Correction (m)	Final Elevation (m)	Error (m)	Point Description
101	900.32826	782.3677	91.2443	72.49	163.73	± 0.20	T2
102	901.70021	825.6547	91.25678	72.49	163.75	± 0.20	T2
103	846.73467	855.7994	93.48027	72.49	165.97	± 0.20	T2
104	846.76339	855.775	93.4744	72.49	165.96	± 0.20	T2
105	795.84658	860.8219	95.03469	72.49	167.52	± 0.20	T3
Note: These elevations are tied to the Benchmark MAYOAZMK (160.75 m ± 0.05 m) on the bridge north of here via: TOWR Pt 69 = TOM2 Pt 21; TOM2 Pt 3 = Benchmark							

Huntington River Location Audubon 1							
Point Number	Northing (m)	Easting (m)	Measured Elevation (m)	Correction (m)	Final Elevation (m)	Error (m)	Point Description
1	1000.000	1000.000	100.000	71.21	171.21	± 0.20	T3
2	1000.000	1000.000	100.000	71.21	171.21	± 0.20	T3
3	971.703	971.895	102.010	71.21	173.22	± 0.20	T4
4	974.071	974.260	100.415	71.21	171.62	± 0.20	SLOPE
5	984.606	986.198	100.023	71.21	171.23	± 0.20	T3
6	1000.107	992.330	99.833	71.21	171.04	± 0.20	T3
7	1015.869	999.835	99.534	71.21	170.74	± 0.20	T3
8	1024.889	1009.400	99.325	71.21	170.53	± 0.20	T3
9	1029.308	1014.780	99.424	71.21	170.63	± 0.20	T3
10	1031.243	1017.343	98.767	71.21	169.97	± 0.20	SLOPE
11	1034.825	1021.400	97.559	71.21	168.76	± 0.20	T2
12	1045.570	1029.329	97.298	71.21	168.50	± 0.20	T2
13	1057.599	1037.808	97.126	71.21	168.33	± 0.20	T2
14	1070.100	1043.431	96.896	71.21	168.10	± 0.20	T2
15	1081.525	1051.829	96.467	71.21	167.67	± 0.20	T2
16	1097.176	1061.037	96.622	71.21	167.83	± 0.20	T2
17	1112.816	1071.657	96.351	71.21	167.56	± 0.20	T2
18	1130.899	1078.773	95.477	71.21	166.68	± 0.20	T1
19	1145.175	1089.147	95.531	71.21	166.74	± 0.20	T1
20	1164.465	1103.558	95.326	71.21	166.53	± 0.20	T1
21	1183.214	1115.973	95.085	71.21	166.29	± 0.20	T1
22	1205.612	1128.800	94.500	71.21	165.71	± 0.20	T1
23	1225.723	1138.715	94.290	71.21	165.50	± 0.20	T1
24	1245.919	1139.079	94.164	71.21	165.37	± 0.20	T1
25	1283.739	1130.172	94.029	71.21	165.23	± 0.20	T1
26	1289.628	1133.001	93.780	71.21	164.99	± 0.20	T1
27	1295.640	1135.060	93.657	71.21	164.86	± 0.20	T1
28	1300.952	1137.302	93.352	71.21	164.56	± 0.20	SLOPE
29	1305.540	1139.368	93.251	71.21	164.46	± 0.20	SLOPE
30	1309.892	1141.834	92.778	71.21	163.98	± 0.20	RIVER
31	1314.027	1143.948	92.680	71.21	163.89	± 0.20	RIVER
32	1315.982	1144.770	92.635	71.21	163.84	± 0.20	RIVER
33	1315.952	1144.867	92.635	71.21	163.84	± 0.20	RIVER
34	1319.308	1146.472	92.079	71.21	163.28	± 0.20	RIVER
35	1323.387	1148.286	91.970	71.21	163.18	± 0.20	RIVER
36	1327.208	1149.769	91.790	71.21	163.00	± 0.20	RIVER
37	1205.201	1062.557	95.829	71.21	167.03	± 0.20	T2
38	1200.072	1059.520	95.851	71.21	167.06	± 0.20	T2
39	1130.260	976.255	99.196	71.21	170.40	± 0.20	T3
40	1141.004	983.622	99.305	71.21	170.51	± 0.20	T3
41	1145.559	986.016	99.111	71.21	170.32	± 0.20	T3
42	1149.788	986.914	98.371	71.21	169.58	± 0.20	SLOPE
43	1149.784	986.908	98.371	71.21	169.58	± 0.20	SLOPE
44	1164.723	987.923	97.729	71.21	168.93	± 0.20	T2
45	1164.721	987.920	97.729	71.21	168.93	± 0.20	T2
46	1178.634	990.183	97.500	71.21	168.71	± 0.20	T2
47	1190.150	991.824	97.528	71.21	168.73	± 0.20	T2
48	1196.418	994.326	96.963	71.21	168.17	± 0.20	T2
49	1201.834	996.810	96.170	71.21	167.38	± 0.20	T2
50	1206.635	1001.770	95.571	71.21	166.78	± 0.20	T2
51	1207.722	1012.309	95.920	71.21	167.13	± 0.20	T2
52	1205.349	1024.773	95.942	71.21	167.15	± 0.20	T2
53	1204.251	1038.350	95.588	71.21	166.79	± 0.20	SLOPE
54	1101.599	968.075	102.557	71.21	173.76	± 0.20	T4

Huntington River Location Audubon 1							
Point Number	Northing (m)	Easting (m)	Measured Elevation (m)	Correction (m)	Final Elevation (m)	Error (m)	Point Description
55	1194.086	985.621	97.499	71.21	168.70	± 0.20	T2
56	1187.286	997.021	96.938	71.21	168.14	± 0.20	T2
57	1182.372	1001.406	95.988	71.21	167.19	± 0.20	T2
58	1176.613	1006.685	95.482	71.21	166.69	± 0.20	T2
59	1163.492	1019.708	95.571	71.21	166.78	± 0.20	T2
60	1148.711	1034.154	95.308	71.21	166.51	± 0.20	T2
61	1130.591	1051.136	94.490	71.21	165.70	± 0.20	T1
62	1120.450	1062.040	94.591	71.21	165.80	± 0.20	T1
63	1112.345	1069.270	93.923	71.21	165.13	± 0.20	T1
64	1106.060	1075.527	93.755	71.21	164.96	± 0.20	T1
65	1100.205	1080.988	94.345	71.21	165.55	± 0.20	T1
66	1098.912	1079.790	94.343	71.21	165.55	± 0.20	T1
67	1115.515	1094.684	94.064	71.21	165.27	± 0.20	T1
68	1114.168	1098.406	93.537	71.21	164.74	± 0.20	T1
69	1135.320	1088.423	93.507	71.21	164.71	± 0.20	T1
70	1138.469	1084.218	93.592	71.21	164.80	± 0.20	T1
71	1142.262	1078.629	94.132	71.21	165.34	± 0.20	T1
72	1148.683	1069.533	94.431	71.21	165.64	± 0.20	T1
73	1152.501	1064.134	94.916	71.21	166.12	± 0.20	T2
74	1164.746	1044.205	95.206	71.21	166.41	± 0.20	T2
75	1176.325	1022.027	95.315	71.21	166.52	± 0.20	T2
76	1184.013	1007.840	96.071	71.21	167.28	± 0.20	T2
77	1188.269	998.065	97.060	71.21	168.27	± 0.20	T2
78	1191.944	989.601	97.504	71.21	168.71	± 0.20	T2
79	1199.302	1018.997	96.952	71.21	168.16	± 0.20	T2
80	1199.384	1023.071	97.436	71.21	168.64	± 0.20	T2
81	1199.229	1025.607	98.573	71.21	169.78	± 0.20	SLOPE
82	1199.848	1028.394	99.678	71.21	170.88	± 0.20	T3
83	1130.358	1094.940	93.887	71.21	165.09	± 0.20	T1
84	1194.075	985.640	97.292	71.21	168.50	± 0.20	T2
85	1192.245	1142.655	94.458	71.21	165.66	± 0.20	T1
86	1193.399	1119.958	99.992	71.21	171.20	± 0.20	T4
87	1189.817	1115.817	100.380	71.21	171.59	± 0.20	T4
88	1188.508	1119.673	99.949	71.21	171.15	± 0.20	T4
89	1186.971	1117.444	100.335	71.21	171.54	± 0.20	T4
90	1182.539	1117.008	99.838	71.21	171.04	± 0.20	T4
91	1180.346	1120.181	98.496	71.21	169.70	± 0.20	T4
92	1181.382	1122.723	97.310	71.21	168.51	± 0.20	SLOPE
93	1183.777	1125.718	95.771	71.21	166.98	± 0.20	T2
94	1183.734	1128.437	94.879	71.21	166.08	± 0.20	SLOPE
95	1188.039	1132.148	94.736	71.21	165.94	± 0.20	T2
96	1186.330	1136.026	94.522	71.21	165.73	± 0.20	T2
97	1165.718	1123.030	93.206	71.21	164.41	± 0.20	T2
98	1249.353	1212.840	93.563	71.21	164.77	± 0.20	T2
99	1249.339	1212.823	93.563	71.21	164.77	± 0.20	T2
100	1243.990	1207.623	93.703	71.21	164.91	± 0.20	T2
101	1240.479	1202.771	93.798	71.21	165.00	± 0.20	T2
102	1235.576	1197.026	94.009	71.21	165.21	± 0.20	T2
103	1235.564	1197.012	94.009	71.21	165.21	± 0.20	T2
104	1231.647	1192.244	94.071	71.21	165.28	± 0.20	T2
105	1227.338	1186.508	94.113	71.21	165.32	± 0.20	T2
106	1223.587	1180.456	94.156	71.21	165.36	± 0.20	T2

Huntington River Location Audubon 1							
Point Number	Northing (m)	Easting (m)	Measured Elevation (m)	Correction (m)	Final Elevation (m)	Error (m)	Point Description
108	1212.074	1166.835	94.184	71.21	165.39	± 0.20	T2
109	1206.795	1160.254	94.258	71.21	165.46	± 0.20	T2
110	1201.307	1153.368	94.335	71.21	165.54	± 0.20	T2
111	1173.810	1168.173	89.923	71.21	161.13	± 0.20	RIVER
112	1170.707	1174.157	90.442	71.21	161.65	± 0.20	RIVER
113	1168.692	1179.824	90.568	71.21	161.77	± 0.20	RIVER
114	1166.704	1187.777	90.679	71.21	161.88	± 0.20	RIVER
115	1164.556	1196.070	90.639	71.21	161.84	± 0.20	RIVER
116	1160.217	1204.303	90.660	71.21	161.87	± 0.20	RIVER
117	1159.693	1212.662	90.556	71.21	161.76	± 0.20	RIVER
118	1157.487	1225.307	90.375	71.21	161.58	± 0.20	RIVER
119	1147.552	1236.466	90.327	71.21	161.53	± 0.20	RIVER
120	1148.865	1247.938	89.931	71.21	161.14	± 0.20	RIVER
121	1140.783	1257.466	89.975	71.21	161.18	± 0.20	RIVER
122	1139.241	1267.666	88.737	71.21	159.94	± 0.20	RIVER
123	1139.137	1262.046	89.416	71.21	160.62	± 0.20	RIVER
124	1138.074	1272.499	88.780	71.21	159.98	± 0.20	RIVER
125	1135.238	1279.679	89.109	71.21	160.31	± 0.20	RIVER
126	1133.608	1285.922	89.236	71.21	160.44	± 0.20	RIVER
127	1133.100	1292.483	88.790	71.21	159.99	± 0.20	RIVER
128	1132.286	1299.681	88.788	71.21	159.99	± 0.20	RIVER
129	1132.096	1305.500	88.775	71.21	159.98	± 0.20	RIVER
130	1129.583	1310.575	89.369	71.21	160.57	± 0.20	RIVER
131	1129.182	1321.026	89.063	71.21	160.27	± 0.20	RIVER
132	1127.971	1327.917	88.585	71.21	159.79	± 0.20	RIVER
133	1127.946	1343.825	88.415	71.21	159.62	± 0.20	RIVER
134	1120.992	1350.207	88.387	71.21	159.59	± 0.20	RIVER
135	1123.721	1364.647	88.543	71.21	159.75	± 0.20	RIVER
136	1122.439	1368.199	89.140	71.21	160.35	± 0.20	RIVER
137	1121.438	1370.944	89.868	71.21	161.07	± 0.20	RIVER
138	1121.444	1370.905	89.869	71.21	161.07	± 0.20	RIVER
139	1120.800	1376.196	91.645	71.21	162.85	± 0.20	T1
140	1117.796	1377.759	91.427	71.21	162.63	± 0.20	T1
141	1117.328	1377.890	91.334	71.21	162.54	± 0.20	T1
142	1115.127	1380.665	91.389	71.21	162.59	± 0.20	T1
143	1113.497	1382.361	91.302	71.21	162.51	± 0.20	T1
144	1111.823	1382.391	90.694	71.21	161.90	± 0.20	RIVER
145	1114.859	1374.291	90.076	71.21	161.28	± 0.20	RIVER
146	1117.115	1370.862	89.431	71.21	160.64	± 0.20	RIVER
147	1132.884	1297.093	88.724	71.21	159.93	± 0.20	RIVER
148	1130.731	1296.633	89.597	71.21	160.80	± 0.20	RIVER
149	1129.868	1295.355	90.406	71.21	161.61	± 0.20	RIVER
150	1129.886	1295.312	90.407	71.21	161.61	± 0.20	RIVER
151	1128.912	1294.884	91.024	71.21	162.23	± 0.20	SLOPE
152	1127.671	1295.697	92.134	71.21	163.34	± 0.20	SLOPE
153	1126.934	1295.753	93.025	71.21	164.23	± 0.20	T1
154	1126.169	1294.740	93.252	71.21	164.46	± 0.20	T1
155	1123.452	1298.169	93.328	71.21	164.53	± 0.20	T1
156	1192.750	1184.957	92.289	71.21	163.49	± 0.20	T1
157	1194.925	1180.689	92.921	71.21	164.13	± 0.20	T1

Huntington River Location Audubon 1							
Point Number	Northing (m)	Easting (m)	Measured Elevation (m)	Correction (m)	Final Elevation (m)	Error (m)	Point Description
158	1196.090	1178.059	93.386	71.21	164.59	± 0.20	T1
159	1196.088	1178.063	93.386	71.21	164.59	± 0.20	T1
160	1196.488	1174.152	94.242	71.21	165.45	± 0.20	T1
161	1104.149	1325.742	91.993	71.21	163.20	± 0.20	SLOPE
162	1108.970	1319.783	92.296	71.21	163.50	± 0.20	SLOPE
163	1111.242	1313.815	92.153	71.21	163.36	± 0.20	SLOPE
164	1112.865	1308.868	92.830	71.21	164.04	± 0.20	T2
165	1115.655	1304.578	93.361	71.21	164.57	± 0.20	T2
166	1115.668	1304.567	93.361	71.21	164.57	± 0.20	T2
167	1111.786	1296.452	93.139	71.21	164.34	± 0.20	T2
168	1103.891	1285.509	93.007	71.21	164.21	± 0.20	T2
169	1091.808	1272.743	92.705	71.21	163.91	± 0.20	T2
170	1082.260	1260.258	92.871	71.21	164.08	± 0.20	T2
171	1078.273	1256.814	93.380	71.21	164.59	± 0.20	T2
172	1072.504	1252.491	93.862	71.21	165.07	± 0.20	T2
173	1064.362	1243.923	93.824	71.21	165.03	± 0.20	T2
174	1055.649	1241.941	93.821	71.21	165.03	± 0.20	T2
175	1041.830	1237.973	93.628	71.21	164.83	± 0.20	T2
176	1028.897	1235.168	93.491	71.21	164.70	± 0.20	T2
177	1020.457	1233.001	94.247	71.21	165.45	± 0.20	T2
178	1017.160	1232.240	95.366	71.21	166.57	± 0.20	T2
179	1013.483	1230.992	96.971	71.21	168.18	± 0.20	T3
180	1010.714	1228.423	96.812	71.21	168.02	± 0.20	T3
181	1015.458	1221.098	95.956	71.21	167.16	± 0.20	T3
182	1019.012	1219.411	94.581	71.21	165.79	± 0.20	T2
183	1023.141	1216.373	93.714	71.21	164.92	± 0.20	T2
184	1024.930	1207.471	93.770	71.21	164.97	± 0.20	T2
185	1024.891	1207.436	93.770	71.21	164.98	± 0.20	T2
186	1013.461	1181.658	93.600	71.21	164.81	± 0.20	T2
187	1008.195	1158.066	93.847	71.21	165.05	± 0.20	T2
188	978.729	1133.118	93.972	71.21	165.18	± 0.20	T2
189	994.672	1190.672	96.732	71.21	167.94	± 0.20	T3
190	995.140	1211.784	96.658	71.21	167.86	± 0.20	T3
191	993.099	1221.784	96.643	71.21	167.85	± 0.20	T3
192	979.734	1243.993	96.441	71.21	167.65	± 0.20	SLOPE
193	977.954	1248.578	95.724	71.21	166.93	± 0.20	T3
194	976.701	1253.683	94.075	71.21	165.28	± 0.20	T2
195	975.021	1261.580	92.509	71.21	163.71	± 0.20	T2
196	987.197	1268.826	92.585	71.21	163.79	± 0.20	T2
197	1010.833	1277.296	93.087	71.21	164.29	± 0.20	T2
198	1030.332	1281.812	92.977	71.21	164.18	± 0.20	T2
199	1043.793	1285.156	92.465	71.21	163.67	± 0.20	T2
200	1034.616	1295.579	91.639	71.21	162.84	± 0.20	T1
201	1039.804	1308.229	91.437	71.21	162.64	± 0.20	T1
202	1049.313	1312.800	91.547	71.21	162.75	± 0.20	T1
203	1062.864	1311.062	91.768	71.21	162.97	± 0.20	T1
204	1075.114	1309.515	91.370	71.21	162.58	± 0.20	T1
205	1083.159	1305.466	91.734	71.21	162.94	± 0.20	T1
206	1096.161	1294.393	92.976	71.21	164.18	± 0.20	T2
207	1087.536	1322.717	91.776	71.21	162.98	± 0.20	T1

Huntington River Location Audubon 1							
Point Number	Northing (m)	Easting (m)	Measured Elevation (m)	Correction (m)	Final Elevation (m)	Error (m)	Point Description
208	1092.432	1317.030	91.634	71.21	162.84	\pm 0.20	T1
209	987.764	1219.644	96.357	71.21	167.56	\pm 0.20	SLOPE
210	951.109	1255.247	94.758	71.21	165.96	\pm 0.20	T2

Note: These elevations are tied to the Benchmark MAYOAZMK (160.75 m \pm 0.05 m) on the bridge north of here via: AUD1 Pt 210 = TOWR Pt 104; TOWR Pt 69 = TOM2 Pt 21; TOM2 Pt 3 = Benchmark

Huntington River Location Audubon 2							
Point Number	Northing (m)	Easting (m)	Measured Elevation (m)	Correction (m)	Final Elevation (m)	Error (m)	Point Description
1	1000.000	1000.000	100.000	75.23	175.23	± 0.20	T5
2	1000.000	1000.000	100.000	75.23	175.23	± 0.20	T5
3	1012.956	1000.177	100.144	75.23	175.37	± 0.20	T5
4	1016.731	1000.175	98.934	75.23	174.17	± 0.20	SLOPE
5	1053.825	1009.217	95.975	75.23	171.21	± 0.20	T3
6	951.842	996.387	101.142	75.23	176.37	± 0.20	T5
7	947.814	999.576	101.361	75.23	176.59	± 0.20	T5
8	960.195	996.907	100.187	75.23	175.42	± 0.20	T5
9	963.085	996.531	99.902	75.23	175.13	± 0.20	T5

Note: These elevations are tied to the Benchmark MAYOAZMK (160.75 m ± 0.05 m on the bridge north of here via: AUD2 Pt 5 = AUD1 Pt 1; AUD1 Pt 210 = TOWR Pt 104; TOWR Pt 69 = TOM2 Pt 21; TOM2 Pt 3 = Benchmark

Huntington River Location Audubon 3							
Point Number	Northing (m)	Easting (m)	Measured Elevation (m)	Correction (m)	Final Elevation (m)	Error (m)	Point Description
1	1000.000	1000.000	100.000	75.23	175.23	± 0.20	T5
2	1000.000	1000.000	100.000	75.23	175.23	± 0.20	T5
3	1033.904	931.349	98.272	75.23	173.50	± 0.20	T4
4	1023.067	913.744	98.833	75.23	174.06	± 0.20	SLOPE
5	1015.808	891.714	99.085	75.23	174.32	± 0.20	T5
6	1012.183	850.526	98.426	75.23	173.66	± 0.20	T4
7	1018.135	799.870	98.168	75.23	173.40	± 0.20	T4
8	1018.134	799.877	98.173	75.23	173.40	± 0.20	T4
9	999.535	786.844	98.207	75.23	173.44	± 0.20	T4
10	987.916	817.466	98.612	75.23	173.84	± 0.20	T4
11	978.514	853.761	99.244	75.23	174.47	± 0.20	T5
12	978.514	853.764	99.244	75.23	174.47	± 0.20	T5
13	975.837	885.790	98.545	75.23	173.78	± 0.20	T4
14	975.836	885.786	98.545	75.23	173.78	± 0.20	T4
15	995.162	943.966	98.096	75.23	173.33	± 0.20	T4
16	990.827	945.807	98.489	75.23	173.72	± 0.20	T4
17	986.650	947.312	99.104	75.23	174.33	± 0.20	T5
18	978.291	948.021	99.720	75.23	174.95	± 0.20	T5
19	978.311	948.033	99.727	75.23	174.96	± 0.20	T5
20	945.486	936.175	99.630	75.23	174.86	± 0.20	T5
21	925.367	909.828	99.606	75.23	174.84	± 0.20	T5
22	920.327	896.272	99.575	75.23	174.81	± 0.20	T5
23	914.526	888.603	99.282	75.23	174.51	± 0.20	T5
24	910.098	881.242	99.144	75.23	174.38	± 0.20	T5
25	903.001	864.276	99.600	75.23	174.83	± 0.20	T5
26	898.031	852.989	100.546	75.23	175.78	± 0.20	FANTOE
27	875.734	834.427	109.008	75.23	184.24	± 0.20	APEX
28	900.252	866.211	99.761	75.23	174.99	± 0.20	T5
29	901.531	896.568	99.045	75.23	174.28	± 0.20	T5
30	909.650	924.053	98.764	75.23	173.99	± 0.20	SLOPE
31	921.823	950.600	99.171	75.23	174.40	± 0.20	T5
32	953.622	958.099	99.826	75.23	175.06	± 0.20	T5
33	989.847	1019.937	99.909	75.23	175.14	± 0.20	T5
34	980.888	1042.728	100.020	75.23	175.25	± 0.20	T5
35	973.487	1054.320	100.762	75.23	175.99	± 0.20	T5
36	973.492	1054.299	100.763	75.23	175.99	± 0.20	T5
37	973.439	1049.995	100.797	75.23	176.03	± 0.20	T5
38	970.311	1050.954	101.277	75.23	176.51	± 0.20	SLOPE
39	967.569	1051.180	101.786	75.23	177.02	± 0.20	SLOPE
40	963.958	1046.858	101.947	75.23	177.18	± 0.20	SLOPE
41	953.721	1049.370	102.119	75.23	177.35	± 0.20	SLOPE
42	965.020	1052.958	101.529	75.23	176.76	± 0.20	SLOPE
43	963.289	1056.284	99.364	75.23	174.60	± 0.20	T5
44	960.184	1059.013	97.325	75.23	172.56	± 0.20	SLOPE
45	955.186	1061.223	95.757	75.23	170.99	± 0.20	SLOPE
46	956.695	1064.554	94.680	75.23	169.91	± 0.20	T2
47	966.506	1066.411	94.548	75.23	169.78	± 0.20	T2
48	979.179	1068.948	94.916	75.23	170.15	± 0.20	T2
49	988.923	1079.949	93.488	75.23	168.72	± 0.20	T2

Note: These elevations are tied to the Benchmark MAYOAZMK (160.75 m ± 0.05 m on the bridge)

Huntington River Location Audubon 3							
Point Number	Northing (m)	Easting (m)	Measured Elevation (m)	Correction (m)	Final Elevation (m)	Error (m)	Point Description
north of here via: AUD3 Pt 1 = AUD2 Pt 1; AUD2 Pt 5 = AUD1 Pt 1; AUD1 Pt 210 = TOWR Pt 104; TOWR Pt 69 = TOM2 Pt 21; TOM2 Pt 3 = Benchmark							

1	949.942	1146.000	949.942	0.000	949.942	0.000	
2	911.183	1146.000	911.183	0.000	911.183	0.000	
3	862.764	1146.000	862.764	0.000	862.764	0.000	
4	816.194	1146.000	816.194	0.000	816.194	0.000	
5	745.604	1146.000	745.604	0.000	745.604	0.000	
6	681.937	1146.000	681.937	0.000	681.937	0.000	
7	624.803	1146.000	624.803	0.000	624.803	0.000	
8	618.75	1146.000	618.75	0.000	618.75	0.000	
9	624.512	1146.000	624.512	0.000	624.512	0.000	
10	676.614	1146.000	676.614	0.000	676.614	0.000	
11	619.198	1146.000	619.198	0.000	619.198	0.000	
12	624.198	1146.000	624.198	0.000	624.198	0.000	
13	624.198	1146.000	624.198	0.000	624.198	0.000	
14	624.198	1146.000	624.198	0.000	624.198	0.000	
15	624.198	1146.000	624.198	0.000	624.198	0.000	
16	624.198	1146.000	624.198	0.000	624.198	0.000	
17	624.198	1146.000	624.198	0.000	624.198	0.000	
18	700.000	1146.000	700.000	0.000	700.000	0.000	
19	876.404	1146.000	876.404	0.000	876.404	0.000	
20	906.388	1146.000	906.388	0.000	906.388	0.000	
21	906.388	1146.000	906.388	0.000	906.388	0.000	
22	986.24	1146.000	986.24	0.000	986.24	0.000	
23	972.814	1146.000	972.814	0.000	972.814	0.000	
24	1013.014	1146.000	1013.014	0.000	1013.014	0.000	
25	1013.014	1146.000	1013.014	0.000	1013.014	0.000	
26	1042.814	1146.000	1042.814	0.000	1042.814	0.000	
27	1053.847	1146.000	1053.847	0.000	1053.847	0.000	
28	1080.0	1146.000	1080.0	0.000	1080.0	0.000	
29	1120.75	1146.000	1120.75	0.000	1120.75	0.000	
30	1051.277	1146.000	1051.277	0.000	1051.277	0.000	
31	1105.004	1146.000	1105.004	0.000	1105.004	0.000	
32	1105.004	1146.000	1105.004	0.000	1105.004	0.000	
33	1105.004	1146.000	1105.004	0.000	1105.004	0.000	
34	1147.004	1146.000	1147.004	0.000	1147.004	0.000	
35	1213.22	1146.000	1213.22	0.000	1213.22	0.000	
36	1213.22	1146.000	1213.22	0.000	1213.22	0.000	
37	1053.847	1146.000	1053.847	0.000	1053.847	0.000	
38	1053.847	1146.000	1053.847	0.000	1053.847	0.000	
39	1076.24	1146.000	1076.24	0.000	1076.24	0.000	
40	1076.24	1146.000	1076.24	0.000	1076.24	0.000	
41	1076.24	1146.000	1076.24	0.000	1076.24	0.000	
42	1076.24	1146.000	1076.24	0.000	1076.24	0.000	

Note: Elevations in feet above sea level.

Huntington River Location 2							
Point Number	Northing (m)	Easting (m)	Measured Elevation (m)	Correction (m)	Final Elevation (m)	Error (m)	Point Description
1	1000.000	1000.000	100.000	106.48	206.48	± 1.0	T9
2	1100.000	1000.000	100.000	106.48	206.48	± 1.0	T9
3	959.993	1190.534	113.026	106.48	219.51	± 1.0	T10
4	911.151	1191.385	113.398	106.48	219.88	± 1.0	T10
5	862.555	1189.427	112.846	106.48	219.33	± 1.0	T10
6	815.194	1193.614	112.622	106.48	219.11	± 1.0	T10
7	745.880	1191.880	111.352	106.48	217.84	± 1.0	T10
8	661.911	1183.334	108.970	106.48	215.45	± 1.0	T10
9	624.808	1127.198	100.327	106.48	206.81	± 1.0	T9
10	618.781	1062.921	96.609	106.48	203.09	± 1.0	T9
11	624.012	1037.934	94.778	106.48	201.26	± 1.0	T9
12	675.617	1014.967	88.156	106.48	194.64	± 1.0	T7
13	697.509	983.191	86.522	106.48	193.01	± 1.0	T7
14	994.129	1031.202	100.166	106.48	206.65	± 1.0	T9
15	976.887	983.308	99.437	106.48	205.92	± 1.0	T9
16	965.530	820.908	86.251	106.48	192.74	± 1.0	T7
17	968.881	788.411	84.722	106.48	191.21	± 1.0	T7
18	1000.000	1000.002	100.073	106.48	206.56	± 1.0	T9
19	976.436	639.123	74.925	106.48	181.41	± 1.0	T4
20	968.882	788.399	84.750	106.48	191.23	± 1.0	T7
21	963.161	732.627	77.673	106.48	184.16	± 1.0	T5
22	968.261	710.268	76.449	106.48	182.93	± 1.0	T5
23	973.506	697.651	75.058	106.48	181.54	± 1.0	T4
24	1010.266	633.686	74.528	106.48	181.01	± 1.0	T4
25	1013.062	627.024	73.883	106.48	180.37	± 1.0	T3
26	1016.180	619.073	73.722	106.48	180.21	± 1.0	T3
27	1042.686	615.659	72.730	106.48	179.21	± 1.0	T3
28	1053.845	607.520	72.614	106.48	179.10	± 1.0	T3
29	1060.103	591.974	70.596	106.48	177.08	± 1.0	T2
30	1120.808	449.665	70.605	106.48	177.09	± 1.0	T2
31	1126.648	443.344	69.433	106.48	175.92	± 1.0	T2
32	1089.588	528.209	71.483	106.48	177.97	± 1.0	T2
33	1100.029	514.181	70.587	106.48	177.07	± 1.0	T2
34	1122.849	379.400	69.128	106.48	175.61	± 1.0	T1
35	1146.739	256.168	70.292	106.48	176.78	± 1.0	T1
36	1211.297	298.814	69.472	106.48	175.96	± 1.0	T1
37	1217.955	305.342	70.370	106.48	176.85	± 1.0	T1
38	1035.781	299.481	70.896	106.48	177.38	± 1.0	T1
39	1023.032	287.827	69.856	106.48	176.34	± 1.0	T1
40	1016.497	278.979	70.269	106.48	176.75	± 1.0	T1
41	1016.734	273.299	69.214	106.48	175.70	± 1.0	T1
42	1020.542	253.180	68.822	106.48	175.31	± 1.0	RIVER

Note: Elevations at this site are tied to a contour line, elevation 720.00 ft or 219.51 m via Pt 3.

Huntington River Location Sarah-Al							
Point Number	Northing (m)	Easting (m)	Measured Elevation (m)	Correction (m)	Final Elevation (m)	Error (m)	Point Description
1	1000.000	1000.000	100.000	124.61	224.61	± 0.20	T9
2	960.121	908.296	100.000	124.61	224.61	± 0.20	T9
3	851.394	658.275	80.326	124.61	204.94	± 0.20	T0
4	864.563	672.577	81.715	124.61	206.32	± 0.20	T1
5	872.246	691.427	81.499	124.61	206.11	± 0.20	T1
6	877.526	705.352	81.516	124.61	206.13	± 0.20	T1
7	882.998	718.439	81.455	124.61	206.06	± 0.20	T1
8	884.229	721.211	81.618	124.61	206.23	± 0.20	T1
9	884.235	721.208	81.618	124.61	206.23	± 0.20	T1
10	885.667	725.408	81.677	124.61	206.29	± 0.20	T1
11	890.413	737.327	81.518	124.61	206.13	± 0.20	T1
12	893.077	744.913	81.548	124.61	206.16	± 0.20	T1
13	893.482	749.042	81.799	124.61	206.41	± 0.20	SLOPE
14	894.301	752.889	81.841	124.61	206.45	± 0.20	SLOPE
15	896.664	760.343	81.985	124.61	206.59	± 0.20	T2
16	898.295	765.364	82.149	124.61	206.76	± 0.20	T2
17	899.208	767.470	82.309	124.61	206.92	± 0.20	T2
18	902.174	777.322	82.192	124.61	206.80	± 0.20	T2
19	904.132	783.634	82.212	124.61	206.82	± 0.20	T2
20	905.552	787.396	82.513	124.61	207.12	± 0.20	T2
21	906.712	791.506	82.876	124.61	207.48	± 0.20	SLOPE
22	911.074	809.671	83.179	124.61	207.79	± 0.20	SLOPE
23	915.844	822.045	83.787	124.61	208.40	± 0.20	T5
24	923.369	834.986	83.896	124.61	208.50	± 0.20	T5
25	933.701	851.478	84.044	124.61	208.65	± 0.20	T5
26	940.415	865.106	84.374	124.61	208.98	± 0.20	T5
27	943.037	870.567	85.217	124.61	209.83	± 0.20	ROAD
28	946.223	876.715	85.349	124.61	209.96	± 0.20	ROAD
29	928.810	878.011	85.051	124.61	209.66	± 0.20	ROAD
30	923.537	892.411	85.188	124.61	209.80	± 0.20	ROAD
31	967.124	866.628	84.660	124.61	209.27	± 0.20	ROAD
32	948.133	879.695	84.520	124.61	209.13	± 0.20	T5
33	953.637	892.890	84.295	124.61	208.90	± 0.20	T5
34	971.680	873.001	83.982	124.61	208.59	± 0.20	T5
35	1034.740	826.296	87.013	124.61	211.62	± 0.20	SLOPE
36	1074.224	803.022	86.926	124.61	211.53	± 0.20	ROAD
37	1067.223	822.956	87.394	124.61	212.00	± 0.20	T6
38	1058.068	847.247	88.501	124.61	213.11	± 0.20	SLOPE
39	1058.069	847.244	88.501	124.61	213.11	± 0.20	SLOPE
40	1044.498	879.302	90.124	124.61	214.73	± 0.20	SLOPE
41	1039.153	894.029	90.919	124.61	215.53	± 0.20	SLOPE
42	1034.225	907.257	92.193	124.61	216.80	± 0.20	SLOPE
43	1030.131	918.991	93.217	124.61	217.83	± 0.20	SLOPE
44	1026.194	931.259	93.920	124.61	218.53	± 0.20	SLOPE
45	1026.195	931.253	93.917	124.61	218.53	± 0.20	SLOPE
46	1022.723	941.240	94.720	124.61	219.33	± 0.20	SLOPE
47	1019.375	951.037	95.955	124.61	220.56	± 0.20	SLOPE
48	1015.717	961.480	96.920	124.61	221.53	± 0.20	SLOPE
49	1011.804	971.365	97.732	124.61	222.34	± 0.20	SLOPE
50	1007.727	981.035	98.903	124.61	223.51	± 0.20	SLOPE

Huntington River Location Sarah-Al							
Point Number	Northing (m)	Easting (m)	Measured Elevation (m)	Correction (m)	Final Elevation (m)	Error (m)	Point Description
51	1003.780	991.661	99.647	124.61	224.26	± 0.20	T9
52	1003.917	1011.387	100.286	124.61	224.90	± 0.20	T9
53	1006.995	1027.695	100.606	124.61	225.22	± 0.20	T9
54	1010.435	1043.455	100.953	124.61	225.56	± 0.20	T9
55	1012.947	1061.380	101.608	124.61	226.22	± 0.20	T9
56	1012.847	1061.386	101.594	124.61	226.20	± 0.20	T9
57	1017.017	1080.907	102.356	124.61	226.96	± 0.20	T9
58	1022.629	1101.607	102.630	124.61	227.24	± 0.20	T9
59	1029.723	1122.872	102.777	124.61	227.39	± 0.20	T9
60	1029.722	1122.871	102.777	124.61	227.39	± 0.20	T9
61	1040.739	1166.695	103.740	124.61	228.35	± 0.20	T9
62	1046.995	1187.845	104.127	124.61	228.74	± 0.20	T9
63	1053.364	1210.315	104.603	124.61	229.21	± 0.20	T9
64	1058.357	1233.359	105.015	124.61	229.62	± 0.20	T9
65	1062.104	1255.678	105.384	124.61	229.99	± 0.20	T9
66	1065.185	1279.197	106.047	124.61	230.66	± 0.20	T9
67	1070.791	1300.638	106.649	124.61	231.26	± 0.20	T9
68	1078.570	1323.878	107.038	124.61	231.65	± 0.20	T9
69	1063.196	1337.142	107.385	124.61	231.99	± 0.20	T9
70	1208.561	419.064	81.651	124.61	206.26	± 0.20	T1
71	1208.547	419.104	81.652	124.61	206.26	± 0.20	T1
72	1208.548	419.103	81.652	124.61	206.26	± 0.20	T1
73	1209.256	419.344	81.652	124.61	206.26	± 0.20	T1
74	1198.383	375.038	81.160	124.61	205.77	± 0.20	TERRACE1
75	1241.860	1031.335	88.072	124.61	212.68	± 0.20	SLOPE
76	1233.541	1010.945	87.679	124.61	212.29	± 0.20	T6
77	1226.669	989.096	87.373	124.61	211.98	± 0.20	T6
78	1220.594	968.998	87.519	124.61	212.13	± 0.20	T6
79	1208.742	949.173	87.398	124.61	212.01	± 0.20	T6
80	1192.615	933.970	87.462	124.61	212.07	± 0.20	T6
81	1177.764	922.301	87.964	124.61	212.57	± 0.20	SLOPE
82	1162.581	912.881	89.046	124.61	213.66	± 0.20	T7
83	1147.490	903.847	90.311	124.61	214.92	± 0.20	SLOPE
84	1125.086	913.910	91.259	124.61	215.87	± 0.20	T8
85	1114.834	920.629	91.486	124.61	216.09	± 0.20	T8
86	1107.460	912.726	91.375	124.61	215.98	± 0.20	T8
87	1084.044	886.144	89.922	124.61	214.53	± 0.20	T7
88	1071.597	871.863	89.457	124.61	214.07	± 0.20	T7
89	1058.422	856.702	88.885	124.61	213.49	± 0.20	T7
90	1045.360	840.852	88.299	124.61	212.91	± 0.20	SLOPE
91	1034.843	826.309	87.069	124.61	211.68	± 0.20	SLOPE
92	1033.624	854.324	88.919	124.61	213.53	± 0.20	T7
93	1022.650	867.085	89.237	124.61	213.85	± 0.20	T7
94	1037.406	869.118	89.509	124.61	214.12	± 0.20	T7
95	1046.270	874.542	89.802	124.61	214.41	± 0.20	T7
96	1030.803	826.512	86.983	124.61	211.59	± 0.20	ROAD
97	1026.817	828.859	86.988	124.61	211.60	± 0.20	ROAD
98	1024.584	821.309	86.917	124.61	211.53	± 0.20	ROAD
99	1039.085	853.308	89.159	124.61	213.77	± 0.20	T7
100	1042.003	852.017	89.135	124.61	213.74	± 0.20	T7

Huntington River Location Sarah-Al							
Point Number	Northing (m)	Easting (m)	Measured Elevation (m)	Correction (m)	Final Elevation (m)	Error (m)	Point Description
101	1059.170	889.360	90.480	124.61	215.09	± 0.20	SLOPE
102	1056.515	891.030	90.621	124.61	215.23	± 0.20	SLOPE
103	1091.768	945.578	91.960	124.61	216.57	± 0.20	T8
104	1089.146	947.274	92.051	124.61	216.66	± 0.20	T8
105	958.674	1040.912	99.598	124.61	224.21	± 0.20	T9
106	1000.004	999.996	99.986	124.61	224.60	± 0.20	T9
107	792.739	950.624	87.138	124.61	211.75	± 0.20	ROAD
108	776.226	960.019	87.207	124.61	211.82	± 0.20	ROAD
109	803.199	946.732	86.901	124.61	211.51	± 0.20	ROAD
110	806.972	952.865	86.931	124.61	211.54	± 0.20	ROAD
111	818.207	953.134	86.049	124.61	210.66	± 0.20	TERRACE2
112	832.261	967.890	85.963	124.61	210.57	± 0.20	TERRACE2
113	843.651	978.698	86.193	124.61	210.80	± 0.20	TERRACE2
114	854.548	990.718	86.053	124.61	210.66	± 0.20	TERRACE2
115	865.939	1001.953	86.306	124.61	210.92	± 0.20	TERRACE2
116	872.965	1016.056	86.471	124.61	211.08	± 0.20	TERRACE2
117	887.853	1021.293	86.708	124.61	211.32	± 0.20	TERRACE2
118	894.243	1024.708	86.791	124.61	211.40	± 0.20	TERRACE2
119	899.541	1027.246	87.191	124.61	211.80	± 0.20	SLOPE
120	904.610	1030.192	88.312	124.61	212.92	± 0.20	SLOPE
121	910.144	1031.231	88.997	124.61	213.61	± 0.20	SLOPE
122	915.707	1032.443	89.332	124.61	213.94	± 0.20	TERRACE3
123	915.521	1034.963	89.539	124.61	214.15	± 0.20	TERRACE3
124	912.054	1037.155	89.445	124.61	214.05	± 0.20	TERRACE3
125	874.568	1034.262	86.937	124.61	211.55	± 0.20	TERRACE2
126	863.789	1082.059	85.684	124.61	210.29	± 0.20	RIVER
127	869.177	1079.599	85.712	124.61	210.32	± 0.20	RIVER
128	872.378	1078.044	87.054	124.61	211.66	± 0.20	TERRACE1
129	880.719	1074.410	86.886	124.61	211.50	± 0.20	TERRACE1
130	886.769	1072.573	86.644	124.61	211.25	± 0.20	TERRACE1
131	889.170	1071.677	86.991	124.61	211.60	± 0.20	SLOPE
132	892.441	1070.279	86.718	124.61	211.33	± 0.20	TERRACE1A
133	894.185	1069.242	87.189	124.61	211.80	± 0.20	SLOPE
134	899.660	1067.162	87.316	124.61	211.93	± 0.20	TERRACE1B
135	906.665	1063.469	87.550	124.61	212.16	± 0.20	TERRACE1B
136	914.043	1064.280	87.587	124.61	212.20	± 0.20	TERRACE1B
137	917.352	1062.997	87.825	124.61	212.43	± 0.20	SLOPE
138	920.189	1062.065	87.770	124.61	212.38	± 0.20	SLOPE
139	933.743	1063.390	87.159	124.61	211.77	± 0.20	T2
140	926.419	1059.058	87.332	124.61	211.94	± 0.20	T2
141	904.392	1134.333	87.431	124.61	212.04	± 0.20	TERRACE1
142	905.671	1132.005	88.082	124.61	212.69	± 0.20	TERRACE1
143	909.356	1126.711	87.929	124.61	212.54	± 0.20	TERRACE1
144	913.831	1120.427	87.861	124.61	212.47	± 0.20	TERRACE1
145	914.447	1119.287	88.236	124.61	212.85	± 0.20	SLOPE
146	915.458	1117.885	88.688	124.61	213.30	± 0.20	SLOPE
147	921.198	1111.081	88.599	124.61	213.21	± 0.20	T2
148	923.005	1100.968	88.589	124.61	213.20	± 0.20	T2
149	931.092	1098.405	88.114	124.61	212.72	± 0.20	T2
150	935.075	1112.031	88.162	124.61	212.77	± 0.20	T2

Huntington River Location Sarah-Al							
Point Number	Northing (m)	Easting (m)	Measured Elevation (m)	Correction (m)	Final Elevation (m)	Error (m)	Point Description
151	944.556	1112.879	87.804	124.61	212.41	± 0.20	T2
152	947.082	1110.951	88.280	124.61	212.89	± 0.20	SLOPE
153	948.890	1110.627	88.663	124.61	213.27	± 0.20	SLOPE
154	955.398	1110.276	88.784	124.61	213.39	± 0.20	T3
155	956.170	1102.841	88.722	124.61	213.33	± 0.20	T3
156	954.193	1123.642	89.081	124.61	213.69	± 0.20	T3
157	954.171	1123.645	89.080	124.61	213.69	± 0.20	T3
158	954.739	1135.349	89.237	124.61	213.85	± 0.20	T3
159	953.803	1135.216	89.206	124.61	213.81	± 0.20	T3
160	951.964	1134.899	88.330	124.61	212.94	± 0.20	T2
161	944.794	1137.327	88.320	124.61	212.93	± 0.20	T2
162	946.434	1155.467	88.550	124.61	213.16	± 0.20	T2
163	945.704	1177.838	88.992	124.61	213.60	± 0.20	T2
164	973.822	1329.424	91.907	124.61	216.52	± 0.20	T2
165	974.527	1373.140	93.115	124.61	217.72	± 0.20	T2
166	963.151	1408.050	93.537	124.61	218.15	± 0.20	T2
167	949.944	1408.701	93.721	124.61	218.33	± 0.20	T2
168	946.065	1408.897	93.778	124.61	218.39	± 0.20	T2
169	948.551	1440.840	94.187	124.61	218.80	± 0.20	T2
170	945.318	1466.570	94.870	124.61	219.48	± 0.20	T2
171	943.557	1500.305	95.944	124.61	220.55	± 0.20	T2
172	950.552	1517.463	96.121	124.61	220.73	± 0.20	T2
173	950.618	1537.625	96.515	124.61	221.12	± 0.20	T2
174	952.416	1544.086	97.281	124.61	221.89	± 0.20	T3

Note: These elevations are tied to the Benchmark BAMBI (206.26 m ± 0.05 m) on the bridge
north of here via: SAAL Pt 70 = Benchmark

Huntington River Location 4-Landslide							
Point Number	Northing (m)	Easting (m)	Measured Elevation (m)	Correction (m)	Final Elevation (m)	Error (m)	Point Description
1	1000.000	1000.000	100.000	126.60	226.60	± 1.0	T7
2	1100.000	1000.000	100.000	126.60	226.60	± 1.0	T7
3	937.016	1185.780	105.451	126.60	232.05	± 1.0	T9
4	950.141	1130.416	104.483	126.60	231.08	± 1.0	T9
5	995.165	1027.709	101.265	126.60	227.87	± 1.0	T8
6	995.166	1027.707	101.265	126.60	227.86	± 1.0	T8
7	995.671	1007.795	100.423	126.60	227.02	± 1.0	T8
8	1004.824	977.755	99.332	126.60	225.93	± 1.0	T7
9	923.716	882.409	94.527	126.60	221.13	± 1.0	T6
10	835.742	679.816	94.260	126.60	220.86	± 1.0	T6
11	898.977	635.312	92.293	126.60	218.89	± 1.0	T2
12	876.338	697.016	91.637	126.60	218.24	± 1.0	T2
13	925.929	629.873	90.628	126.60	217.23	± 1.0	T1
14	1087.518	614.008	90.020	126.60	216.62	± 1.0	T1
15	1196.146	490.130	111.205	126.60	237.80	± 1.0	T10
16	1179.661	452.127	113.308	126.60	239.91	± 1.0	T10
17	1194.474	720.535	87.697	126.60	214.30	± 1.0	RIVER
18	1205.632	721.596	88.451	126.60	215.05	± 1.0	RIVER
19	1178.054	742.404	88.396	126.60	215.00	± 1.0	RIVER
20	1147.153	785.468	89.223	126.60	215.82	± 1.0	RIVER

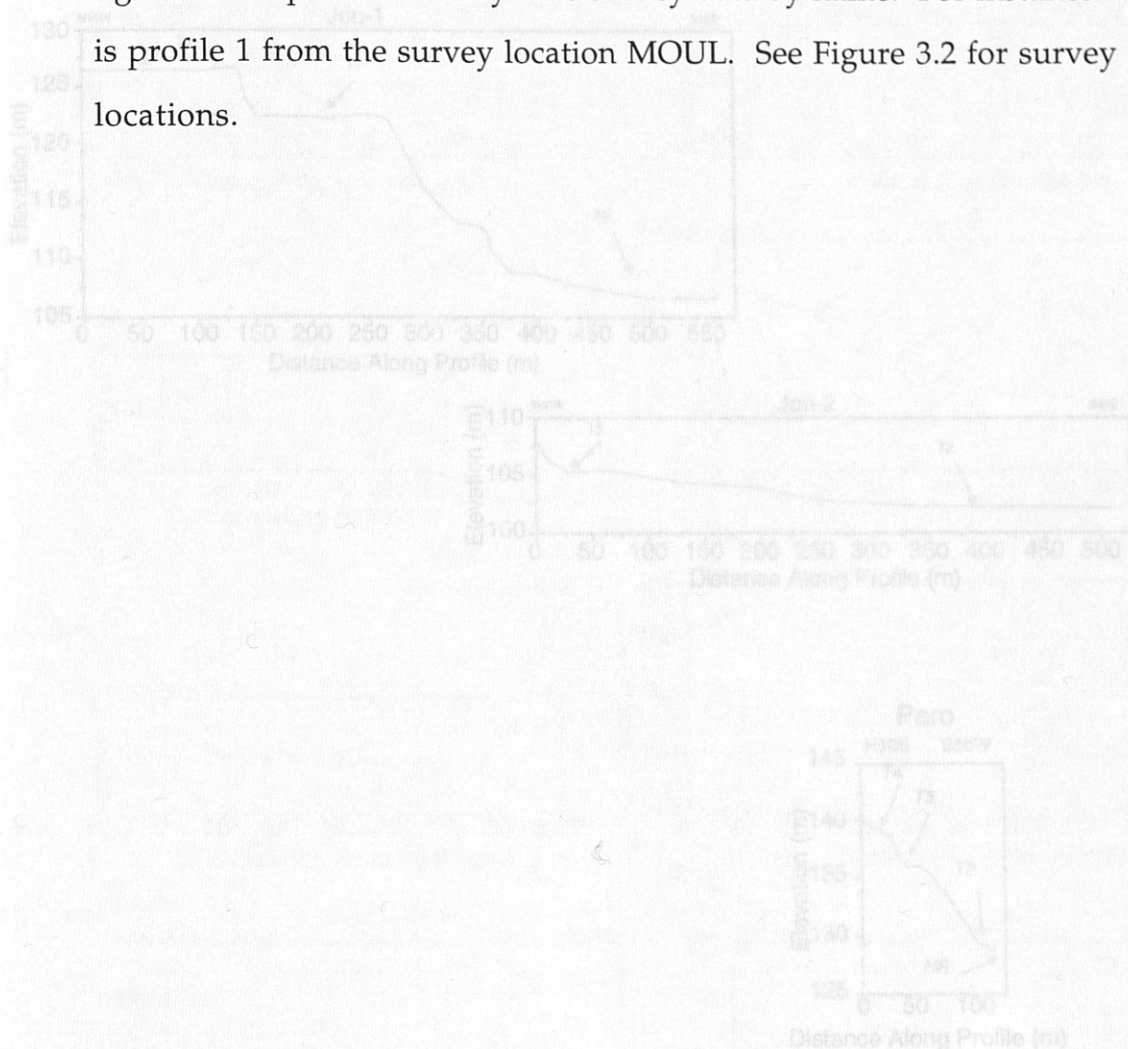
Note: Elevations at this site are tied to a contour line, elevation 780.00 ft or 237.80 m via Pt 15.

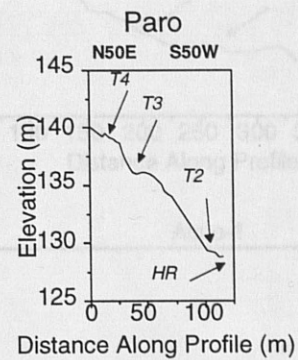
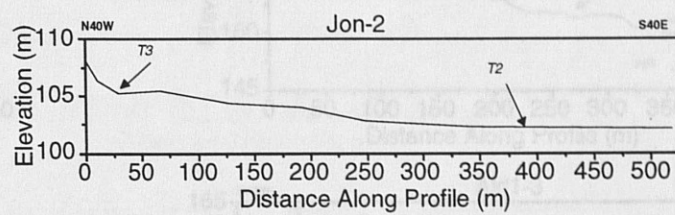
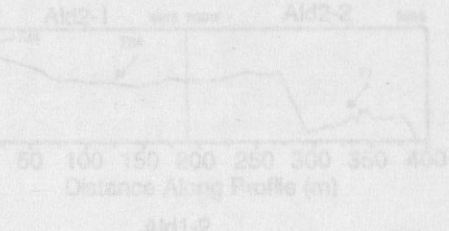
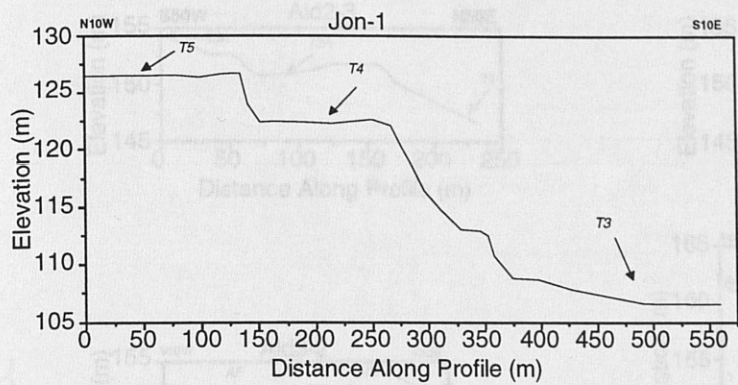
Huntington River Location 3-Cemetery							
Point Number	Northing (m)	Easting (m)	Measured Elevation (m)	Correction (m)	Final Elevation (m)	Error (m)	Point Description
1	1000.000	1000.000	100.000	222.82	322.82	± 1.0	T9
2	1100.000	1000.000	100.000	222.82	322.82	± 1.0	T9
3	983.543	966.020	91.073	222.82	313.89	± 1.0	RIVER
4	981.059	968.264	92.257	222.82	315.08	± 1.0	T1
5	996.161	983.012	92.861	222.82	315.68	± 1.0	T1
6	994.323	996.181	99.960	222.82	322.78	± 1.0	T9
7	989.426	1007.970	100.486	222.82	323.31	± 1.0	T9
8	997.758	1019.940	100.636	222.82	323.46	± 1.0	T9
9	1004.315	1039.273	100.640	222.82	323.46	± 1.0	T9
10	1034.680	1014.098	102.359	222.82	325.18	± 1.0	SLOPE
11	999.981	999.992	100.010	222.82	322.83	± 1.0	T9
12	1124.978	1008.109	112.545	222.82	335.37	± 1.0	T10
13	1134.384	1004.926	112.627	222.82	335.45	± 1.0	T10

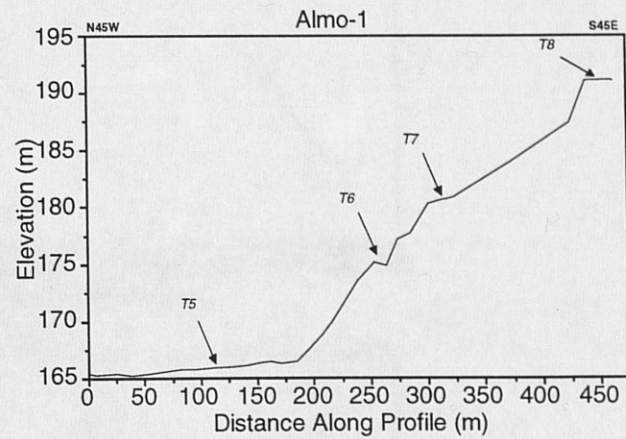
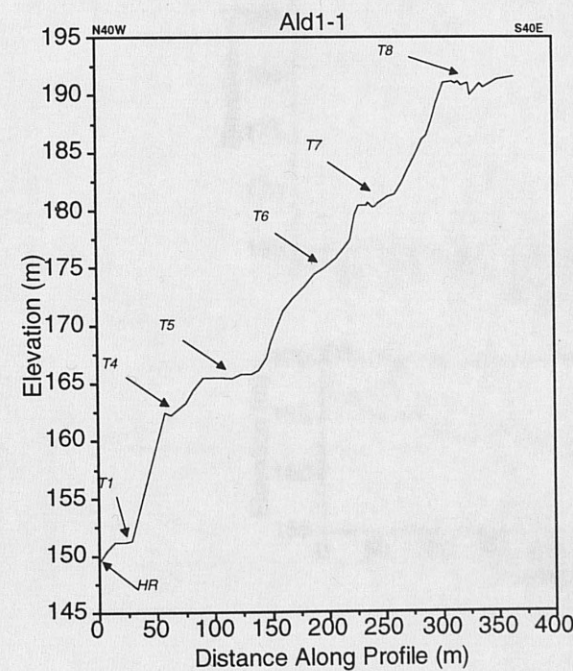
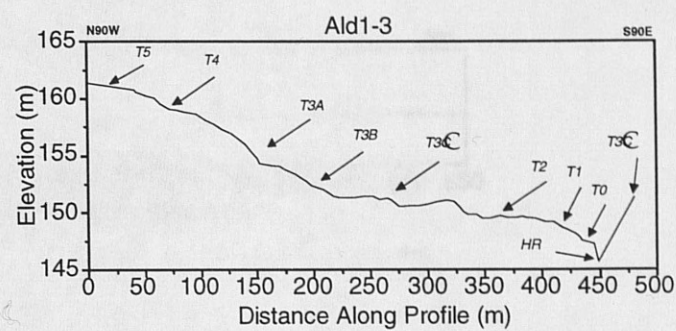
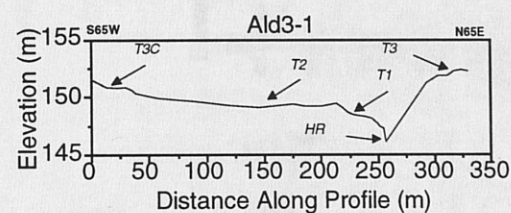
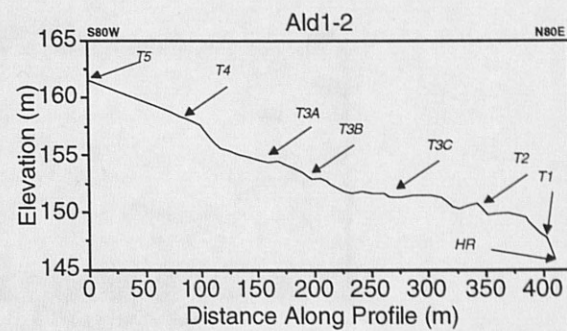
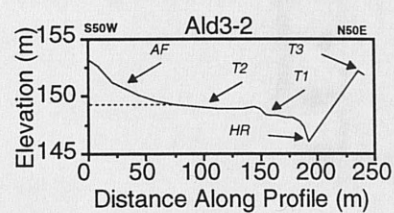
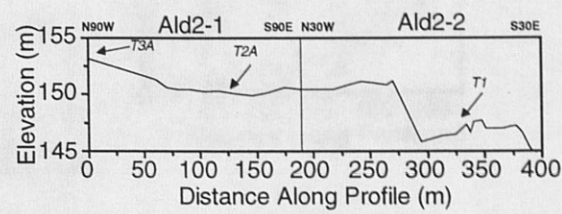
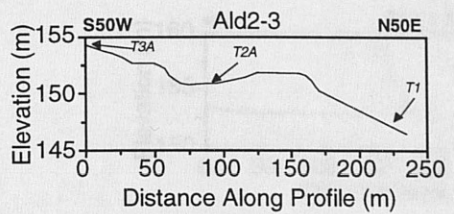
Note: Elevations at this site are tied to a contour line, elevation 1100.00 ft or 335.37 m via Pt. 12.

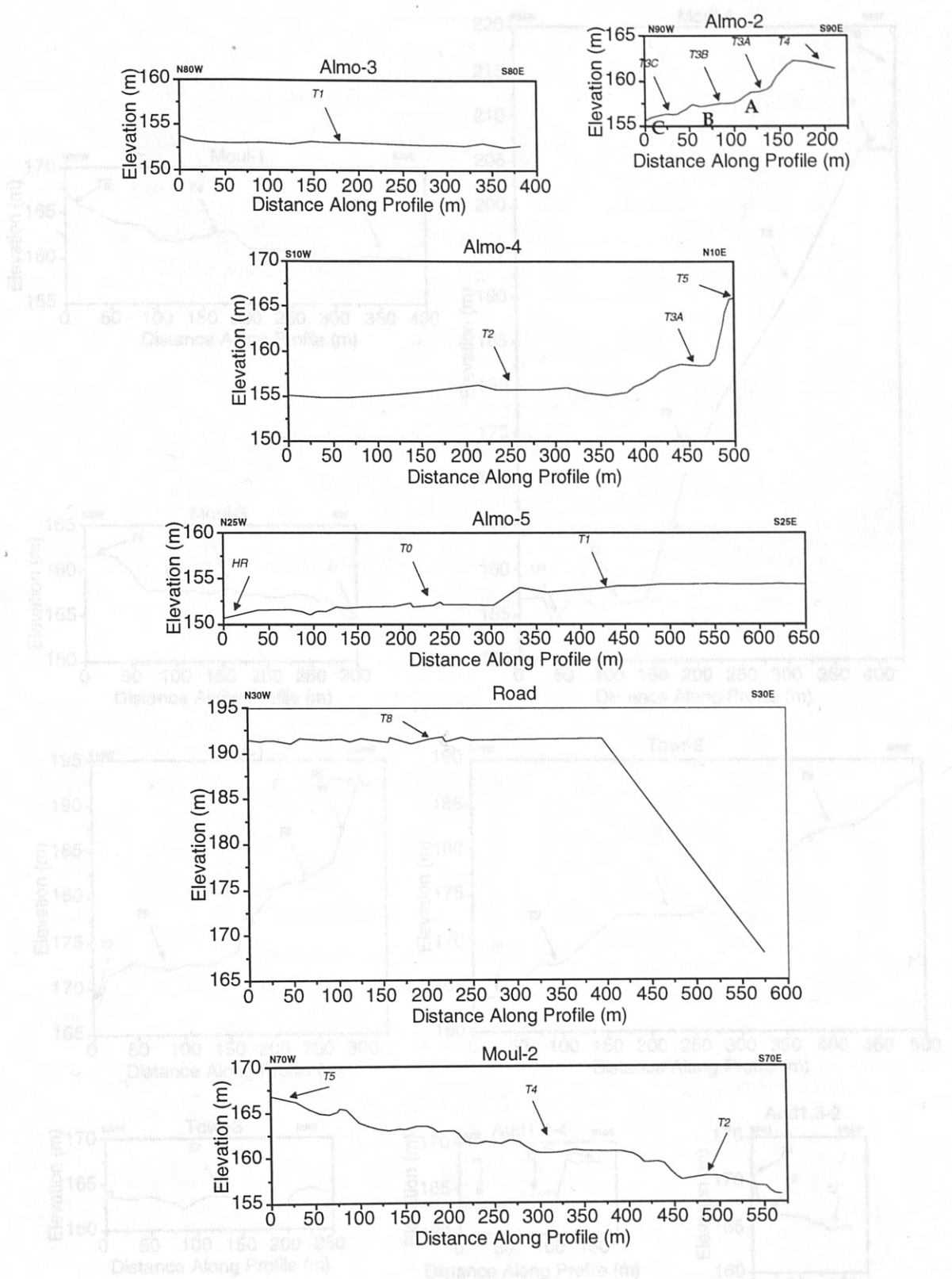
HUNTINGTON RIVER CROSS-VALLEY PROFILES

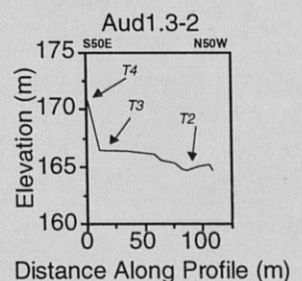
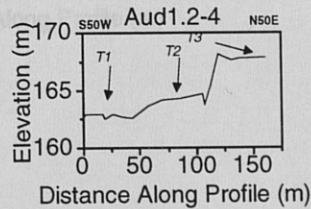
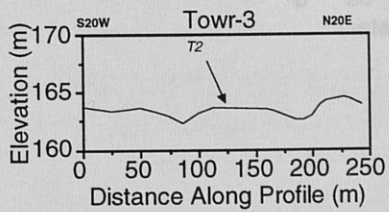
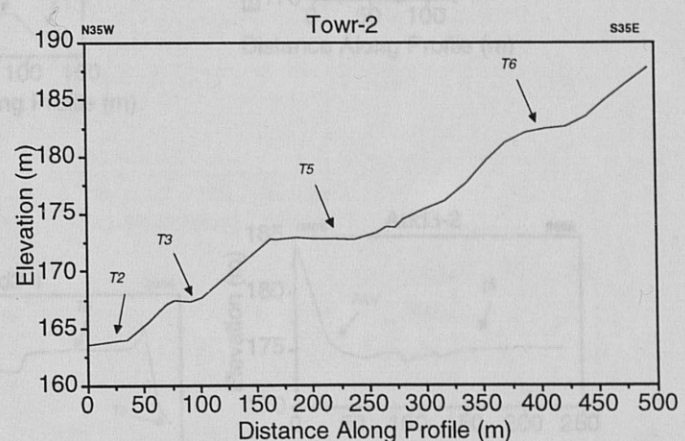
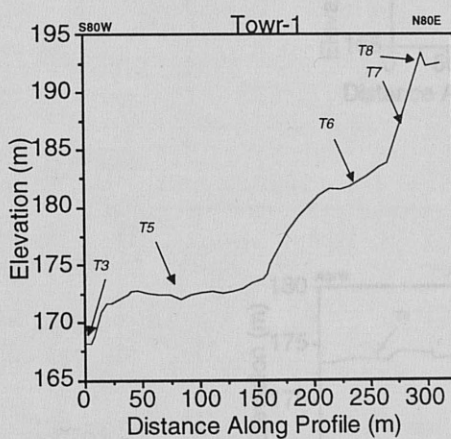
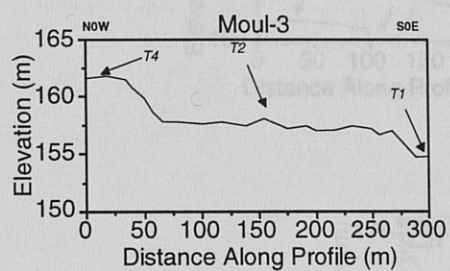
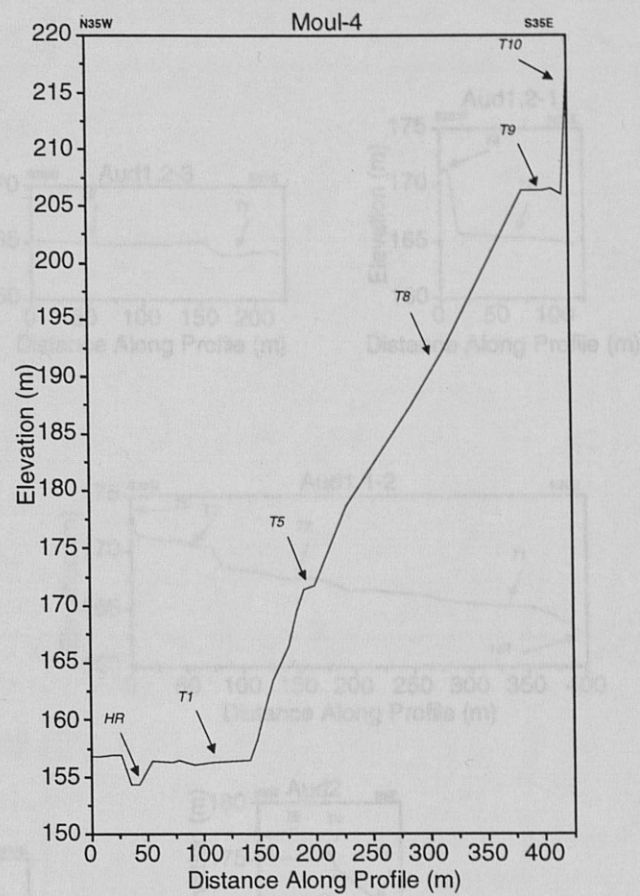
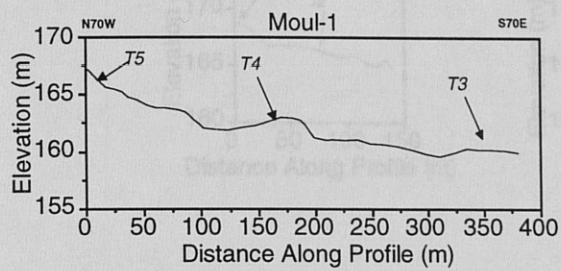
The Huntington River cross-valley profiles are presented in the following figures. The profiles are keyed to survey data by name. For instance MOUL-1 is profile 1 from the survey location MOUL. See Figure 3.2 for survey locations.

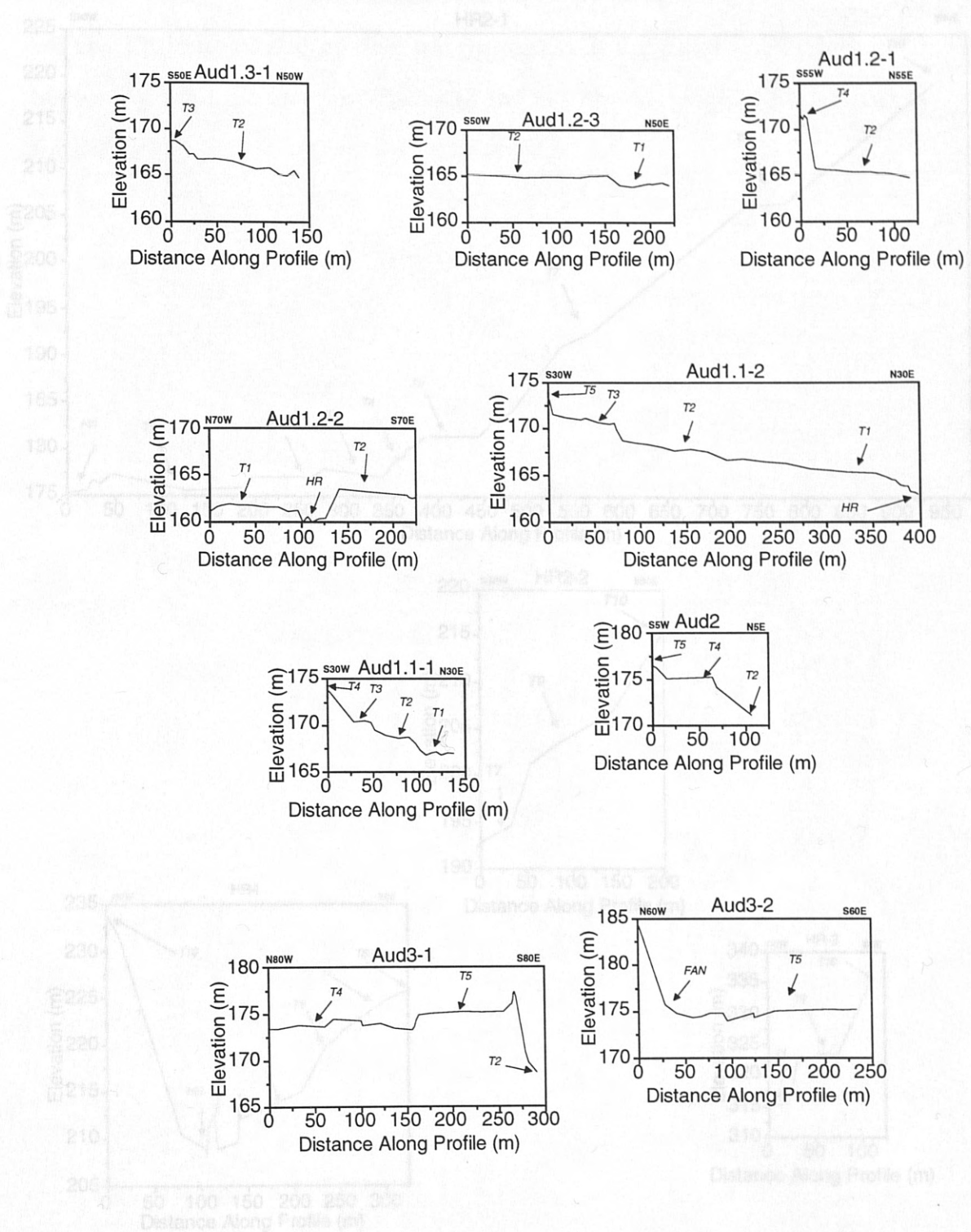






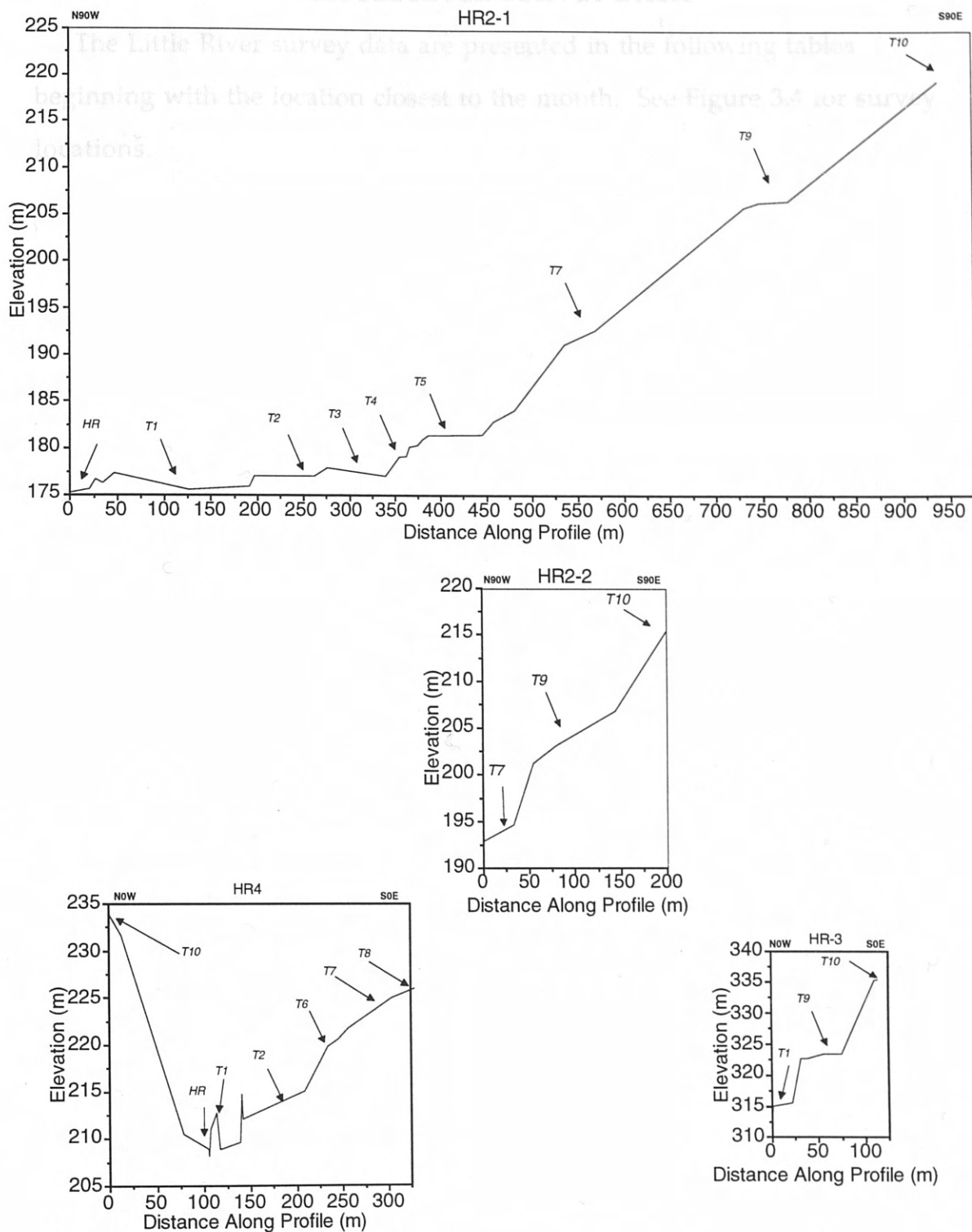






APPENDIX C: LITTLE RIVER DATA

LITTLE RIVER SURVEY DATA



APPENDIX C: LITTLE RIVER DATA

Point Number	Location (m)	Station Number	Section	Final Elevation	Point Description
1	100.000	1000.000	100.000	57.25	TBA
2	101.545	1015.545	101.545	57.25	TBA
3	103.089	1030.089	103.089	57.25	TBA
4	104.633	1040.633	104.633	57.25	TBA
5	106.177	1038.563	106.177	57.25	TBA
6	107.721	1030.563	107.721	57.25	TBA
7	109.365	1030.563	109.365	57.25	TBA
8	110.909	1012.363	110.909	57.25	TBA
9	112.453	1012.212	112.453	57.25	TBA
10	113.997	1010.021	113.997	57.25	TBA
11	115.541	1010.021	115.541	57.25	TBA
12	117.085	1005.674	117.085	57.25	TBA
13	118.629	1010.160	118.629	57.25	TBA
14	119.650	1020.046	119.650	57.25	TBA
15	120.659	1015.460	120.659	57.25	TBA
16	121.477	1014.700	121.477	57.25	TBA
17	122.195	1007.593	122.195	57.25	TBA
18	122.893	994.007	122.893	57.25	TBA
19	123.606	1021.968	123.606	57.25	TBA
20	123.925	972.268	123.925	57.25	TBA
21	124.774	976.774	124.774	57.25	TBA
22	125.822	985.208	125.822	57.25	TBA
23	126.849	931.007	126.849	57.25	TBA
24	126.871	581.008	126.871	57.25	TBA
25	127.011	1031.040	127.011	57.25	TBA
26	128.074	963.212	128.074	57.25	TBA
27	128.387	1081.412	128.387	57.25	TBA
28	129.924	1031.050	129.924	57.25	TBA
29	130.236	1010.003	130.236	57.25	TBA
30	130.550	1289.353	130.550	57.25	TBA
31	130.966	875.815	130.966	57.25	TBA
32	132.343	942.805	132.343	57.25	TBA
33	132.824	1003.528	132.824	57.25	TBA
34	133.305	989.614	133.305	57.25	TBA
35	134.359	973.912	134.359	57.25	TBA
36	135.621	1003.528	135.621	57.25	TBA
37	136.336	872.183	136.336	57.25	TBA
38	137.057	921.343	137.057	57.25	TBA
39	137.757	934.583	137.757	57.25	TBA
40	138.346	802.256	138.346	57.25	TBA
41	139.028	803.555	139.028	57.25	TBA
42	139.637	853.308	139.637	57.25	TBA
43	140.168	1010.728	140.168	57.25	TBA
44	140.736	981.568	140.736	57.25	TBA
45	142.362	1038.844	142.362	57.25	TBA
46	144.004	1040.481	144.004	57.25	TBA
47	145.251	1041.582	145.251	57.25	TBA
48	146.316	1131.025	146.316	57.25	TBA
49	148.056	872.738	148.056	57.25	TBA

The Little River survey data are presented in the following tables

beginning with the location closest to the mouth. See Figure 3.4 for survey locations.

Little River Location 2-Mouth							
Point Number	Northing (m)	Easting (m)	Measured Elevation (m)	Correction (m)	Final Elevation (m)	Error (m)	Point Description
1	1000.000	1000.000	100.000	57.25	157.25	± 0.30	T5A
2	1100.000	1000.000	100.000	57.25	157.25	± 0.30	T5A
3	1049.067	1045.352	88.566	57.25	145.82	± 0.30	SLOPE
4	1015.459	1038.322	100.369	57.25	157.62	± 0.30	T5A
5	1015.454	1038.308	100.369	57.25	157.62	± 0.30	T5A
6	993.538	1038.626	100.499	57.25	157.75	± 0.30	T5A
7	985.030	1030.633	98.564	57.25	155.82	± 0.30	T5B
8	945.001	1012.168	98.509	57.25	155.76	± 0.30	T5B
9	944.802	1012.212	98.503	57.25	155.75	± 0.30	T5B
10	936.901	1014.021	97.887	57.25	155.14	± 0.30	T5B
11	1000.036	999.992	100.020	57.25	157.27	± 0.30	T5A
12	920.852	1005.674	98.487	57.25	155.74	± 0.30	T5B
13	900.960	1010.100	92.922	57.25	150.17	± 0.30	T4
14	845.598	1020.646	91.196	57.25	148.45	± 0.30	T4
15	883.659	1015.400	92.295	57.25	149.55	± 0.30	T4
16	874.477	1016.708	91.159	57.25	148.41	± 0.30	T4
17	838.100	1037.535	91.195	57.25	148.45	± 0.30	T4
18	835.891	991.007	92.191	57.25	149.44	± 0.30	T4
19	845.605	1020.668	91.271	57.25	148.52	± 0.30	T4
20	779.025	972.259	97.977	57.25	155.23	± 0.30	T5B
21	796.774	978.255	92.897	57.25	150.15	± 0.30	T4
22	808.982	985.209	92.627	57.25	149.88	± 0.30	T4
23	835.888	991.007	92.259	57.25	149.51	± 0.30	T4
24	835.871	991.003	92.249	57.25	149.50	± 0.30	T4
25	701.011	1031.040	78.012	57.25	135.26	± 0.30	ROAD
26	808.974	985.212	92.753	57.25	150.01	± 0.30	T4
27	655.387	1051.432	73.317	57.25	130.57	± 0.30	ROAD
28	700.994	1031.050	78.056	57.25	135.31	± 0.30	ROAD
29	532.236	1019.003	68.715	57.25	125.97	± 0.30	T0
30	485.950	1099.361	68.057	57.25	125.31	± 0.30	T0
31	482.986	996.615	71.326	57.25	128.58	± 0.30	T1
32	488.349	942.805	98.777	57.25	156.03	± 0.30	SLOPE
33	316.624	1001.528	73.771	57.25	131.02	± 0.30	ROAD
34	483.005	996.614	71.390	57.25	128.64	± 0.30	T1
35	210.359	923.310	72.824	57.25	130.08	± 0.30	ROAD
36	316.621	1001.526	73.778	57.25	131.03	± 0.30	ROAD
37	123.366	802.197	71.682	57.25	128.93	± 0.30	T1
38	210.357	923.307	72.897	57.25	130.15	± 0.30	ROAD
39	67.757	981.563	69.005	57.25	126.26	± 0.30	T0
40	123.348	802.256	71.736	57.25	128.99	± 0.30	T1
41	90.088	803.965	68.892	57.25	126.14	± 0.30	T0
42	28.637	953.308	66.516	57.25	123.77	± 0.30	T0
43	8.168	1019.128	70.730	57.25	127.98	± 0.30	T1
44	67.749	981.568	69.033	57.25	126.28	± 0.30	T0
45	72.667	1036.344	67.446	57.25	124.70	± 0.30	T0
46	64.004	1040.431	64.560	57.25	121.81	± 0.30	T0
47	53.251	1044.522	63.831	57.25	121.08	± 0.30	T0
48	-19.316	1131.025	85.264	57.25	142.52	± 0.30	T3
49	-83.935	882.736	63.393	57.25	120.64	± 0.30	RIVER

Little River Location 2-Mouth							
Point Number	Northing (m)	Easting (m)	Measured Elevation (m)	Correction (m)	Final Elevation (m)	Error (m)	Point Description
Note: Elevations at this site are tied to the Waterbury Dam (elevation 633.00 ft or 192.99 m) via: LR2 Pt 3 = LR1 Pt172.							
3	873.042	1002.324	100.248	-0.05	100.193	+ 0.00	TBA
4	992.107	1002.310	100.250	-0.05	100.195	+ 0.30	TB
5	863.631	1010.678	100.088	-0.05	100.033	+ 0.30	TB
6	973.703	1014.573	97.244	-0.05	97.189	+ 0.30	TB
7	992.165	1016.709	98.796	-0.05	98.741	+ 0.30	TB
8	908.794	1071.642	99.467	-0.05	99.412	+ 0.30	TCA
9	994.753	1083.937	98.313	-0.05	98.258	+ 0.30	TCA
10	965.025	1120.073	96.878	-0.05	96.823	+ 0.30	TCA
11	983.214	1129.563	95.703	-0.05	95.648	+ 0.30	TCA
12	1060.602	939.986	92.046	-0.05	91.991	+ 0.30	TG
13	1060.603	982.977	100.011	-0.05	99.956	+ 0.30	TG
14	975.981	1150.813	95.526	-0.05	95.471	+ 0.30	TG
15	978.020	1150.822	96.429	-0.05	96.374	+ 0.30	TG
16	978.367	1160.770	96.034	-0.05	95.979	+ 0.30	TG
17	965.959	1158.927	96.324	-0.05	96.269	+ 0.30	TG
18	1000.687	1172.529	94.921	-0.05	94.866	+ 0.30	TG
19	1001.59	1204.482	75.126	-0.05	75.071	+ 0.30	TG
20	1004.839	1208.892	74.311	-0.05	74.256	+ 0.30	TG
21	876.737	1159.949	95.540	-0.05	95.485	+ 0.30	TG
22	1082.658	1127.792	79.637	-0.05	79.582	+ 0.30	TG
23	645.630	1135.183	70.510	-0.05	70.455	+ 0.30	T
24	849.189	1149.404	74.020	-0.05	73.965	+ 0.30	TG
25	874.479	1123.555	75.247	-0.05	75.192	+ 0.30	TG
26	669.915	1141.995	71.112	-0.05	71.057	+ 0.30	SLOPE
27	886.501	1143.924	78.368	-0.05	78.313	+ 0.30	TG
28	848.067	1159.789	78.522	-0.05	78.467	+ 0.30	TG
29	280.478	1154.287	78.716	-0.05	78.661	+ 0.30	SLOPE
30	832.503	1159.583	77.721	-0.05	77.666	+ 0.30	SLOPE
31	893.103	1172.876	75.170	-0.05	75.115	+ 0.30	TG
32	827.813	1161.978	70.890	-0.05	70.835	+ 0.30	TG
33	861.711	1167.940	76.227	-0.05	76.172	+ 0.30	TG
34	867.570	1284.708	72.385	-0.05	72.330	+ 0.30	TG
35	691.451	1184.125	72.094	-0.05	72.039	+ 0.30	SLOPE
36	845.643	1178.175	75.529	-0.05	75.474	+ 0.30	TG
37	709.879	1153.372	76.172	-0.05	76.117	+ 0.30	SLOPE
38	663.271	1140.333	76.328	-0.05	76.273	+ 0.30	SLOPE
39	1050.671	1179.476	77.841	-0.05	77.786	+ 0.30	SLOPE
40	643.73	1177.262	77.141	-0.05	77.086	+ 0.30	SLOPE
41	910.635	1154.946	76.101	-0.05	76.046	+ 0.30	SLOPE
42	801.24	1171.638	77.524	-0.05	77.469	+ 0.30	SLOPE
43	848.189	1164.732	80.413	-0.05	80.358	+ 0.30	TGA
44	536.1984	1132.232	78.624	-0.05	78.569	+ 0.30	TG
45	811.673	1148.330	76.489	-0.05	76.434	+ 0.30	TG
46	511.670	1151.958	75.369	-0.05	75.314	+ 0.30	TG
47	639.743	1178.948	75.681	-0.05	75.626	+ 0.30	TG
48	607.644	1167.417	72.375	-0.05	72.320	+ 0.30	TG
49	599.642	1180.532	72.164	-0.05	72.109	+ 0.30	TG
50	866.150	1146.596	75.010	-0.05	74.955	+ 0.30	TG

Little River Location 1-State Park							
Point Number	Northing (m)	Easting (m)	Measured Elevation (m)	Correction (m)	Final Elevation (m)	Error (m)	Point Description
1	1000.000	1000.000	100.000	64.65	164.65	± 0.30	T6
2	1099.369	1011.219	100.000	64.65	164.65	± 0.30	T6
3	1579.524	1065.431	128.339	64.65	192.99	± 0.30	Dam
4	982.107	1002.110	100.256	64.65	164.90	± 0.30	T6
5	983.891	1010.078	100.083	64.65	164.73	± 0.30	T6
6	978.707	1018.923	97.444	64.65	162.09	± 0.30	T5A
7	992.185	1049.079	96.796	64.65	161.44	± 0.30	T5A
8	988.794	1078.642	96.457	64.65	161.11	± 0.30	T5A
9	984.755	1093.937	96.319	64.65	160.97	± 0.30	T5A
10	985.025	1135.976	95.844	64.65	160.49	± 0.30	T5B
11	983.214	1129.593	95.843	64.65	160.49	± 0.30	T5B
12	1000.002	999.988	99.994	64.65	164.64	± 0.30	T6
13	1000.003	999.977	100.010	64.65	164.66	± 0.30	T6
14	978.361	1150.313	95.626	64.65	160.27	± 0.30	T5B
15	978.089	1158.025	90.429	64.65	155.08	± 0.30	T4
16	978.362	1160.920	89.834	64.65	154.48	± 0.30	T4
17	986.999	1188.227	75.594	64.65	140.24	± 0.30	T1
18	1000.381	1212.129	74.291	64.65	138.94	± 0.30	T0
19	1001.759	1234.582	73.528	64.65	138.18	± 0.30	T0
20	1004.336	1208.892	74.331	64.65	138.98	± 0.30	T0
21	978.332	1150.249	95.560	64.65	160.21	± 0.30	T5B
22	1012.058	1250.790	73.607	64.65	138.26	± 0.30	T0
23	848.856	1186.183	76.510	64.65	141.16	± 0.30	T1
24	999.789	1142.404	74.090	64.65	138.74	± 0.30	T0
25	874.179	1123.666	95.247	64.65	159.90	± 0.30	T5B
26	883.915	1141.995	87.215	64.65	151.86	± 0.30	SLOPE
27	885.501	1149.924	84.388	64.65	149.04	± 0.30	T3
28	888.067	1156.780	83.539	64.65	148.19	± 0.30	T3
29	890.476	1164.957	78.733	64.65	143.38	± 0.30	SLOPE
30	892.500	1169.853	77.713	64.65	142.36	± 0.30	SLOPE
31	893.105	1172.378	75.755	64.65	140.40	± 0.30	T2
32	895.845	1180.973	75.890	64.65	140.54	± 0.30	T2
33	895.711	1187.340	74.020	64.65	138.67	± 0.30	T1
34	872.670	1264.708	73.385	64.65	138.03	± 0.30	T1
35	691.251	1144.828	77.596	64.65	142.24	± 0.30	SLOPE
36	848.843	1186.179	76.269	64.65	140.92	± 0.30	T2
37	709.879	1135.372	79.124	64.65	143.77	± 0.30	SLOPE
38	693.271	1140.339	78.420	64.65	143.07	± 0.30	SLOPE
39	650.470	1168.436	77.648	64.65	142.30	± 0.30	SLOPE
40	643.734	1156.759	77.743	64.65	142.39	± 0.30	SLOPE
41	610.659	1147.646	76.405	64.65	141.05	± 0.30	SLOPE
42	691.247	1144.836	77.524	64.65	142.17	± 0.30	SLOPE
43	640.499	1098.732	96.418	64.65	161.07	± 0.30	T5A
44	616.284	1137.239	76.824	64.65	141.47	± 0.30	T2
45	611.525	1148.330	76.432	64.65	141.08	± 0.30	T2
46	611.409	1151.055	75.559	64.65	140.21	± 0.30	T2
47	609.093	1159.839	75.521	64.65	140.17	± 0.30	T2
48	607.844	1167.417	72.375	64.65	137.02	± 0.30	T1
49	599.647	1226.132	72.184	64.65	136.83	± 0.30	T1
50	666.159	1145.656	75.010	64.65	139.66	± 0.30	T2

Little River Location 1-State Park							
Point Number	Northing (m)	Easting (m)	Measured Elevation (m)	Correction (m)	Final Elevation (m)	Error (m)	Point Description
51	673.035	1145.272	74.960	64.65	139.61	± 0.30	T2
52	759.965	1172.713	72.353	64.65	137.00	± 0.30	T1
53	610.673	1147.648	76.361	64.65	141.01	± 0.30	SLOPE
54	717.587	1243.078	95.510	64.65	160.16	± 0.30	T5A
55	747.997	1188.903	73.007	64.65	137.66	± 0.30	T1
56	751.003	1180.952	72.861	64.65	137.51	± 0.30	T1
57	745.196	1162.914	70.990	64.65	135.64	± 0.30	T0
58	749.336	1107.608	71.144	64.65	135.79	± 0.30	T0
59	748.382	1101.197	69.425	64.65	134.07	± 0.30	T0
60	748.266	1088.678	69.454	64.65	134.10	± 0.30	T0
61	742.849	1015.586	69.525	64.65	134.17	± 0.30	T0
62	746.051	1013.905	71.460	64.65	136.11	± 0.30	T1
63	747.935	1011.303	71.599	64.65	136.25	± 0.30	T1
64	747.667	1002.658	74.820	64.65	139.47	± 0.30	T2
65	610.678	1147.642	76.331	64.65	140.98	± 0.30	T2
66	740.446	994.411	75.053	64.65	139.70	± 0.30	T2
67	740.860	987.402	74.986	64.65	139.63	± 0.30	T2
68	741.987	987.605	74.932	64.65	139.58	± 0.30	T2
69	741.961	987.617	74.932	64.65	139.58	± 0.30	T2
70	725.495	1172.873	72.420	64.65	137.07	± 0.30	T2
71	765.626	948.635	95.005	64.65	159.65	± 0.30	T5B
72	765.630	948.633	95.009	64.65	159.66	± 0.30	T5B
73	610.664	1147.617	76.314	64.65	140.96	± 0.30	T2
74	676.597	1137.991	74.236	64.65	138.88	± 0.30	T1
75	676.583	1137.986	74.289	64.65	138.94	± 0.30	T1
76	683.605	1132.871	72.664	64.65	137.31	± 0.30	T1
77	694.168	1123.389	71.892	64.65	136.54	± 0.30	T0
78	694.166	1123.385	71.892	64.65	136.54	± 0.30	T0
79	696.377	1120.083	71.274	64.65	135.92	± 0.30	T0
80	981.447	1218.115	70.813	64.65	135.46	± 0.30	T0
81	759.923	1172.704	72.265	64.65	136.91	± 0.30	T0
82	872.802	1306.068	96.906	64.65	161.55	± 0.30	T5A
83	893.885	1298.543	92.989	64.65	157.64	± 0.30	T5B
84	901.158	1288.279	83.742	64.65	148.39	± 0.30	T3
85	906.516	1284.150	82.867	64.65	147.52	± 0.30	T3
86	926.572	1287.302	81.749	64.65	146.40	± 0.30	T3
87	936.756	1270.911	76.348	64.65	141.00	± 0.30	SLOPE
88	950.471	1255.703	75.560	64.65	140.21	± 0.30	SLOPE
89	957.355	1243.944	70.757	64.65	135.41	± 0.30	T2
90	986.012	1194.140	71.067	64.65	135.72	± 0.30	T2
91	985.605	1190.837	69.672	64.65	134.32	± 0.30	T2
92	985.800	1189.065	69.353	64.65	134.00	± 0.30	T2
93	1187.347	1242.308	94.092	64.65	158.74	± 0.30	T5B
94	1187.921	1242.294	94.202	64.65	158.85	± 0.30	T5B
95	981.444	1218.115	70.751	64.65	135.40	± 0.30	T2
96	1265.186	1255.118	93.876	64.65	158.52	± 0.30	T5B
97	1187.901	1242.291	94.248	64.65	158.90	± 0.30	T5B
98	1253.309	1278.839	93.322	64.65	157.97	± 0.30	T5B
99	1252.344	1280.653	93.852	64.65	158.50	± 0.30	T5B
100	1217.643	1344.611	93.925	64.65	158.57	± 0.30	T5B

Little River Location 1-State Park							
Point Number	Northing (m)	Easting (m)	Measured Elevation (m)	Correction (m)	Final Elevation (m)	Error (m)	Point Description
101	1214.165	1355.910	95.330	64.65	159.98	± 0.30	T5A
102	1212.401	1359.513	95.535	64.65	160.18	± 0.30	T5A
103	1214.792	1351.418	95.407	64.65	160.06	± 0.30	T5A
104	1199.439	1380.356	95.819	64.65	160.47	± 0.30	T5A
105	1196.948	1384.358	96.789	64.65	161.44	± 0.30	T5A
106	1218.271	1391.347	96.924	64.65	161.57	± 0.30	T5A
107	1218.451	1393.077	97.206	64.65	161.85	± 0.30	T5A
108	1222.198	1412.197	98.234	64.65	162.88	± 0.30	T5A
109	1223.194	1418.054	99.342	64.65	163.99	± 0.30	T6
110	1217.740	1344.224	93.826	64.65	158.47	± 0.30	T5B
111	1330.796	1217.735	68.445	64.65	133.09	± 0.30	T1
112	1274.188	1267.680	93.862	64.65	158.51	± 0.30	T5B
113	1317.334	1228.444	69.194	64.65	133.84	± 0.30	T1
114	1330.890	1219.614	68.859	64.65	133.51	± 0.30	T1
115	1331.819	1213.968	66.383	64.65	131.03	± 0.30	T0
116	1339.059	1194.954	64.341	64.65	128.99	± 0.30	RMER
117	1392.174	1196.836	68.476	64.65	133.12	± 0.30	T1
118	1330.760	1217.747	68.345	64.65	132.99	± 0.30	T1
119	1379.521	1200.882	65.140	64.65	129.79	± 0.30	T0
120	1361.745	1180.365	64.257	64.65	128.91	± 0.30	T0
121	1398.143	1205.052	68.501	64.65	133.15	± 0.30	T1
122	1438.451	1233.689	93.419	64.65	158.07	± 0.30	T5B
123	1452.225	1167.497	70.831	64.65	135.48	± 0.30	T2
124	1452.231	1167.467	70.819	64.65	135.47	± 0.30	T2
125	1392.177	1196.835	68.499	64.65	133.15	± 0.30	T1
126	1540.718	1218.327	66.353	64.65	131.00	± 0.30	T0
127	1540.712	1218.324	66.353	64.65	131.00	± 0.30	T0
128	1452.231	1167.459	70.935	64.65	135.58	± 0.30	T2
129	1677.921	1421.479	66.448	64.65	131.10	± 0.30	T1
130	1540.716	1218.329	66.080	64.65	130.73	± 0.30	T1
131	1605.630	1430.562	92.335	64.65	156.98	± 0.30	T5B
132	1650.276	1435.146	71.572	64.65	136.22	± 0.30	T2
133	1662.455	1432.258	69.956	64.65	134.60	± 0.30	T2
134	1668.648	1430.267	66.747	64.65	131.40	± 0.30	T1
135	1680.904	1432.598	66.778	64.65	131.43	± 0.30	T1
136	1690.015	1435.793	63.969	64.65	128.62	± 0.30	RMER
137	1707.478	1438.218	63.808	64.65	128.46	± 0.30	RMER
138	1683.906	1479.251	66.402	64.65	131.05	± 0.30	T1
139	1677.917	1421.436	66.489	64.65	131.14	± 0.30	T1
140	1669.731	1480.684	66.950	64.65	131.60	± 0.30	T1
141	1665.829	1480.849	66.926	64.65	131.57	± 0.30	T1
142	1609.919	1497.822	88.877	64.65	153.53	± 0.30	SLOPE
143	1637.095	1539.659	77.558	64.65	142.21	± 0.30	SLOPE
144	1642.841	1539.925	76.743	64.65	141.39	± 0.30	SLOPE
145	1661.167	1525.613	67.044	64.65	131.69	± 0.30	T1
146	1676.177	1527.059	66.328	64.65	130.98	± 0.30	T1
147	1680.478	1528.172	64.572	64.65	129.22	± 0.30	T0
148	1668.286	1558.752	66.635	64.65	131.28	± 0.30	T1
149	1685.039	1587.428	65.135	64.65	129.78	± 0.30	T0
150	1683.906	1479.262	66.436	64.65	131.08	± 0.30	T1

Little River Location 1-State Park							
Point Number	Northing (m)	Easting (m)	Measured Elevation (m)	Correction (m)	Final Elevation (m)	Error (m)	Point Description
151	1634.698	1639.193	93.673	64.65	158.32	± 0.30	T5A
152	1687.760	1601.901	64.870	64.65	129.52	± 0.30	T0
153	1698.882	1591.172	64.542	64.65	129.19	± 0.30	T0
154	1702.541	1588.028	63.521	64.65	128.17	± 0.30	T0
155	1729.284	1582.917	62.361	64.65	127.01	± 0.30	T0
156	1731.575	1583.155	61.093	64.65	125.74	± 0.30	RIVER
157	1734.682	1583.189	60.826	64.65	125.47	± 0.30	RIVER
158	1807.404	1675.320	64.653	64.65	129.30	± 0.30	T0
159	1807.403	1675.319	64.653	64.65	129.30	± 0.30	T0
160	1685.043	1587.431	65.171	64.65	129.82	± 0.30	T0
161	1812.534	1717.043	85.000	64.65	149.65	± 0.30	T4
162	1906.846	1665.990	65.181	64.65	129.83	± 0.30	T1
163	1906.892	1665.985	65.181	64.65	129.83	± 0.30	T1
164	1807.442	1675.315	64.619	64.65	129.27	± 0.30	T1
165	2113.389	1533.352	64.794	64.65	129.44	± 0.30	T1
166	2033.741	1635.517	66.207	64.65	130.86	± 0.30	T2
167	2041.812	1624.602	65.306	64.65	129.95	± 0.30	T1
168	2072.077	1570.677	65.461	64.65	130.11	± 0.30	T1
169	2081.361	1555.133	64.960	64.65	129.61	± 0.30	T1
170	2081.603	1548.591	61.688	64.65	126.34	± 0.30	T0
171	2083.207	1532.064	61.480	64.65	126.13	± 0.30	T0
172	2195.060	1564.880	81.169	64.65	145.82	± 0.30	SLOPE

Note: Elevations at this site are tied to the Waterbury Dam, elevation 633.00 ft or 192.99 m.

Little River Location 7-Waterbury Dam							
Point Number	Northing (m)	Easting (m)	Measured Elevation (m)	Correction (m)	Final Elevation (m)	Error (m)	Point Description
1	1000.000	1000.000	106.251	86.74	192.99	± 0.30	dam
2	1100.000	1000.000	106.251	86.74	192.99	± 0.30	dam
3	1035.566	1034.950	92.965	86.74	179.70	± 0.30	water
4	1035.558	1034.950	92.967	86.74	179.70	± 0.30	water
5	911.623	1071.290	79.544	86.74	166.28	± 0.30	T6
6	888.176	1127.499	76.933	86.74	163.67	± 0.30	T6

Note: Elevation of dam is 633.00 ft or 192.99 m

Note: Elevation of dam is 633.00 ft or 192.99 m
Water level in Gage

Little River Location 6-Canoe Access							
Point Number	Northing (m)	Easting (m)	Measured Elevation (m)	Correction (m)	Final Elevation (m)	Error (m)	Point Description
1	1000.000	1000.000	100.000	88.09	188.09	± 0.30	T7
2	1100.000	1000.000	100.000	88.09	188.09	± 0.30	T7
3	1008.949	978.410	100.152	88.09	188.25	± 0.30	T7
4	992.776	1006.500	99.926	88.09	188.02	± 0.30	T7
5	973.197	1024.873	97.593	88.09	185.69	± 0.30	T6
6	931.929	1069.687	97.747	88.09	185.84	± 0.30	T6
7	1000.006	999.994	100.057	88.09	188.15	± 0.30	T7
8	896.785	1074.710	97.521	88.09	185.62	± 0.30	T6
9	931.943	1069.685	97.792	88.09	185.89	± 0.30	T6
10	862.905	1099.378	97.068	88.09	185.16	± 0.30	T6
11	896.757	1074.730	97.553	88.09	185.65	± 0.30	T6
12	766.795	1075.633	94.596	88.09	182.69	± 0.30	T5
13	862.812	1099.355	97.099	88.09	185.19	± 0.30	T6
14	828.356	1087.521	97.096	88.09	185.19	± 0.30	T6
15	789.108	1083.013	94.761	88.09	182.86	± 0.30	T5
16	763.483	1069.994	94.399	88.09	182.49	± 0.30	T5
17	745.054	1059.773	93.112	88.09	181.21	± 0.30	T4
18	636.525	999.856	92.608	88.09	180.70	± 0.30	T4
19	634.129	998.944	91.609	88.09	179.70	± 0.30	Water Level
20	757.181	1080.746	91.533	88.09	179.63	± 0.30	Water Level
Note: Elevations at this site are tied to the water elevation in reservoir at LR7.							
Water level measured at 179.70 m at dam so correction is 88.09 m.							

Little River Location 3-Stowe Farm							
Point Number	Northing (m)	Easting (m)	Measured Elevation (m)	Correction (m)	Final Elevation (m)	Error (m)	Point Description
1	1000.000	1000.000	100.000	105.71	205.71	± 0.20	T6
2	1100.000	1000.000	100.000	105.71	205.71	± 0.20	T6
3	1058.685	1085.502	100.065	105.71	205.78	± 0.20	T6
4	1068.932	1062.061	93.763	105.71	199.47	± 0.20	T4
5	1117.582	928.447	92.820	105.71	198.53	± 0.20	T4
6	1087.349	901.415	90.597	105.71	196.31	± 0.20	T4
7	1032.363	832.422	92.275	105.71	197.99	± 0.20	T4
8	1011.922	832.081	92.527	105.71	198.24	± 0.20	T4
9	1006.973	838.488	93.876	105.71	199.59	± 0.20	T4
10	974.915	808.386	96.824	105.71	202.54	± 0.20	SLOPE
11	963.027	815.390	100.009	105.71	205.72	± 0.20	T6
12	843.011	969.895	101.876	105.71	207.59	± 0.20	T7
13	820.807	1182.596	106.302	105.71	212.01	± 0.20	SLOPE
14	999.997	1000.003	99.988	105.71	205.70	± 0.20	T6
15	868.018	1108.512	102.215	105.71	207.93	± 0.20	BM
16	839.689	1207.684	111.313	105.71	217.02	± 0.20	SLOPE

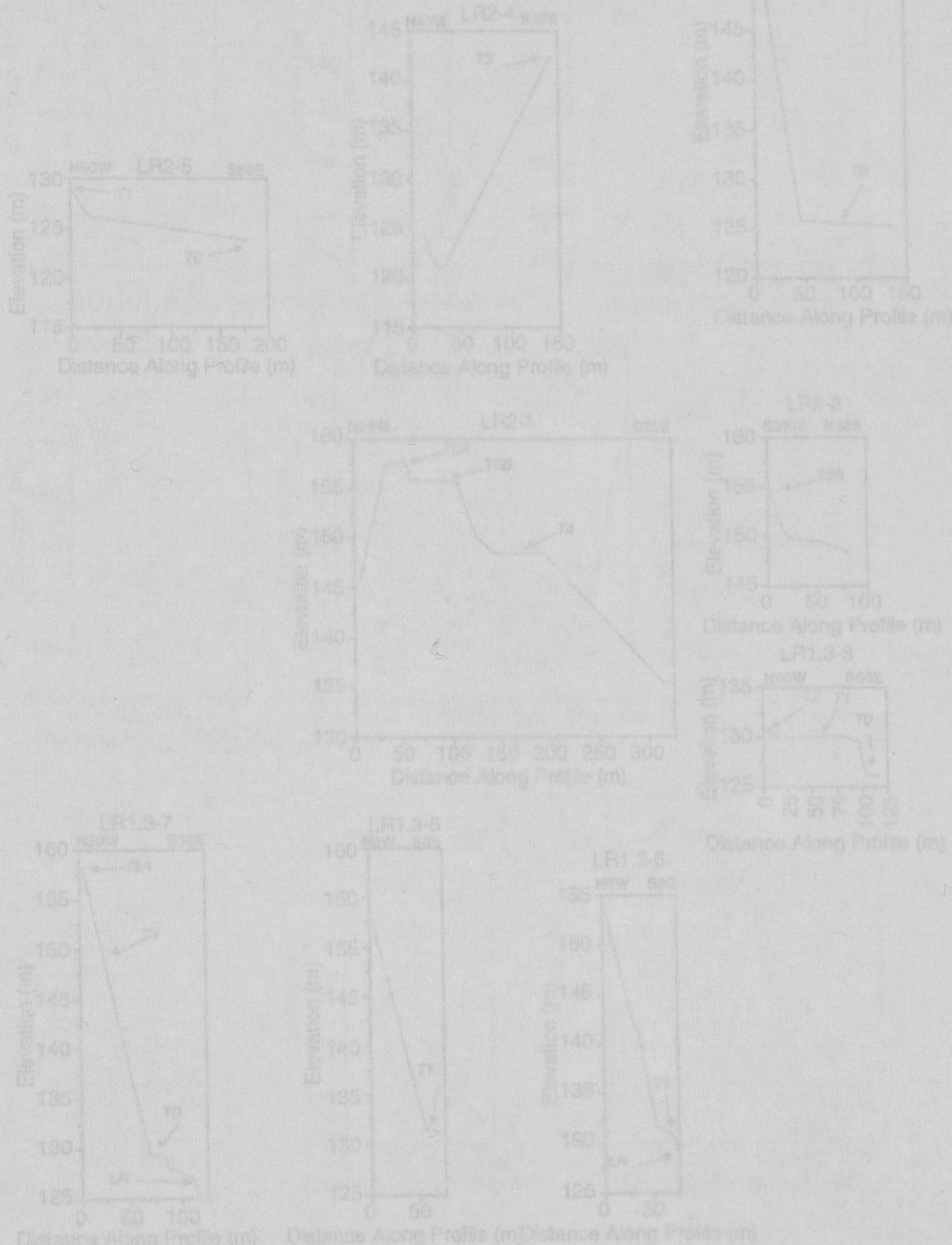
Note: Elevations at this site are tied to Benchmark 57 HBC 1967 (elevation 682.00 ft or 207.93 m)
via: LR3 Pt 15 = Benchmark.

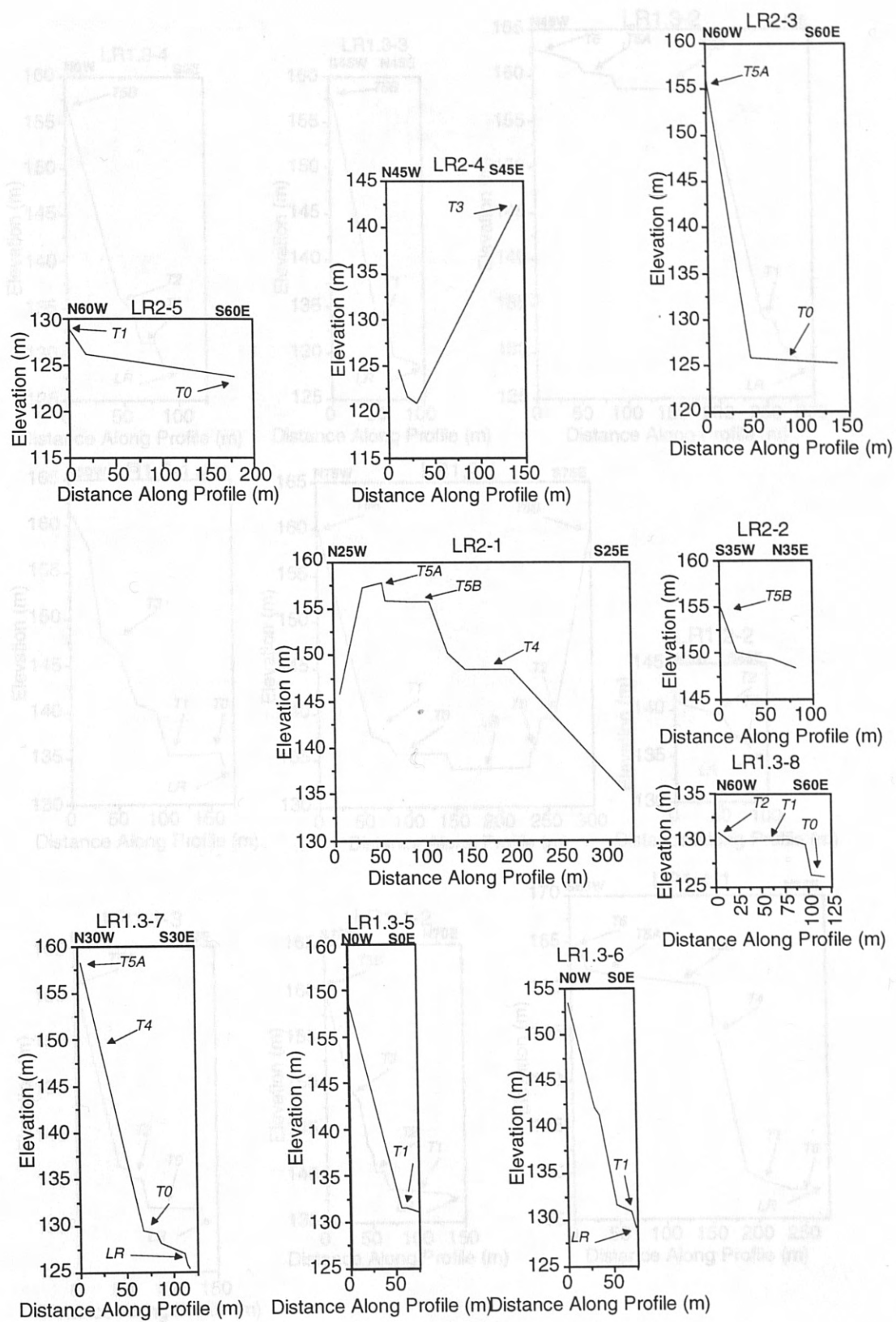
Little River Location 4-Moulton Lane							
Point Number	Northing (m)	Easting (m)	Measured Elevation (m)	Correction (m)	Final Elevation (m)	Error (m)	Point Description
1	1000.000	1000.000	100.000	130.07	230.07	± 1.0	T8
2	1100.000	1000.000	100.000	130.07	230.07	± 1.0	T8
3	1064.644	868.207	109.393	130.07	239.46	± 1.0	T9
4	1061.995	883.759	108.352	130.07	238.42	± 1.0	T9
5	1042.830	915.333	101.615	130.07	231.69	± 1.0	T8
6	1038.690	961.140	100.460	130.07	230.53	± 1.0	T8
7	1035.611	968.739	100.765	130.07	230.84	± 1.0	T8
8	1048.187	1015.312	100.819	130.07	230.89	± 1.0	T8
9	1036.613	1025.963	99.465	130.07	229.54	± 1.0	T7
10	1019.160	1118.079	99.414	130.07	229.49	± 1.0	T7
11	1017.891	1046.595	98.671	130.07	228.74	± 1.0	T6
12	940.007	1052.458	97.929	130.07	228.00	± 1.0	RIVER
13	956.946	1040.195	98.703	130.07	228.77	± 1.0	T6

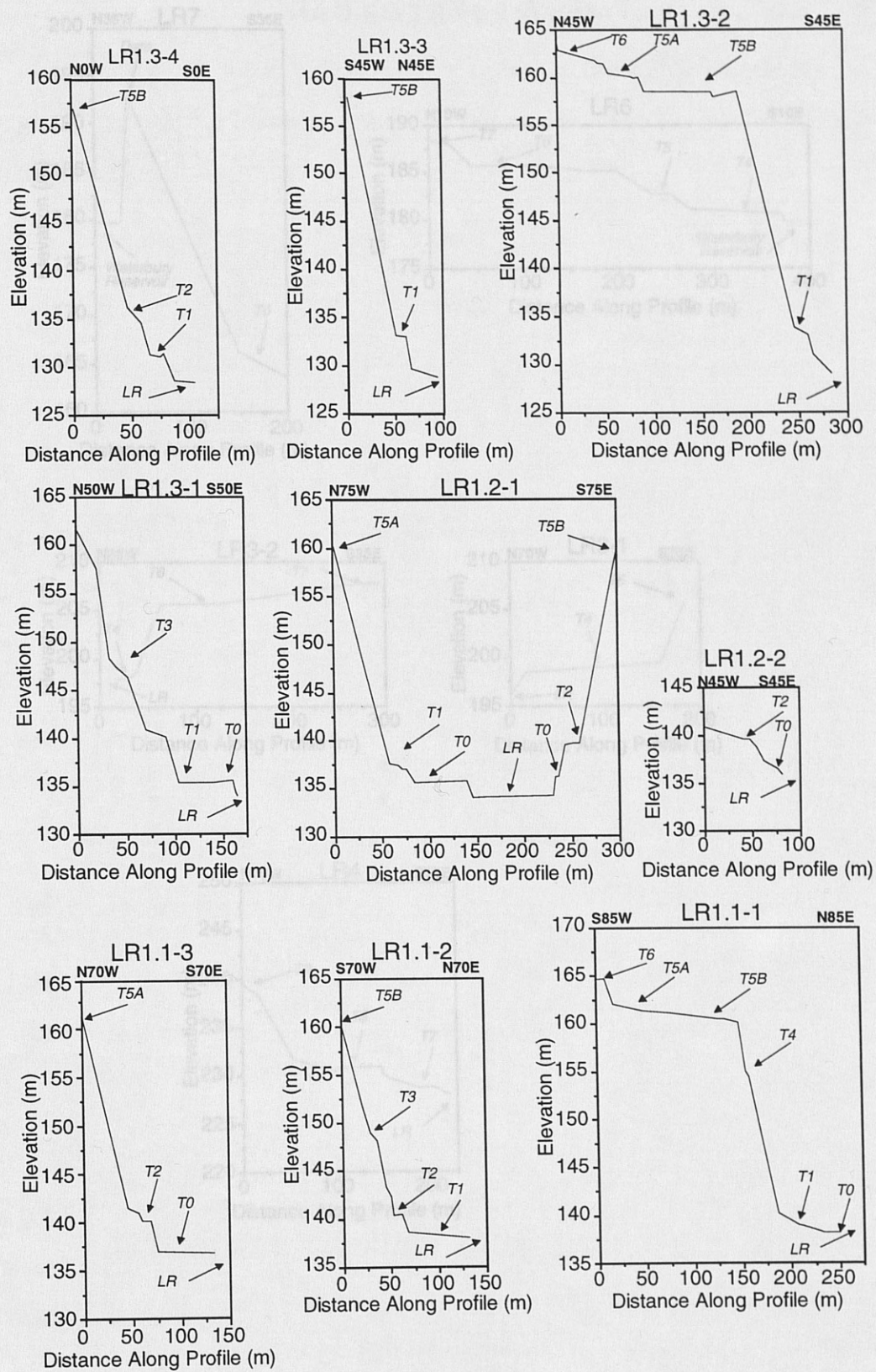
Note: Elevations at this site are tied to a contour line, elevation 960.00 ft or 228.00 m.

LITTLE RIVER CROSS-VALLEY PROFILES

The Little River cross-valley profiles are presented in the following figures. The profiles are keyed to survey data by name. For instance LR3-1 is profile 1 from the survey location LR3. See Figure 3.4 for survey locations.

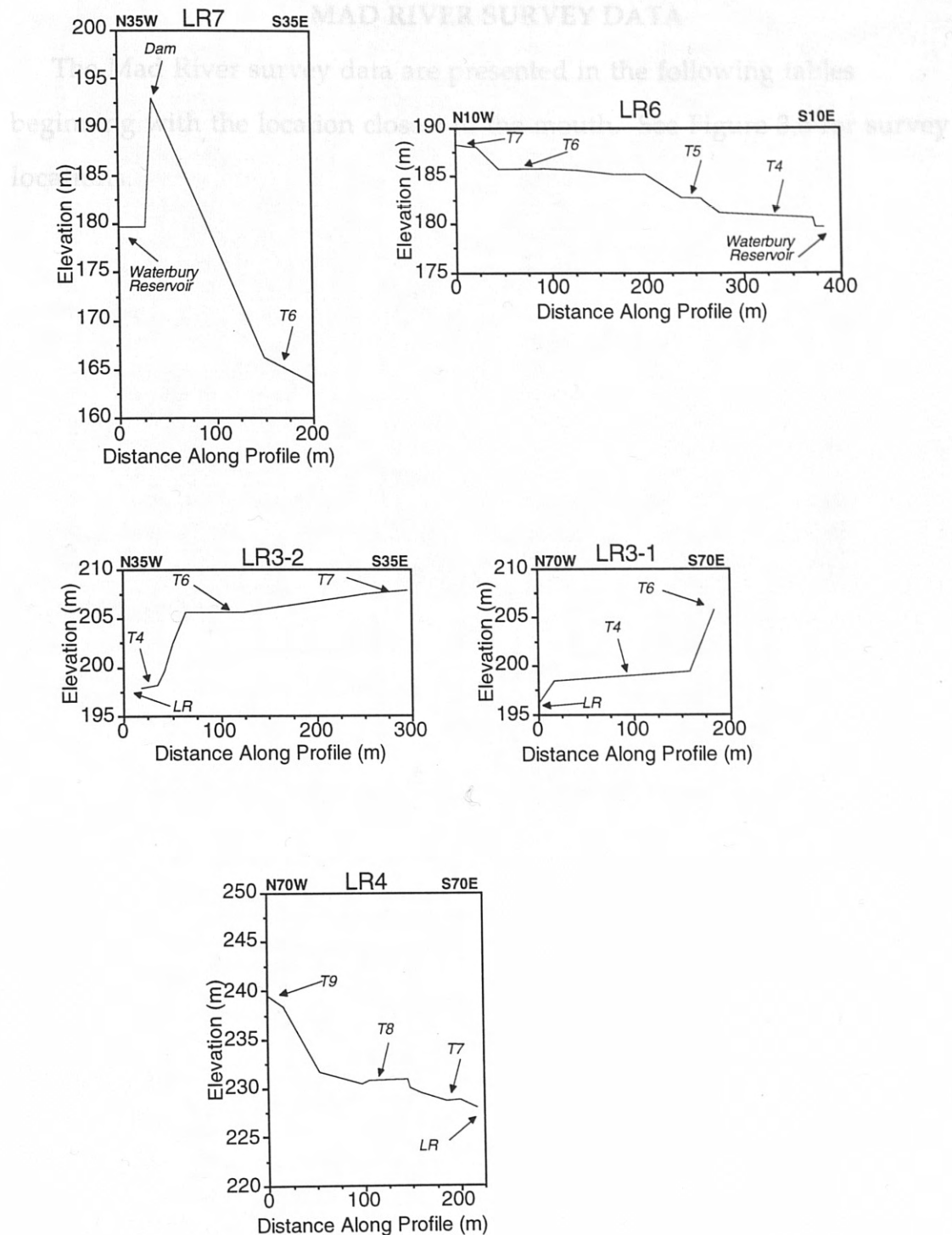






APPENDIX D: MAD RIVER DATA

MAD RIVER SURVEY DATA



APPENDIX D: MAD RIVER DATA

MAD RIVER SURVEY DATA

The Mad River survey data are presented in the following tables beginning with the location closest to the mouth. See Figure 3.6 for survey locations.

Point	Station	Easting (ft)	Northing (ft)	Point	Station	Easting (ft)	Northing (ft)
1	124-946	11233.320	77.824	8	80-93	134.42	± 0.20
2	127-386	1140.951	78.626	9	86-53	135.20	± 0.20
3	1000.044	1000.048	84.877	10	86-61	136.13	± 0.20
4	1231.860	901.558	78.478	11	86-75	132.72	± 0.20
5	1255.919	916.935	79.560	12	86-83	132.53	± 0.20
6	1258.520	1078.983	82.268	13	86-83	142.88	± 0.20
7	1234.415	1074.417	85.195	14	86-83	160.12	± 0.20
8	1215.293	1054.131	82.145	15	86-83	152.77	± 0.20
9	1405.562	937.852	86.945	16	86-83	133.08	± 0.20
10	1328.757	1103.321	79.468	17	86-83	156.09	± 0.20
11	1419.454	919.118	79.381	18	86-83	165.99	± 0.20
12	1108.701	1200.874	81.058	19	86-83	167.68	± 0.20
13	1785.546	1130.655	78.137	20	86-83	154.74	± 0.20
14	1800.389	1080.481	77.931	21	86-83	154.57	± 0.20
Note: Locations 21-25 S18 21S 21E 800.10' apart; Total length (elevation 850.00 ft or 107.65 m) = 42.47 ft. Pt 14 is a Benchmark.							

Mad River Location 17-Mouth							
Point Number	Northing (m)	Easting (m)	Measured Elevation (m)	Correction (m)	Final Elevation (m)	Error (m)	Point Description
1	1000.000	1000.000	100.000	86.63	186.63	± 0.20	T7
2	1100.000	1000.000	100.000	86.63	186.63	± 0.20	T7
3	993.575	1012.309	100.342	86.63	186.97	± 0.20	T7
4	1007.614	1014.119	100.075	86.63	186.70	± 0.20	T7
5	1102.934	1017.477	87.879	86.63	174.50	± 0.20	T6
6	1128.934	1021.236	88.006	86.63	174.63	± 0.20	T6
7	1784.340	1133.326	77.854	86.63	164.48	± 0.20	T5
8	1777.744	1140.951	76.656	86.63	163.28	± 0.20	T5
9	1000.044	1000.008	99.807	86.63	186.43	± 0.20	T7
10	1231.360	901.136	76.078	86.63	162.70	± 0.20	T5
11	1205.919	916.695	79.902	86.63	166.53	± 0.20	T5
12	1266.920	1078.983	62.258	86.63	148.88	± 0.20	T4
13	1233.475	1074.417	63.495	86.63	150.12	± 0.20	T4
14	1215.298	1054.131	66.143	86.63	152.77	± 0.20	T4
15	1406.383	950.529	51.435	86.63	138.06	± 0.20	T2
16	1828.707	1203.592	79.468	86.63	166.09	± 0.20	T5
17	1819.454	1197.113	79.361	86.63	165.99	± 0.20	T5
18	1839.401	1200.874	81.058	86.63	167.68	± 0.20	T5
19	1785.545	1130.635	78.117	86.63	164.74	± 0.20	T5
20	1860.189	1080.389	77.941	86.63	164.57	± 0.20	T5

Note: Elevations at this site are tied to Benchmark Westover (elevation 550.00 ft or 167.68 m) via:
MR17 Pt 18 = Benchmark.

Mad River Location 13-Horse Farm							
Point Number	Northing (m)	Easting (m)	Measured Elevation (m)	Correction (m)	Final Elevation (m)	Error (m)	Point Description
1	1000.000	1000.000	100.000	70.40	170.40	± 0.30	T2
2	1100.000	1000.015	100.000	70.40	170.40	± 0.30	T2
3	1002.287	1041.332	96.441	70.40	166.84	± 0.30	RIVER
4	1001.887	1047.959	98.426	70.40	168.82	± 0.30	T1
5	1002.575	1105.999	98.494	70.40	168.89	± 0.30	T1
6	979.883	1073.227	99.930	70.40	170.33	± 0.30	T2
7	958.669	1086.339	100.288	70.40	170.68	± 0.30	T2
8	952.042	1093.875	103.001	70.40	173.40	± 0.30	T3
9	897.738	1106.928	104.212	70.40	174.61	± 0.30	T3
10	798.978	1085.674	114.599	70.40	185.00	± 0.30	T5
11	693.174	1061.527	133.627	70.40	204.02	± 0.30	T7
12	593.358	1165.166	136.427	70.40	206.82	± 0.30	T7
13	617.704	1124.195	134.814	70.40	205.21	± 0.30	T7
14	693.359	1061.474	133.607	70.40	204.00	± 0.30	T7
15	1111.688	1312.839	131.823	70.40	202.22	± 0.30	T7
16	1072.595	1246.437	116.488	70.40	186.88	± 0.30	T5
17	1123.962	1235.171	116.907	70.40	187.30	± 0.30	T5
18	1120.732	1218.907	114.050	70.40	184.45	± 0.30	T5
19	1043.595	1149.919	101.650	70.40	172.05	± 0.30	T3
20	998.813	1003.347	100.334	70.40	170.73	± 0.30	BM 560 ft

Note: Elevations at this site are tied to Benchmark 44 HBC 1967 (elevation 560.00 ft or 170.73 m)
via: MR13 Pt 20 = Benchmark.

1	1301.081	1318.645	177.280	77.17	174.48	± 0.20	T3
2	1195.749	816.786	127.280	77.17	204.43	± 0.20	T7
3	1186.619	976.777	123.013	77.17	200.18	± 0.20	T7
4	1195.692	1001.367	125.211	77.17	200.43	± 0.20	T7
5	1197.896	1337.454	118.655	77.17	183.84	± 0.20	5.5 ft
6	1053.706	1036.341	107.387	77.17	184.56	± 0.20	5.5 ft
7	1093.543	1057.657	99.324	77.17	176.56	± 0.20	5.5 ft
8	1160.657	8112.556	104.350	77.17	181.62	± 0.20	5.5 ft
9	1168.055	8738.546	102.367	77.17	179.54	± 0.30	5.5 ft
10	1192.612	1167.954	99.376	77.17	177.15	± 0.20	5.5 ft
11	1190.937	8157.481	100.876	77.17	178.05	± 0.20	5.5 ft

Note: Elevations at this site are tied to Benchmark 44 HBC 1967 (elevation 564.00 ft or 171.93 m) via Pt 20

Mad River Location 14-Pink House							
Point Number	Northing (m)	Easting (m)	Measured Elevation (m)	Correction (m)	Final Elevation (m)	Error (m)	Point Description
1	1000.000	1000.000	100.000	77.17	177.17	± 0.20	T4
2	1100.000	1000.005	100.000	77.17	177.17	± 0.20	T4
3	770.825	1069.641	129.622	77.17	206.80	± 0.20	T7
4	777.307	1059.601	129.134	77.17	206.31	± 0.20	T7
5	786.725	1036.647	128.106	77.17	205.28	± 0.20	T7
6	790.834	1029.572	127.426	77.17	204.60	± 0.20	T7
7	835.395	1081.293	119.278	77.17	196.45	± 0.20	SLOPE
8	824.273	998.748	117.721	77.17	194.90	± 0.20	SLOPE
9	939.157	990.666	103.942	77.17	181.12	± 0.20	T4
10	920.128	955.650	103.417	77.17	180.59	± 0.20	T4
11	939.430	957.185	101.104	77.17	178.28	± 0.20	T4
12	978.090	961.609	100.514	77.17	177.69	± 0.20	T4
13	984.077	967.930	100.366	77.17	177.54	± 0.20	T4
14	1036.713	1063.960	96.902	77.17	174.08	± 0.20	T3
15	1022.906	1052.891	97.439	77.17	174.61	± 0.20	T3
16	1011.459	1038.857	99.010	77.17	176.18	± 0.20	T4
17	1012.396	994.709	97.039	77.17	174.21	± 0.20	T3
18	1014.901	994.434	96.913	77.17	174.09	± 0.20	T3
19	1100.450	1105.289	93.399	77.17	170.57	± 0.20	T1
20	1103.765	1107.421	94.864	77.17	172.04	± 0.20	T2
21	1106.753	1106.371	96.324	77.17	173.50	± 0.20	T2
22	1249.473	1238.842	98.192	77.17	175.37	± 0.20	T4
23	1245.236	1250.938	95.118	77.17	172.29	± 0.20	T2
24	1287.162	1284.391	97.414	77.17	174.59	± 0.20	T3
25	1301.061	1316.545	97.289	77.17	174.46	± 0.20	T3
26	1185.749	918.784	127.260	77.17	204.43	± 0.20	T7
27	1186.889	976.777	123.012	77.17	200.19	± 0.20	T7
28	1195.602	1001.347	123.229	77.17	200.40	± 0.20	T7
29	1197.906	1037.454	118.665	77.17	195.84	± 0.20	SLOPE
30	1143.706	1036.341	107.387	77.17	184.56	± 0.20	SLOPE
31	1093.541	1037.967	99.364	77.17	176.54	± 0.20	T4
32	1180.257	1112.686	104.350	77.17	181.52	± 0.20	SLOPE
33	1168.055	1108.546	102.367	77.17	179.54	± 0.20	T4
34	1192.612	1157.854	99.976	77.17	177.15	± 0.20	T4
35	1190.927	1157.481	100.876	77.17	178.05	± 0.20	T4

Note: Elevations at this site are tied to Benchmark (elevation 584.00 ft or 178.05 m) via Pt 35

Mad River Location 15-Austin							
Point Number	Northing (m)	Easting (m)	Elevation (m)	Correction (m)	Final Elevation (m)	Error (m)	Point Description
1	5000.000	5000.000	100.000	111.13	211.13	± 0.20	T8
2	4936.373	4922.853	100.000	111.13	211.13	± 0.20	T8
3	4536.580	4125.367	89.682	111.13	200.81	± 0.20	T5
4	4073.236	3721.162	82.925	111.13	194.06	± 0.20	T3
5	4838.450	3962.771	98.931	111.13	210.06	± 0.20	T8
6	5091.609	4865.735	97.896	111.13	209.03	± 0.20	T7
7	5084.326	4836.388	97.403	111.13	208.53	± 0.20	T7
8	5075.195	4779.535	93.584	111.13	204.71	± 0.20	T6
9	5065.692	4728.922	93.170	111.13	204.30	± 0.20	T6
10	4970.759	4637.663	80.030	111.13	191.16	± 0.20	T1
11	4962.147	4613.948	80.312	111.13	191.44	± 0.20	T1
12	4806.321	4682.148	81.000	111.13	192.13	± 0.20	T2
13	4853.823	4727.445	80.000	111.13	191.13	± 0.20	T2
14	4862.797	4739.037	81.336	111.13	192.47	± 0.20	T3
15	4879.733	4765.231	81.195	111.13	192.33	± 0.20	T3
16	4946.320	4903.114	84.888	111.13	196.02	± 0.20	T4
17	4949.397	4910.620	85.519	111.13	196.65	± 0.20	T4
18	4902.847	4995.494	102.259	111.13	213.39	± 0.20	T8

Note: Elevations at this site are tied to Benchmark Goodwin (elevation 645.00 ft or 196.65 m) via:
MR 15 Pt 4 = MR 16 Pt 3; MR16 Pt 4 = Benchmark.

Mad River Location 16- Austin to Goodwin							
Point Number	Northing (m)	Easting (m)	Elevation (m)	Correction (m)	Final Elevation (m)	Error (m)	Point Description
1	1000.000	1000.000	100.000	97.30	197.30	± 0.20	ROAD
2	1030.666	1095.182	100.000	97.30	197.30	± 0.20	ROAD
3	1743.872	1157.060	96.756	97.30	194.06	± 0.20	Pt 4 on MR15
4	982.982	981.105	99.351	97.30	196.65	± 0.20	Goodwin

Note: Elevations at this site are tied to Benchmark Goodwin (elevation 645.00 ft or 196.65 m) via:
MR16 Pt 4 = Benchmark.

10	1012.817	1091.029	100.000	97.30	197.30	± 0.20	ROAD
11	997.161	1146.137	100.000	97.30	197.30	± 0.20	ROAD
12	997.136	1155.046	100.000	97.30	197.30	± 0.20	ROAD
13	980.207	1101.862	100.000	97.30	197.30	± 0.20	ROAD
14	833.225	1103.657	100.000	97.30	197.30	± 0.20	ROAD
15	835.890	1120.152	100.000	97.30	197.30	± 0.20	ROAD
16	843.000	1160.136	100.000	97.30	197.30	± 0.20	ROAD
17	821.310	1170.550	100.000	97.30	197.30	± 0.20	ROAD
18	910.004	1172.310	100.000	97.30	197.30	± 0.20	ROAD
19	801.932	1180.725	100.000	97.30	197.30	± 0.20	ROAD
20	927.197	1195.745	100.000	97.30	197.30	± 0.20	ROAD
21	909.105	1191.900	100.000	97.30	197.30	± 0.20	ROAD
22	897.615	1140.277	100.000	97.30	197.30	± 0.20	ROAD
23	866.533	1149.321	100.000	97.30	197.30	± 0.20	ROAD
24	956.616	1146.280	100.000	97.30	197.30	± 0.20	ROAD
25	1000.000	1000.000	100.000	97.30	197.30	± 0.20	ROAD
26	898.918	1006.257	100.000	97.30	197.30	± 0.20	ROAD
27	956.615	1146.280	100.000	97.30	197.30	± 0.20	ROAD
28	879.581	991.471	100.000	97.30	197.30	± 0.20	ROAD

Note: Elevations at this site are tied to Benchmark Goodwin (elevation 645.00 ft or 196.65 m) via:
MR12 Pt 26 = Benchmark.

Mad River Location 12-Turner Farm							
Point Number	Northing (m)	Easting (m)	Measured Elevation (m)	Correction (m)	Final Elevation (m)	Error (m)	Point Description
1	1000.000	1000.000	100.000	113.33	213.33	± 0.20	T8
2	1100.000	1000.000	100.000	113.33	213.33	± 0.20	T8
3	662.690	1935.704	106.462	113.33	219.79	± 0.20	T8
4	1066.504	695.020	103.541	113.33	216.87	± 0.20	T8
5	943.417	951.281	100.679	113.33	214.01	± 0.20	T8
6	946.723	958.182	98.890	113.33	212.22	± 0.20	T7
7	942.161	1003.463	97.965	113.33	211.29	± 0.20	T7
8	933.333	1028.520	94.482	113.33	207.81	± 0.20	T6
9	949.185	1044.477	93.534	113.33	206.86	± 0.20	T6
10	1009.897	1068.024	89.374	113.33	202.70	± 0.20	T5
11	997.103	1086.197	88.452	113.33	201.78	± 0.20	T5
12	997.136	1085.949	88.447	113.33	201.77	± 0.20	T5
13	980.237	1101.868	82.506	113.33	195.83	± 0.20	T4
14	963.225	1116.557	81.319	113.33	194.65	± 0.20	T3
15	955.890	1129.122	81.070	113.33	194.40	± 0.20	T3
16	943.006	1168.181	80.391	113.33	193.72	± 0.20	T3
17	941.310	1178.858	79.735	113.33	193.06	± 0.20	T3
18	910.004	1247.318	79.942	113.33	193.27	± 0.20	T3
19	907.832	1260.778	78.731	113.33	192.06	± 0.20	T2
20	927.187	1348.746	78.409	113.33	191.74	± 0.20	T2
21	969.185	1391.905	78.060	113.33	191.39	± 0.20	T1
22	967.405	1420.277	76.853	113.33	190.18	± 0.20	T1
23	966.539	1430.228	76.850	113.33	190.18	± 0.20	T1
24	956.616	1146.280	80.717	113.33	194.04	± 0.20	T3
25	1000.000	1000.000	99.974	113.33	213.30	± 0.20	T7
26	698.318	1005.257	83.756	113.33	197.08	± 0.20	T4
27	956.615	1146.280	80.682	113.33	194.01	± 0.20	T3
28	679.691	991.471	83.323	113.33	196.65	± 0.20	T4

Note: Elevations at this site are tied to Benchmark Goodwin (elevation 645.00 ft or 196.65 m) via:
MR12 Pt 28 = Benchmark.

Mad River Location 18-Neil Farm							
Point Number	Northing (m)	Easting (m)	Measured Elevation (m)	Correction (m)	Final Elevation (m)	Error (m)	Point Description
1	1000.000	1000.000	100.000	99.34	199.34	± 1.0	T4
2	1100.000	1000.000	100.000	99.34	199.34	± 1.0	T4
3	423.810	952.854	116.653	99.34	215.99	± 1.0	T8
4	447.671	955.561	116.849	99.34	216.19	± 1.0	T8
5	479.892	958.204	113.233	99.34	212.57	± 1.0	T7
6	576.807	969.356	112.696	99.34	212.04	± 1.0	T7
7	584.850	956.346	109.939	99.34	209.28	± 1.0	T6
8	617.473	959.776	108.094	99.34	207.43	± 1.0	T6
9	679.358	963.326	104.303	99.34	203.64	± 1.0	T4
10	692.182	954.713	103.590	99.34	202.93	± 1.0	T4
11	647.482	1018.423	112.053	99.34	211.39	± 1.0	T7
12	666.599	1017.586	107.722	99.34	207.06	± 1.0	T7
13	697.458	1005.868	107.234	99.34	206.57	± 1.0	T7
14	710.806	998.822	103.744	99.34	203.08	± 1.0	T4
15	993.042	1011.327	99.923	99.34	199.26	± 1.0	T4
16	1030.064	966.164	99.892	99.34	199.23	± 1.0	T4
17	1037.851	956.721	98.882	99.34	198.22	± 1.0	T3
18	1136.922	892.113	97.819	99.34	197.16	± 1.0	T3
19	1146.197	883.153	97.105	99.34	196.45	± 1.0	T2
20	1227.676	718.760	96.895	99.34	196.23	± 1.0	T2
21	1221.044	710.596	95.727	99.34	195.07	± 1.0	T1
22	1218.925	707.268	95.782	99.34	195.12	± 1.0	T1
23	1285.816	701.085	99.138	99.34	198.48	± 1.0	Bridge

Note: Elevations at this site are tied to a contour line (elevation 640.00 ft or 195.12 m) via:
MR18 Pt 22 = contour line.

Mad River Location 10- Waitsfield							
Point Number	Northing (m)	Easting (m)	Measured Elevation (m)	Correction (m)	Final Elevation (m)	Error (m)	Point Description
1	1000.000	1000.000	100.000	130.30	230.30	± 0.20	T7
2	988.381	1099.323	100.000	130.30	230.30	± 0.20	T7
3	981.496	1158.181	102.374	130.30	232.67	± 0.20	T8
4	994.165	1123.920	101.741	130.30	232.04	± 0.20	T8
5	996.001	1110.310	101.292	130.30	231.59	± 0.20	T8
6	1001.238	1011.789	99.582	130.30	229.88	± 0.20	T7
7	991.810	941.300	98.490	130.30	228.79	± 0.20	SLOPE
8	1090.982	867.997	95.907	130.30	226.20	± 0.20	T6
9	999.991	999.992	100.008	130.30	230.31	± 0.20	T7
10	1061.046	904.451	96.006	130.30	226.30	± 0.20	T6
11	1095.881	861.380	95.708	130.30	226.01	± 0.20	T6
12	1119.079	860.973	94.565	130.30	224.86	± 0.20	T5
13	1141.112	847.194	93.465	130.30	223.76	± 0.20	T5
14	1259.062	760.506	83.355	130.30	213.65	± 0.20	T2
15	1090.981	867.998	95.878	130.30	226.18	± 0.20	T5
16	1149.391	830.382	89.373	130.30	219.67	± 0.20	T4
17	1165.386	822.089	88.399	130.30	218.70	± 0.20	T4
18	1200.009	805.078	83.907	130.30	214.20	± 0.20	T2
19	1175.909	766.193	81.886	130.30	212.18	± 0.20	T1
20	1331.208	673.734	82.597	130.30	212.89	± 0.20	T1
21	1230.364	623.110	83.412	130.30	213.71	± 0.20	T2
22	1353.680	706.971	82.503	130.30	212.80	± 0.20	T1

Note: Elevations at this site are tied to Benchmark 693 (elevation 693.00 ft or 212.80 m) via:
MR10 Pt 22 = Benchmark.

Mad River Location 7-Hap							
Point Number	Northing (m)	Easting (m)	Measured Elevation (m)	Correction (m)	Final Elevation (m)	Error (m)	Point Description
1	1000.000	1000.000	100.000	125.61	225.61	± 1.0	T4
2	1100.000	1000.000	100.000	125.61	225.61	± 1.0	T4
3	766.809	1211.136	115.699	125.61	241.31	± 1.0	T8
4	789.973	1166.208	113.112	125.61	238.72	± 1.0	T8
5	835.270	1115.262	103.441	125.61	229.05	± 1.0	T5
6	843.707	1084.473	103.640	125.61	229.25	± 1.0	T5
7	865.505	1066.598	100.626	125.61	226.24	± 1.0	T4
8	923.510	1012.526	100.703	125.61	226.31	± 1.0	T4
9	887.702	995.689	96.956	125.61	222.57	± 1.0	T3
10	875.536	946.666	97.131	125.61	222.74	± 1.0	T3
11	882.509	936.859	96.362	125.61	221.97	± 1.0	T1
12	1002.574	734.517	96.705	125.61	222.31	± 1.0	T2
13	1002.901	731.041	95.840	125.61	221.45	± 1.0	T1
14	1008.355	724.576	96.079	125.61	221.69	± 1.0	T1
15	1008.635	722.439	95.604	125.61	221.21	± 1.0	T1
16	956.810	714.978	95.604	125.61	221.21	± 1.0	T1
17	960.402	733.542	95.866	125.61	221.48	± 1.0	T1
18	962.767	744.082	96.194	125.61	221.80	± 1.0	T1
19	963.872	746.988	96.636	125.61	222.25	± 1.0	T2
20	1014.412	1025.130	100.582	125.61	226.19	± 1.0	T4

Note: Elevations at this site are tied to a contour line (elevation 740.00 ft or 225.61 m) via:
MR7 Pt 1 = contour line.

Note: Elevations at this site are tied to a contour line (elevation 800.00 ft or 243.80 m).

MR5 Pt 15 = contour line.

Mad River Location 5-Guys							
Point Number	Northing (m)	Easting (m)	Measured Elevation (m)	Correction (m)	Final Elevation (m)	Error (m)	Point Description
1	1000.000	1000.000	100.000	131.60	231.60	± 1.0	T4
2	1100.000	1000.007	100.000	131.60	231.60	± 1.0	T4
3	924.107	1049.642	93.906	131.60	225.51	± 1.0	RIVER
4	930.245	1050.858	95.270	131.60	226.87	± 1.0	T1
5	960.399	1052.813	96.518	131.60	228.12	± 1.0	T2
6	982.072	1070.243	96.225	131.60	227.83	± 1.0	T1
7	986.959	1075.369	97.244	131.60	228.85	± 1.0	T2
8	1020.846	1111.885	96.730	131.60	228.33	± 1.0	T2
9	1038.035	1108.830	97.624	131.60	229.23	± 1.0	T2
10	1058.959	1148.881	97.939	131.60	229.54	± 1.0	T2
11	1059.358	1163.231	98.670	131.60	230.27	± 1.0	T3
12	1077.351	1200.604	98.567	131.60	230.17	± 1.0	T3
13	1082.602	1206.519	99.385	131.60	230.99	± 1.0	T3
14	1099.352	1239.251	99.064	131.60	230.67	± 1.0	T3
15	983.930	1301.867	112.296	131.60	243.90	± 1.0	T8
16	993.583	1266.802	99.262	131.60	230.87	± 1.0	T3
17	982.181	1242.813	99.191	131.60	230.80	± 1.0	T3
18	982.912	1234.020	98.419	131.60	230.02	± 1.0	T3
19	980.623	1186.097	98.576	131.60	230.18	± 1.0	T3
20	978.392	1172.698	96.705	131.60	228.31	± 1.0	T2
21	980.231	1082.668	97.304	131.60	228.91	± 1.0	T2
22	979.284	1073.269	96.193	131.60	227.80	± 1.0	T1
23	986.652	1027.517	96.084	131.60	227.69	± 1.0	T1
24	994.568	1009.140	99.601	131.60	231.21	± 1.0	T4
25	1014.055	986.648	99.540	131.60	231.14	± 1.0	T4
26	1036.435	954.409	94.572	131.60	226.18	± 1.0	T1
Note: Elevations at this site are tied to a contour line, elevation 800.00 ft or 243.90 m.							
MR5 Pt 15 = contour line.							

Mad River Location 8- Rodger							
Point Number	Northing (m)	Easting (m)	Measured Elevation (m)	Correction (m)	Final Elevation (m)	Error (m)	Point Description
1	1000.000	1000.000	100.000	161.88	261.88	± 1.0	T8
2	1100.000	1000.000	100.000	161.88	261.88	± 1.0	T8
3	1006.766	958.469	100.504	161.88	262.38	± 1.0	T8
4	1012.486	1001.615	100.206	161.88	262.09	± 1.0	T8
5	1000.232	1017.793	96.704	161.88	258.58	± 1.0	T7
6	996.379	1039.403	96.682	161.88	258.56	± 1.0	T7
7	977.844	1047.134	96.675	161.88	258.56	± 1.0	T7
8	976.060	1053.483	96.738	161.88	258.62	± 1.0	T7
9	965.389	1060.127	95.269	161.88	257.15	± 1.0	T6
10	956.940	1077.882	95.475	161.88	257.36	± 1.0	T6
11	962.237	1091.149	94.381	161.88	256.26	± 1.0	T5
12	985.784	1142.077	94.875	161.88	256.76	± 1.0	T5
13	988.128	1183.931	95.093	161.88	256.97	± 1.0	T5
14	1000.000	999.998	100.018	161.88	261.90	± 1.0	T8
15	919.733	1140.724	90.092	161.88	251.97	± 1.0	T3
16	898.993	1170.665	90.322	161.88	252.20	± 1.0	T3
17	908.348	1188.626	87.314	161.88	249.19	± 1.0	T2
18	897.997	1210.945	87.463	161.88	249.34	± 1.0	T2
19	895.382	1221.157	86.472	161.88	248.35	± 1.0	T1
20	879.533	1259.857	87.002	161.88	248.88	± 1.0	T1
21	867.730	1258.545	85.933	161.88	247.81	± 1.0	RMER
22	853.088	1248.197	85.782	161.88	247.66	± 1.0	RMER
23	851.020	1248.474	85.411	161.88	247.29	± 1.0	RMER
24	841.921	1248.002	85.555	161.88	247.44	± 1.0	RMER
25	886.224	1154.825	89.673	161.88	251.55	± 1.0	T2
26	874.521	1151.194	89.842	161.88	251.72	± 1.0	T2
27	651.029	1000.361	90.022	161.88	251.90	± 1.0	T2
28	988.128	1183.931	94.991	161.88	256.87	± 1.0	T5
29	866.167	1126.526	87.495	161.88	249.38	± 1.0	T1
30	840.837	1117.037	87.678	161.88	249.56	± 1.0	T1
31	865.013	1146.597	86.931	161.88	248.81	± 1.0	T1
32	850.428	1147.826	87.022	161.88	248.90	± 1.0	T1
33	619.699	1049.714	86.135	161.88	248.02	± 1.0	RMER
34	623.070	1047.124	87.370	161.88	249.25	± 1.0	T1
35	635.180	1019.238	87.583	161.88	249.46	± 1.0	T1
36	640.827	1011.812	89.603	161.88	251.48	± 1.0	RT 100
37	647.883	1003.534	89.235	161.88	251.12	± 1.0	RT100
38	654.935	993.699	90.177	161.88	252.06	± 1.0	T3
39	656.923	989.753	91.039	161.88	252.92	± 1.0	T3
40	668.673	974.795	91.722	161.88	253.60	± 1.0	T4
41	678.426	964.646	92.702	161.88	254.58	± 1.0	T4
42	685.703	949.253	92.655	161.88	254.54	± 1.0	T4
43	706.771	946.181	95.622	161.88	257.50	± 1.0	T5
44	721.080	933.830	95.783	161.88	257.66	± 1.0	T5
45	724.705	903.223	101.809	161.88	263.69	± 1.0	T8
46	349.992	853.626	98.702	161.88	260.58	± 1.0	T8
47	651.014	1000.354	90.136	161.88	252.02	± 1.0	T4
48	220.259	852.104	104.263	161.88	266.14	± 1.0	T8

Note: Elevations at this site are tied to a contour line (elevation 960.00 ft or 292.68 m) via:

MR8 Pt 48 = MR4 Pt 20; MR4 Pt 18 = contour line.

Mad River Location 8- Rodger 2							
Point Number	Northing (m)	Easting (m)	Measured Elevation (m)	Correction (m)	Final Elevation (m)	Error (m)	Point Description
1	1000.000	1000.000	100.000	164.78	264.78	± 1.0	T8
2	966.012	1094.047	100.000	164.78	264.78	± 1.0	T8
3	938.721	1093.132	87.123	164.78	251.90	± 1.0	T2
4	995.566	1008.187	99.733	164.78	264.51	± 1.0	T8
5	1011.910	973.872	100.307	164.78	265.09	± 1.0	T8
6	1031.401	925.714	126.729	164.78	291.51	± 1.0	T9
7	1000.001	999.998	100.035	164.78	264.82	± 1.0	T8
8	1038.873	874.618	127.012	164.78	291.79	± 1.0	T9
9	1046.640	803.989	127.044	164.78	291.82	± 1.0	T9
10	1031.398	925.740	126.717	164.78	291.50	± 1.0	T9
11	1177.533	941.387	126.759	164.78	291.54	± 1.0	T9
12	1158.838	922.358	126.289	164.78	291.07	± 1.0	T9
13	1067.413	811.956	126.766	164.78	291.55	± 1.0	T9
14	1062.092	818.420	126.696	164.78	291.48	± 1.0	T9
15	1046.341	840.693	123.224	164.78	288.00	± 1.0	TRIBUTARY
16	1051.295	864.056	122.771	164.78	287.55	± 1.0	TRIBUTARY

Note: Elevations at this site are tied to a contour line (elevation 960.00 ft or 292.68 m) via:
MR8-2 Pt 3 = MR8 Pt 27; MR8 Pt 48 = MR4 Pt 20; MR4 Pt 18 = contour line

Mad River Location 4-Seasons							
Point Number	Northing (m)	Easting (m)	Measured Elevation (m)	Correction (m)	Final Elevation (m)	Error (m)	Point Description
1	1000.000	1000.000	100.000	165.80	265.80	± 1.0	T8
2	1029.483	904.445	100.000	165.80	265.80	± 1.0	T8
3	1014.058	954.503	100.257	165.80	266.06	± 1.0	T8
4	995.702	1014.702	97.107	165.80	262.91	± 1.0	T7
5	991.434	1029.074	97.090	165.80	262.89	± 1.0	T7
6	989.135	1041.525	94.426	165.80	260.23	± 1.0	T5
7	987.172	1048.460	94.078	165.80	259.88	± 1.0	T5
8	991.364	1063.114	91.921	165.80	257.72	± 1.0	T4
9	991.513	1073.336	91.415	165.80	257.22	± 1.0	T4
10	977.615	1075.765	88.952	165.80	254.76	± 1.0	T2
11	969.383	1105.961	88.810	165.80	254.61	± 1.0	T2
12	967.047	1111.495	87.492	165.80	253.30	± 1.0	T1
13	961.904	1126.235	87.020	165.80	252.82	± 1.0	T1
14	960.712	1128.205	85.627	165.80	251.43	± 1.0	RMER
15	957.996	1134.138	85.509	165.80	251.31	± 1.0	RMER
16	1015.560	950.725	102.296	165.80	268.10	± 1.0	RT 100
17	1018.259	934.689	102.228	165.80	268.03	± 1.0	RT 100
18	1090.209	899.705	126.877	165.80	292.68	± 1.0	T9
19	941.543	920.521	106.025	165.80	271.83	± 1.0	RT 100
20	1025.485	981.809	100.340	165.80	266.14	± 1.0	T8

Note: Elevations at this site are tied to a contour line (elevation 960.00 ft or 292.68 m) via: Pt 18

MAD RIVER CROSS-VALLEY PROFILES

The Mad River cross-valley profiles are presented in the following figures. The profiles are keyed to survey data by name. For instance MR8-1 is profile 1 from the survey location MR8. See Figure 3.6 for survey locations.

